MEDICINAL CHEMISTRY

A Series of Monographs

EDITED BY

GEORGE DESTEVENS

CIBA Pharmaceutical Company, A Division of CIBA Corporation
Summit, New Jersey

Volume 1. GEORGE DESTEVENS. Diuretics: Chemistry and Pharmacology. 1963

Volume 2. RODOLFO PAOLETTI (ED.). Lipid Pharmacology. Volume I. 1964. RODOLFO PAOLETTI AND CHARLES J. GLUECK (EDS.). Volume II. 1976

Volume 3. E. J. ARIENS (ED.). Molecular Pharmacology: The Mode of Action of Biologically Active Compounds. (In two volumes.) 1964

Volume 4. MAXWELL GORDON (ED.). Psychopharmacological Agents. Volume I. 1964. Volume II. 1967. Volume III. 1974. Volume IV. 1976

Volume 5. GEORGE DESTEVENS (ED.). Analgetics. 1965

Volume 6. ROLAND H. THORP AND LEONARD B. COBBIN. Cardiac Stimulant Substances. 1967

Volume 7. EMIL SCHLITTLER (ED.). Antihypertensive Agents. 1967

Volume 8. U. S. VON EULER AND RUNE ELIASSON. Prostaglandins. 1967

Volume 9. G. D. CAMPBELL (ED.). Oral Hypoglycaemic Agents: Pharmacology and Therapeutics. 1969

Volume 10. LEMONT B. KIER. Molecular Orbital Theory in Drug Research. 1971

Volume 11. E. J. ARIENS (ED.). Drug Design. Volumes I and II. 1971. Volume III. 1972. Volume IV. 1973. Volumes V and VI. 1975. Volume VII. 1976

Volume 12. PAUL E. THOMPSON AND LESLIE M. WERBEL. Antimalarial Agents: Chemistry and Pharmacology. 1972

Volume 13. ROBERT A. SCHERRER AND MICHAEL W. WHITEHOUSE (Eds.). Antiinflammatory Agents: Chemistry and Pharmacology. (In two volumes.) 1974

Volume 14. LEMONT B. KIER AND LOWELL H. HALL. Molecular Connectivity in Chemistry and Drug Research. 1976

In Preparation

JULIUS A. VIDA. Anticonvulsants

Molecular Orbital Theory in Drug Research

LEMONT B. KIER
Biochemistry Division
Battelle Memorial Institute
Columbus, Ohio

1971

ACADEMIC PRESS New York San Francisco London
A Subsidiary of Harcourt Brace Jovanovich, Publishers

ACADEMIC PRESS, INC.
111 Fifth Avenue, New York, New York 10003

United Kingdom Edition published by
ACADEMIC PRESS, INC. (LONDON) LTD.
24/28 Oval Road, London NW1

LIBRARY OF CONGRESS CATALOG CARD NUMBER: 73-137616

PRINTED IN THE UNITED STATES OF AMERICA

To my wife
Martha
and my children
Sarah, Lemont, Jr., Andrew, Peter, Katherine

PREFACE

It is apparent from a survey of the literature of the past decade that a growing number of scientists are employing theoretical chemistry to probe biological events at the molecular level. The increasing use of molecular orbital theory in medicinal chemistry, chemical pharmacology, and biochemistry directed toward drug studies has made it desirable to incorporate a presentation and review of the subject in one source.

This book evolved from a series of lectures I presented to graduate students in medicinal chemistry at the University of Michigan. It is directed to the advanced undergraduate or graduate student in medicinal chemistry or pharmacology, to the practicing scientist interested in acquiring some understanding of this approach, and to the theoretical chemist seeking information on biological phenomena amenable to semiempirical molecular orbital study.

The chapters dealing with the applications of molecular orbital theory have been organized on the basis of physical chemical phenomena concluded from the studies described to be involved in the biological activity. Discussion of the chemistry or pharmacology relating to the studies is limited to information pertinent to a background description of the problem and to the validity of the predictions. Major emphasis is placed on the use of molecular orbital theory in each case and the conclusions drawn.

A large number of colleagues have been consulted on many of the topics discussed in the book. Grateful acknowledgment is made to Mr. Gordon Amidon, Dr. Richard Falb, Dr. James Hoyland, Dr. Jackson Lynn, Mr. Victor Marquez, Dr. Brian Myhr, Miss Judith Raisch, Dr. Edward Roche, Mr. Richard Stein, Dr. James Stubbins, and Dr. Edward Truitt. I would also like to gratefully acknowledge the excellent typing done by Mrs. Lucyle Arrowsmith. Finally I want to thank my wife for her patience and understanding.

Chapter I

GENERAL CONSIDERATIONS OF DRUG PHENOMENA

I. Drug–Receptor Interactions

A. The Receptor Concept

One of the most intriguing observations in man's experience is the witnessing of a dramatic change throughout his body as the result of the ingestion or administration of a minuscule quantity of some chemical. The drying of a secretion, the lowering of a pulse, the relief of a pain, even the altering of his own ability to contemplate himself can occur with a quantity of matter which may not be detectable to his naked eye. Accompanying this remarkable power of chemicals to influence life is the equally remarkable specificity that many have in eliciting a particular type of change in the body. We have come to regard the fact of biological influence and the type of biological response as a function of the molecular structure of the chemical, which is designated a drug.

Informed opinion is directed toward the view that many drug molecules engage some highly specialized and selective sites in a tissue, in a chemical or physical event leading to a characteristic biological response. The site is termed the receptor and is regarded as being a pattern of atoms or groups on a macromolecule. The term drug will be used in a broad sense hereafter to include natural transmitter agents, as well as foreign substances with a well-defined pharmacological activity. This view of recep-

tors is supported by the observations that many drugs possess biological activities highly sensitive to molecular modification, and that their activities can be selectively antagonized by another group of structurally similar molecules.

As a consequence of the engagement of drug and receptor in a particular manner, a chain of events ensues leading to macroscopic, widely diffuse and frequently whole-body phenomena, generally termed a pharmacological (or physiological) response. Apparently only a very few molecules are necessary to invoke this response involving tissues and organs. Thus, the initial engagement is capable of massive amplification.

To achieve this response, there are two basic conditions necessary. The drug must be accessible to the receptor, and the drug must possess the necessary features in its structure to insure an efficacious engagement of the receptor. The necessary features of the drug molecule have been termed the pharmacophoric pattern. To date, efforts have been directed primarily toward studying the pharmacophoric pattern in order to reach some conclusions about the nature of the receptor. In contrast, attempts to isolate and probe the receptor structure directly have not yet been fruitful. This latter approach would appear to be a difficult one, even though potentially informative, and will be discussed again later.

B. Theories of Drug Reactions

Two measurable quantities are available in the drug–receptor system: the dose and the response. The dose may be defined as the quantity administered, or an attempt may be made to relate this to the concentration which appears in the environment of the receptor. The limiting conditions between administration and presence near the receptor include absorption, transport, barrier passage, and metabolism. By the careful design of experiments, using isolated tissue, we can estimate the dose or concentration of drug near the receptor, a region termed the biophase.

The measurement of the response is really the measurement of some physical phenomenon such as blood pressure or muscle contraction, which hopefully relates to the receptor being engaged by the drug. The correlation between dose–response and drug–receptor interaction is presumed to be related, even though many molecular events are recognized as intervening between the two. This postulated relationship is all we have now, hence it must stand as a measure of the receptor involvement. The relationship between two quantites, dose and response, then is used to study what is taking place between two molecules, drug and receptor.

A number of hypotheses have been proposed to relate dose–response phenomena and drug–receptor events. Clark employed the Langmuir isotherm to describe drug–receptor interaction [*1*]. He assumed that (*a*) the

intensity of response is directly related to the number of receptors occupied by a drug, (*b*) an all-or-none response is elicited by the drug at each receptor, (*c*) the drug and receptor have a rigid "lock and key" relationship, and (*d*) occupation of a receptor does not influence the function of other receptors.

More recent work by Furchgott [*2*] and Nickerson [*3*] have indicated that, at least in some systems, all of the accessible receptors need not be occupied to achieve a maximum response. By using blocking agents with a low dissociation rate from the receptor (an irreversible blocking agent) they found that most of the receptors could be denied access to the drug and yet the remaining free receptors, when exposed to the drug in sufficient concentration, produced a maximum response.

Ariens [*4*] and Furchgott [*5*] have questioned the all-or-none response concept. Stephenson made further modifications to receptor theory by proposing that only a small percentage of the receptors need be occupied in order to produce a maximum response, and that the response is not linearly related to receptor occupancy [*6*]. He further proposed that drugs had differing abilities to induce a response, although occupancy may be identical. This ability to induce a response is termed the efficacy of the drug. In these theories, efficacy is a property, separate from molecular reactivity (or affinity) of the drug with the receptor. Van Rossum and Ariens have used the term intrinsic activity to define a property quite similar to efficacy [*7*].

It is instructive to consider graphically the meanings of drug efficacy and affinity for receptor sites. Figure 1 shows the comparative log dose versus response profiles for two given drugs. Since both drugs are shown to yield

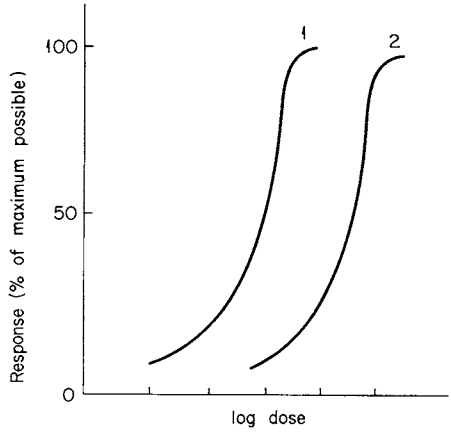

Fig. 1. Drug molecules with equal maximal efficacy but with molecule 2 requiring a higher dose, presumably due to a lower affinity for the receptor relative to molecule 1.

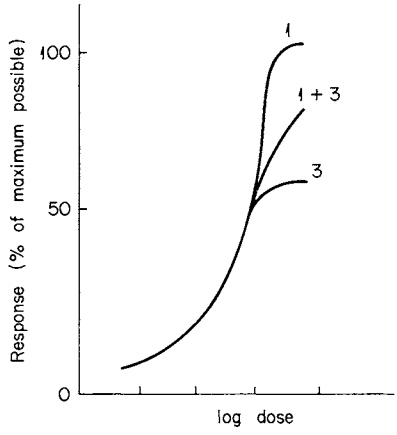

Fig. 2. Drug molecules 1 and 3 with equal affinity but with molecule 3 possessing a lower efficacy. The resultant of the mixture of 1 and 3 is designated as 1 + 3.

identical maximum response levels, their efficacies or intrinsic activities are the same. The response being maximal with sufficient concentration, we term the molecules agonists. However, we require one order of magnitude more of molecule 2 than of molecule 1 to achieve the maximum response. It is presumed that this differential is due to a lower affinity of molecule 2 for the receptor, if it is presumed that the biophase concentrations of the two drugs are related identically to the dose levels.

In Fig. 2, the response of a third drug, molecule 3, is compared with the dose–response curve of molecule 1. Because the inflection points of the two curves occur at nearly the same dose levels, the two drugs are said to have equal affinities for the receptor. The maximum response to drug 3, however, is found to be much lower. Thus molecule 3 is only partially efficacious, relative to molecule 1, and it is termed a partial agonist relative to molecule 1.

A third case is illustrated in Fig. 3. If a molecule 4 had an affinity equal to 1, but did not cause the receptor to elicit any response (no efficacy) it would, of course, compete with 1 for receptors and lead to the necessity of a higher dose of 1 to achieve its maximal response level. This situation is characteristic of competitive antagonism.

A theory by Paton proposed that a drug effect is not due to the proportion of receptors occupied, but is due to the rate at which they are occupied [*8*]. The key event in the hypothesis is the occupation process rather than the physical association formed. Each association event leads to a transient excited state that ultimately produces the observed response. It is expected that the response would be greatest upon initial introduction of the drug to the biophase, followed by some diminution or fade upon equili-

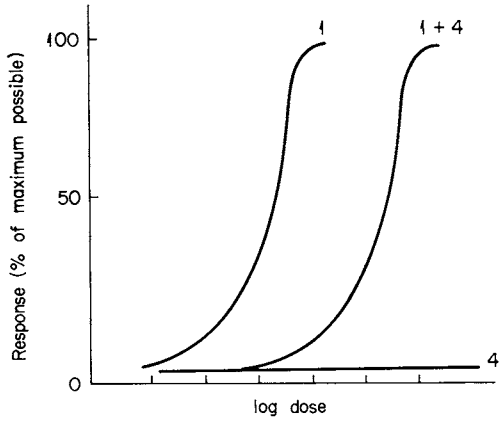

Fig. 3. Drug molecules 1 and 4 with equal affinities but with 4 possessing no efficacy. Molecule 4 competitively antagonizes 1 when mixed with it, requiring a larger dose of 1 to achieve a maximum response.

bration of the association–dissociation events. Such a response profile has been noted for some drugs.

The status of these theories remains an open question for study. Both general theories can find support in existing experimental evidence. Waud has recently critically reviewed both [9].

II. Drug–Receptor Interaction Forces

Preliminary to a consideration of techniques of studying drug receptor phenomena, it is desirable to review the forces involved in intermolecular interaction. These have structural and distance dependencies which determine their presence in a particular association, and which in turn determine the strength or energy of bonding.

It has been a conventional practice to consider the binding of two molecular entities by dissecting the total energy of binding into discrete forces. These individual forces are then defined in terms of specific kinds of bonds and attempts are made to measure and estimate the energies involved. This approach has led to categories such as covalent, electrostatic, dipole, hydrogen, dispersion, and hydrophobic bonding.

A. The Covalent Bond

This type of binding is, in selected cases, associated with drug receptor interactions. A few cases can be cited postulating covalent bonding with drugs such as certain adrenergic inhibitors and the fluorosphosphate enzyme inhibitors. Because of the strength of the bond, 50–100 kcal/mole, a rapid dissociation would not occur, hence these systems are usually treated

as being irreversible. These bonds are characterized by being highly directional, permitting the closest approach of atoms (1–2 Å) and having very high bonding energies.

These bonds form as a result of a mutual (although not necessarily equal) sharing of two electrons. If atoms of different electronegativity are involved, the electrons in the bond will be displaced, in their most probable location, toward one atom. This results in a permanent electric dipole, permitting the bonded system to interact with its environment.

The intuition of the organic chemist is developed primarily to cope with the problem of explaining and predicting the course of covalent bond making and breaking reactions. This intuition has been carried over by the medicinal chemist to the prediction of drug molecule events at the receptor. Considerable complication can be expected at the receptor in contrast to *in situ* experience. The multiplicity of bond types likely between drug and receptor and the very important role played by molecular stereochemistry, places definite limits on the *in situ* derived intuition. Clearly, drug–receptor reactions must be studied using a more inclusive consideration of all of the structural features and bonding forces involved.

An excellent example is the enzymic hydrolysis of an ester. This process occurs at a rate greatly exceeding the rate found by digesting the ester in alkali. Secondary binding forces and optimized conformation contribute to the greatly increased rate due to the enzyme. These added influences must be considered in any rigorous study of the effect of structural modification on the gross phenomenon of enzymic covalent bond breaking.

B. Electrostatic Interaction

This type of bonding is the result of the interaction between two charged species. The potential energy of the system is

$$E = q_1 q_2 / dD$$

where q is the charge, d the distance separating the points, and D the dielectric constant of the medium. Two opposite unit charges separated by 5 Å in water would have an energy of about 65 kcal/mole.

Charged molecules are prevalent among drugs and enzyme substrates. At physiological pH, many amino groups can be expected to be protonated, hence charged. These molecules are certainly not point charges since the charge of the onium group is distributed over the molecule. Further, in a polar solvent, such as water intervening between charged molecules, it is expected that the energy of interaction would be somewhat dissipated. In dilute solution, this energy can be approximated if the dielectric constant, D, is included in the expression, along with the numerical value of the charges, q and q_2.

Chemical intuition can qualitatively assess this binding force, but without a reasonable estimate of the charges on two interacting species, quantitation or prediction of binding strength and ranking in a series of molecules is not very reliable.

C. Dipolar Interactions

The unequal sharing of electrons in a bond between two atoms of substantially different electronegativity will lead to a permanent displacement of the electron probability in the bond toward the more electronegative atom. Thus a carbonyl group would be expected to have a negatively charged oxygen atom and a positively charged carbon atom. This permanent dipole is capable of interaction with another permanent dipole to form a bond. The strength of this bond depends upon the spatial orientation of the interacting dipoles, their distance apart, and the extent of charge separation in each dipole. In a head-to-tail interaction of two dipoles, the energy of the bond is

$$E = 2\mu_a\mu_b/d^3D$$

where μ is the dipole moment for each dipole and d is the distance between the centers of the two moments.

It would be expected that this type of bonding would be prevalent in aqueous solution with water contributing one of the species. Many drug molecules possess carbonyl groups and other heteroatoms, creating permanent dipoles. The interaction of these with polar features of proteins could be expected to lead to dipolar bonds.

Weaker bonds can form from the interaction of a permanent dipole with a nonpolar molecule causing the induction of a dipole, giving rise to a weak interaction between the two. This interaction is highly distance-dependent, falling off as the sixth power of the separating distance. Although the strength of these bonds is very small, they may be important in many drugs where a weak secondary binding site in a drug molecule must be present to impart a stereoselective biological activity.

D. Hydrogen Bonds

The hydrogen bond if formed between a proton initially covalently bound to an electronegative atom, X, and another electronegative atom, Y.

$$X\text{——}H\cdots\cdots Y$$

The bond energy ranges from 2 to about 10 kcal/mole and is essentially, but not completely, an electrostatic phenomena. A group capable of hy-

drogen bonding is also capable of aqueous solvation, with little difference in energetic preference. There is no doubt that this type of bond is found extensively in drug and receptor phenomena.

E. Dispersion Forces

These forces, also known as London or van der Waal's forces, are due to the interaction of the instantaneous electrical moment in one molecule with the induced electrical moment in a neighboring molecule. The instantaneous moment in a molecule is due to fluctuations in the positions of the electrons. This instantaneous moment can induce a moment in another molecule at short range, leading, always, to an attractive force at short range in the ground state. These attractive forces are also referred to as charge fluctuation interactions.

The energy of this bond can be approximated for two neutral identical molecules as

$$E = -3\Delta\bar{E}\alpha^2/4d^6$$

where $\Delta\bar{E}$ is an average excitation energy and α is the polarizability of each group. The attraction between two CH_2 groups 5 Å apart is thus calculated to be about 0.1 kcal/mole. The forces are additive, hence the interaction energy is the sum of the pair interaction energies along a chain. For adjacent methylene groups in the system shown in Fig. 4 the calculated total binding energy is approximately 0.9 kcal/mole [*11*]. The additive nature indicates that sizable binding energies can be achieved if a large number of groups are spatially permitted intimate contact. These forces are associated with all molecules, but they are especially prominent in neutral molecules and groups since they are the only attractive force to be found. The forces are highly sensitive to distance, falling off with at least the sixth power of the distance, and probably, due to retardation phenomena, at a greater power of the distance. It is to be expected that dispersion forces would be greater between unsaturated bonds in adjacent molecules, since these bonds are more polarizable.

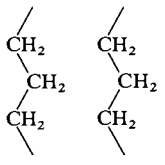

Fig. 4. Adjacent methylene groups illustrating enhancement of dispersion binding in molecules from the interaction of identical groups.

F. Hydrophobic Bonds

The observed tendency of nonpolar portions of biopolymers to avoid contact with aqueous medium and thus to become associated among themselves has been termed "hydrophobic bonding" by Kauzmann [*12*]. The phenomenon is presumed to be due to favorable entropy since the interspersion of nonpolar groups among water molecules would, if it were to occur, result in considerable ordering of the water around the nonpolar groups. This increased entropy is avoided by the water and the nonpolar groups remaining associated with their own kind [*12*].

A more direct explanation for this phenomenon may be possible by considering the events at the molecular level. Certainly the forces binding water molecules are large, involving primarily electrostatic, but including some dispersion forces as well. This energy is 5–6 kcal/mole. The forces of attraction between nonpolar groups, such as methyls or methylenes, in a nonpolar chain can be considerable, especially if chains of some length are involved. Any interaction between a nonpolar group and water would involve a dispersion force. Thus water bonding to water and nonpolar group bonding to nonpolar group is certainly favored from the comparative enthalpies. Thus entropy considerations may not have to be invoked to explain this phenomenon.

III. Consequences of Drug–Receptor Interaction

A. General Considerations

Before going on to a brief discussion of structural requirements for receptor activation, it is of interest to dwell on the events subsequent to the drug–receptor engagement. The consequences of this association can only be speculated upon since we have no precise knowledge to date of what specifically a receptor is or what structures it engages to propagate a stimulus.

In a recent review, Mautner has classified most drugs into three categories based upon the results of receptor engagement [*13*]. They are (*a*) drugs inhibiting or altering enzymes, (*b*) drugs altering membrane permeability, and (*c*) drugs altering template molecules. The first two categories may actually be the same event. Examples can be cited in each category, but the central concept emerges that a biopolymer is altered in some way by the drug.

In the case of certain drugs, the altered biopolymer has been identified as an enzyme, and the consequences of the reaction with that enzyme are clear and measurable. However, in many cases the drug appears to combine loosely with unknown biopolymers which have been given the label,

receptor molecules, or simply, receptors, to imply their activity. Many receptors show evidence of being located in or near the outer cell membrane based upon the rapidity of response produced when they are activated. Most receptors are generally assumed to be proteins or lipoproteins, which are known components of most cell membranes. Calculations of the number of drug molecules required to activate cells indicate that a receptor could occupy only a small portion of the cell surface. Within the cell, certain macromolecules known to exert controlling influences, such as DNA and RNA, are also certainly candidates for consideration as receptors. However, the reactions they produce would necessarily be slower than for membrane-controlled events.

In some cases the effect of a drug on the receptor protein might be viewed as resulting in a conformational change in the protein if the interaction is known to be reversible. This event could lead to a subsequent perturbation and/or alteration in some function of the protein with the end result of a large-scale response. This is consistent with the highly reversible action of many drugs, since only a nonbonded interaction of low energy would be required to produce a conformational change in the protein, and the weak bond formed would be capable of facile dissociation.

B. Physicochemical Consequences

The most important effect that has been identified for drugs acting on membrane receptors has been the consequence of an altered permeability of the membrane to electrolyte ions. Drugs may act upon excitable membranes either to increase membrane permeability, which may cause depolarization, or to decrease permeability, which results in hyperpolarization. Acetylcholine produces increased permeability, allowing a rapid influx of the external Na^+ ions, followed by an efflux of the internally high concentration of K^+ ions. General anesthetics such as diethyl ether may impede or block this depolarizing action of acetylcholine as it is released from preganglionic nerve endings or, more likely, inhibit the effect of this acetylcholine on the postsynaptic terminals. Some local anesthetics appear to impede the progress of an electrical signal along nerve trunks by a similar impedence of ionic flux across the membrane. Diphenylhydantoin has been shown to increase the stability of cortical neurons against convulsive discharge by reducing the intracellular Na^+ and maintaining a greater electronegativity in the membrane potential that is less easily discharged by abnormal brain wave signals in epileptics.

Caffeine is an example of a drug acting in or near the sarcoplasmic membrane to produce an increased dissociation of bound calcium. Increased calcium dissociation initiates several intracellular energy mechanisms and may be involved in the release of high energy phosphate from adenosine

triphosphate (ATP) leading to the restoration of normal membrane polarization by the pumping out of Na^+ and the reentrance of K^+ ions.

C. Biochemical Consequences

A growing number of drugs can be identified as reactants at specific enzymes in their mechanism of action. The primary effect most often seen is an inhibition of the enzyme activity. This may be either reversible, with little detriment to the protein structure, or irreversible damage leading to denaturation of the protein. Most reversible drugs are attached only transiently and may compete with normal body cofactors and substrates for the enzyme.

A well-known example of this type is the competition of the drug disulfiram (Antabuse) with the coenzyme factor nicotinamide adenine dinucleotide (NAD, formerly DPN) with the enzyme aldehyde dehydrogenase. This leads to an abnormally slow breakdown of acetaldehyde and accumulation of this metabolite of alcohol causing unpleasant consequences.

Acetazoleamide is a carbonic anhydrase inhibitor which alters the normal ability of cells to release hydrogen ions, and alters acid–base balance. This leads to diuretic effects in the kidney, reduced gastric pH in the stomach, and an anticonvulsant effect in the brain.

Cholinesterase inhibitors include many drugs and insecticides, the latter of which may destroy cholinesterase irreversibly. The consequence of cholinesterase inhibition or destruction is an abnormal persistence of large amounts of acetylcholine. Similarly, monoamine oxidase inhibitors result in unusually high concentrations of the biogenic amine neurotransmitters, 5-hydroxytryptamine (serotonin) and norepinephrine (noradrenaline).

D. Neurochemical Consequences

In some examples recently identified, interaction of a drug with a receptor may stimulate neurochemical reactions by the release, or blockage of release, of a neurotransmitter substance. Tyramine, ephedrine, and many other sympathomimetic amines cause the release of norepinephrine from storage granules in nerve endings to bring about their vasoconstrictor actions indirectly. Excessive release and the almost total depletion of the biogenic amines norepinephrine and 5-hydroxytryptamine by drugs such as reserpine may produce effects owing to the failure of sufficient neurotransmitter compounds. One can remedy the deficiency of a neurohormone by giving large amounts of its precursor compound such as the administration of high doses of *l*-(3,4-dihydroxyphenyl)alanine (*l*-dopa) which forms dopamine at the site of the Parkinson's disease lesion in the brain. Another neurochemical mechanism recently identified is the potentiation of the re-

leased norepinephrine neurotransmitter that results when its reuptake into the nerve ending is blocked by drugs such as cocaine, imipramine, and certain antihistamine compounds.

IV. The Study of Drug–Receptor Events

Research into the nature of drug–receptor events has been directed toward the elucidation of the structure of the receptor and the macromolecule of which it is a part, as well as the salient features of the drug molecule which confers upon it receptor specificity. These studies have ranged from theoretical considerations and physical measurements to analog synthesis and testing.

A. Receptor Molecule Isolation

An approach to the drug–receptor phenomenon might be the isolation and characterization of biopolymers implicated as being receptors. If a measurable function of the biopolymer exists, it could then be used to monitor the isolation and serve as a criterion of purity. This function, as, for example, the catalytic activity of an enzyme, would have to be relatable to the pharmacological response produced by the drug. If no such relationship is known or if the receptor biopolymer, when detached from its environment, produced no measurable activity, it would be difficult to establish the isolated substance as a receptor molecule.

Gaddum has outlined a general scheme of receptor isolation similar to active site studies on enzymes [*14*]. The receptor is protected with a competitive blocking agent and other sites of attachment are occupied with a covalent bonding nonradioactive molecule. The receptor-blocking molecule is then washed out and the receptors are exposed to a radioactive form of the covalent bonding molecule. Subsequent isolation steps could now be monitored by detection of a radioactive label [*15*].

B. Physical Measurements of Receptor Molecule Changes

Changes in the ultraviolet absorption of chromophoric groups in protein molecules recorded as difference spectra, have been used to study conformational changes by Scheraga [*16*].

Optical rotatory dispersion measurements have been made of biopolymers in contact with drug and substrate molecules. The changes in optical rotation as a result of molecular alteration of the helical content of proteins have been useful in detecting and understanding conformation changes [*18*].

Perutz has studied the conformation changes occurring in hemoglobin upon oxidation by using X-ray diffraction techniques [*19*]. Enzyme inhibi-

tor complexes have also been studied by Phillips by this method [*20*]. These studies are done on crystals rather than molecules in solution.

Nuclear magnetic resonance (NMR) measurements have been employed to study the binding of small molecules to proteins. Burgen *et al.* have examined the binding of quaternary ammonium compounds to enzymes [*21*].

C. Chemical Studies

A great number of molecules have been synthesized over the past few decades with the intention of using these as molecular probes to gain further insight into the chemical nature of the receptor and the mode of interaction with a drug molecule. Broadly, this approach can be categorized into studies using analogs of agonists or antagonists of a particular potent receptor substrate.

1. Structure–Activity Studies on Agonists

Some information has been accumulated on the essential nature of certain groups and atoms in agonist molecules and their analogs by synthesizing large numbers of molecules in which minor structural variations have been introduced. This approach has permitted the assignment of pharmacophoric patterns to agonist molecules in several pharmacological classes. The approach presumes that the essential electronic structure can be intuitively assessed from a study of graded variations on a basic molecular theme. The intuition has had its roots in valence bond or resonance theory reasoning. In the case of aromatic molecules or the aromatic portions of molecules, the intuition has centered almost exclusively on the π-electron portion. Comparative chemical reactivities have also been deduced from a consideration of comparative electron distributions. This, however, is generally a poor criterion of chemical reactivity [*22*].

Another problem that has persisted in the synthetic analog approach is the difficulty in predicting conformational preference in molecules containing single bonds. Where this has involved portions of the pharmacophoric pattern, as in the case of acetylcholine, a knowledge of the conformation is indeed critical.

A number of investigators have recently attempted to cope with conformational problems by preparing molecules in which the assumed essential features of the parent agonist are contained in a rigid structure [*23*, *24*, *25*]. The method involves the synthesis of rigid molecules containing the essential pharmacodynamic groups in known configurations approximating the likely spatial arrangements in the agonist molecule. By testing the various molecules, it was hoped that the most active analog could be presumed to have the key groups in a configuration most closely approximating the parent agonist, in its functional or preferred conformation.

Unfortunately, in the process of constraining the essential groups into a

rigid configuration, numerous additional atoms have been added to the basic agonist molecule. As a result, the influence of these additional atoms at the receptor site could become a factor in the activity of the molecule. The finding of markedly lowered agonist activity among most of these rigid analogs suggests that perhaps what has been synthesized are partial antagonists. The correspondence between the activity of the rigid analog and the functional conformation of the parent agonist is thus in question. Further, the additional atoms influence electronic structure in the rigid analog, introducing a new variable in these comparative studies. If the rigid analog could be kept quite simple in terms of structural departure from the original agonist molecule, these problems would be minimized and a comparison would become more realistic. Armstrong and co-workers have made cyclopropyl analogs of acetylcholine and found, in one case, comparable activity to acetylcholine [*26*]. The distance between the nitrogen and ether oxygen in this active analog corresponds more closely to the conformational prediction of acetylcholine based upon NMR [*27*] and theoretical predictions [*28*] than to the conformation predicted from studies on a decalin analog [*25*]. In the cyclopropyl studies then the formation of a rigid molecule has not led to a sacrifice of the relevance of key features to the receptor.

The fruitful direction that this approach can take is thus evident. The rigid analogs could serve as models for physical measurements, such as NMR, of the influence of groups and atoms on the properties of each other. These could be used to compare with agonist molecules with the hope of deducing conformation by physical means.

2. *Structure–Activity Studies of Antagonists*

Another approach to drug–receptor information has centered around the study of antagonist or antimetabolite molecules. Again, systematic structural variation accompanied by biological testing can reveal trends which influence activity. The assumption is made that receptor affinity depends upon specific structural features, regardless of whether the molecule is efficacious (an agonist) or not (an antagonist). An irreversible inhibitor may function by covalently attaching to a portion of the receptor or an adjacent feature. Hence, studies of this type may lead to information concerning the immediate environment of the receptor. A competitive inhibitor, on the other hand, has structural features more closely related to the agonist molecule. Hence comparative activities of this type of inhibitor take on the significance discussed previously for agonist variation.

D. Theoretical Studies Based on Quantum Mechanics

It is becoming increasingly apparent to many medicinal chemists, phar-

macologists, and biochemists, that studies of biological events, designed to elucidate mechanisms at the receptor, must be directed toward the fundamental particles controlling these events. Specifically, this means an understanding of the structural features of molecules imparting chemical (hence biological) activity. The structural features are, of course, the energies and distributions of valence electrons and the spatial arrangement of their cores (nonvalence electrons plus nuclei).

The fundamental description of matter is known as wave mechanics or quantum mechanics. It seeks to describe in mathematical terms the nature of physical reality. Its success is truly remarkable, but because of the intractability of the many-electron equations, it is limited to very simple atomic and molecular systems for exact or nearly exact descriptions. More approximate, hence less rigorous, treatments of larger molecules are possible through approximations of quantum theory. These approximations have followed two general lines of development, valence bond theory and molecular orbital theory.

1. Valence Bond Theory

Valence bond theory seeks to describe the structure of a molecule as a resultant of the weighted contributions of numerous possible structures, where the electron composition of each contributing structure is considered to be made up of a whole number of electrons. Thus for benzene, the contributing structures are

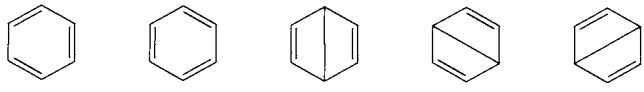

The number of valence bond structures which must be considered for naphthalene increases to 42 and for anthracene to 429. Solutions to larger molecules with less symmetry are very complex indeed. The advantage of valence bond theory is that it lends itself to pictorial description if the more probable contributions only are considered. The organic chemist has seized upon this pictorial simplicity and has developed a useful tool, known as resonance theory, to approximate molecular properties without the use of calculations, but with only some of the pictorial descriptions derived from the mathematics.

Resonance theory has been the intuition of the chemist, and more recently the drug scientist, for deducing electronic structures and predicting reactivities of molecules of interest. This intuition is severely limited to simple, usually aromatic, molecules or molecules of high symmetry. The geometry of nonaromatic molecules or the electron distributions in heterocyclic systems is more elusive to resonance theory prediction.

2. Molecular Orbital Theory

The alternative approximation of rigorous quantum mechanics is known as molecular orbital (MO) theory. This theory depicts the electrons of a molecule as being associated with the entire molecule rather than being uniquely associated with a particular nucleus. Thus the electrons are described in terms of molecular orbitals. The theory is intensely mathematical and does not lend itself to pictorial description. The mathematical complexity of molecular orbital theory has prevented its use, except in simple molecules, until the postwar development of high-speed digital computers. The inability of the calculations to yield results easily portrayed has been a barrier to its use or study by many nonmathematically oriented scientists.

Nevertheless, molecular orbital theory offers greater promise in calculating electronic structures and predicting properties of drug molecules than does valence bond theory or its nonmathematical offshoot, resonance theory. The success of MO theory to predict chemical and physical events has been encouraging, as witnessed by a steady increase in its use in the literature. Within the past two decades, MO theory has been introduced into the area of biochemistry under the pioneering leadership of the Pullmans [*22*].

More recently, MO theory has found its way into the hands of a few medicinal chemists and pharmacologists to explain drug phenomena. Although the number of such studies on drug molecules is yet small, the successes achieved have been encouraging and portend a wider use of MO theory. In the ensuing chapters in this book, many of these studies will be described.

In the next three chapters, the reader will be brought to a level of understanding and competence in the use of approximate MO techniques that will allow him to read with understanding the current literature in which MO theory is applied to drug studies. The serious student may be equipped with a background sufficient for the actual employment of MO theory as a research tool.

In the chapters following the general treatment of MO theory, the applications of this theory to drug studies will be described. It must be emphasized that these chapters are not treatments of quantum chemistry nor are they intended to be discussions of topics in medicinal chemistry or pharmacology. Rather, the organization is based on chemical or physical phenomena in which MO theory has or can play a role in illuminating various aspects of drug action. These application chapters, therefore, are not based on molecular types or on pharmacological classes of drugs, but are based upon the general types of physical events in which drug molecules have been thought to participate. The discussions in these chapters will lay emphasis on what has been done and what can be done with MO theory to

elucidate drug mechanisms. In depth discussions of the chemistry or the pharmacological consequences of MO-correlated activities or predicted mechanisms will not be considered beyond what is necessary to reflect on the validity of the conclusions of the studies described. The applications chapters are intended to demonstrate to the drug scientist how MO theory has been used, and how it can be used. They are also intended to show to the quantum chemist how his theoretical knowledge may be brought to bear on biological problems and what some of those problems are.

References

1. A. J. Clark, "Mode of Action of Drugs on Cells." Arnold, London, 1933.
2. R. F. Furchgott, *J. Pharmacol. Exp. Ther.* **111**, 265 (1954).
3. M. Nickerson, *Nature (London)* **178**, 697 (1956).
4. E. J. Ariens, *Arch. Int. Pharmacodyn. Ther.* **99**, 32 (1954).
5. R. F. Furchgott, *Pharmacol. Rev.* **7**, 183 (1954).
6. R. P. Stephenson, *Brit. J. Pharmacol.* **11**, 379 (1956).
7. J. M. Van Rossum and E. J. Ariens, *Arch. Int. Pharmacodyn. Ther.* **136**, 385 (1962).
8. W. D. M. Paton, *Proc. Roy. Soc., Ser. B* **154**, 21 (1961).
9. D. R. Waud, *Pharmacol. Rev.* **20**, 49 (1968).
10. L. B. Kier, *J. Med. Chem.* **11**, 441 (1968).
11. L. Salem, *in* "Electronic Aspects of Biochemistry" (B. Pullman, ed.), p. 293. Academic Press, New York, 1962.
12. W. Kauzmann, *Advan. Protein Chem.* **14**, 1 (1959).
13. H. G. Mautner, *Pharmacol. Rev.* **19**, 107 (1967).
14. J. H. Gaddum, *in* "Enzymes and Drug Action" (J. L. Mougar and A. V. S. de Reuck, eds.), p. 449. Little, Brown, Boston, Massachusetts, 1962.
15. S. Ehrenpreis, J. H. Fleisch, and T. W. Mittag, *Pharmacol. Rev.* **21**, 131 (1969).
16. H. A. Scheraga, "Protein Structure." Academic Press, New York, 1961.
17. B. H. Havsteen and G. P. Hess, *J. Amer. Chem. Soc.* **85**, 791 (1963).
18. E. Breslow, S. Beychok, K. D. Hardman, and F. R. R. Gurd, *J. Biol. Chem.* **240**, 304 (1965).
19. M. F. Perutz, *Sci. Amer.* **211**, 64 (1964).
20. D. C. Phillips, *Sci. Amer.* **215**, 78 (1966).
21. A. S. V. Burgen, O. Jardetzky, J. C. Metcalf, and N. Wade-Jardetzky, *Proc. Nat. Acad. Sci. U.S.* **58**, 447 (1967).
22. B. Pullman and A. Pullman, "Quantum Biochemistry." Wiley (Interscience), New York, 1963.
23. F. W. Schueler, *J. Amer. Chem. Soc.* **78**, 197 (1956).
24. S. Archer, A. M. Lands, and T. R. Lewis, *J. Med. Chem.* **5**, 423 (1962).
25. E. E. Smissman, W. L. Nelson, J. B. Lapidus, and J. L. Day, *J. Med. Chem.* **9**, 458 (1966).
26. P. D. Armstrong, J. G. Cannon, and J. P. Long, *Nature (London)* **220**, 65 (1968).
27. C. C. J. Culvenor and N. S. Ham, *Chem. Commun.* p. 537 (1966).
28. L. B. Kier, *Mol. Pharmacol.* **3**, 487 (1967).

Chapter II

GENERAL CONSIDERATIONS OF QUANTUM THEORY

I. Classical Mechanics

A. General Principles

Until the turn of this century, it was felt that all reality was describable by Newton's laws. The material world was considered to be composed of particles of matter which either moved or were at rest in space. From Newton's First Law, a particle at rest remained at rest, whereas a particle in motion remained in motion in the same direction, unless some force altered the rest or moving state. Forces were defined in terms of their effects on particles; thus, from the Second Law, a force was measured by the change it produced in the velocity of a body on which it acted, multiplied by the mass of the body. These laws, or Newtonian mechanics, were, for the first time in philosophical history, based on experimental results rather than speculation and conjecture. The theories were also free from restrictions limiting them to the earth's surface. Thus they were able to act as a foundation for astronomical application.

Extensions of Newtonian mechanics appeared to be capable of handling natural objects from planet-sized bodies, through man-sized objects, down to particles of minute size such as electrons and positive rays (α particles). Matter was thought to be composed of atoms of different types, and these different types in turn had the property of combination to form molecules. From experiment the view was held that atoms in turn consisted of a collec-

tion of electrons, negatively charged particles, associated with a particle of comparable positive charge. In the field of optics, light was considered to be an undulatory phenomenon, propagated as waves of varying frequencies. Phenomena such as diffraction and interference could be explained by this concept.

Thus physical philosophy at the turn of the century envisaged reality as matter and undulatory radiation, existing and moving in a continuum of space and time. Classical mechanics had experienced conspicuous success in explaining and predicting phenomena in the man-sized world and astronomy; however, some lacunae existed in explaining atomic phenomenon. This failure was to grow and eventually to spawn an entirely new concept of matter.

B. Failures of Classical Theory

The failure of classical mechanics occurs at the atomic level of reality. It is not in the province of classical mechanics to explain the unchanging size of an atom or its stability alone or in combination in a molecule. According to classical theory, the charges within an atom cannot stand at rest or they will coalesce. Neither can they be in motion or they will be a perpetual motion device not permitted in classical mechanics.

Another disharmony in classical theory occurs with a consideration of light phenomenon. The wave concept can explain interference and diffraction; however, the photoelectric effect implicates a particulate nature for light. In this latter phenomenon, light appears to have a definite energy and momentum, depending on the frequency. Thus particulate or corporeal properties may be attributed to light as with other particles such as electrons. A fraction of this light particle is never observed.

The failure of these classical ideas can be seen not only from experimental evidence, but from general philosophical considerations. In the classical theory, the behavior of matter must be deduced from the behavior of its constituent parts. This, however, leaves unexplained the nature of these constituent parts. A consideration of these constituent parts seems to demand that these smaller parts in turn reflect the behavior of even smaller parts comprising them. There would be no end to this logic in explaining the properties of ultimate particles.

II. Quantum Mechanics

A. Theory of Quanta

The dawn of the present century saw also a dawn of new concepts in man's consideration of the nature of reality. In the first three decades of this cen-

tury, we have seen perhaps the most significant advance in physical philosophy since the days of Newton. In 1901, Planck cleared up an anomaly in the explanation of blackbody radiation. He suggested that energy was emitted from heated bodies, not as waves, but as discrete particles or quanta. The theory stated that radiation was particulate in its structure just like matter, but differing in that there are an infinite number of different kinds of radiation depending on their wavelength. The relationship between wavelength, λ, frequency, v, and light velocity, c, being

$$\varepsilon = hv = hc/\lambda \tag{1}$$

with h being a proportionality constant. This constant, Planck's constant, has since come to be regarded as a universal constant. It is a constant of least action having a value of 6.626×10^{-27} erg sec.

Planck's theory was immediately applied to a successful explanation of the photoelectric effect. When ultraviolet light falls on a metal surface, a stream of electrons emanates from the metal. If the radiation is weakened the number of electrons emitted is reduced but their energy remains the same. The number of electrons emitted is proportional to the intensity of the radiation. Further, when an electron is emitted, the total energy absorbed by it is exactly one whole quantum. Some of this energy is dissipated in detaching the electron from the metal. Low-frequency radiation has quanta of low energy as was shown by Planck's equation, Eq. (1), hence this energy may not be sufficient to liberate an electron. The limiting frequency for electron liberation is the threshold frequency. From the corpuscular concept of light, this explanation was consistent with experiments.

Einstein expanded upon this theory by proposing that an atom could only emit radiation in complete units or quanta. He pictured each emitted quantum as traveling through space in the form of a compact indivisible unit. He referred to this packet of radiation as a light-arrow. The term used today is photon. According to this picture, a beam of radiation or light is a shower of photons. Upon striking a metal surface, each photon may strike an electron imparting the energy of the photon, one quantum, to the electron.

The quantum concept of Planck was applied to a theory of atomic structure of Bohr in 1913 [*1*]. He utilized classical mechanics to describe an electron orbiting the nucleus of the atom. To account for the stability of this orbit, he imposed a quantum condition on the electron, consigning it only to orbits of definite energy. He further postulated that an electron could jump from one orbit to another if the energy absorbed or emitted was a multiple of the frequency, as shown in Eq. 1. This theory was able to explain the spectrum of hydrogen; however, it was deficient in explaining the spectra of other elements.

B. The New Quantum Theory

The shortcomings of the Bohr picture of the atom and the dichotomy of the wave-particle picture of light resulted in a more extensive departure from classical concepts during the decade of the 1920's. From the wave picture of light, the energy of each photon is related to the frequency as a multiple of Planck's constant [Eq. (1)]. Einstein had shown from relativity theory that the energy of a photon relates to the mass, m, and the velocity of light, c,

$$\varepsilon = mc^2$$

In 1924, DeBroglie combined these two ideas into a relationship between mass and frequency.

$$mc^2 = h\nu$$

hence the relationship involving velocity, v, and momentum, p, becomes [2, 3]

$$p = mv = h\nu/c = h/\lambda$$

The prediction was that particles such as electrons have associated with them waves of a frequency dependent on the mass and their velocity. This was experimentally verified by Davisson and Germer [4] and by Thompson [5] when they demonstrated the diffraction of a stream of electrons. We will touch on the significance of these waves of matter later. In 1926, Schrödinger incorporated these ideas into an equation in which the behavior of a particle could be described by a wave equation [6].

C. The Schrödinger Wave Equation

There is no derivation of the wave equation. It is a postulated relationship which gives logical coherence to most experimental observations. There are some analogies between quantum theory and classical mechanics which can serve as a point of departure for the development of the wave equation. From classical mechanics, the law of energy conservation can be expressed as in Eq. (2)

$$T + V = E \tag{2}$$

where E is the total energy and T and V are kinetic and potential energies, respectively. If we consider a single particle of mass, m, moving along the x-axis in a potential field, V, with a velocity, v, Eq. (2) becomes

$$\tfrac{1}{2}mv^2 + V = E \tag{3}$$

Using the momentum relationship, $p = mv$, Eq. (3) becomes

$$p^2/2m + V = E \tag{4}$$

To convert Eq. (4) into a wave equation, the momentum, p, is replaced by the differential operator

$$p \rightarrow \frac{h}{2\pi i}\frac{d}{dx}$$

where h is Planck's constant and $i = \sqrt{-1}$. Equation (4) thus becomes

$$-\frac{h^2}{8\pi^2 m}\frac{d^2}{dx^2} + V = E \tag{5}$$

The left side of Eq. (5) is an operator requiring an operand. This operand is ψ, the wavefunction. Its inclusion completes the one-dimensional Schrödinger equation in differential form.

$$\left(-\frac{h^2}{8\pi^2 m}\frac{d^2}{dx^2} + V\right)\psi = E\psi$$

The more common form is Eq. (6).

$$\frac{d^2\psi}{dx^2} + \frac{8\pi^2 m}{h^2}(E - V)\psi = 0 \tag{6}$$

In the more usual case, the particle moves in three-dimensional space thus the kinetic energy term is expressed as in Eq. (7),

$$T = \tfrac{1}{2}m(v_x^2 + v_y^2 + v_z^2) = \frac{p_x^2 + p_y^2 + p_z^2}{2m} \tag{7}$$

where the subscripts denote the dimensional components of velocity, v, and momentum, p. Again converting the momentum components into a form suitable for a wave equation

$$p_x \rightarrow \frac{h}{2\pi i}\frac{d}{dx} \qquad p_y \rightarrow \frac{h}{2\pi i}\frac{d}{dy} \qquad p_z \rightarrow \frac{h}{2\pi i}\frac{d}{dz}$$

The wave equation in three dimensions now becomes

$$\frac{d^2\psi}{dx^2} + \frac{d^2\psi}{dy^2} + \frac{d^2\psi}{dz^2} + \frac{8\pi^2 m}{h^2}(E - V)\psi = 0$$

The expression is shortened to Eq. (8) by substituting the Laplacian operator ∇^2 for the partial differentials,

$$\nabla^2\psi + (8\pi^2 m/h^2)(E - V)\psi = 0 \tag{9}$$

ψ is the dependent variable in Eq. (8), being a function of the coordinates of the particle. It represents the amplitude of the particle wave, hence is called the wavefunction. Neither ψ nor its complex conjugate ψ^* (in which the i in ψ is replaced by $-i$) have any physical significance. Only the product $\psi\psi^*$ or $|\psi|^2$ has physical significance. This is interpreted as the probability of finding the particle at some point in space. The greater the wave amplitude, ψ, the greater the probability of finding the particle at that point.

Certain constraints must be met if ψ is to be physically meaningful. It must be single-valued; in other words, it must have only one value at a given point in space. Also the probability of finding the particle in all space must be unity, that is,

$$\int |\psi|^2 \, dx \, dy \, dz = 1$$

The statistical interpretation of ψ^2 emerges from the principle of indeterminancy of Heisenberg. This fundamental concept states that two conjugate quantities cannot be determined exactly for small particles. Thus the position and momentum of an electron cannot be simultaneously known with precision, for in the act of measuring one quantity, we alter the other. Attempts to measure the momentum, p, render the position, x, uncertain. The product of these uncertainties is a multiple of Planck's constant,

$$\Delta x \, \Delta p = h/2\pi$$

A pictorial but less accurate way of viewing the wavefunction ψ is to regard the electron as traveling over a region of the system from which it cannot escape. Over a finite period of time, the electron can be regarded as being "spread out" over this domain in the form of a cloud. Thus $|\psi|^2$ would give the "density" of the charge at any point in this domain. Putting it another way, if the electron could be photographed in its domain, we would see a dot denoting its position. Repeating this process in three dimensions, we would eventually obtain a pattern of dots of varying density throughout the domain of the electron. This would be the charge cloud of the electron.

Of course, the electron cannot be photographed, let alone precisely located; hence, the charge cloud picture is, strictly speaking, inaccurate, although useful. This simplistic view enables us to draw contours of equal values of ψ or ψ^2 and thus to obtain pictorial representations of the domains of electrons associated with atoms. As we shall see later, these domains have a bearing on the effective size of the atom, the stereochemical relationships of atoms in molecules, and other chemical and physical properties.

III. Atomic and Molecular Structure

A. Atomic Orbitals

The concept of the atomic orbital can be developed from a consideration of the simplest atom, hydrogen. The hydrogen-like atom is composed of a single electron with a charge of $-e$, and a nucleus with a charge of $+Ze$ where Z is the atomic number. If the electron and the nucleus are separated by a distance, r, then from Coulomb's law the potential energy of attraction V is

$$V = -Ze^2/r$$

If we adopt the simplifying assumption that because the nucleus is so much heavier than the electron, we can assume it is the center of mass of the atom and is stationary relative to the electron. The Schrödinger equation for the electron then is Eq. (9).

$$\nabla^2\psi + \frac{8\pi^2 m}{h^2}\left(E + \frac{Ze^2}{r}\right)\psi = 0 \tag{9}$$

Since the potential energy of attraction between the nucleus and the electron is spherically symmetrical for some solutions of the wavefunction, it is more convenient for the solution to convert Eq. (9) to polar coordinates. The relationship between Cartesian and polar coordinates is shown in Fig. 1 and the equations are as follows:

$$x = r \sin\theta \cos\phi$$

$$y = r \sin\theta \sin\phi$$

$$z = r \cos\theta$$

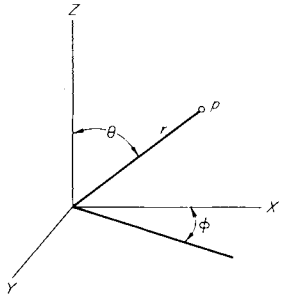

Fig. 1. Relationship between Cartesian and polar coordinates.

It can be shown that solutions of the wave equation [Eq. (9)] involve an angular component, involving θ and ϕ and a radial component involving r. Thus ψ may be expressed as in Eq. (10),

$$\psi = R(r)\Theta(\theta)\Phi(\phi) \tag{10}$$

where R, Θ, and Φ are functions only of r, θ, and ϕ, respectively. Acceptable solutions of the radial term R in Eq. (10) require the use of a constant, n, with an integral value. This constant is the principle quantum number which determines the distance of the most probable location of the electron from the nucleus. Acceptable solutions of the angular components θ and ϕ in Eq. (10) require two new constants with integer values, namely, l and m. These values determine the spatial disposition of the domain of the electron. The constant l is the azimuthal quantum number and the constant m, the magnetic quantum number. The allowed values for n are 1, 2, 3, ..., for l are 0, 1, 2, ... $(n-1)$, and for m are l, $l-1$, $l-2$,...0... $-(l-1)$, $-l$. A fourth quantum number appears when the wave equation is made relativistically satisfactory. This is known as the "spin" quantum number and has the values $s = +1/2$ and $s = -1/2$. The solutions for some of the wavefunctions for hydrogen are given in Table I. Since the probability of finding the electron in all space is 1, solutions of ψ must be normalized, that is multiplied by a constant so that Eq. (11) holds.

$$\int \psi^2 \, d\tau = 1 \tag{11}$$

TABLE I
SOLUTIONS FOR SOME WAVE FUNCTIONS OF THE HYDROGEN ATOM

Quantum numbers				
n	l	m	State	$\psi(r$ in Bohr radii)
1	0	0	1s	$(Z^3/\pi)^{1/2}e^{-Zr}$
2	0	0	2s	$\frac{1}{4}(Z^3/2\pi)^{1/2}(2-Zr)e^{-Zr/2}$
2	1	0	$2p_z$	$\frac{1}{4}(Z^5/2\pi)^{1/2}Ze^{-Zr/2}$
2	1	+1	$2p_x$	$\frac{1}{4}(Z^5/2\pi)^{1/2}e^{-Zr/2}r\sin\theta\cos\phi$
2	1	−1	$2p_y$	$\frac{1}{4}(Z^5/2\pi)^{1/2}e^{-Zr/2}r\sin\theta\sin\phi$
3	0	0	3s	$\frac{1}{81}(Z^3/3\pi)(27-18Zr+2Z^2r^2e^{-Zr/3})$
3	1	0	$3p_z$	$\frac{1}{81}(Z^5/\pi)^{1/2}(6-Zr)Ze^{-Zr/3}$
3	1	+1	$3p_x$	$\frac{1}{81}(2Z^5/\pi)^{1/2}(6-Zr)e^{-Zr/3}r\sin\theta\cos\phi$
3	1	−1	$3p_y$	$\frac{1}{81}(2Z^5/\pi)^{1/2}(6-Zr)e^{-Zr/3}r\sin\theta\sin\phi$

The radial part of the wave equation contains the orbital energy term, E, and the quantum numbers n and l, but not m. Thus the orbital energy is independent of m. In the special case of one-electron atoms like hydrogen, the orbital energy E depends only on n,

$$E = -Z^2e^2/2a_0n^2$$

where a_0 is the radius of the first orbit of hydrogen and replaces the r term in the general equation. This is known as the Bohr radius from Bohr's theory of the hydrogen atom.

$$a_0 = h^2/4\pi^2me^2 = 0.529 \text{ Å}$$

The transition of an electron from an orbital with a principle quantum number $n = 2$ to $n = 1$ should be accompanied by the emission of light of predictable frequency

$$En_2 - En_1 = \frac{Z^2e^2}{2a_0n_2^2} - \frac{Z^2e^2}{2a_0n_1^2} = h\nu = \frac{hc}{\lambda}$$

This is in agreement with experiment.

The orbitals are designated by the numerical values of the principle quantum number, $n = 1, 2, 3, \ldots$, and a letter designating the azimuthal quantum number $l = 0, 1, 2, 3 \equiv s, p, d, f$. The orbital with the lowest energy is the $1s$ where $n = 1$ and $l = 0$. The electron in this orbital is maximally bound in the hydrogen atom. At higher energies, the hydrogen electron can occupy $2s$, $2p$, $3s$, $3p$, $3d$, etc. The electron cannot exist in a $1p$ orbital from the selection rules.

All s-type orbitals are spherically symmetrical, hence the orbitals are a function only of the radius r. Other orbitals are nonspherically symmetrical and their probability distributions describe characteristic shapes. Some of the shapes of the electron domains for various solutions of ψ are shown in Fig. 2.

A more careful analysis of these domain shapes is instructive. It must be remembered that the surfaces shown in Fig. 2 are contours of equal values of ψ in that state. Showing a planar view of the $1s$ orbital through the nucleus (Fig. 3) a series of concentric circles can be used to depict iso-ψ positions. The squared values of ψ yield equiprobable contours.

If we are interested in the most probable location of the electron in, say, the $1s$ orbital, it is necessary to plot the radius, r, versus the radial density or radial probability since the volume elements we are considering increase as a function of r^2. The plot in Fig. 4 shows that this relationship exhibits a maximum value of the probability at $r = a_0$, in precise agreement with Bohr's theory of the hydrogen atom.

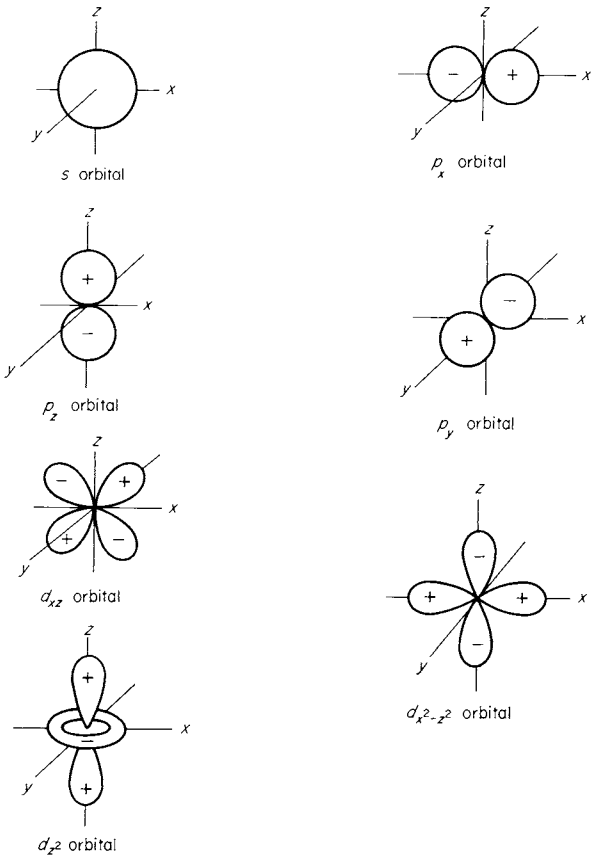

Fig. 2. Domain shapes from solutions of the wave equation.

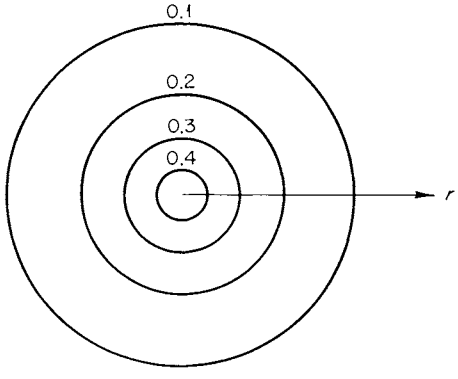

Fig. 3. Planar view of contours of equal ψ value for the 1*s* orbital.

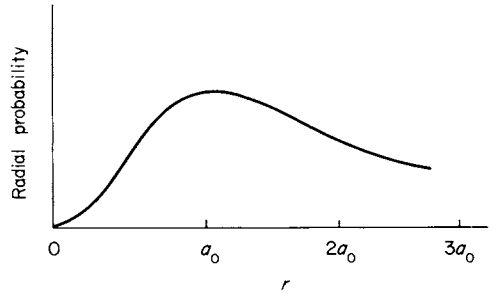

Fig. 4. Radial probability of an electron as a function of distance from the nucleus in a 1*s* orbital.

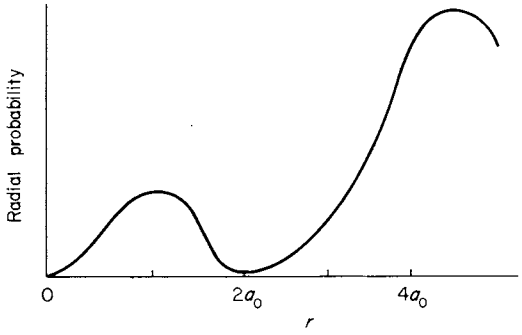

Fig. 5. Radial probability of an electron as a function of distance from the nucleus in a 2*s* orbital.

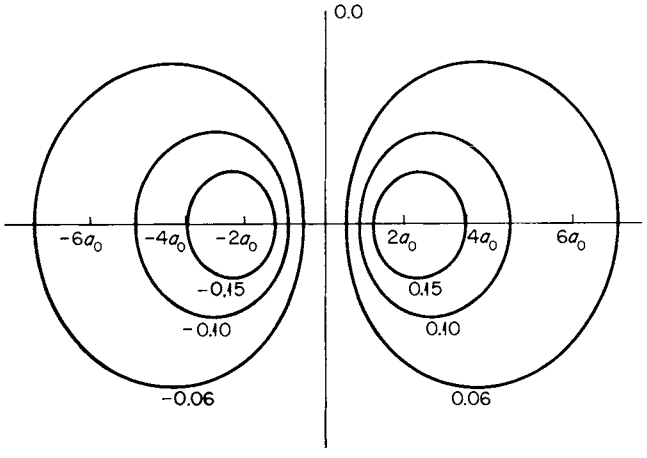

Fig. 6. Planar view of contours of equal ψ value for the 2*p* orbital.

A similar plot for the 2*s* orbital (Fig. 5) indicates that the probability is essentially zero that the electron will be found in a thin spherical region bounded by $r = 2a_0 - \delta$ and $r = 2a_0 + \delta$, where δ is a very small quantity. The wavefunction has a value of zero at $r = 2a_0$ and this is termed a node. The 3*s* state has two such nodes.

A more detailed analysis of the domain of the p orbitals shown in Fig. 2 reveals a directional character to these surfaces. A planar view of the 2*p* orbital is shown in Fig. 6 with contours of equal ψ values of the electron in that state.

The *p* orbitals are oriented along the appropriate Cartesian axes as represented by the sketches in Fig. 2. The three *p* orbitals are of equal energy and are termed degenerate. The two regions of the *p* orbital are designated as being positive and negative in sign and are separated by a region of zero value of ψ or a node. There is no physical significance to the sign. Only ψ^2 has meaning and this, interpreted as a probability, is always positive. The positive and negative regions of the 2*p* and higher asymmetric states is analogous to the two regions of the amplitude of a light wave (Fig. 7a).

The signs of the amplitude are important in light interference phenomena (Fig. 7b, c) and the signs of the orbitals are important in determining whether bonding will occur between two orbitals.

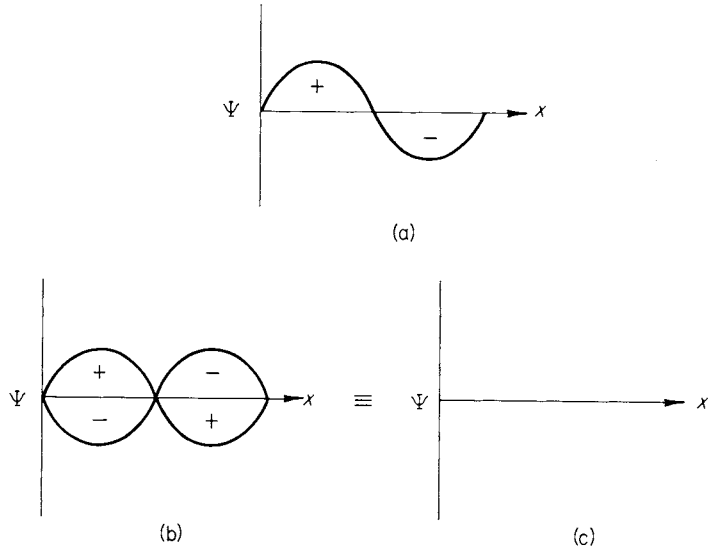

Fig. 7. Consequences of interference of wavefunction (a) by another wavefunction (b) leading to complete cancellation (c).

B. Multielectron Atoms

The atoms above hydrogen in the periodic table are all polyelectronic; therefore, a general approach to the solution of the wave equation for these cases is necessary. The simplest case is the helium atom with two electrons moving around an assumed fixed nuclear charge of $+2e$ at the origin of the axes, as depicted in Fig. 8.

Returning to Eq. (7), the kinetic energy of the two-electron system can be expressed

$$T = T_1 + T_2 = \frac{p_{x_1}^2 + p_{y_1}^2 + p_{z_1}^2 + p_{x_2}^2 + p_{y_2}^2 + p_{z_2}^2}{2m}$$

and the potential energy as

$$V = -\frac{2e^2}{r_1} - \frac{2e^2}{r_2} + \frac{e^2}{r_{12}}$$

Equation (9) now expands to Eq. (12):

$$(\nabla_1^2 + \nabla_2^2)\psi + \frac{8\pi^2 m}{h^2}\left(E + \frac{2e^2}{r_1} + \frac{2e^2}{r_2} - \frac{e^2}{r_{12}}\right)\psi = 0 \tag{12}$$

the wave equation for a two-electron atom. Equation (12) contains a term for the repulsive potential between the two electrons.

$$V_{12} = e^2/r_{12}$$

The potential energy of the system is now dependent on the relative positions of the electrons with respect to each other as well as with respect to the nucleus. The term V_{12} couples the motion of the two electrons in such a way that Eq. (12) cannot be solved in closed analytical form for energies and wavefunctions. Therefore, approximate means of solution must be utilized.

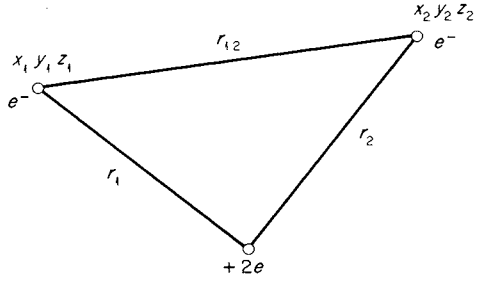

Fig. 8. Helium atom showing relationship between electrons and nucleus.

A method was proposed by Hartree and Fock for reducing the multi-electron Eq. (12) to a sum of single-electron equations, capable of approximate solution [7] [8]. The approach known as the self-consistent field (SCF) method, is to make an initial guess of the wavefunction based upon filled or partly filled shells in accordance with the Aufbau principle. It is then assumed that each electron moves in the potential field of the nucleus and the average potential field of all other electrons in the atom. This assumption then leads to an equation which can be solved numerically for a new improved set of orbitals. A new potential field is then calculated and the process is repeated until the orbitals resulting from two successive cycles are the same to within a small predetermined error.

The wavefunctions resulting from these calculations can be approximated by analytical solutions which are convenient for visualization and use. These approximate wavefunctions, due to Slater, use parameters which give good agreement with the SCF wavefunctions [9]. These are found in Table II. The N terms are normalization factors, i.e., values employed to make the probability ψ^2 over all space, unity. The c is an effective nuclear charge obtained by modifying the atomic number, Z, with a shielding constant, S; $c = Z - S$. The shielding constants are derived from contributions from the environment of the electron.

1. $S = 0$ for all electrons outside of the principal quantum number being considered

2. $S = 0.35$ for each electron with the same principal quantum number. The value $S = 0.30$ is used for consideration of the $1s$ orbital.

3. If the orbital being considered is an s or p, $S = 0.85$ from each electron in the next inner shell, and $S = 1.00$ for each electron further in. It can be shown then that the effective nuclear charges for some commonly considered orbitals are: $C_{(1s)} = 5.70$, $C_{(2p)} = 3.25$, $N_{(2p)} = 3.90$, $O_{(2p)} = 4.55$.

TABLE II
SLATER WAVEFUNCTIONS[a]

n	l	State	ψ
1	0	$1s$	Ne^{-cr}
2	0	$2s$	$Nre^{-cr/2}$
2	1	$2p_x$	$Nxe^{-cr/2}$
3	0	$3s$	$Nr^2e^{-cr/3}$
3	1	$3p_x$	$Nxre^{-cr/3}$

[a] Slater [9].

C. Molecules

The simplest polynuclear, polyelectron molecule is hydrogen (H_2). A consideration of it illustrates the complexities of solution of the wave equation, but at the same time points out how certain reasonable simplifications can be brought in to permit an approximate solution which will be in harmony with experiment. In the hydrogen molecule (Fig. 9) the kinetic energy term T expands in terms of the momentum, p, as shown in Eq. (7).

The potential energy term, V, expands to

$$V = \frac{-e^2}{r_{1A}} + \frac{-e^2}{r_{2A}} + \frac{-e^2}{r_{1B}} + \frac{-e^2}{r_{2B}} + \frac{e^2}{r_{12}} + \frac{e^2}{R_{AB}}$$

The wave equation derived from Eq. (8) becomes

$$(\nabla_1^2 + \nabla_2^2)\psi + \frac{8\pi^2 m}{h^2}\left(E + \frac{e^2}{r_{1A}} + \frac{e^2}{r_{2A}} + \frac{e^2}{r_{1B}} + \frac{e^2}{r_{2B}} - \frac{e^2}{r_{12}} - \frac{e^2}{R_{AB}}\right)\psi = 0$$

The exact solution of this problem is not possible just as in the case for the helium atom, since the potential terms for each electron are dependent on the other electron. We can achieve approximate solutions by assuming that each electron moves in a potential field which is the average of all other electron distributions and nuclei. The Hartree-Fock equations can then, in principle, be solved to obtain a wavefunction for the molecule using the same procedure outlined previously. This has never been done numerically for a molecule, however, because the loss of spherical symmetry creates mathematical problems which thus far have not been overcome.

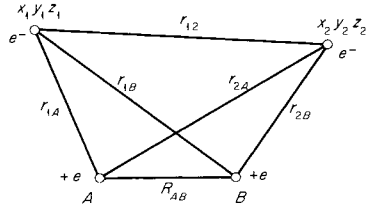

Fig. 9. Hydrogen molecule showing relationship between electrons and nuclei.

IV. Molecular Orbitals

The concept of the SCF treatment of the hydrogen molecule leads to a general approach to the solution of larger molecules. The concept of molecular orbitals (MO) is a natural extension of the treatment of atomic orbitals. It is assumed that the orbitals of electrons in a molecule extend over the entire molecule and are subject to the potentials of all the nuclei and the potentials of the charge distributions of all other electrons. Electrons occupy these MO's according to the same restrictions imposed on electrons in atomic orbitals; i.e., in pairs of electrons with opposed spins. The orbitals are polycentric (over all nuclei). If the MO's, ψ, are normalized so that Eq. (11) holds, then ψ^2 measures the probability of finding the electron at some point in space. This permits us to draw contours of constant probability around the molecule for the electrons and to conceptualize where regions of high and low probability (or charge) are located. For molecules in which a closed-shell structure is found, each MO, ψ, can be thought of as an approximate eigenfunction of a one-electron Hartree-Fock Hamiltonian, F,

$$F\psi = \varepsilon\psi$$

and the value of ε is approximately equal to the negative of the energy necessary to ionize an electron described by ψ from the molecule. The MO for H_2 contains the two electrons, one from each atom, contributing to the bond. We cannot locate either electron precisely; however, a reasonable assumption can be made that when one electron is in the vicinity of one nucleus, say A, then the forces acting on it are approximately those found in a single hydrogen atom, hence the wavefunction for the isolated atom, ψ_a, should be a contributor to the wavefunction for the H_2 molecule. Likewise, if one electron is near nucleus B then ψ_b should approximate that contribution to the MO. If the MO is characterized by contributions from ψ_a and ψ_b, it is reasonable to assume that some combination, a linear combination of atomic orbitals (LCAO approximation) could represent the MO, as expressed in Eq. (13),

$$\psi = C_a\psi_a + C_b\psi_b \tag{13}$$

where the coefficients, C, weight the contributions of the two atomic orbitals.

A general MO for any molecule is expressed by Eq. (14).

$$\psi = C_a\psi_a + C_b\psi_b \ldots C_n\psi_n \tag{14}$$

For the LCAO approximation to be reasonable, we must consider the nature of the atomic orbitals ψ_a and ψ_b to be summed in Eq. (13) to give us the MO. The energies associated with the orbitals ψ_a and ψ_b must be about

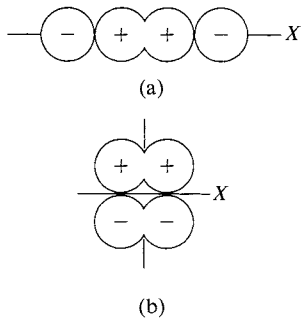

Fig. 10. Schematic illustration of formation of (a) σ bond and (b) π bond between p orbitals.

the same magnitude or Eq. (13) reduces to the wavefunctions of two isolated atomic orbitals and ψ is then not representative of a bond or molecule.

The electron density domains or charge clouds of ψ_a and ψ_b must overlap and the overlapping regions must be of identical sign. Also ψ_a and ψ_b must be suitably oriented for overlap. Thus two p orbitals must be oriented along the same axis to form a σ bond (a) or a π bond (b), as shown in Fig. 10.

Solutions to the wave equation for the molecule must now be sought, specifically for the coefficients to give the charge distribution and for the energies of the MO's. The approach to solution of the coefficients is based on the variation theorem. This theorem states that for a particular MO the best value of the coefficients are those which give the minimum value to the energy, or

$$\frac{\partial E}{\partial C_{i,i=1\cdots n}} = 0$$

The kinetic and potential terms in the Schrödinger equation can be expressed in unspecified form by an unspecified one-electron Hamiltonian, H. It is emphasized that H is not the *true* Hamiltonian operator for the molecule, but should be regarded as an approximation to the *Hartree-Fock* Hamiltonian. The Schrödinger equation [Eq. (8)] thus reduces to Eq. (15),

$$H\psi = E\psi \tag{15}$$

where ψ is a solution for the MO in Eq. (13). Rewriting Eq. (15) we obtain Eq. (16).

$$(H - E)\psi = 0 \tag{16}$$

Expanding Eq. (16) in terms of the atomic orbitals as in Eq. (13), we obtain Eq. (17).

$$C_a(H - E)\psi_a + C_b(H - E)\psi_b = 0 \tag{17}$$

Since only ψ^2 has any meaning, as the probability of finding the electron in a region of space, and since over all space this probability is 1,

$$\int \psi^2 \, d\tau = 1 \tag{18}$$

then it follows that Eq. (17) should be multiplied through by the two wavefunctions for the two atomic orbitals ψ_a and ψ_b and integrated over all space. This results in Eqs. (19) and (20).

$$C_a \int \psi_a(H - E)\psi_a \, d\tau + C_b \int \psi_a(H - E)\psi_b \, d\tau = 0 \tag{19}$$

$$C_a \int \psi_b(H - E)\psi_a \, d\tau + C_b \int \psi_b(H - E)\psi_b \, d\tau = 0 \tag{20}$$

A set of standard notations is used to represent certain of the integrals in these equations. In general terms, these are

$$\alpha_i = \int \psi_i H \psi_i \, d\tau \tag{21}$$

$$\beta_{ij} = \int \psi_i H \psi_j \, d\tau \tag{22}$$

$$S_{ij} = \int \psi_i \psi_j \, d\tau \tag{23}$$

$$E = \int \psi_i E \psi_i \, d\tau \tag{24}$$

Equation (23) is true since we have employed normalized atomic orbitals, i.e., orbitals modified by a constant N so that Eq. (18) obtains.

Equations (19) and (20) now reduce to Eqs. (25) and (26),

$$C_a(\alpha_a - E) + C_b(\beta_{ab} - ES_{ab}) = 0 \tag{25}$$

$$C_a(\beta_{ba} - ES_{ba}) + C_b(\alpha_b - E) = 0 \tag{26}$$

which is a set of equations in two unknowns, the C's and E.

We are interested only in nontrivial solutions, that is solutions other than $C_a = C_b = 0$. Nontrivial solutions will be obtained only if the multipliers of the C's in Eqs. (25) and (26) in determinant form, are zero. The determinant can thus be expressed

$$\begin{vmatrix} \alpha_a - E & \beta_{ab} - ES_{ab} \\ \beta_{ba} - ES_{ba} & \alpha_b - E \end{vmatrix} = 0$$

This determinant, second-degree in E when solved, will give two roots or values of E. The lower value of E when substituted into Eqs. (25) and (26) give solutions for C_a and C_b which are then solutions for Eq. (13). In the two-atom problem we are considering, this solution to Eq. (13) gives the lowest energy MO which is a bonding orbital. From the second root of the determinant, a higher value of E, solution of the coefficient values in Eqs. (25) and (26), and insertion into Eq. (13) gives Eq. (27).

$$\psi = C_a^1 \psi_a - C_b^1 \psi_b \tag{27}$$

This MO expressed by Eq. (27) is of higher energy, is antibonding, and is an approximation to the first excited state MO.

It is evident that this approach to the solution of the wavefunction of the two-atom molecule can now be extended to polyatomic molecules by similar treatment of the general expression in Eq. (14).

References

1. N. Bohr, *Phil. Mag.* **26**(1), 476 (1913).
2. L. de Broglie, *Phil. Mag.* **47**, 446 (1924).
3. L. de Broglie, *Ann. Phys. (Paris)* **3**, 22 (1926).
4. C. J. Davisson and L. H. Germer, *Phys. Rev.* **30**, 705 (1927).
5. G. P. Thompson, *Proc. Roy. Soc., Ser. A* **117**, 600 (1928).
6. E. Shrödinger, *Ann. Phys. (Leipzig)* **79**, 361 (1926).
7. D. R. Hartree, *Proc. Cambridge Phil. Soc.* **24**, 89, 111, 426 (1927).
8. V. Fock, *Z. Phys.* **62**, 795 (1930).
9. J. C. Slater, *Phys. Rev.* **36**, 57 (1930).

Supplemental Reading

C. A. Coulson, "Valence." Oxford Univ. Press, London and New York, 1961.
J. N. Murrell, S. F. A. Kettle, and J. M. Tedder, "Valence Theory." Wiley, New York, 1965.
C. W. N. Cumper, "Wave Mechanics for Chemists." Academic Press, New York, 1966.

Chapter III

MOLECULAR ORBITAL CALCULATIONS

Exact solutions of the wave equation are not within our grasp except for the simplest molecules. It is necessary then to apply approximations, the severity of which depends upon the size of the molecule under study. A graph relates these in a meaningful way in Fig. 1.

Since throughout this book and throughout the domain of interest to the medicinal chemist and pharmacologist we will be speaking of molecules of appreciable size, it is necessary then only to discuss MO methods which can, at the present time, be practically used to treat such molecules.

I. Hückel π-Electron Approximation

A. The π-Electron Approximation

A simplifying feature is present in molecules containing unsaturated bonds between atoms in the first row of the periodic table. Each of these atoms involved in an unsaturated bond contributes usually a single π electron in a p orbital (not directed between adjacent nuclei) to the delocalized system of atoms. The p orbitals forming these π bonds are orthogonal (do not overlap) to other orbitals on the same atom. As a result, the interaction between the π orbital and σ orbitals on the same atom may be regarded as minimal. This leads to the assumption that the σ and π bonds in these molecules may be regarded separately and that an MO treatment of just the π-electron system, if it is entirely planar, gives a reasonable approximation of many properties of the entire molecule. The MO treatment of the simplest

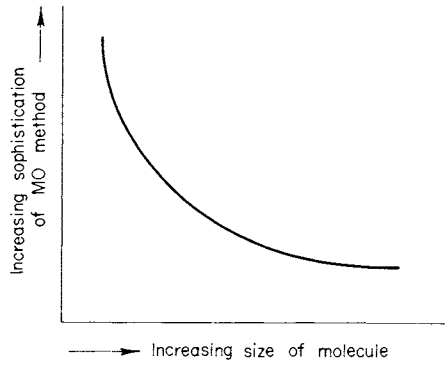

Fig. 1. Relationship between MO method sophistication and their ability to treat molecules of various sizes.

unsaturated molecule, ethylene, using the π-electron approximation, reduces to the same procedure as was illustrated for the hydrogen molecule in the previous chapter.

B. The Hückel Approximations

For ethylene we write down an expression [Eq. (1)] for the MO as a linear combination of π atomic orbitals ϕ_1 and ϕ_2.

$$\psi = C_1\phi_1 + C_2\phi_2 \tag{1}$$

The associated wave equation, $H\psi = E\psi$, now contains an effective Hamiltonian operator, H, which is considered for the π system only and embodies the kinetic and potential energy of one electron in the field of its nucleus and other electrons on the same atom (core). The repulsive and attractive potentials between each electron and neighboring electrons and cores are neglected. This is referred to as a one-electron Hamiltonian operator and is the basis of Hückel molecular orbital (HMO) theory [*1*].

Expanding Eq. (1) in terms of the π orbitals, as shown in Eqs. (15)–(26) in Chapter II, we can write the secular determinant for ethylene

$$\begin{vmatrix} \alpha_1 - E & \beta_{12} - ES_{12} \\ \beta_{21} - ES_{21} & \alpha_2 - E \end{vmatrix} = 0$$

In the Hückel scheme, the terms defined in Eqs. (21)–(23) in Chapter II, and used in the secular determinant above, have special meaning.

The α term [Eq. (21) in Chapter II] is called the Coulomb integral. It is probably best to regard these Coulomb integrals as an empirical property of the atoms and not attempt to attach physical significance to them. It is commonly assumed that this is the energy necessary to remove the electron

from the orbital. Since the π system in ethylene is made up of identical cores (a carbon nucleus and the remaining electrons), all α's are assumed equal.

The β term [Eq. (22) in Chapter II] is called the resonance integral. It represents the energy of interaction of two atomic orbitals, ϕ_1 and ϕ_2 in the ethylene case. Since the energy depends on the distance between the two orbitals, the energies of π orbitals of atoms not bonded by σ bonds should be small. This energy is usually neglected, hence $\beta_{ij} = 0$ where i and j are not formally bonded. Where i and j are bonded, as in the ethylene case, the β values are considered to be equal for all identical atoms.

The S term [Eq. (23) in Chapter II] is called the overlap integral. If the orbitals are normalized then $S_{ii} = 1$. For large distances between two orbitals, $S_{ij} = 0$. If atoms i and j are σ-bonded, a simplifying assumption is made that $S_{ij} = 0$. This is the zero differential overlap (ZDO) approximation.

Using these approximations, the matrix for ethylene reduces to

$$\begin{vmatrix} \alpha_1 - E & \beta_{12} \\ \beta_{21} & \alpha_2 - E \end{vmatrix} = 0$$

Note that the main diagonal terms of the matrix contain the Coulomb integrals and the energies (eigenvalues). The off-diagonal terms are the resonance integrals. The matrix is symmetrical around the main diagonal.

1. *Solution of Energy Values*

The determinant can be reduced to a more manageable form by dividing each term by β and setting $X = \alpha - E/\beta$. The determinant becomes

$$\begin{vmatrix} X & 1 \\ 1 & X \end{vmatrix} = 0$$

The solution of this second-order determinant is a second-order polynomial, $X^2 - 1 = 0$. There are two roots to this equation, $X = 1$ and $X = -1$, hence $E = \alpha + \beta$ and $E = \alpha - \beta$. Since both α and β are negative energy quantities, it follows that the two π electrons possess the lowest energy, $E = \alpha + \beta$, for $X = -1$. Using an energy level diagram (Fig. 2) the ethylene π-electron occupancy can be illustrated. The zero of energy is taken as α, and the lower energy level, $\alpha + \beta$, is filled according to aufbau principles with electrons of paired spins.

The total energy of the two π electrons is $E = 2(\alpha + \beta)$. The energy of two π electrons on isolated $2p$ carbon orbitals is 2α; therefore, the π-bond energy is 2β. The $\alpha + \beta$ energy level is associated with the lowest energy MO, ψ_{I}, in the π-electron approximation. The higher energy level $\alpha - \beta$ is associated with the highest energy MO, ψ_{II}. The latter is unoccupied and is called a virtual orbital which is antibonding.

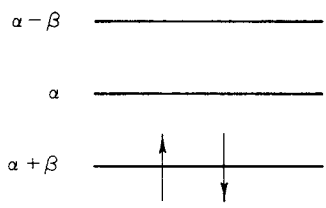

Fig. 2. Occupancy of ethylene Hückel π-electron energy levels.

The value of β is not stated since the Hamiltonian is undefined. Expressing the energies in terms of some standard β, it is possible to compare series of molecules in a relative way. Approximations to the value of β can be obtained by analyses of experimental data on a series of molecules, but it will be found that these values of β vary with the experimental data and the series. A more thorough consideration of properties related to the energies of eigenvalues of the MO equations will be found in the next chapter.

2. *Solution of Coefficients*

It is now necessary to use the energy terms from the solution of the determinant to solve for the coefficients corresponding to each energy value. We can rewrite the secular equations [Eqs. (25) and (26) in Chapter II] using $X = \alpha - E/\beta$ and obtain Eqs. (2) and (3).

$$C_1X + C_2 = 0 \tag{2}$$

$$C_1 + C_2X = 0 \tag{3}$$

The lowest determinants root, $X = -1$, is first used to solve for the C's. Equations (2) and (3) reduce to

$$C_1 = C_2$$

From the normalizing of the orbitals, we know that

$$C_1^2 + C_2^2 = 1$$

hence

$$C_1 = C_2 = 1/\sqrt{2}$$

The lowest energy MO, ψ_1, for the ethylene π electrons is then

$$\psi_{\mathrm{I}} = (1/\sqrt{2})\phi_1 + (1/\sqrt{2})\phi_2$$

For the next highest energy level, $X = 1$, or $E = \alpha - \beta$ it can be shown that

$$\psi_{\mathrm{II}} = (1/\sqrt{2})\phi_1 - (1/\sqrt{2})\phi_2$$

We can now describe the contributions from each atomic orbital to the

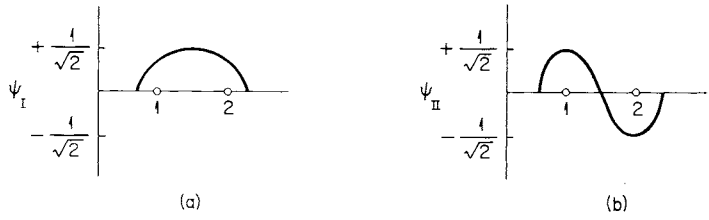

Fig. 3. MO wavefunctions for the ethylene π system (a) bonding MO, (b) antibonding MO.

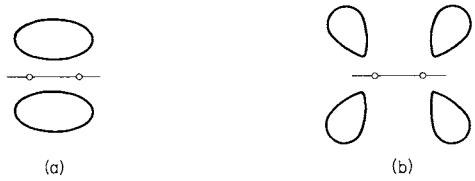

Fig. 4. ψ Contours for the π electrons of ethylene (a) bonding MO, (b) antibonding MO.

total MO in each energy state by plotting the coefficient value along the electron chain. The lowest energy MO, ψ_I, is bonding (Fig. 3a) since adjacent electrons have the same sign. The next highest MO, ψ_{II}, is antibonding (Fig. 3b).

Note that in Fig. 3b the value of ψ between the nuclei vanishes at a node.

Plotting the ψ contours gives another picture of the two π electrons in the bonding (Fig. 4a) and antibonding (Fig. 4b) energy levels.

The nonoverlapping, hence antibonding, nature of the orbitals, is evident in Fig. 4b.

C. Hückel π-Electron Treatment of Larger Molecules

The butadiene molecule is typical of the more complex molecules to be considered in future chapters. First, we write down the π-electron skeleton and number it in any manner.

$$C_1 = C_2 - C_3 = C_4$$

From the LCAO equation,

$$\psi = C_1\phi_1 + C_2\phi_2 + C_3\phi_3 + C_4\phi_4 \tag{4}$$

we can write the polynomial equations directly in determinant form

$$\begin{vmatrix} \alpha_1 - E & \beta_{12} & 0 & 0 \\ \beta_{21} & \alpha_2 - E & \beta_{23} & 0 \\ 0 & \beta_{32} & \alpha_3 - E & \beta_{34} \\ 0 & 0 & \beta_{43} & \alpha_4 - E \end{vmatrix} = 0$$

The subscripts denote the Coulomb integrals for the appropriate atoms and resonance integrals for the appropriate bonds. In the butadiene molecule as in other conjugated molecules, the π electrons are considered delocalized over the entire system despite the fact that a single bond is conventionally written for the C-2 to C-3 bond. Insight into the nature of these bonds emerges from the calculations.

We can simplify the butadiene determinant using the $X = \alpha - E/\beta$ relationship described for the ethylene solution.

$$\begin{vmatrix} X & 1 & 0 & 0 \\ 1 & X & 1 & 0 \\ 0 & 1 & X & 1 \\ 0 & 0 & 1 & X \end{vmatrix} = 0$$

Expansion of this secular determinant gives the fourth-order polynomial

$$X^4 - 3X^2 + 1 = 0$$

Solutions to this are

$$X = \pm 1.62 \qquad X = \pm 0.62$$

At this juncture, it should be pointed out that these determinants can be solved by hand calculation; however, it is tedious and certainly subject to error. The ready access to most scientists of high-speed digital computers and suitable programs, makes these computations easy, fast, and without arithmetic error.

The energy values can be illustrated for the π system of butadiene in an energy level diagram (Fig. 5).

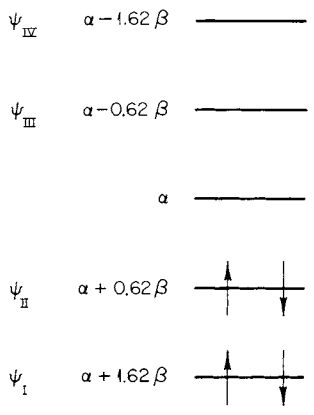

Fig. 5. Hückel π-electron energy levels for butadiene.

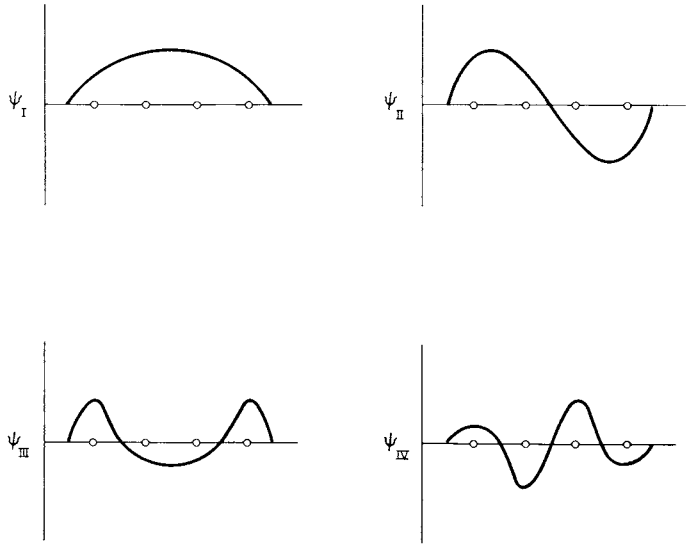

Fig. 6. MO wavefunctions for the π electrons of butadiene.

The lowest energy levels are filled with two electrons each, of opposite spin. The MO's represented by ψ_I and ψ_{II} are bonding orbitals, whereas ψ_{III} and ψ_{IV} are antibonding orbitals. The total π energy for butadiene is $4\alpha + 4.472\beta$.

Solution of the coefficients for each MO and insertion into Eq. (4) gives the following equations.

$$\psi_I \text{ for } E = \alpha + 1.62\beta, \quad \psi_I = 0.37\phi_1 + 0.60\phi_2 + 0.60\phi_3 + 0.37\phi_4$$

$$\psi_{II} \text{ for } E = \alpha + 0.62\beta, \quad \psi_{II} = 0.60\phi_1 + 0.37\phi_2 - 0.37\phi_3 - 0.60\phi_4$$

$$\psi_{III} \text{ for } E = \alpha - 0.62\beta, \quad \psi_{III} = 0.60\phi_1 - 0.37\phi_2 - 0.37\phi_3 + 0.60\phi_4$$

$$\psi_{IV} \text{ for } E = \alpha - 1.62\beta, \quad \psi_{IV} = 0.37\phi_1 - 0.60\phi_2 + 0.60\phi_3 - 0.37\phi_4$$

We can now describe the contributions of each atomic orbital to the total MO in each energy state, by plotting the coefficient value along the chain in butadiene (Fig. 6).

Plotting the ψ contours gives another concept of the electron domains for each MO (Fig. 7).

From these two illustrations, the general picture of the π-electron distribution in butadiene can be obtained. In the lowest energy MO, ψ_I, in Fig. 7, the electron domains for each atomic orbital coalesce into a single distribution cloud, hence the π-bonding encompasses all of the atomic cores in the molecule. There are then three π bonds in this MO. In the next highest energy MO, ψ_{II}, there is π-bonding between atom cores 1 and 2 and also

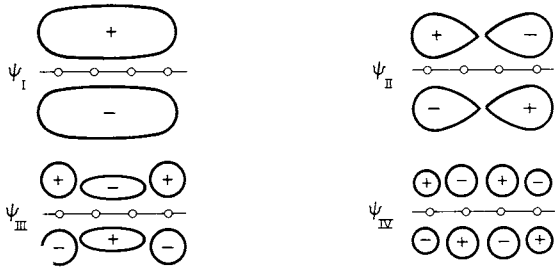

Fig. 7. ψ Contours for the π electrons of butadiene.

3 and 4. The situation between atoms 2 and 3 is reminiscent of the second energy level MO of ethylene. There is a change of sign between the ψ lobes, hence in ψ_{II} atom cores 2 and 3 are antibonding. With two bonds and one antibond in ψ_{II}, the net effect is still a bonding situation for ψ_{II}. In ψ_{III}, there are two antibonds, atom cores 1 and 2 and also 3 and 4. There is only one bonding condition, hence ψ_{III} is net antibonding. Finally ψ_{IV}, the highest energy MO, has three antibonds.

Energy level α, on the energy level diagram (Fig. 5), is the energy of the isolated atoms in the molecules. This is taken as the zero of energy. It is obvious from the diagram then that the two net antibonding MO's, ψ_{III} and ψ_{IV}, are less favored energetically than the isolated atoms. For electrons to occupy these MO's, energy must be put into the molecule in the form of light. Occupancy of these higher energy MO's then is a transient situation, since the electrons return to lower lying orbitals when the source of energy input is removed. These are then spectroscopic states and the promotion to and return from these higher energy MO's determine the spectroscopic properties of molecules.

A general approach to the approximate solution of π-electron properties of large conjugated hydrocarbons is now at hand. As a further illustration, consider the benzene molecule.

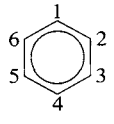

The π skeleton is written and numbered in a convenient manner. The simplified secular determinant can now be written directly.

$$\begin{vmatrix} X & 1 & 0 & 0 & 0 & 1 \\ 1 & X & 1 & 0 & 0 & 0 \\ 0 & 1 & X & 1 & 0 & 0 \\ 0 & 0 & 1 & X & 1 & 0 \\ 0 & 0 & 0 & 1 & X & 1 \\ 1 & 0 & 0 & 0 & 1 & X \end{vmatrix} = 0$$

Note that atom 1 is bonded to atoms 2 and 6, hence this is reflected in the determinant off-diagonal terms in the first row, columns 2 and 6, and the sixth row, columns 1 and 5.

Solution of the benzene determinant gives a sixth-order equation

$$X^6 - 6X^4 + 9X^2 - 4 = 0$$

The solution gives six roots:

$$X = 2, 1, 1, -1, -1, -2$$

The energy values can be described as in Fig. 8. Four of the roots occur in pairs of identical values, hence two of the energy levels are equivalent or degenerate. Orbital occupancy is assigned according to the aufbau principle. The total π energy is seen to be $6\alpha + 8\beta$.

Determination of the coefficients gives the following equations for the MO's of benzene

$$E = \alpha + 2\beta \qquad \psi_{\mathrm{I}} = \frac{1}{6^{1/2}}(\phi_1 + \phi_2 + \phi_3 + \phi_4 + \phi_5 + \phi_6)$$

$$E = \alpha + \beta \qquad \psi_{\mathrm{II}} = \frac{1}{12^{1/2}}(2\phi_1 + \phi_2 - \phi_3 - 2\phi_4 - \phi_5 + \phi_6)$$

$$E = \alpha + \beta \qquad \psi_{\mathrm{III}} = \frac{1}{4^{1/2}}(\phi_2 + \phi_3 - \phi_5 - \phi_6)$$

$$E = \alpha - \beta \qquad \psi_{\mathrm{IV}} = \frac{1}{4^{1/2}}(\phi_2 - \phi_3 + \phi_5 - \phi_6)$$

$$E = \alpha - \beta \qquad \psi_{\mathrm{V}} = \frac{1}{12^{1/2}}(2\phi_1 - \phi_2 - \phi_3 + 2\phi_4 - \phi_5 - \phi_6)$$

$$E = \alpha - 2\beta \qquad \psi_{\mathrm{IV}} = \frac{1}{6^{1/2}}(\phi_1 - \phi_2 + \phi_3 - \phi_4 + \phi_5 - \phi_6)$$

From the signs of the coefficient it can be seen that the lowest energy MO, ψ_{I}, is bonding between six centers. Orbital ψ_{II} is bonding between four pairs of atoms, while orbital ψ_{III} is bonding between two pairs of atoms. In ψ_{III} the coefficients of atomic orbitals ϕ_1 and ϕ_4 are zero. These atoms are then at nodes and do not participate in the π-bonding for that MO.

D. Treatment of Heteroatoms

Most molecules of biological significance contain heteroatoms, particularly nitrogen and oxygen. These two atoms, being in the first row of the periodic table along with carbon, can form π-electron bonds, hence may be

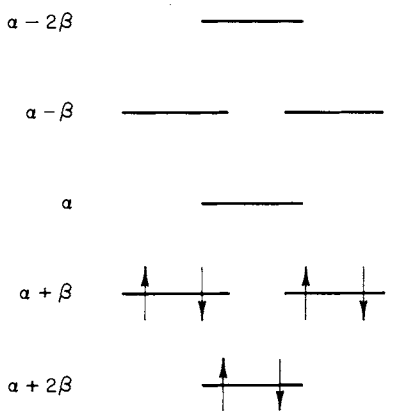

Fig. 8. Hückel π-electron energy levels for benzene.

involved in conjugated systems. Because of the difference in electronic structure among these atoms, it is obvious that the standard Coulomb integral, α, and resonance integral, β, adopted for a carbon π electron must be modified.

The Coulomb integral is a measure of the attraction between a π electron and its atomic core, in HMO theory. With an increasing attraction for the electron, there is a corresponding increase in the absolute value of the Coulomb integral. This attraction is reflected by the electronegativity, χ, of atoms. Since

$$\chi_O > \chi_N > \chi_C$$

this same ordering should prevail for the Coulomb integral. Wheland and Pauling approached this problem by retaining the standard π electron α for carbon and modifying this value with some value of β, the resonance integral [*2*] [Eq. (5)]. For nitrogen, Eq. (5) is expressed as

$$\alpha_N = \alpha_C + h_N\beta \tag{5}$$

The parameter, h, must be determined for the heteroatoms.

Oxygen and nitrogen π electrons can participate in conjugated molecules in two ways. In the case of the nitrogen atom in the pyridine molecule, the valence electrons are distributed in $tr^2trtr\,\pi$ orbitals, hence the core charge is $+1$. In the case of pyrrole, the electrons are distributed in $trtrtr\,\pi^2$ orbitals, hence the core charge is $+2$. The electronegativity of the pyrrole nitrogen should be greater than a pyridine nitrogen, hence it would be expected that $h_{\dot{N}} > h_{\dot{N}}$ in Eq. (5). The same situation holds for the oxygen

atom in a carbonyl group, $tr^2tr^2tr\,\pi$, and in an ether or hydroxyl group, $tr^2trtr\,\pi^2$, so that $h_{\ddot{O}} > h_{\dot{O}}$ in Eq. (5) would be expected.

Bonds involving heteroatoms could not be expected to use the same standard resonance integral, β, but must be suitably modified to reflect the difference in the electronegativity of the two atoms in the bond. Wheland and Pauling have adopted a modifying parameter to reflect these differences [2]. Thus for a C—N bond

$$\beta_{C-\dot{N}} = k_{C-\dot{N}}\beta_{CC}$$

where the value of k_{C-N} is the modifier of the standard β value.

A variety of methods and theories have been applied to select suitable heteroatom parameter values. Parameter sets vary depending on whether energy or coefficient-related properties are being studied. Some proposed sets are shown in Table I which are proposed to be consistent within themselves in reproducing some molecular properties.

Using Streitwieser's parameters [3] for the calculation of pyridine, the secular determinant is written

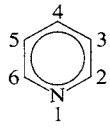

$$\begin{vmatrix} X+0.5 & 1 & 0 & 0 & 0 & 1 \\ 1 & X & 1 & 0 & 0 & 0 \\ 0 & 1 & X & 1 & 0 & 0 \\ 0 & 0 & 1 & X & 1 & 0 \\ 0 & 0 & 0 & 1 & X & 1 \\ 1 & 0 & 0 & 0 & 1 & X \end{vmatrix} = 0$$

and is solved for the energies and coefficients in the usual way. The energy levels are illustrated in Fig. 9.

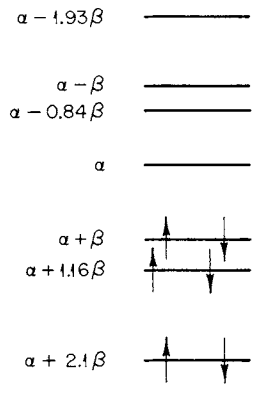

Fig. 9. Hückel π-electron energy levels for pyridine.

Note that pyridine no longer possesses the degenerate orbitals found in benzene. The total π energy is calculated to be $6\alpha + 8.55\beta$. Solution of the coefficient values gives, for the three occupied MO's

$$\psi_{\mathrm{I}} = 0.52\phi_1 + 0.42\phi_2 + 0.36\phi_3 + 0.34\phi_4 + 0.36\phi_5 + 0.42\phi_6$$

$$\psi_{\mathrm{II}} = -0.57\phi_1 - 0.19\phi_2 + 0.35\phi_3 + 0.50\phi_4 + 0.35\phi_5 - 0.19\phi_6$$

$$\psi_{\mathrm{III}} = -0.50\phi_2 - 0.50\phi_3 + 0.50\phi_5 + 0.50\phi_6$$

In molecules such as aniline and phenol, the atoms in the heteroatom-containing group NH_2 or OH are usually considered collectively as extending the conjugation, and the parameters shown in Table I for these groups are utilized. These groups are treated as though they contributed two electrons to the π system. As an example, the secular determinant for phenol, using Pullman's parameters [*4*] can be written

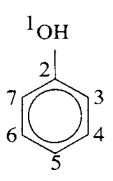

$$\begin{vmatrix} X+2.0 & 0.9 & 0 & 0 & 0 & 0 & 0 \\ 0.9 & X & 1 & 0 & 0 & 0 & 1 \\ 0 & 1 & X & 1 & 0 & 0 & 0 \\ 0 & 0 & 1 & X & 1 & 0 & 0 \\ 0 & 0 & 0 & 1 & X & 1 & 0 \\ 0 & 0 & 0 & 0 & 1 & X & 0 \\ 0 & 1 & 0 & 0 & 0 & 1 & X \end{vmatrix} = 0$$

Note that there are three off-diagonal resonance integrals written for atom 2 since it is π-bonded to three other atoms. Note also, that the matrix is symmetrical about the main diagonal Coulomb integral terms. Thus the supradiagonal elements of the matrix completely describe the matrix. Advantage of this simplification is taken in introducing data for computer calculations.

A quaternary atom such as a protonated pyridine molecule or the anilinium ion can be calculated by recognizing that, although the π electron is not involved in the new bond, it is now present in a potential field of the core, made more electronegative by the sharing of the lone-pair electrons with another atom. This should alter the Coulomb integral, hence the h parameter in Eq. (5) would be higher for these atoms.

A methyl group bonded to a conjugated system is known to have a modest effect on the π-electron system, although a π bond of the conventional form cannot be written. There are three ways that the methyl group effect can be introduced into π-electron calculations.

The methyl group can be regarded as a heteroatom group similar to NH_2 and OH, in which two "π-like" electrons are considered available to the delocalized π system [*5*, *6*]. Since these are conceded to weakly interact with the π system, a large Coulomb integral is used to reflect this. Similarly,

the low values of the resonance integral reflects this weak interaction. Values for the heteroatom model of the methyl group are found in Table I.

A second way of considering the methyl group influence is to regard its effect on the attached atom of the π system as strictly an inductive effect through the π electrons [2]. This electron enrichment of the bonded carbon core should result in a modest lowering of the core electronegativity. This in turn would be reflected by a modest lowering of the Coulomb integral for the attached carbon of the π system. Thus the parameter, h, in Eq. (5), for this carbon would have a modest negative value (see Table I).

The third model, known as the conjugation molecule, envisages the three hydrogen atoms functioning like a pseudoatom with a π orbital which can extend the conjugation of the system to which it is attached [7].

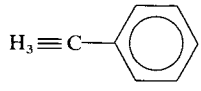

Thus toluene, in this model, is treated by assigning a Coulomb integral value to the H_3 pseudoatom and a resonance integral to the $H_3{\equiv}C$ bond (Table I).

A consideration of other heteroatom parameters and group parameters will be deferred until examples arise requiring their consideration. The basic concepts outlined here prevail in their selection.

TABLE I
SIMPLE HÜCKEL MO PARAMETERS FOR HETEROATOMS

Streitwieser values[a]		Pullman values[b]	
h	k	h	k
$\dot{N} = 0.5$	$C—\dot{N} = 1.0$	$\dot{N} = 0.4$	$C—\dot{N} = 1.0$
$\ddot{N} = 1.5$	$C—\ddot{N} = 0.8$	$\ddot{N} = 1.0$	$C—\ddot{N} = 0.9$
$\dot{O} = 1.0$	$C—\dot{O} = 1.0$	$\dot{O} = 1.2$	$C—\dot{O} = 2.0$
$\ddot{O} = 2.0$	$C—\ddot{O} = 0.8$	$\ddot{O} = 2.0$	$C—\ddot{O} = 0.9$
$\dot{N}^{\oplus} = 2.0$	$C—\dot{N}^{\oplus} = 1.0$	$\dot{N}^{\oplus} = 2.0$	$C—\dot{N}^{\oplus} = 1.0$
$\dot{C}H_3 = 2.0$[c]	$C—\dot{C}H_3 = 0.7$[c]	$\dot{C}_\alpha = -0.1$[d]	$C_\alpha—C = 0.7$[d]
$\dot{C}_\alpha = -0.1$[d]	$C_\alpha—\dot{C} = 0.8$[d]	$—\dot{C}{\equiv} = 2.0$[d]	$C{\equiv}H_3 = 2.0$[d]
${\equiv}H_3 = -0.5$[d]	$C{\equiv}H_3 = 3.0$[d]		

[a] Streitwieser [3].
[b] Pullman [4].
[c] Parameters for heteroatom model of methyl group.
[d] Parameters for conjugative model of methyl group $C_\alpha—C{\equiv}H_3$.

E. Delocalization Energy

The total π energy calculated for butadiene was found to be $4\alpha + 4.472\beta$. If we regarded butadiene as two ethylene molecules with no delocalization of π electrons across bond 2 and 3, then the total π energy would be $2(2\alpha + 2\beta)$ or $4\alpha + 4\beta$. Thus the energy gained by delocalizing the π system along the entire molecule is 0.472β. This is called the delocalization energy, E_D. Similarly the E_D for benzene can be seen to be 2β over the localized cyclohexatriene model. Generally, the delocalization energy can be defined as the calculated additional bonding energy resulting from delocalized electrons, in reference to isolated double bonds. With suitable restrictions, the delocalization energies can be correlated with experimental resonance energies. The delocalization energies are useful in predicting relative equilibrium constants. This will be discussed in more detail in the next chapter.

F. Electron Densities

The probability of finding any electron in a small volume element, $d\tau$, has been shown to be $|\psi|^2 d\tau$. In the LCAO-Hückel approximation, the wavefunction, ϕ_i, for each atomic orbital in any MO has been assumed to be the same and its contribution to a MO wavefunction, ψ, is weighted by a constant, C_i. The probability of finding the electron in the region of space associated with atomic orbital ϕ_i is then C_i^2. The probability can be expressed in terms of a fractional charge or electron density, q, at atom r based upon our charge cloud concept of electron distribution in its domain. Since there are two electrons in a filled MO, the electron density at atom r in the ith MO is $q_r^i = 2C_r^2$. The total density at atom r is then a sum of the electron densities at atom r for all occupied MO's.

$$q_r = \sum_{i\,\mathrm{oc}} 2C_{ir}^2$$

In butadiene, ψ_{I} and ψ_{II} are the occupied MO's. The π-electron density at atom 1, for example, is $q_1 = 2(0.37)^2 + 2(0.60)^2 = 1$. For atom 4, $q = 2(0.37)^2 + 2(-0.60)^2 = 1$. Similarly $q_2 = q_3 = 1$.

For pyridine, using the calculations previously described, the nitrogen π-electron density, $q_N = 2(0.52)^2 + 2(-0.57)^2 + 2(0.00)^2 = 1.19$. For the

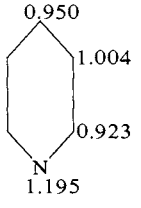

Fig. 10. Hückel-calculated pyridine π-electron densities.

entire pyridine molecule, the π-electron densities from these calculations are shown in Fig. 10.

Another way of expressing the charge is to state the net charge on an atom relative to the number of electrons contributed to the π system at each atom. This is the charge density, Q_r, which is

$$Q_r = N - q_r$$

where N is the number of π electrons contributed by the atom r. This value of N is the same numerically as the core charge. A useful check on calculations of these values is the knowledge that the sum of all q values should equal the number of π electrons in the system and the sum of all Q values should be zero.

The charge densities are a calculated index of certain properties of the molecule which will be discussed in the next chapter.

G. Bond Order

The concept of the partial mobile bond order, p_{rs}, or simply the bond order was introduced by Coulson in 1939 [8]. The bond order in any MO between atoms r and s is

$$p_{rs}^{i} = C_{ir}C_{is}$$

therefore, the bond order between two atoms as a result of the contribution from all occupied MO's is

$$p_{rs} = \sum_{i\,\mathrm{occ}} 2C_{ir}C_{is}$$

This quantity is associated with the binding power of a π bond. Adjacent atoms with large coefficients of like sign are strongly π-bonded. When the signs of the coefficients change between atoms, the bond order is negative, typical of a node at a nonbonding site.

Calculations of p_{12} and p_{23} for butadiene give

$$p_{12} = 2(0.37)(0.60) + 2(0.60)(0.37) = 0.89$$

$$p_{23} = 2(0.60)(0.60) + 2(0.37)(-0.37) = 0.45$$

It is evident from these values that the 1–2 and 3–4 bonds in butadiene have significant π bond strength, whereas the 2–3 bond is appreciably weaker in π-bonding strength. This is consistent with the usual way of writing the molecule.

$$CH_2{=}CH{-}CH{=}CH_2$$

Another way of looking at the bond order is to regard a pure single bond as having a bond order of 1, a pure double bond as having a bond order of 2, and a pure triple bond as having a bond order of 3. The 1–2 bond in butadiene has a π bond order of 0.89, to which is added 1 for the σ bond to give a total bond order of 1.89. This is clearly closer to 2 than 1, hence this bond more closely resembles a pure double bond than does say the 2–3 butadiene bond.

It is reasonable to suppose that there should be some relationship between bond order and bond length. A further discussion of this will be undertaken in the next chapter.

Coulson and Longuet-Higgins have derived a relationship between the total π-electron energy and the electron densities and bond orders [*9*].

$$E_\pi = \sum_r q_r\alpha + 2\sum_{r<s}\sum p_{rs}\beta_{rs}$$

H. Free Valence

The concept of free valence, F, was proposed by Coulson as being a residual bonding affinity of a π electron on an atom [*10*]. It is the difference between the maximum bond orders around an atom, N_{max}, and the calculated bond orders around that atom, N_r

$$F = N_{max} - N_r$$

The maximum bond order around an atom is taken to be $3 + \sqrt{3}$ which is derived from the central atom of trimethylenemethane

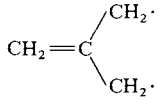

although the middle atom of propargylene can be shown to have a larger bond order [*11*]. The free valence is an index of reactivity at an atom, a higher numerical value predicting greater susceptibility, in selected cases. This will be dealt with in the next chapter.

II. Modified π-Electron Hückel Methods

A. Inclusion of Overlap

In the simple Hückel scheme thus far described, the overlap term S_{ij} was taken to be zero. Actually overlap between neighboring atoms is not zero but can be large, i.e., $S = 0.25$ between benzene carbon π orbitals. Retention of an overlap term between bonded atoms in butadiene results in a matrix

$$\begin{vmatrix} \alpha - E & \beta - SE & 0 & 0 \\ \beta - SE & \alpha - E & \beta - SE & 0 \\ 0 & \beta - SE & \alpha - E & \beta - SE \\ 0 & 0 & \beta - SE & \alpha - E \end{vmatrix} = 0$$

It is assumed that $S_{12} = S_{23}$ though these bonds differ in length. The solution of this determinant can be simplified by introducing the parameter $\gamma = \beta - S\alpha$ which makes the off-diagonal terms $\gamma + S(\alpha - E)$. If we divide all terms by γ and let $X = \alpha - E/\gamma$ the matrix reduces to

$$\begin{vmatrix} X & 1 + SX & 0 & 0 \\ 1 + SX & X & 1 + SX & 0 \\ 0 & 1 + SX & X & 1 + SX \\ 0 & 0 & 1 + SX & X \end{vmatrix} = 0$$

If we let $b = 1 + SX$, the solution of the matrix is in terms of b. Using $S = 0.25$ for all overlap integrals, the energies of the occupied orbitals of butadiene become $E_1 = \alpha + 1.152\gamma$ and $E_2 = \alpha + 0.535\gamma$. When overlap is included, the pairing property of bonding and antibonding orbital energies, $\alpha + m\beta$ and $\alpha - m\beta$ is destroyed.

Calculation of coefficients reveals that the inclusion of overlap integrals does not change the ratio of atomic orbital coefficients of a given MO since they are multiplied by the same factor. Thus in conjugated hydrocarbons, the inclusion of overlap integrals does not change the charge densities or bond orders, thereby supplying some justification for the neglect of overlap in the usual Hückel treatment. This would not be expected to be true in the case of heteroatom molecules since the same α and S values would not be used throughout. In general, the refinement of the inclusion of overlap is seldom used, since it appears to be an oversophistication of a simple MO method and because the HMO method apparently works well in many situations without it.

B. An Iterative Hückel Technique

In the simple Hückel calculations, the values of the Coulomb integrals, α, for each π electron were assumed identical. It is apparent that if the charges on each atom are not the same, then the values of α cannot really be the same. In the case of an atom with a $q > 1$, the core charge is more effectively neutralized and the attraction of the core for any π electron is reduced. This should result in a less negative value of α. Conversely, if $q < 1$, the α should be more negative. Wheland and Mann suggested that α could be related to the charge by

$$\alpha_i = \alpha_0 + (1 - q_i)\omega\beta_0$$

where α_0 and β_0 are initial parameters and ω is a dimensionless parameter chosen to fit experimental data [*12*]. In essence, this iterative procedure introduces some recognition of electron repulsion into the calculations. Streitwieser has studied this technique and suggested a value $\omega = 1.4$.

The calculations begin in the usual Hückel framework using α_0 and β_0 parameters. A series of charges thus calculated are used to calculate a new set of α_i values. The calculations are iterated to a constant value of the charges. The application to heteroatom molecules requires the use of different parameters than for the simple Hückel scheme. Some of these sets of parameters are shown in Table II.

A further modification of the simple Hückel method involves the variation of the β parameter as a function of the calculated bond order. A relationship commonly used is

$$\beta_{ij} = (1 + 0.5p_{ij})\beta_0$$

TABLE II
OMEGA HÜCKEL MO PARAMETERS[a]

Streitwieser values[b]		Kier-Roche values[c]	
h	*k*	*h*	*k*
$\dot{N} = 0.3$	$C—\dot{N} = 0.8$	$\dot{N} = 0.8$	$C—\dot{N} = 1.0$
$\ddot{N} = 1.7$	$C—\ddot{N} = 0.7$	$\ddot{N} = 1.7$	$C—\ddot{N} = 0.7$
$\dot{O} = 1.3$	$C—\dot{O} = 0.8$	$\dot{O} = 1.3$	$C—\dot{O} = 0.8$
$\ddot{O} = 2.7$	$C—\ddot{O} = 0.6$	$\ddot{O} = 2.7$	$C—\ddot{O} = 0.6$
$\ddot{Cl} = 2.8$	$C—\ddot{Cl} = 0.37$	$\ddot{Cl} = 2.8$	$C—\ddot{Cl} = 0.5$
$\dot{C}H_3 = 3.0$	$C—CH_3 = 0.7$	$\dot{C}H_3 = 3.0$	$C—\dot{C}H_3 = 0.7$
			$\dot{N}—\dot{O} = 0.9$
			$\dot{N}—\ddot{O} = 0.5$
			$\dot{N}—\ddot{N} = 0.9$

[a] ω value is 1.4 for both sets of parameters.
[b] Streitwieser [*12*].
[c] Roche and Kier [*13*].

III. Self-Consistent Field π-Electron Method

A. THEORY

In simple Hückel theory we have neglected electron repulsion and have considered a generalized Hamiltonian to reflect the potential of one π

electron in the field of its core. In SCF theory these interactions are included to various degrees depending upon the level of sophistication chosen in the SCF framework. A semiempirical method applicable to the π electrons of molecules of a size of interest to the biological scientist is available and known as the Pairiser, Parr [*14*], and Pople [*15*] SCF method.

For a π-electron system, a Hamiltonian operator is expressed by Eq. (6).

$$H = \sum H_i^{\text{core}} + \frac{1}{2} \sum_{i \neq j} \frac{e^2}{r_{ij}} \tag{6}$$

As used in this discussion, subscripts k and l denote atomic orbitals, μ and ν, MO's, 1, 2 or i and j, electrons. The first term in Eq. (6) includes the attraction energy of the core for the π electron. The second term is the electron repulsion term summing all repulsions between π electrons. Each e^2/r_{ij} term in the summation involves the coordinates of both electrons simultaneously, hence cannot be evaluated exactly. This term can be approximated by considering the electron 1 in the average field of another electron, 2. This average field is

$$\int \psi^2(2) \frac{e^2}{r_{12}} d\tau_2$$

Electron exchange between orbitals μ and ν is considered by including the term

$$\int \psi_\mu(2) \psi_\nu \frac{e^2}{r_{12}} d\tau_2$$

An expanded expression can now be written in wave equation form

$$\left(\sum H^{\text{core}} + 2 \sum \int \psi_\nu^2(2) \frac{e^2}{r_{12}} d\tau_2 \right) \psi_\mu(1) - \sum_{\nu \text{ occ}} \left(\psi_\nu(2) \psi_\mu(2) \frac{e^2}{r_{12}} d\tau_2 \right) \psi_\nu(1) = E_\mu \psi_\mu(1)$$

Since electrons occupy energy levels doubly, the average field term will be double; however, the exchange term represents only one possible exchange, hence will remain a single term. The average field term is abbreviated as J or a Coulomb operator, and the exchange term, K, or an exchange operator. The equation now reduces to

$$(\sum H^{\text{core}} + \sum (2J_\nu - K_\nu)) \psi_\mu(1) = E_\mu \psi_\mu(1)$$

This operator is an effective Fock operator and the wave equation can be written as in Eq. (7).

$$F \psi_\mu = E_\mu \psi_\mu \tag{7}$$

As in Hückel theory, the MO's are built up as LCAO ($2p$ π orbitals).

$$\psi_\mu = \sum_k C_{k\mu}\phi_k$$

From the variation theorem we multiply the Fock wave equation [Eq. (7)] through by ϕ_2 and integrate to obtain

$$\sum_k C_{k\mu} \int \phi_l F \phi_k \, d\tau = E_\mu \sum_k C_{k\mu} \int \phi_l \phi_k \, d\tau$$

As in Hückel formalism, we can abbreviate

$$\int \phi_k F \phi_k \, d\tau = F_{kk} = \alpha_k$$

$$\int \phi_k F \phi_l \, d\tau = F_{kl} = \beta_{kl}$$

$$\int \phi_k \phi_l \, d\tau = S_{kl}$$

The α and β terms resemble the same terms in Hückel theory except in SCF formalism, these terms depend upon the coordinates of more than one electron. The overlap term S is the same as in Hückel theory. The coefficients are determined from solution of the secular equations, which in determinant form are

$$\begin{vmatrix} \alpha_{11} - E & \beta_{12} - ES_{12} & \beta_{13} - ES_{13} & — & — & — \\ \beta_{21} - ES_{21} & \alpha_{22} - E & \beta_{23} - ES_{23} & — & — & — \\ — & — & — & & & \\ — & — & — & & & \end{vmatrix} = 0$$

Evaluation of the diagonal, α, and off-diagonal terms, β, can be shown to be approximated by the equations

$$\alpha_k = \alpha_k^{\text{core}} + \tfrac{1}{2}q_k(kk|kk) + \sum_{l \neq k} q_l(kk|ll)$$

$$\beta_{kl} = \beta_k^{\text{core}} - \tfrac{1}{2}p_{kl}(kk|ll)$$

where q_k is the total π-electron density on atom k, α_k^{core} and β_{kl}^{core} the values of the one-electron portion of the Hamiltonian integrated over one (α_k) and two centers (β_{kl}), p the π-electron bond order between atoms k and l, $(kk|kk)$ the integral describing the repulsion between two electrons in the field of the same core, and $(kk|ll)$ the integral describing the repulsions between two electrons on neighboring cores k and l.

With these equations for the α's and β's, the secular determinant can be solved for the coefficients, thence the charges and bond orders. This

set of q and p values is used to compute an improved set of α and β values and the process is iterated until some value of the charges is obtained which is consistent within prescribed limits. The energies are obtained for each MO as eigenvalues of the determinant.

As in Hückel theory, in the PPP-SCF method, the overlap S_{kl} is 0 unless $k = l$ where it is 1. The value of β_{kl} is commonly assumed to be 0 for non-neighbor atoms.

The equations just described are based on sound theoretical principles; however, the evaluation of some of the integrals as parameters for calculations requires empiricism in order to achieve useful results which mirror physical experience. A considerable amount of attention has been paid to the selection of parameter values, a detailed review of which is outside the scope of this book. The interested reader can better inform himself by consulting several recent papers [*16*, *18*].

A few general comments can be made to guide the selection of these parameters.

B. Parameter Selection

1. α *Core*

Evaluation of the one-electron, one-center terms is not directly possible since this term involves an effective nuclear attraction for the electron. The Goeppert-Mayer and Sklar approximation equates this energy with ionization potential, I, of the electron in this orbital as well as the potential from the other cores, which is approximated by the two-center repulsion integrals [*10*].

$$\alpha_i^{\text{core}} = -I_i - \sum (ii|jj)$$

2. β *Core*

The one-electron, two-center terms are selected empirically. A wide range of values have been proposed based on several theoretical approaches to this parameter. Based on overlap and valence state ionization potential values, Mulliken has proposed a relationship [*20*].

$$\beta_{kl} = \frac{S_{kl}}{1 + S_{kl}} \frac{I_k + I_l}{2}$$

Another empirical relationship has been suggested by Flurry and Bell [*21*].

$$\beta_{kl} = \frac{(2 - S_{kl})S_{kl}}{2 - S_{kl}^2} (I_k I_l)^{1/2}$$

Fischer-Hjalmars derived an equation involving electron repulsion integrals [*22*].

$$\beta_{kl} = S_{kl}\{0.4297[(kk|kk) + (ll|ll)] - 2.581(kk|ll)\}$$

Empirically derived values are frequently employed which give calculated properties in agreement with experiment. Some commonly used values for β_{cc} are -1.75, -2.06, and -2.39 eV. Detailed discussions of this parameter choice are available [*23*].

3. *Electronic Repulsion Integrals*

These can be computed from Slater orbitals but the results do not agree with spectral data. The one-center, two-electron repulsion integral, $(kk|kk)$, can be shown to be approximately the difference between the ionization potential, I, and the electron affinity of the atom in its valence state

$$(kk|kk) = I - A$$

This value is 11.13 eV for a carbon $2p$ electron.

The two-electron, two-center repulsion integrals, $(kk|ll)$, may be calculated from two prominent procedures, the first proposal is by Parr [*24*]

$$(kk|ll) = \tfrac{1}{2}[(kk|kk) + (ll|ll)] - aR - bR^2$$

where a and b are determined by parabolic fitting to the values at internuclear distance $R = 2.8$ Å and $R = 3.7$ Å. This gives integral values for $R < 2.8$ Å. When $R > 2.8$ Å

$$(kk|ll) \approx \frac{13.6 \text{ eV}}{R_{kl}}$$

The second procedure, proposed by Nishimoto and Mataga is

$$(kk|ll) = \frac{14.397}{R + a}$$

where

$$a = \frac{14.397}{\tfrac{1}{2}[(kk|kk) + (ll|ll)]}$$

Typical values for C—C integrals are $(kk|kk) = 10.84$ eV and $(kk|ll) = 7.38$ or 5.28 eV [*25*].

With numerical values for the integrals, the appropriate secular determinant can now be set up and solved for the energies and coefficients. Iterating the calculations using the charges and bond orders gives improved sets of matrix elements until the charges are constant to a predetermined range.

The total π energy cannot be computed as a sum of the occupied energy levels times the orbital occupancy, as in Hückel theory, since this would include all electron repulsion terms twice. The total electronic energy is the sum of the energies of the Fock matrix and the core matrix summed over all occupied orbitals.

IV. Methods of Treating σ Bonds

Historically, π-electron systems of any size were the first studied quantum mechanically. A major reason, of course, lies in the fact that, by considering only the π electrons, we can consider much larger molecules. The planarity of conjugated systems makes many approximations reasonable so that less sophisticated MO theories have a better chance of success.

The neglect of the σ-bonded framework is not completely justifiable in any π-only MO method. A more compelling reason to consider σ-bonded molecules is the fact that these molecules are part or all of many of the compounds which are of interest to the chemist, particularly the biological chemist.

Del Re has proposed a simple method whereby the bond charges, calculated in a Hückel formalism are summed around an atom to give the total σ charge [*26*]. Each bond is treated as a localized, double occupied MO. The influence of adjacent bonds is considered through an inductive effect on the bond orbital. Each bond orbital can then be described

$$\psi_{AB} = C_A\phi_A + C_B\phi_B$$

This, upon expansion, yields a determinant in the conventional Coulomb, α, and resonance integral, β, terms with the neglect of overlap.

$$\begin{vmatrix} \alpha_A - E_{AB} & \beta_{AB} \\ \beta_{BA} & \alpha_B - E_{AB} \end{vmatrix} = 0$$

A standard α_0 and β_0 terms are based on carbon–carbon bonds, hence bonds involving heteroatoms would be modified using the Wheland and Mann convention [*27*].

$$\alpha_A = \alpha_0 + \delta_A^0\beta_0$$

$$\beta_{AB} = \varepsilon_{AB}\beta_0$$

The inductive effects on an atom are introduced by modifying the Coulomb parameter δ_A to include a fraction of the Coulomb parameters of adjacent atoms

$$\delta_A = \delta_A^0 + \sum \gamma_{AB}\delta_B$$

where γ_{AB} is an inductive parameter. It is assumed that ε_{AB} is independent of surroundings, i.e., is not modified inductively. Thus parameters δ_A^0, γ_{AB}, and ε_{AB} must be chosen empirically. This has been done to give agreement with dipole moments of selected molecules.

The charge of atom A in bond AB can be calculated

$$q_A^{(B)} = \frac{\delta_B - \delta_A}{\left[1 + \left(\frac{\delta_B - \delta_A}{2\varepsilon_{AB}}\right)^2\right]^{\frac{1}{2}}}$$

The total charge on atom A then is a sum of all bond charges in which atom A is involved

$$Q_A = \sum_B q_A^{(B)}$$

TABLE III
DEL RE MO PARAMETERS[a]

$\delta_A - \sum_{\text{linked to } A} \gamma_{AB}\delta_B = \delta_A^\circ$				
Atom (A)	Atom (B) linked to (A)	δ_A°	γ_{AB}	ε_{AB}
C	H	0.07	0.30	1.00
C	C	0.07	0.10	1.00
C	N	0.07	0.10	1.00
C	N	0.07	0.10	1.33
C	O	0.07	0.10	0.95
C	$O^{-1/2}$	0.07	0.10	0.80
C	S	0.07	0.20	0.75
C	Cl	0.07	0.20	0.65
N	C	0.24	0.10	1.00
N	H	0.24	0.30	0.45
N	N	0.24	0.10[b]	1.00[b]
N	O	0.24	0.10[b]	1.00[b]
N	C	0.31	0.10	1.33
N	H	0.31	0.30	0.60
O	C	0.40	0.10	0.95
O	H	0.40	0.30	0.45
O	N	0.40	0.10[b]	1.00[b]
H	C	0.00	0.40	1.00
H	N	0.00	0.40	0.45
H	N	0.00	0.40	0.60
H	O	0.00	0.40	0.45
Cl	C	0.35	0.40	0.60
S	C	0.07	0.40	0.75
S	S	0.07	0.10	0.60

[a] Del Re [28].
[b] Kier and Roche [38].

The σ-electron energy of the AB bond can be calculated as

$$E_{AB} = 2\alpha + \beta\left\{\delta_A + 2\varepsilon_{AB}\left(\frac{\delta_B - \delta_A}{2\varepsilon_{AB}}\right) + \left[1 + \left(\frac{\delta_B - \delta_A}{2\varepsilon_{AB}}\right)^2\right]^{\frac{1}{2}}\right\}$$

The σ-electron energy for the molecule is thus

$$E = \sum_{\text{all bonds}} E_{AB}$$

Parameters derived for δ_A, γ_{AB}, and ε_{AB} are shown in Table III.

The dipole moments of simple molecules have been approximated and the charges by this method, when added to π-electron charges have approximated dipole moments of aromatic molecules [*29*, *30*].

V. All-Valence Methods

The idea of overlaying π-electron and σ-electron MO calculations on the same molecule to obtain a reasonable description of certain properties of an aromatic, conjugated, or mixed aryl–aliphatic molecule is based on the concept of orthogonality of these two systems and complete noninteraction. Clearly this assumption is not strictly valid, although some calculated properties can be obtained which are useful. These methods, however, fail to predict anything of the preferred conformation of the saturated portion of molecules.

Two comparatively recent treatments now make it possible to consider all valence electrons (σ and π), their mutual effects, hence to be sensitive to the geometry of saturated molecules.

A. Extended Hückel Theory

Hoffmann has proposed a one-electron LCAO method known as extended Hückel theory (EHT) [*31*]. The method employs a one-electron Hamiltonian; however, overlap integrals are retained and the two-center integrals H_{ij} are considered between all atoms, bonded and otherwise. The Coulomb integrals, H_{jj}, are approximated as the valence state ionization potentials for the appropriate atomic orbital. The off-diagonal elements H_{ij} are taken as being proportional to the overlap.

$$H_{ij} = 0.5K(H_{ii} + H_{jj})S_{ij}$$

The parameter K is assigned a value of 1.75, the overlap integrals are calculated using Slater orbitals and Slater's effective nuclear charges. Since the calculation of S_{ij} requires interatomic distances and since all S_{ij} and H_{ij} values between all-valence electron orbitals (hydrogen 1*s*, first row atom

2*s*, 2*p*), long range interaction is introduced and the method becomes sensitive to geometry.

Cusachs has proposed an alternative formula for H_{ij} [*32*].

$$H_{ij} = S_{ij}(2 - |S_{ij}|)(H_{ii} + H_{jj})/2$$

The total energy is calculated as the sum of orbital energies multiplied by their orbital occupancy. Some parameters commonly used are shown in Table IV.

The charges are calculated by a Mulliken population analysis.

$$q_r = 2 \sum_{i,\ \text{occ}\ s} \sum C_{ir} C_{is} S_{rs}$$

Although these tend to be exaggerated, they appear to be correctly ordered. The method has been used to calculate equilibrium conformations of molecules by regularly varying bond rotational angles and calculating the total energy as a function of this angle.

TABLE IV
EXTENDED HÜCKEL MO PARAMETERS[a,b]

Coulomb integrals		Slater exponents	
Electron	Value (eV)	Atom	Value
N 2*s*	−26.00	H	1.000
N 2*p*	−13.40	C	1.625
O 2*s*	−35.30	N	1.950
O 2*p*	−17.76	O	2.275
C 2*s*	−21.40		
C 2*p*	−11.40		

[a] Hoffmann [*31*].
[b] Kier [*39*].

B. SELF-CONSISTENT FIELD METHOD

Pople has described a method based on SCF formalism in which there is complete neglect of differential overlap (CNDO) [*33*]. This is the same approximation made in π-electron Hückel theory. As a result, all two-center overlap integrals vanish, greatly simplifying the calculations. The Fock matrix elements are

$$F_{ii} = -\tfrac{1}{2}(I_i + A_i) + [(P_{aa} - Z_a) - \tfrac{1}{2}(P_{ii} - 1)](aa|aa) + \sum(P_{bb} - Z_b)(aa|bb)$$

$$F_{ij} = \beta_{ij}{}^{\circ} S_{ij} - \tfrac{1}{2} P_{ij}(aa|bb)$$

The one-center, one-electron term, $-\frac{1}{2}(I_i + A_i)$ is derived from the ionization potential, I, and the electron affinity, A, of the electron in its valence state. The P terms are charges and bond orders for P_{aa}, total atom charge on atom a, P_{ii} charge on orbital i, P_{ab}, bond order between atoms a and b, and P_{ij} bond order between orbitals i and j. The β_{ab}° terms are derived by calibrating the results of calculations to accurate Hartree-Fock calculations on small molecules.

$$\beta_{ij} = S_{ij}(\beta_a^{\circ} + \beta_b^{\circ})/2$$

The value of β_{ij} vanishes if orbitals i and j are on the same atom.

The solution to a problem is the same as for the π-electron SCF method previously described.

VI. Analysis of Methods

The Hückel theory is computationally simpler than the SCF methods due to a number of assumptions. The most severe Hückel theory assumption is the neglect of electron repulsion terms. The Hamiltonian is defined in terms of one π electron in the field of its core with no consideration given to the effects of π electrons on neighboring cores. This failure to consider electron repulsion leads to a poor approximation of excited state phenomena. In closely related series of molecules, this neglect tends to be minimal in its influence, hence, some satisfactory correlations between Hückel-calculated energy level transitions and spectroscopic properties may be obtained. The general situation is, however, not encouraging.

Because of the unspecified nature of the one-electron Hamiltonian the energy terms, α and β, are likewise unspecified. From calculations on series of molecules, β values may be obtained by regression analyses, but the value so obtained differs from a value of β obtained from some other series of experiments on a different molecular property. This is due to the fact that the properties being studied should be dealt with using a complete Hamiltonian, not the artificial one used in Hückel theory.

It is equally apparent that the assumption of equal α and equal β values is not justified. With any change in molecular environment there should be some compensatory change in the α and β parameters. Some attempt is made to account for differing environment by using a variable α term, dependent on charge density, in the Wheland and Mann or ω technique. Some improvement in relating calculations to physical experience is possible by this consideration.

The neglect of overlap has been commented on before. It is present in both Hückel and in Pairiser, Parr, Pople SCF methods. Because of the crudeness of the Hückel approximations it is not particularly meaningful

to overlay more sophisticated techniques on it and expect to obtain more refined results.

The neglect of overlap in the simpler SCF methods is perhaps more severe than in Hückel theory in view of the consideration of repulsion terms. The empirical choice of some SCF parameters lays the method open to some criticism, although in general the theoretical foundation is stronger than in Hückel theory. SCF calculations are certainly superior in the treatment of excited state phenomena. Charge densities are probably more realistic due to consideration of electron correlation.

The Del Re bond orbital treatment of σ-bonded systems is computationally very simple and gives charge densities which in some cases may be reasonable. The energies derived from such a method are not of much value due to the failure to consider nonbonded interactions. The method makes no account of geometry of σ-bonded molecules. Its use as a method of assessing the σ bond charges in a π system and then the numerical summing of these charges with the π Hückel or π SCF charges has been demonstrated. In a few cases, experimental properties have been mirrored; however, the noninteraction of σ and π frameworks is not theoretically justifiable.

It is becoming increasingly evident to biological scientists, already using MO theory in their research, that π-electron MO methods are giving only half of the story in regard to the structures of interest to them. Attempts to overlay σ-bond orbital calculations onto π-electron MO calculated charges are useful in very simple systems, but are doomed to failure when heteroatoms are involved. The all-valence electron MO methods currently used are clearly a step in the right direction for the study of molecules of biological importance. The potential ability to predict conformation with these methods is a giant step ahead in the area of theoretical molecular studies.

It is thus of great importance to consider in detail the comparative values of EHT and CNDO/2 MO techniques so that proper application of them can be made to biologically important molecules. Hoyland has made a detailed comparison and review of these two methods [*34*].

Extended Hückel theory is the simplest of the methods, and, as such, is the least satisfactory for anything other than very qualitative prediction. It is best suited to molecules in which the charge distribution is quite uniform (such as hydrocarbons), as shown by Blyholder and Coulson [*35*]. Since EHT neglects both electron–electron and nuclear–nuclear repulsions, it cannot be used to predict bond lengths, but is capable under certain conditions of yielding satisfactory angles [*36*]. The charge distribution calculated by EHT is unsatisfactory for molecules containing atoms with large differences of electronegativity, leading to grossly exaggerated dipole moments.

EHT has been relatively successful in the prediction of preferred conformations and it may be that it is within this area that it has its greatest utility, in spite of the fact that predicted barriers to internal rotation are often exaggerated. Finally, it is felt that application of EHT to unsaturated molecules must be undertaken with caution since the virtual orbital levels indicate that the π system is not treated correctly.

Some iterative Hückel schemes (IEHT) have been developed in an effort to overcome some of the shortcomings of EHT with regard to charge distribution. These methods appear capable of predicting adequate dipole moments, provided these are computed with the exact quantum mechanical prescription. Ionization potentials are usually predicted somewhat better by IEHT than by EHT, but application to unsaturated molecules is not warranted in its present form. Although not much work has appeared on conformational calculations or on prediction of bond angles, it is felt that IEHT should be as good as EHT for conformation.

Methods based on neglect of differential overlap, most notably CNDO and INDO, appear to be generally useful for computing dipole moments and geometry. The CNDO/2 procedure as outlined originally by Pople, Santry, and Segal [*33*] generally overemphasizes bond strengths and does not lead to good potential functions for bond stretching or contraction. Furthermore, CNDO/2 does not give good energy levels, especially for unsaturated molecules, and conformational information is liable to be poor. Alternative parametrization [*37*] leads to better energy levels and has proved adequate for binding energies, but cannot be used for the prediction of bond lengths since the nuclear–nuclear repulsion is not evaluated in the proper manner for such a calculation.

These faults and advantages also apply to INDO (intermediate neglect of differential overlap) which has a further advantage in being able to adequately predict ESR hyperfine coupling constants in radicals. It would appear that CNDO and INDO have many fine features and a more careful parametrization and a better system of integral evaluation may be able to cope with some of the difficulties of the original theories.

In view of the above discussion, it is difficult to recommend the use of one method for all types of calculations. It appears best to decide which formulation seems to be most adequate for the calculation of the properties of interest. Further work on all of these methods is needed to overcome some of the most glaring faults, especially with regard to unsaturated molecules. This necessarily means that complete rotational invariance must be sacrificed, as has been done in the nonempirical MO formulations. This is a small price to pay for better accuracy in the energy levels.

More work should be done with IEHT directed toward building a set

of rules for choosing appropriate diagonal elements for atoms in various molecular environments. This could lead to a method requiring no iteration and producing results of comparable value to a full IEHT calculation.

It is expected that within the next few years significant improvement in existing semiempirical methods will be made and new and better schemes devised which will be more generally applicable to the calculation of a wider variety of properties. Hopefully, a greater amount of this effort will go into the prediction of chemical reactivities and a more fundamental understanding of such topics as linear free energy relationships, aromatic substitution, acidity and basicity, and other areas of interest to biochemists.

References

1. E. Hückel, *Z. Phys.* **76**, 628 (1932).
2. G. W. Wheland and L. Pauling, *J. Amer. Chem. Soc.* **57**, 2086 (1935).
3. A. Streitwieser, "Molecular Orbital Theory for Organic Chemists," p. 135. Wiley, New York, 1961.
4. B. Pullman, "Quantum Biochemistry." Wiley (Interscience), New York, 1963.
5. F. A. Matsen, *J. Amer. Chem. Soc.* **72**, 5243 (1950).
6. D. P. Stevenson, cited in A. Streitwieser "Molecular Orbital Theory for Organic Chemists," p. 133. Wiley, New York, 1961.
7. R. S. Mulliken, C. A. Rieke, and W. G. Brown, *J. Amer. Chem. Soc.* **63**, 41 (1941).
8. C. A. Coulson, *Proc. Roy. Soc., Ser. A* **169**, 413 (1939).
9. C. A. Coulson and H. C. Longuet-Higgins, *Proc. Roy. Soc., Ser. A* **191**, 39 (1947).
10. C. A. Coulson, *Discuss. Faraday Soc.* **2**, 9 (1947).
11. C. Finder, *J. Org. Chem.* **32**, 1672 (1967).
12. A. Streitwieser, *J. Amer. Chem. Soc.* **82**, 4123 (1960).
13. E. B. Roche and L. B. Kier, *Tetrahedron* **24**, 1673 (1968).
14. R. Pariser and R. G. Parr, *J. Chem. Phys.* **21**, 466, 767 (1953).
15. J. A. Pople, *Trans. Faraday Soc.* **49**, 1375 (1953).
16. R. L. Flurry and J. J. Bell, *Theor. Chim. Acta* **10**, 1 (1968).
17. K. Nishimoto and L. S. Forster, *Bull. Chem. Soc. Jap.* **41**, 2254 (1968).
18. I. Fischer-Hjalmers and M. Sundbom, *Acta Chem. Scand.* **22**, 607 (1968).
19. M. Goeppert-Mayer and A. L. Sklar, *J. Chem. Phys.* **6**, 645 (1938).
20. R. S. Mulliken, *J. Chem. Phys.* **56**, 292 (1952).
21. R. L. Flurry, Jr. and J. J. Bell, *J. Amer. Chem. Soc.* **89**, 525 (1967).
22. I. Fischer-Hjalmers, *in* "Molecular Orbitals in Chemistry, Physics, and Biology" (P. Lowdin, ed.), p. 361. Academic Press, New York, 1964.
23. R. L. Flurry, "Molecular Orbital Theories of Bonding in Organic Molecules," p. 208. Dekker, New York, 1968.
24. R. L. Parr, *J. Chem. Phys.* **20**, 1499 (1952),
25. K. Nishimoto and N. Mataga, *Z. Phys. Chem. (Frankfurt am Main)* **12**, 335 (1957).
26. G. Del Re, *J. Chem. Soc., London* p. 4031 (1958).
27. G. W. Wheland and D. E. Mann, *J. Chem. Phys.* **17**, 264 (1949).
28. G. Del Re, *in* "Electronic Aspects of Biochemistry" (B. Pullman, ed.), p. 221. Academic Press, New York, 1964.
29. L. B. Kier, *Tetrahedron Lett.* **37**, 3273 (1965).
30. H. Berthod and B. Pullman, *J. Chem. Phys.* 942 (1965).
31. R. Hoffmann, *J. Chem. Phys.* **39**, 1397 (1963).

32. L. C. Cusachs, *J. Chem. Phys.* **43**, 5157 (1965).
33. J. A. Pople, D. P. Santry, and G. A. Segal, *J. Chem. Phys.* **43**, 5129 (1965).
34. J. R. Hoyland, *in* "Molecular Orbital Studies in Chemical Pharmacology" (L. Kier, ed.), p. 31. Springer-Verlag, New York, 1970.
35. G. Blyholder and C. A. Coulson, *Theor. Chim. Acta* **10**, 316 (1968).
36. L. C. Allen and J. D. Russell, *J. Chem. Phys.* **46**, 1029 (1967).
37. J. M. Sichel and M. A. Whitehead, *Theor. Chim. Acta* **11**, 239 (1968).
38. L. B. Kier and E. B. Roche, *J. Pharm. Sci.* **55**, 807 (1966).
39. L. B. Kier, *Mol. Pharmacol.* **3**, 487 (1967).

Chapter IV

SIGNIFICANCE OF MOLECULAR ORBITAL INDICES

The value of MO theory, in the hands of the chemist or biologist lies, hopefully, in its ability to derive information concerning the properties of molecules of interest to him, without major reliance on the performance of an experiment. With an exact solution of the wave equation for a molecule, this ideal would be fully realized. As we have seen, with increasing molecular complexity, we are forced further and further away from a theoretically justifiable wave equation toward an approximate one resting on many assumptions. In essence we have lost the ability to calculate from first principles the properties of interest to us. It is then necessary to rely on some available experimental information with which to calibrate our parameters in approximate MO methods, in order to achieve some ability to reproduce physical experience. We thus are semiempirical in our approach.

With suitable choices of parameters and judicious choices of models, MO theory has often succeeded in correlating well with experimental data. The extrapolation of correlation is prediction and this is the goal of the biological scientist in selecting MO theory as a powerful research tool.

In this chapter, we shall describe some of the physical and chemical properties which are, at least in part, interpretable using MO theory, and to describe this connection. The discussion will center on those properties which are of interest to the biological scientist primarily, recognizing that a more detailed and more extensive consideration of these and other properties is possible.

I. Properties Related to Total Energy

In the π-only methods previously described, it is apparent that a calculated total energy can only pertain to π electrons, whereas in all-valence electron MO methods, we are calculating a more detailed, but not a complete molecular energy. It is obvious that π-only energies and all-valence electron energies from these two treatments should be unrelated. Each has a degree of physical significance, however, and will accordingly be considered in its own right.

A. π-Electron Delocalization Energy

The delocalization energy, DE_π, is the calculated total π energy in excess of the total π energy which would be calculated for the same conjugated system in which the delocalization did not exist, and where the electrons were isolated in double bonds. The total π energy calculated for butadiene using simple Hückel theory is $4\alpha + 4.472\beta$. Two isolated double bonds result in a total π energy of $4\alpha + 4\beta$. The DE_π for butadiene is thus 0.472β, from this MO method. Simple Hückel calculations on benzene give a total π energy of $6\alpha + 8\beta$. This same system using an isolated bond model has a total π energy of $6\alpha + 6\beta$. The DE_π is thus 2β for benzene. The isolated bond model used as a reference in this case corresponds to a Kekule benzene structure. The DE_π calculated for benzene then should bear a relationship to the resonance energy. A study of the DE_π values for a series of aromatic hydrocarbons [*1*] calculated from simple Hückel theory revealed a good correlation with empirical resonance energies [*2*] (see Fig. 1 and Table I).

Resonance energy is a measure of aromatic stability. Calculations of DE_π have been used to predict the stability of unusual aromatic molecules such as cyclobutadiene and azulene. Simple HMO calculations on a square model of cyclobutadiene (Fig. 2a), show that the molecule has a DE_π of zero. The degenerate singly occupied orbitals with energy α are nonbonded MO's and correspond to a diradical. Assuming a rectangular shape (Fig. 2b), the calculations show no degeneracy but still indicate a low value of DE_π. SCF calculations on this molecule indicate that it is a typical cyclic polyene with essentially localized double and single bonds. The calculated resonance energy from an SCF calculation is only 0.8 kcal/mole [*3*]. Both MO methods thus predict an unstable molecule, which is borne out by the chemical properties of the synthesized compound [*4*].

Simple HMO calculations on azulene (**I**) and naphthalene (**II**)

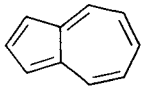

I

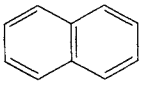

II

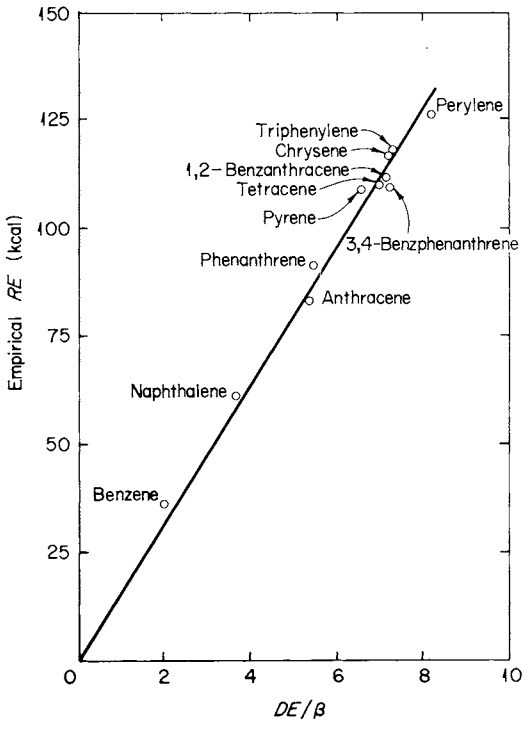

Fig. 1. Empirical resonance energies and HMO DE_π of aromatic hydrocarbons [*1*].

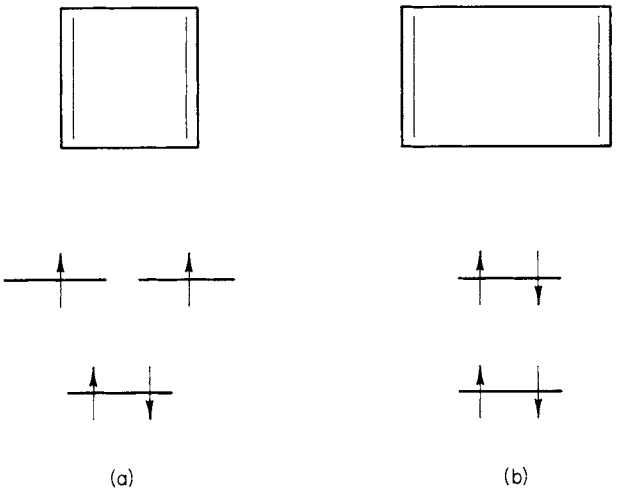

Fig. 2. Calculated π-electron energy levels for (a) square model and (b) rectangular model of cyclobutadiene.

TABLE I
RESONANCE AND DELOCALIZATION ENERGIES OF AROMATIC HYDROCARBONS

Hydrocarbon	Hückel *DE* (β)[a]	Empirical *RE* (kcal)[b]
Benzene	2.000	36.0
Naphthalene	3.683	61.0
Anthracene	5.314	83.5
Phenanthrene	5.448	91.3
Tetracene	6.932	110.0
1,2-Benzanthracene	7.101	111.6
Chrysene	7.190	116.5
Triphenylene	7.275	117.7
3,4-Benzphenanthrene	7.187	109.6
Pyrene	6.506	108.9
Perylene	8.245	126.3

[a] Pullman and Pullman [*1*].
[b] Wheland [*2*].

show azulene with $DE_\pi = 3.364\beta$, whereas naphthalene has a $DE_\pi = 3.684\beta$. The theory predicts a larger resonance energy for naphthalene, in agreement with the relative empirical values.

It should be noted that empirical resonance energies are composed of factors other than π-electron delocalization. Contributing to this energy is an energy associated with hybridization changes and bond compression, the latter resulting from the change to an equal bond length delocalized structure from a nonequal bond length Kekule structure. It is not always possible to obtain a reliable estimate of these contributions. Nevertheless, in comparing related molecules, the DE_π is a good criterion of relative stability.

In the case of molecules containing heteroatoms, the situation is somewhat more complicated. In order to compare an MO-calculated π-electron energy with the energy from a localized bond model or Kekule structure, it is necessary to be able to write down unambiguously this localized model. This is not always possible as, for example, in pyridizine (**III** or **IV**),

III

IV

the reference Kekule structure used in a DE_π calculation would have to be specified. The localized structures would likely have different energies.

The situation is further complicated in the case of aromatic heterocycles, for which localized, Kekule structures cannot be written at all. Such a class of molecules are the mesoionic molecules, of which the sydnones (**V**) are an example [*5*].

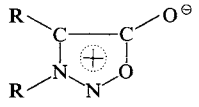

V

The concept of resonance energy is thus not very useful in this case. For comparative stability studies, an alternative value would be the total π energy compared to the energy of the π electrons completely isolated. This latter value would simply be a sum of all of the Coulomb integrals in the molecule. In the butadiene case, the sum of isolated π-electron energies is 4α, the calculated total π-electron energy is $4\alpha + 4.472\beta$, hence the delocalization energy in this reference framework is 4.472β. In the case of pyridine, using an $h_N = 1$ and $k_{CN} = 1.2$, the total π energy is calculated to be $6\alpha + 8.674\beta$. The completely localized energy is the sum of the Coulomb integrals $5\alpha + (\alpha + \beta) = 6\alpha + \beta$. The difference, 7.674β, is the delocalized energy by this technique. It is now possible to compare the calculated stabilities or extent of π delocalization among molecules containing the same number of π electrons. The method can be broadened to permit comparisons between molecules containing a differing number of π electrons by dividing the DE_π calculated in this manner by the number of π electrons in the molecule, thus arriving at a specific DE_π or a DE_π per π electron. For the pyridine case above, this becomes $1.28\beta/\pi$ electron. This method permits comparison of stabilities of heterocyclic isomers containing the heteroatoms in different valence states. Predictions of stability of various isomeric bisoxadiazoles have been based on this concept [*6*].

We have seen that the total π energy may be compared with a reference model containing localized bonds or with a model containing localized electrons in order to estimate the relative stability of a molecule. By the same token, if a reaction course can proceed along more than one path, leading to two or more possible products, it should be possible to predict the relative π-electron stability of the products, hence the equilibria of the

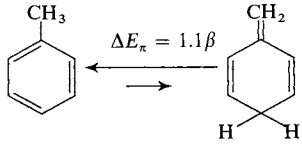

Fig. 3. Calculated resonance energy in toluene equilibrium.

system by comparing the total π-electron energies. An example is furnished in the considering of the equilibria of some methylated aromatic hydrocarbons [7] (Fig. 3). Calculation and comparison of the π-electron energies of each member of a pair, in a series of molecules, Table II, predicts predominance of the methyl form for the first three molecules and an increasingly larger contribution of the methylene form for the last two, in agreement with experience [8].

TABLE II
E_π DIFFERENCE BETWEEN METHYL HYDROCARBON TAUTOMERS[a]

Molecule	Methyl E_π – methylene $E_\pi(\beta)$
Toluene	1.1
α-Methylnaphthalene	0.9
9-Methylanthracene	0.5
5-Methylnaphthacene	0.43
6-Methylpentacene	0.38

[a] Pullman and Pullman [1], p. 250.

B. LOCALIZATION ENERGIES

The π-electron energies derived from MO calculations can be used to compare a molecule in the ground state to the same molecule in a reaction transition state structure (Fig. 4). The energy of the transition from the ground state to the transition state, or free energy of activation, $\Delta F^\ddagger$ is composed of entropy and enthalpy terms. In comparing a related series of molecules undergoing a similar reaction, a first approximation is that the $\Delta F^\ddagger$ values are related primarily to the enthalpy changes, $\Delta H^\ddagger$, in the process [9]. In aromatic substitution reactions, the Wheland model (Fig. 5) of the transition state involves only a perturbation of the electron structure due to the approaching reagent [10]. As such, the σ-electron system is not

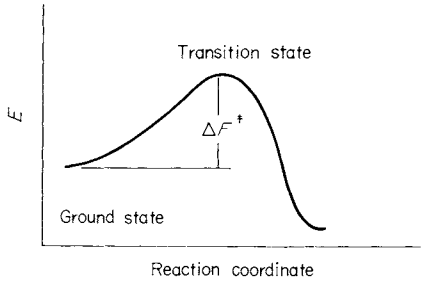

Fig. 4. Free energy relationship between ground and transition state.

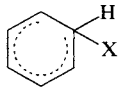

Fig. 5. Wheland model of a reaction intermediate.

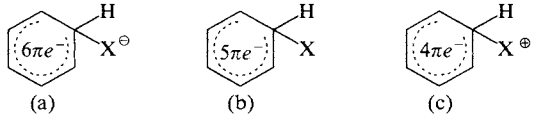

Fig. 6. Wheland models for transition states for (a) nucleophilic, (b) radical, and (c) electrophilic attack.

materially altered and so it would be expected that changes in comparative $\Delta F^{\ddagger}$ values in a related series of molecules should be primarily related to comparative $\Delta E_{\pi}^{\ddagger}$ values between ground and transition states [*9*]. The Wheland intermediate provides a model of the π-electron structure in the transition state on which MO calculations can be performed and comparisons made in related series. In this hypothetical intermediate, the carbon attacked is surrounded by four single bonds, each with an electron pair. As a result, it cannot be part of the delocalized system. The remaining atoms in the delocalized portion of the molecule contain those π electrons not needed to satisfy the electron demands of the attacking reagent. The three types of attacking reagents can be shown to produce the Wheland models shown in Fig. 6. The E_{π} for the transition state model in the nucleophilic attack is calculated from a 5-atom system with 6 π electrons; in the radical attack, a 5-atom system with 5 π electrons; and in the electrophilic attack, a 5-atom system with 4 π electrons. It is possible, using these models and the assumptions previously stated, to correlate $\Delta E_{\pi}^{\ddagger}$ values in a series with relative reaction rate constants [*11*].

As an example, in benzene, the ground state π-electron energy is $E_{\pi} = 6\alpha + 8\beta$. Using the Wheland intermediate for electrophilic attack in which 2π electrons are localized at a carbon (Fig. 6c), there remain 4 electrons delocalized over 5 atoms. Calculations on this system give energy levels $E_1 = \alpha + 1.732\beta$, $E_2 = \alpha + \beta$. Each of these lowest energy MO's is doubly occupied, hence the E_{π} for this transition state (Fig. 6c), is $4\alpha + 5.464\beta$. To this we can add the energies of the two isolated π electrons on the attacked carbon 2α. The $\Delta E_{\pi}^{\ddagger}$, symbolized L_r^+, is

$$L_r^+ = -\Delta E_{\pi} = -[E_{\pi}\text{ (transition state)} - E_{\pi}\text{ (ground state)}]$$
$$= -[(6\alpha + 5.464\beta) - (6\alpha + 8\beta)] = 2.536\beta$$

TABLE III
RELATIVE METHYL RADICAL REACTIVITIES[a]

Compound	Relative reactivity	$L'(\beta)$
Benzene	1	2.55
Biphenyl	5	2.39
Naphthalene	22	2.3
Phenanthrene	27	2.3
Chrysene	57.5	2.25
Pyrene	125	2.2
Stilbene	183	2.16
Benzanthracene	468	2.05
Anthracene	820	2.01
Naphthacene	9250	1.95

[a] Szwarc [*12*].

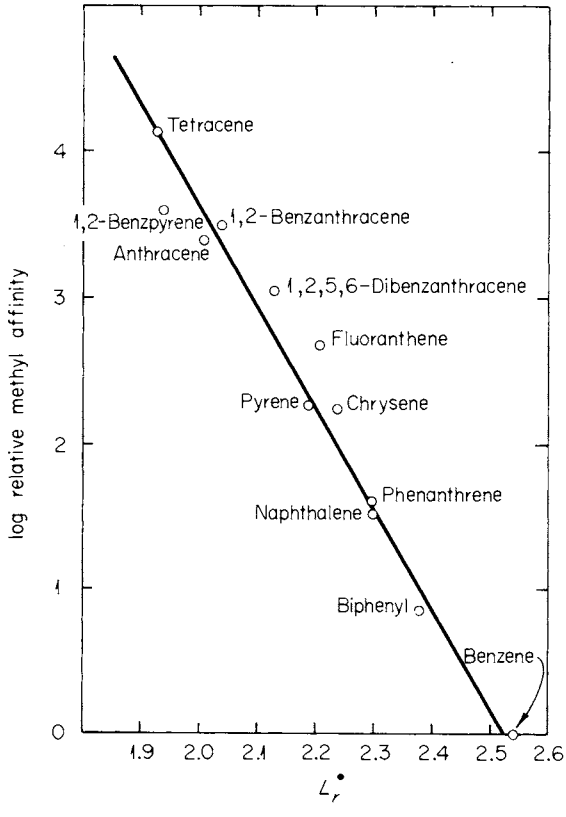

Fig. 7. Methyl affinities and localization energies [*12*].

This energy can be looked upon as the energy necessary to localize the electronic requirement of an attacking species (in this case an electrophile) at a carbon atom of benzene. The smaller the value of L_r^+ at a position, the more susceptible it is to attack.

In comparing relative reaction rates in a closely related series, the approximate relationship holds

$$-RT \log(k_2/k_1) = (L_r^+)_2 - (L_r^+)_1$$

This reactivity index frequently gives good correlation with reactivity data in a related chemical series as shown in Table III and Fig. 7.

Within a molecule, comparative localization energies calculated for different positions frequently lead to a correct prediction of the preferred site of attack. Cases in point are the correct prediction of reaction preference for naphthalene (1 position), anthracene (9 position), biphenyl (2 position), and styrene (β position) [*13*].

The method has been applied to heterocycles and heteroatom conjugated molecules. The base-catalyzed hydrolysis rates of a series of carbonyl compounds has been correlated with the nucleophilic localization energies L_r^-, using the ω-Hückel technique and assuming a transition state model shown in Fig. 8. This relationship is shown in Fig. 9 and Table IV.

TABLE IV
SECOND-ORDER BASE HYDROLYSIS RATE CONSTANTS AND ANION LOCALIZATION ENERGIES FOR SEVERAL CARBONYL COMPOUNDS[a]

Compound	Log k + 5 (mole^{-1}, min^{-1}, 25°)	$L_c^-(\beta)$
Urea	0.250	1.144
Acetamide	1.352	1.002
Urethan	2.079	0.966
Methyl acetate	3.945	0.804
Ethyl carbonate	5.447	0.766
Ethyl chloroformate	6.380	0.643

[a] Kier [*41*].

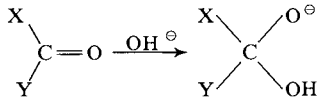

Fig. 8. Reaction model for hydrolysis.

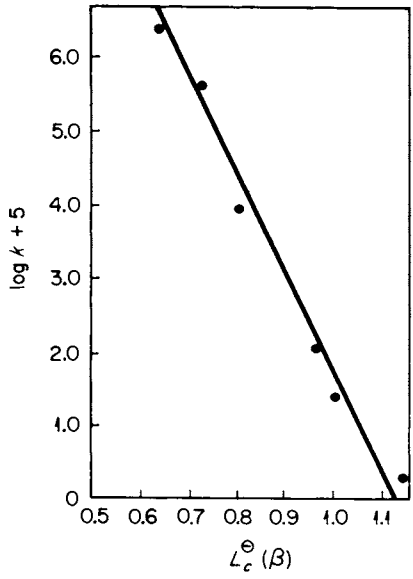

Fig. 9. Correlation between base-catalyzed hydrolysis rate (log k + 5) and MO-calculated localization energy, $L_C^{\ominus}$ [*14*].

C. Total All-Valence Electron Energy

Hoffmann has shown that a sum of occupied energy levels, times the orbital occupancy, from an EHT calculation, gives an energy which can be minimized as a function of geometrical variation in the molecule [*15*]. This provides a quantum mechanical approach to the prediction of preferred conformation. Hoffmann has concluded that the success of this total energy in predicting geometry is due to the fortuitous selection of the off-diagonal matrix elements, H_{ij} [*15*]. This choice apparently simulates, within the calculated electronic energies, the presence of nuclear repulsions at small distances, giving rise to a minimum, frequently mirroring physical experience. Slater has suggested that the sum of one-electron energies $\sum H_{en}$ of a Hartree-Fock Hamiltonian behave approximately as the total molecular energy, since the nuclear–nuclear $\sum H_{nn}$ and electron–electron $\sum H_{ee}$ repulsions in the Hamiltonian roughly cancel [*16*].

$$H = \sum_{en} H_{en} + \sum_{ee'} H_{ee} + \sum_{nn'} H_{nn}$$

A comparison of EHT total energy predictions of conformation with those from Hartree-Fock calculations showed good agreement if the atoms in the molecule did not differ by more than 1.1 electronegativity units in the Pauling scale [*17*].

The prediction of bond length has not met with such success nor can the absolute value of the energies within a molecule be regarded confidently. The problem of bond lengths is not serious since variations in organic molecules are not severe. The usual practice is to adopt a standard bond length for a particular hybrid pattern in a bond.

The barrier heights frequently are exaggerated, hence reliance on them can only be made in a relative sense. Some calculated and experimental values are shown in Table V.

TABLE V
COMPARISON OF CALCULATED WITH EXPERIMENTAL BARRIER HEIGHTS[a]

Molecule	Calculated (kcal)	Experimental (kcal)
CH_3-CH_3	4.0	2.7–3.0
$CH_3-CH_2CH_3$	5.6	3.4
$CH_3-CH_2CH_2CH_3$	10.9	3.4
Cyclohexane	17.5	5.5
e-Methyl cyclohexane	6.5	1.8

[a] Hoffmann [*15*].

The method has been used to predict geometries of fairly large molecules and heteroatom-containing molecules [*18–21*]. Some discrepancies have been noted in calculations involving heteroatoms particularly in a few cases involving carbonyl groups [*22*]. Charged species such as quaternary ammonium compounds can apparently be treated in the cases reported [*23*].

The EHT has been used to calculate energies of ground and transition states, hence to derive a localization energy for a particular position in a reaction [*24–26*]. In one of these studies, Hermann has compared EHT, CNDO/2, and π-only Hückel-calculated localization energies for the protonation of several heterocycles [*26*]. The transition state model (Fig. 10a) shown here for α-position protonation of pyrrole can be subjected to a complete-valence electron total energy calculation using EHT or CNDO/2 methods. Only the π electrons are involved in a simple Hückel localization energy calculation which would use a transition state model shown in Fig. 10b. The results of MO calculation on several heterocycles are shown in Table VI. The position of preferred protonation is correctly predicted in all

(a) (b)

Fig. 10. Protonation transition state models for (a) all-valence electron MO calculation and (b) π-electron MO calculation.

TABLE VI
MO-CALCULATED LOCALIZATION ENERGIES FOR HETEROCYCLE PROTONATION[a]

Compound	EHT energy (au)	CNDO/2 energy (au)	π-Hückel energy (β)
Pyrrole	−17.095	−43.775	− 8.630
Protonated α[b]	−17.264	−44.274	− 6.564
Protonated β[b]	−17.257	−44.266	− 6.390
Indole	−28.710	−73.775	−14.410
Protonated α	−28.873	−74.270	−12.209
Protonated β	−28.876	−74.284	−12.353
Furan	−18.062	−49.762	− 9.466
Protonated α	−18.237	−50.247	− 7.743
Protonated β	−18.218	−50.228	− 7.177
Benzofuran	−29.685	−79.767	−15.268
Protonated α	−29.854	−80.254	−13.123
Protonated β	−29.842	−80.251	−13.145

[a] Herrman [*26*].
[b] Position substituted.

cases by both all-valence electron methods. The π-only Hückel fails with benzofuran. The reaction intermediates have a lower energy in the case of the all-valence electron calculations since the energy needed to abstract the proton from another base was neglected. This situation would prevail for all EHT-calculated systems in which the transition state model contained additional atoms.

II. Properties Related to Orbital Energies

Solving the secular determinant gives rise to a series of energy values corresponding to particular MO's which are solutions of the wave equation. In the Hückel scheme, we take no account of electron repulsions or singlet–triplet excited states, hence the differences in energy levels may be unreliable, especially when excited states are concerned. Nevertheless, some success has been achieved in relating energy levels and differences between energy levels to physical phenomena, using the simple MO techniques.

A. ELECTRONIC SPECTRA

This discussion of the MO relationship to electronic spectra is intended as a brief introduction to acquaint the reader only with some sample MO applications and correlations. Extensive treatments are available [*27*, *28*].

We have seen that the energy levels are filled with pairs of electrons, the completed set comprising the ground electronic state of the molecule.

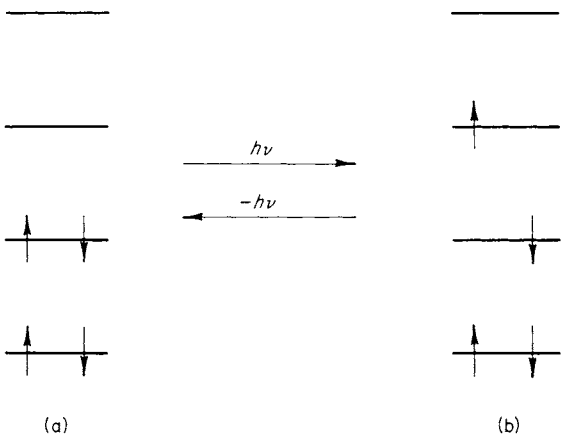

Fig. 11. Energy exchange and energy level occupancy in (a) ground state and (b) electronically excited state.

With an input of a definite amount of energy, $h\nu$, electrons can be promoted to higher lying MO's. The result is a molecule in an electronically excited state. This process is reversible, resulting in an emission of the energy, $h\nu$. In general terms, the phenomenon is depicted in Fig. 11.

In a complex heteroatomic conjugated molecule, the energy levels generally, but not universally, follow a pattern as far as the bonding characteristics of resident electrons. Similarly, the unoccupied energy levels are selectively receptive to electrons promoted from occupied MO's of certain bonding characteristics. The electronic transitions can thus be designated according to the origins of electrons involved and the relative energies of the transitions, as shown in Fig. 12.

The level designated as n is a nonbonding MO. The frequency ν of any transition depends upon the energy difference between ground and excited state energy levels, $h\nu = hc/\lambda = E^* - E = \Delta E$.

An intense absorption band of aromatic hydrocarbons is the $\pi \rightarrow \pi^*$ transition or p band, frequently measurable in the ultraviolet or visible range of the spectrum and a transition which is characteristic of the extent of delocalization in a molecule. It is subject to variation as a result of structural modification. It is a physical phenomenon frequently called upon to identify and classify conjugated and aromatic molecules.

The $\pi \rightarrow \pi^*$ transition, being a promotion of an electron from the highest occupied MO (HOMO) to the lowest empty MO (LEMO) should be related to the difference in the π-electron energies of these levels from MO calculations. If we use the general terms, m, $m - 1$, $m - 2$, etc. to denote the coefficients of β in an energy level diagram, we can designate the levels and transition according to Fig. 13.

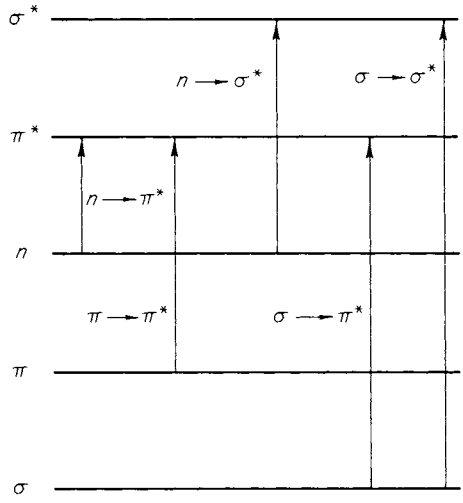

Fig. 12. Electronic transitions of various types showing origins and levels promoted to and relative energies.

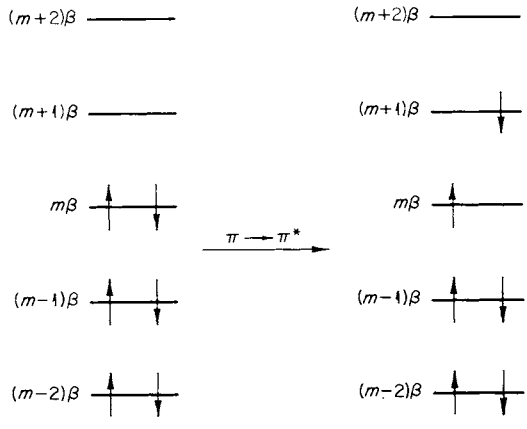

Fig. 13. Designation of π-electron energy levels in units of β.

The transition should then be related to the difference in the coefficients of β

$$\Delta m(\beta) = (m + 1)\beta - m\beta$$

The aromatic hydrocarbons furnish a good example of the correlation which can be obtained. A comparison between simple Hückel calculations of $\Delta m[(m + 1) - m]$ and the p-band λ_{max} for an aromatic series is shown in Table VII and Fig. 14.

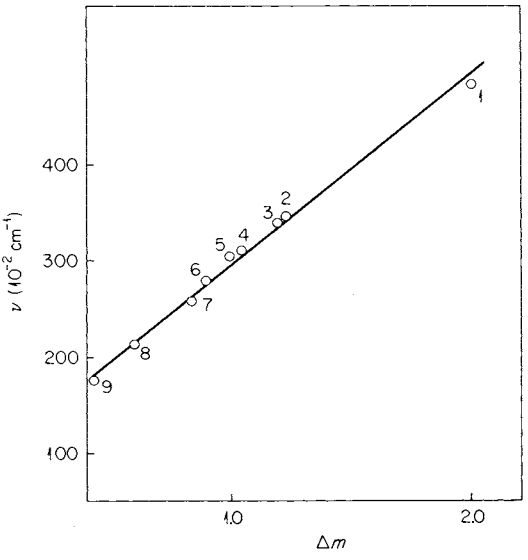

Fig. 14. Relationship between *p*-band absorption frequencies and π-Hückel Δm values in a series of hydrocarbons listed in Table VII.

The relationship has been extended to heterocycles. An example using an ω-Hückel procedure [*29*] is shown in Table VIII and Fig. 15. From the results in Table VII it can be seen that the extension of π conjugation in a series of molecules brings about a displacement of the absorption of the principal band to higher wavelengths (bathochromic displacement). Thus MO calculations correctly anticipate this shift within a related series. Similarly, the direction of the shift in wavelength due to substituents may be predicted in a series, as is shown in Table VII.

TABLE VII
$\pi \rightarrow \pi^*$ TRANSITION WAVELENGTH AND MO-CALCULATED Δm

Compound	$\nu\ 10^{-2}\ \mathrm{cm}^{-1}$ (*p* band)[a]	$\Delta m[(m+1)-m]$[b]
1. Benzene	484	2.000
2. Naphthalene	347	1.236
3. Phenanthrene	340	1.210
4. Chrysene	313	1.040
5. Picene	305	1.004
6. Tetraphene	278	0.905
7. Anthracene	261	0.828
8. Tetracene	212	0.590
9. Pentacene	174	0.439

[a] Clar [*51*].
[b] Streitwieser [*11*], p. 218.

TABLE VIII
MAXIMUM UV ADSORPTION OF THE SYDNONE RING AND CALCULATED VALUES OF ΔM^a

No.	Compound	ν cm^{-1}	$\Delta M(\beta)$
1	3-Methylsydnone	34483	0.481
2	3-Phenyl-4-ethylsydnone	32573	0.451
3	3-(*p*-Tolyl)-4-methylsydnone	32573	0.450
4	3-Phenylsydnone	32258	0.465
5	3-(*m*-Tolyl)sydnone	32258	0.465
6	3-(β-Pyridyl)sydnone	32051	0.461
7	3-(β-Naphthyl)sydnone	31746	0.457
8	3-Phenyl-4-acetylsydnone	30675	0.417
9	3,4-Di-(*p*-tolyl)sydnone	29586	0.405
10	3,4-Diphenylsydnone	29412	0.405

[a] Kier and Roche [29].

The use of SCF-MO methods coupled with configuration interaction is clearly superior to Hückel theory in correlating with and predicting spectral phenomena of any complexity. The interaction of excited electrons plays a prominent part in the generation of a complicated electronic spectra so that Hückel theory holds no hope for a reasonable relationship to these frequencies. SCF methods, on the other hand, have been used extensively for spectral studies.

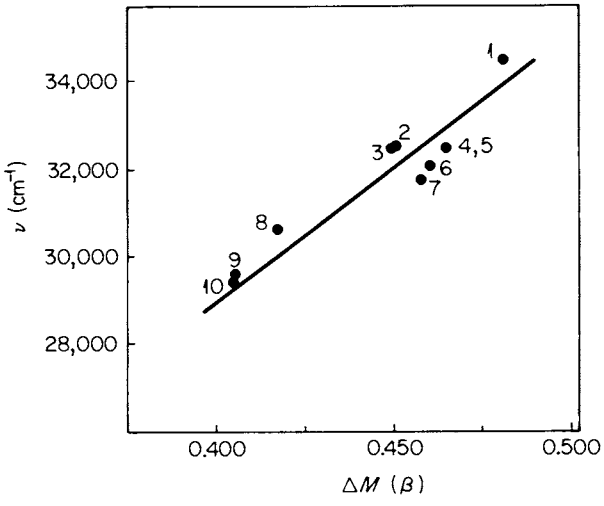

Fig. 15. Relationship between absorption frequencies and π-ω-Hückel Δm values in a series of sydnones listed in Table VIII [15].

B. Phenomena Associated with HOMO

The electron pair in a neutral molecule occupying the highest energy MO is subject to the least attraction to the core. This high-lying pair is on the frontier of the energy levels, to use a term coined by Fukui *et al.* [*30*]. Electrons in this MO have characteristics not shared by other electrons in lower lying energy levels.

1. *Ionization Potential*

The ionization potential, *Ip*, is the energy required to remove an electron from a molecule in the gas phase. The lowest energy *Ip* in a molecule corresponds approximately to the negative of the energy of the HOMO. Experimental values of this energy are obtained by ultraviolet spectroscopy, electron impact (mass spectrometry), or photoionization. Unfortunately the experimental procedures frequently give differing results, probably since somewhat different processes are taking place in the experimental procedures. As a result, correlations of *Ip* values with HOMO energies are not always good.

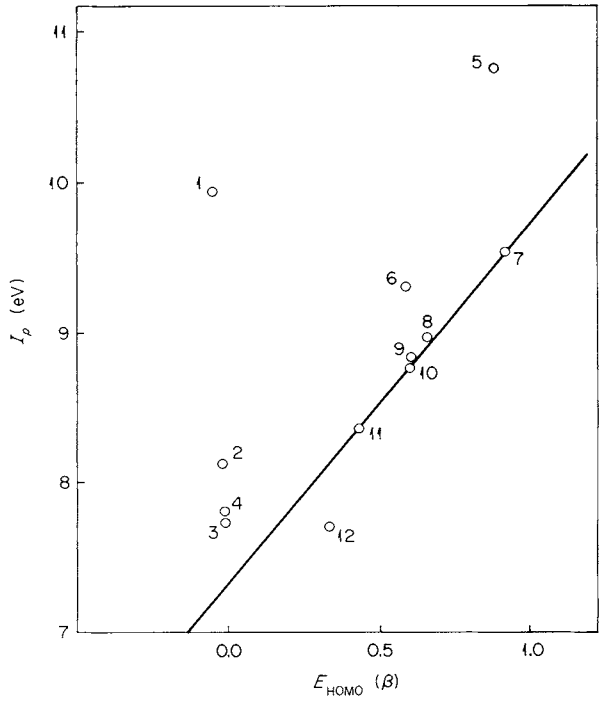

Fig. 16. Relationship between ionization potentials and $E_{(HOMO)}$. Numbering is from Table X [*31*].

TABLE IX
IONIZATION POTENTIALS AND HOMO ENERGIES[a]

Compound	I_{exp} (eV)	M_{HOMO}	X(β)
Benzene	9.57	1.000	0.167
Naphthalene	8.68	0.618	0.592
Phenanthrene	8.62	0.605	0.653
3,4-Benzphenanthrene	8.40	0.568	—
Anthracene	8.20	0.414	0.839
Tetracene	7.71	0.295	—
Ethylene	10.62	1.000	—
Butadiene	9.18	0.618	—
Styrene	8.86	0.622	—

[a] Streitwieser and Nair [*31*].

TABLE X
IONIZATION POTENTIALS FOR π-ELECTRON SYSTEMS[a]

No.	Compound	I_{exp} (eV)	MO(m_j)	$\omega = 1.4$ χ
1	Methyl	9.95	0	0
2	Alklyl	8.16	0	0.785
3	Pentadienyl	7.73	0	1.018
4	Benzyl	7.76	0	1.001
5	Ethylene	10.62	1.000	−0.370
6	Butadiene	9.18	0.618	0.310
7	Benzene	9.52	1.000	0.167
8	Styrene	8.86	0.662	0.445
9	Naphthalene	8.68	0.618	0.592
10	Phenanthrene	8.62	0.605	0.653
11	Anthracene	8.20	0.414	0.839
12	Naphthacene	7.71	0.295	0.982

[a] Streitwieser and Nair [*31*].

Using simple HMO energies for the HOMO, correlations with electron impact data have been reported within a related family of aromatic hydrocarbons [*31*] (see Table IX and Fig. 16). Extension of the correlation to *Ip* values for olefins fails, undoubtedly due to neglect of electron-repulsion terms [*32*].

Streitwieser has modified this calculation in two ways [*32*]. The MO calculations have been made using an ω technique, and the energy relating to *Ip* has been calculated as

$$I = E\,(\text{cation}) - E\,(\text{hydrocarbon}) = \alpha + X\beta$$

The values of X correlate well with *Ip* data (see Table X and Fig. 17).

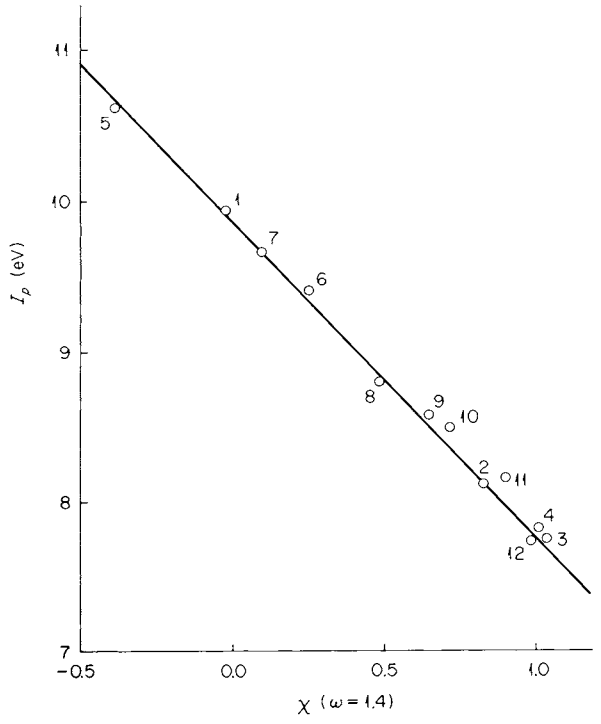

Fig. 17. Relationship between ionization potentials and calculated energy differences. Numbering is from Table X [*31*].

2. *Charge Transfer Phenomena*

Molecular complexes may be formed, in solution or in the solid state, from the transfer of an electron from the donor molecule, *D*, to the acceptor molecule, *A*. The electron donor possesses a weakly bound electron or pair of electrons, while the acceptor molecule is energetically quite receptive to the donation. In the case involving the donation of a pair of electrons as in the system

$$NH_3 \rightarrow BF_3$$

the weakly held electrons are the NH_3 lone pair. These systems have been termed coordinate covalent compounds. When a single electron participates in the transfer, it is frequently a high-lying π electron in the donor which is involved. These complexes are termed charge transfer complexes and are characteristic of many aromatic molecules.

Mulliken has described the phenomenon in quantum mechanical terms [33]. The wavefunctions of the donor and acceptor in isolation are $\psi(D)$ and $\psi(A)$, or the wavefunction of the separated pair is written as in Eq. (1).

$$\psi(D,A) = \psi(D)\psi(A) \tag{1}$$

The wavefunction for the ions D^+ and A^- in isolation will be Eq. (2).

$$\psi(D^+,A^-) = \psi(D^+)\psi(A^-) \tag{2}$$

Bringing the two molecules together may permit sufficient orbital overlap to occur so that electron exchange may take place. The wavefunction of the complex can now be written as a linear combination of the two functions [Eqs. (1) and (2)], describing the extreme cases of electron transfer and no-electron transfer states

$$\psi_{\text{complex}} = a\psi(D,A) + b\psi(D^+,A^-)$$

Solving the secular equations gives two solutions whose wavefunctions are

$$\psi_1 = a_1\psi(D,A) + b_1\psi(D^+,A^-)$$

$$\psi_2 = a_2\psi(D,A) + b_2\psi(D^+,A^-)$$

The energy of the lower energy ψ_1 is less than the energy of either $\psi(D,A)$ or $\psi(D^+,A^-)$ which accounts for the stability of the complex. The electronic transition $\psi_1 \rightarrow \psi_2$ is therefore the characteristic absorption of the complex.

In the π-electron complexes of organic molecules which will be our primary concern, the no-electron transfer state $\psi(D,A)$ will have a much lower energy than the charge transfer state $\psi(D^+,A^-)$. The interaction of these states will be small, resulting in little perturbation of the MO energy levels of the donor or acceptor molecules. As a result, in the ground state of the complex,

$$\psi_1 = a_1\psi(D,A) + b_1\psi(D^+,A^-)$$

b_1 will have a value much less than 1, indicating little charge transfer character. In the excited state of the complex

$$\psi_2 = a_2\psi(D,A) + b_2\psi(D^+,A^-)$$

a_2 will have a value much less than 1, indicating a substantial degree of charge transfer character. The electronic transition $\psi_1 \rightarrow \psi_2$ is then essentially the transfer of an entire electron from the donor to the acceptor. This transition can then be approximated by $\psi(D,A) \rightarrow \psi(D^+,A^-)$. Thus the energy involved is approximately the energy needed to transfer the electron from D to A. This energy depends upon the ionization potential of D and the electron affinity of A. From our previous consideration of the ioniza-

TABLE XI
CHARGE TRANSFER BANDS WITH TRINITROFLUORENONE AND MO-CALCULATED E_{HOMO}[a]

No.	Compound	$\lambda_{complex}(m\mu)$	$\lambda_{donor}(m\mu)$	$E_{HOMO}(\beta)$
1	Acenaphthalene	415	324	0.637
2	Anthracene	541	375	0.414
3	Azulene	535	353	0.477
4	1,2-Benzanthracene	522	359	0.452
5	1,12-Benzoperylene	570	388	0.439
6	1,2-Benzopyrene	510	332	0.497
7	3,4-Benzopyrene	590	385	0.371
8	3,4-Benzotetraphene	561	367	0.405
9	Chrysene	482	319	0.520
10	Coronene	512	342	0.539
11	1,2,3,4-Dibenzanthracene	505	349	0.499
12	1,2,5,6-Dibenzanthracene	525	351	0.473
13	1,2,3,4-Dibenzopyrene	548	402	0.398
14	1,2,4,5-Dibenzopyrene	562	378	0.442
15	Fluoranthene	430	359	0.618
16	Naphthacene	654	471	0.294
17	Naphthalene	430	285	0.616
18	Pentacene	745	576	0.220
19	Perylene	620	434	0.347
20	Phenanthrene	435	293	0.605
21	Picene	470	329	0.501
22	Pyrene	520	334	0.445
23	Triphenylene	425	284	0.684

[a] Lepley [*34*].

TABLE XII
CHARGE TRANSFER BANDS OF INDOLE DERIVATIVES WITH TETRACYANOETHYLENE[a]

Compound	$\lambda_{max}(m\mu)$	$\frac{1}{\lambda} \times 10^4$	$E_{HOMO}(\beta)$
Benzene	384	26.0	1.000
Anisole	470	21.2	0.725
Veratrole	550	18.2	0.562
Naphthalene	505	19.8	0.618
Phenanthrene	490	20.4	0.605
Indole	510	19.6	0.600
4-MeO-indole	715	14.0	0.473
5-MeO-indole	610	16.4	0.592
6-MeO-indole	680	14.7	0.489
7-MeO-indole	660	15.1	0.518
Tryptamine	500	20.2	0.549
5-MeO-tryptamine	615	16.2	0.540
4,5-$(MeO)_2$-indole	720	13.9	0.465

[a] Millie *et al.* [*35*].

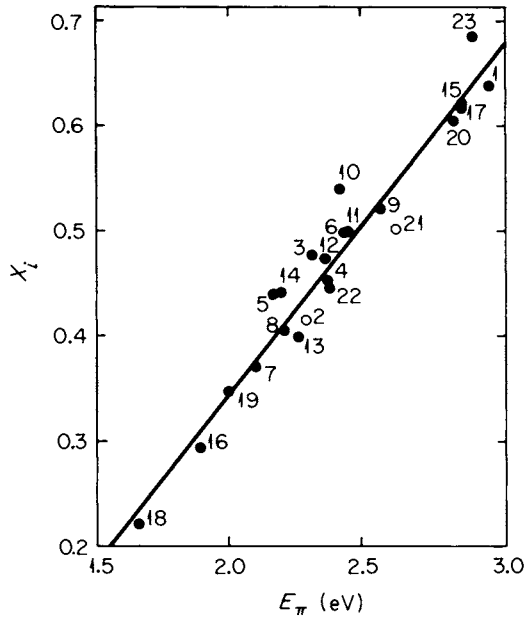

Fig. 18. Charge transfer energies, E_π, against HOMO coefficient, χ_i, for complexes between hydrocarbons designated in Table XI and trinitrofluorenone [*34*].

tion potential we have seen how this energy can be correlated with the energy of the HOMO, in this case, in the donor molecule. Similarly, the electron affinity of a molecule bears a relationship to the energy of the LEMO.

If we are considering a series of donor molecules forming a complex with a common acceptor, the charge transfer bands of the complex should be related to the HOMO energies of the donor molecule. Such a relationship has been found in numerous cases. An example is shown in Table XI and Fig. 18 [*34*].

The relationship between HOMO energy and charge transfer bands has been extended to heterocycles [*35*] (Table XII).

III. Properties Related to Charge

The distribution of electronic charge in a molecule is responsible for a number of observable phenomena, such as the electric dipole moment. The charge distribution may also play a part in the orientation of an attacking reagent, hence may be used in some cases as an index of chemical reactivity.

We have shown that the probability of finding an electron in a volume of space $d\tau$ is $|\psi|^2 d\tau$. For the assumption of the linear combination of atomic orbitals, the probability or charge in the vicinity of an atom is described by Eq. (3)

$$q_i = \sum_{\text{occ}} n_j c_{ij}^2 \tag{3}$$

where n is the orbital occupancy and q the electron density. The charge in excess or deficiency of that needed to neutralize the core charge is the charge density, Q.

$$Q_i = \text{core charge} - q_i$$

A. Dipole Moments

In a simple diatomic molecule such as H_2, the size of the overlapping orbitals will be the same, as will the electronegativity of the cores. As a result, shared electrons will be uniformly distributed between the atoms in the bond. This will result in no differentiation of the electrical character of either atom, and the molecule will have no dipole moment. If the bond were composed of different atoms leading to an unequal sharing of bonding electrons, the displacement toward one atom in the MO leads to a moment, a dipole moment, μ, for the molecule.

Picking an arbitrary point in the molecule and drawing vectors, r, to each charge, q, in each of the three Cartesian axes, we get a moment along each axis approximated by

$$\mu_x = e(q_{1x}r_{1x} + q_{2x}r_{2x} \cdots q_{nx}r_{nx})$$

The moment is independent of the origin of the vectors r, only if the molecule is neutral.

The total moment of a conjugated molecule can be dissected into the moments due to localized σ bonds and the delocalized π systems. This assumes noninteraction of the two systems which is implicit in Hückel theory. The assumption neglects the polarizing influence of strongly electronegative atoms like Cl in the σ system. This polarizing effect may be partially compensated for by a selection of π-Hückel parameters which reflect this effect. The σ-bond moments may be regarded as being relatively uniform in organic molecules, and therefore can be estimated from a consideration of the same σ bond in a variety of molecules which have experimentally derived total moments available [*36*]. A π moment can be calculated by assuming the total charge density to be centered on each atom. The vectors, r, are drawn from some convenient point in the molecule toward the atom with negative charge density and toward the origin if the atom has a positive charge density.

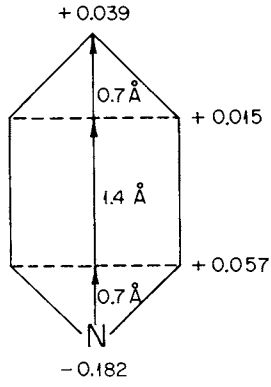

Fig. 19. Calculated π charge densities and dimensions for pyridine used to calculate π dipole moment.

Pyridine serves as a useful example of this calculation (Fig. 19). In this particular case [*37*] uniform bond lengths of 1.40 Å were assumed, the ω-Hückel theory was used for the π charge density calculations, whereas the σ charge densities were calculated by Del Re's bond orbital method [*38*]. The calculations are shown in Eq. (4)

$$\mu_\pi = 4.77[(2)(0.057)(0.7) + 2(0.015)(2.1) + (0.039)(2.8)] = 1.21 \text{ Debye} \quad (4)$$

Advantage is taken of the symmetry of the molecule along the N to C-4 axis so that the vectors coincide with this axis. The value 4.77 is the charge of the electron in the appropriate units. From the σ charge calculations, the value $\mu = 0.74$ Debye is obtained [*37*]. The total $\mu = 1.95$ is in good agreement with the experimental value of 2.15 D. The direction of the moment is away from the nitrogen, toward the C-4.

It is known charges in the simple Hückel calculations tend to be exaggerated since the effect of electron interaction with neighbors is not considered. This electron correlation is treated approximately in the ω treatment resulting in a smoothing out of the charge densities. As a result, more reasonable estimates of dipole moments may be expected from the use of the ω-Hückel techniques.

It is generally true that SCF π charge densities are superior in calculating the dipole moment. Extended Hückel theory has not proven satisfactory for dipole calculations because of exaggerated charges. The SCF all-valence electron CNDO/2 method appears to be superior for at least small molecules. A good example of an SCF all-valence electron calculation of reasonable dipole moments is available using CNDO/2 [*39*] (see Table XIII).

TABLE XIII
CNDO/2 CALCULATIONS OF DIPOLE MOMENT[a]

Compound	Dipole moment	
	Calculated	Observed
Hydrocarbons		
Propane	0.00	0.083
Propene	0.36	0.364
Propyne	0.43	0.75
2-Methylpropane	0.00	0.132
2-Methylpropene	0.65	0.503
2-Methyl-1,3-butadiene	0.25	0.292
Toluene	0.21	0.43
Fluorine compounds		
Hydrogen fluoride	1.85	1.8195
Methyl fluoride	1.66	1.855
Methylene fluoride	1.90	1.96
Fluoroform	1.66	1.645
Ethyl fluoride	1.83	1.96
1,1-Difluoroethane	2.23	2.30
1,1,1-Trifluoroethane	2.18	2.32
Fluoroethylene	1.51	1.427
1,1-Difluoroethylene	1.02	1.37
cis-1,2-Difluoroethylene	2.83	2.42
Fluoroacetylene	1.04	0.75
n-Propyl fluoride (*trans*)	1.84	2.05
trans-1-Fluoropropene	1.67	1.85
cis-1-Fluoropropene	1.59	1.46
2-Fluoropropene	1.69	1.60
3-Fluoropropene (*s-cis*)	1.83	1.765
3,3,3-Trifluoropropene	2.34	2.45
3,3,3-Trifluoropropyne	2.48	2.36
2-Fluoro-1,3-butadiene	1.65	1.417
Fluorobenzene	1.66	1.66
Oxygen compounds		
Water	2.10	1.846
Methanol	1.94	1.69
Dimethyl ether	1.83	1.30
Formaldehyde	1.98	2.339
Acetaldehyde	2.53	2.68
Acetone	2.90	2.90
Acrolein (*s-trans*)	2.63	3.11
Methyl vinyl ketone	2.92	3.16
Ketene	1.30	1.414
Methylketene	1.35	1.79
Formic acid	0.87	1.415
Phenol	1.73	1.55

TABLE XIII *(continued)*

Compound	Dipole moment	
	Calculated	Observed
Nitrogen compounds		
Ammonia	1.97	1.468
Methylamine	1.86	1.326
Dimethylamine	1.76	0.612
Hydrogen cyanide	2.48	2.986
Methyl cyanide	3.05	3.92
Trimethylamine	1.68	0.612
Mixed compounds		
Nitrogen trifluoride	0.43	0.235
Difluoramine	2.13	1.93
Nitrous acid	2.27	1.85
Nitric acid	2.24	2.16
Cyano fluoride	1.55	1.68
Formyl fluoride	2.16	2.02
Carbonyl fluoride	1.42	0.951
Acetyl fluoride	2.84	2.96
Acetyl cyanide	2.80	3.45
Isocyanic acid	1.88	1.59
Methyl isocyanate	1.80	2.81
Formamide	3.79	3.71
Nitromethane	4.38	3.46
Nitrobenzene	5.33	4.28

[a] Pople and Gordon [*39*].

B. Charge Densities and Chemical Reactivity

In a previous discussion of MO indices relating to chemical reactivity, we described the use of the localization energy to approximate the free energy of activation. This was based on the assumption that the transition state was closely approximated by a localized π-electron response at an atom encountering an attacking reagent. This is known as the localization or dynamic model. It assumes that the energy barrier to the reaction occurs with an intimate contact of reactants, resulting in a bond forming between the two, and a significant perturbation of the π electrons.

Another concept of reactivity centers on the view that in some systems, the rate-limiting step leading to the transition state is the formation of a loose complex formed between reactants, determined by the ground state structures of the two molecules. Thus the π system will be little perturbed and the electronic indices such as charge density and free valence will largely

determine the position of reagent attack in a molecule and may correlate with the relative rate among a series of similar molecules. This concept is called the isolated molecule approximation or static model [*40*].

The static model is part of the classical chemical intuition of the chemist and has its roots in the valence bond or resonance concept of "hybrid" structures, giving rise to the accumulation of π-electron charge at one atom and a π-electron deficit at another. The electronic charge pattern is then used to deduce preferred sites of reagent attack. In the MO framework, this implies that the charges, rather than perturbations induced by the reagents on each other, limit the reaction.

This view may be hard to justify from theoretical considerations. The charge densities may be considered to be responsible for the bringing together of the reactants into an orientation in which the transition state may be formed. The localization or dynamic model, however, probably reflects the character of the rate-limiting phenomenon, hence the localization energy may be a better way to approximate the free energy of activation. The static or isolated model of the reaction and the use of charge density indices of reaction may have validity if these charges play a significant role in determining the nature of the subsequent perturbations in the dynamic model. Some successes have been recorded in correlating reactivities with charge densities and in predicting sites of preferential attack.

It is apparent that the static model predicts an electrophilic attack at a site in a molecule with the largest negative charge density, and a nucleophilic attack at a site with the largest positive charge density. Radical attack will be discussed, in the framework of the static model, under a consideration of free valence. Charge density calculations on the azulene molecule illustrate a successful prediction of the position of attack (Fig. 20). Each calculation correctly predicts the 3 position to be most susceptible to

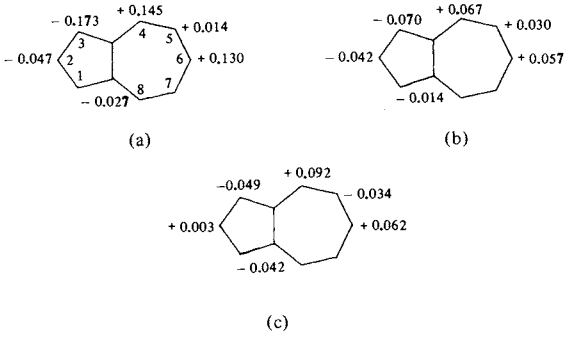

Fig. 20. Calculated π charge densities for azulene using (a) simple Hückel [*41*], (b) ω-Hückel [*42*], and (c) SCF [*43*].

electrophilic attack and the 4 position to be most favored for nucleophilic attack.

This success and a few other correct predictions, as in the monosubstituted benzene reactivities, are overshadowed by the frequent failures encountered. The use of charge density as a reactivity index should be used with caution.

C. Frontier Electron Theory and Reactivity

A different approach to reactivity using the isolated molecule approximation was proposed by Fukui *et al.* [*30*]. The theory presumes that the least tightly bound electron would react preferentially with an electrophilic reagent. The π electrons in the HOMO would thus be important in the reaction. The position in the molecule with the greatest density in these MO's would presumably be the most reactive. These orbitals are known as frontier orbitals and the electrons as frontier electrons.

Nucleophilic reactivity would be predicted to occur at a position in the molecule having the highest density of two ghost electrons in the LEMO. The symbols $f_r^{(E)}$ and $f_r^{(N)}$ are used for the electron density, $2C_{fr}^2$, at atom r for the frontier orbital, f, for electrophilic or nueleophilic attack. The index permits only a comparison of relative reactivities within the same molecule.

The concept was extended to permit comparison of the reactivities of positions in different molecules [*44*]. The index, called superdelocalizability, S_r, is defined as

$$S_r = 2\sum_{j=i}^{m} \frac{C_{jr}^2}{m_j}$$

where m is the HOMO energy (in terms of β) for electrophilic attack or the LEMO energy for nucleophilic attack. The index thus incorporates a consideration of charge transfer capability, along with an orbital charge at a particular atom.

As an example, butadiene in the HOMO has the structure $\psi_{II} = 0.60\phi_1 + 0.37\phi_2 - 0.37\phi_3 - 0.60\phi_4$, $E = \alpha + 0.62\beta$. For the 1 and 2 position, the indices become

$$f_1^{(E)} = 2(0.60)^2 = 0.72; \qquad f_2^{(E)} = 2(0.37)^2 = 0.27$$

$$S_1^{(E)} = 2\left(\frac{0.37^2}{1.62} + \frac{0.60^2}{0.62}\right) = 1.33; \qquad S_2^{(E)} = 2\left(\frac{0.60^2}{1.62} + \frac{0.37^2}{0.62}\right) = 0.89$$

It can be shown that in this case the values of $f^{(N)}$ and $S^{(N)}$ for both positions will be the same as for the electrophilicity indices. The two indices predict

both nucleophilic and electrophilic attack preferentially at the 1(4) position in butadiene. The method has been successfully employed in predicting reactivity in a series of heterocyclic aromatic molecules [*45*].

The superdelocalizability index has also been defined for radical attack where

$$S_r^{(R)} = \sum_{j=1} \frac{C_{jr}}{m_j} + \sum_{j=m+1} \frac{C_{jr}^2}{-m_j}$$

D. Free Valence and Reactivity

The free valence, f_r, at an atom r is the "leftover" π-bonding power when the bond orders centering on atom r are summed and subtracted from the maximum π-bond order which can be achieved. The index has its roots in Thiele's concept of residual affinity. For butadiene the values are

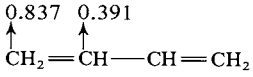

It has been reasoned that this "unused bonding power" renders the positions with higher f_r values more susceptible to attack. Thus the 1(4) position in butadiene is correctly predicted to be the most susceptible to a radical attack. Radical reactivity has been of special interest as far as this index is concerned. Some success has been achieved in predicting free radical reactivity (see Fig. 21) [*46*].

Correlations are only fair in most cases, and appear to be limited to radical reactions. The free valence, like the charge density reflects "early" events along the reaction coordinate, hence may not presage the remainder of the potential energy curve leading to the transition state.

E. Bond Order and Bond Length

The bond order, $p_{rs} = \sum_j n_j C_{jr} C_{js}$, may conceptually be related to the binding power of a bond or a bond electron density. This physically relates to the valency between the bonded atoms or the number of formal bonds which can be assigned. Ethane, ethylene, and acetylene, considered as standards, have π-bond orders of 0, 1, and 2, respectively. This would correspond to bond lengths in these molecules of 1.54, 1.33, and 1.20 Å, respectively. An MO-calculated π-bond order will likely have some intermediate value of p_{rs} denoting a fractional part of a standard bond order, and some intermediate value of the bond length. Thus the bonds in benzene have a π-bond order of 0.67, intermediate between ethane and ethylene, and a bond length of about 1.40 Å, also an intermediate dimensional value.

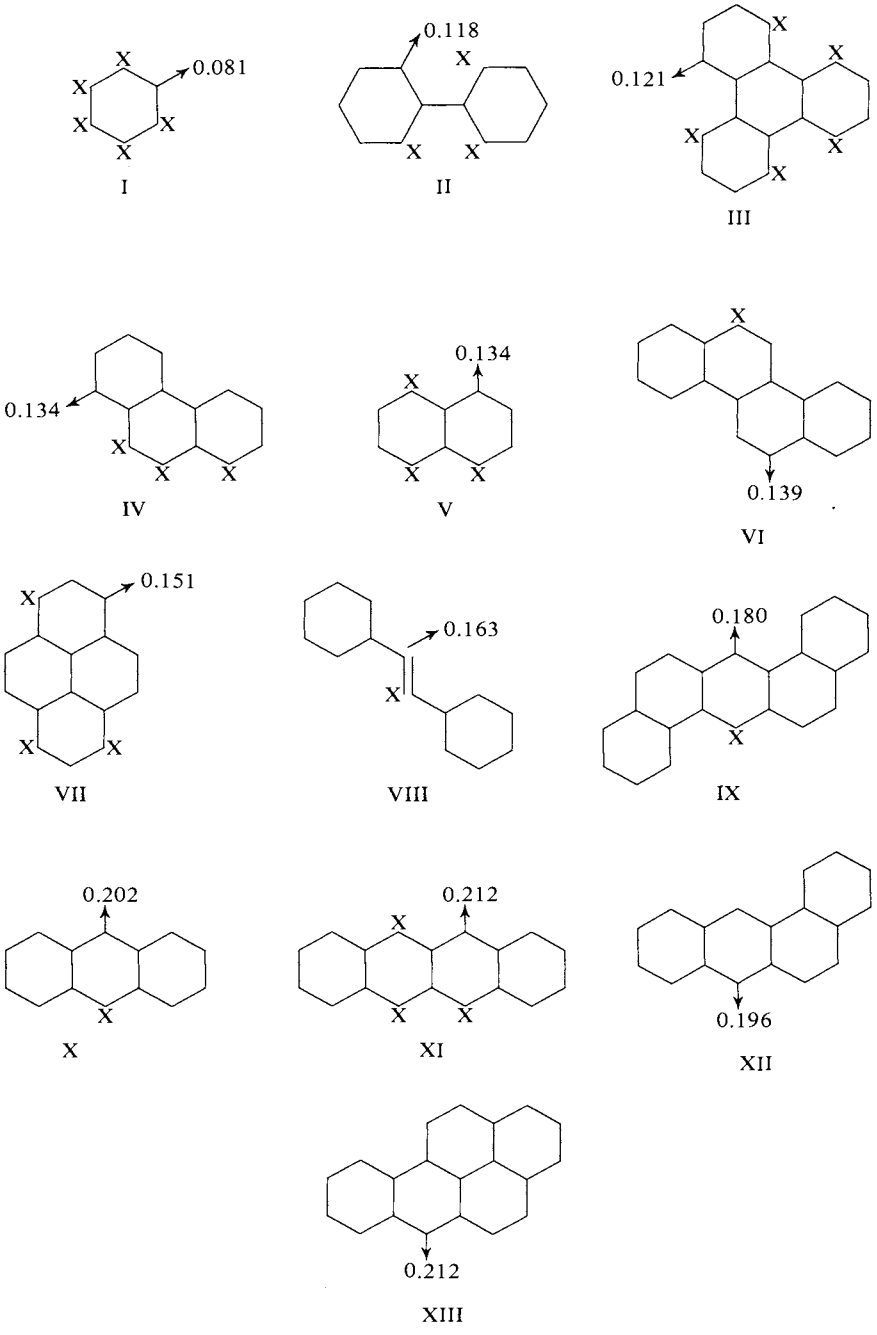

Fig. 21. Positions of maximum free valence in a series of hydrocarbons, with positions equivalent to maximum value identified with X [*46*].

Coulson has derived an approximate relationship between p_{rs} and bond length, R, which in linear form is Eq. (5)

$$R_{rs} = 1.517 - 0.180p_{rs} \tag{5}$$

based on bond orders and bond lengths for ethylene and benzene of 1.000, 1.337 Å and 0.667, 1.397 Å, respectively [*47*].

Using simple Hückel theory, the method fails to predict accurately the bond lengths in butadiene, probably due to the assumption of all equal β's. More advanced MO methods generally improve the treatments of polyenes.

The ω-Hückel procedure leads to a bond order–bond length relationship

$$R_{rs} = 1.524 - 0.194p_{rs}$$

which provides a good fit with experimental data [*48*] (see Table XIV and Fig. 22).

F. Bond Orders and Infrared Frequencies

Transitions between vibrational levels in a molecule give rise to absorption bands in the infrared region of the spectrum. An analysis has indicated that the force constant of a vibration is due to the bond order and bond polarizability [*49*]. The relationship between the π-bond order and the infrared stretching frequency has been tested and found to correlate, even though the σ system is ignored [*50*]. The relationship holds only for a closely related series (see Table XV).

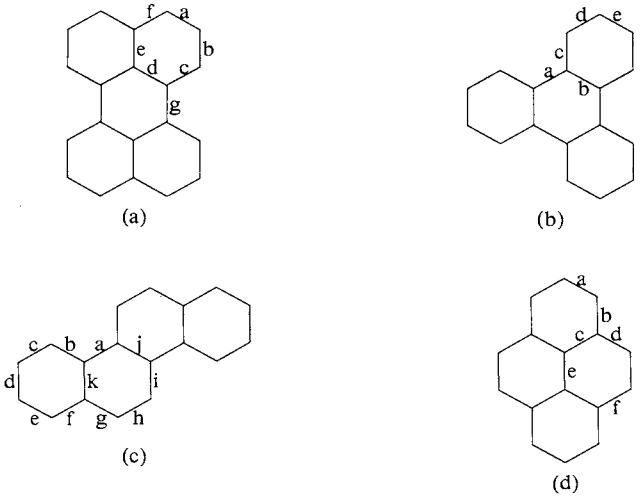

Fig. 22. Bond designations for (a) perylene, (b) triphenylene, (c) chrysene, and (d) pyrene [*48*].

TABLE XIV
OBSERVED AND CALCULATED BOND LENGTHS[a]

Compound	Bond	Calculated R_{rs}	Observed R_{rs}
Perylene	a	1.381	1.370
	b	1.408	1.418
	c	1.391	1.397
	d	1.423	1.425
	e	1.417	1.424
	f	1.420	1.400
	g	1.454	1.471
Triphenylene	a	1.448	1.447
	b	1.410	1.415
	c	1.407	1.416
	d	1.388	1.377
	e	1.403	1.402
Chrysene	a	1.435	1.468
	b	1.414	1.409
	c	1.382	1.381
	d	1.410	1.394
	e	1.381	1.363
	f	1.416	1.428
	g	1.430	1.421
	h	1.371	1.369
	i	1.427	1.428
	j	1.404	1.401
	k	1.414	1.409
Pyrene	a	1.394	1.380
	b	1.405	1.420
	c	1.419	1.417
	d	1.436	1.442
	e	1.425	1.417
	f	1.365	1.320

[a] Boyd and Singer [*48*].

TABLE XV
MO BOND ORDERS AND CARBONYL INFRARED FREQUENCIES[a]

Compound	Bond order	ν_{CO} cm^{-1}
Formaldehyde	0.958	1744
Glyoxal	0.938	1730
Benzaldehyde	0.905	1708
Acrolein	0.895	1700
9,10-Phenanthraquinone	0.885	1683
o-Benzoquinone	0.879	1669
9,10-Anthraquinone	0.860	1679
1,2,5,6-Dibenz-9,10-anthraquinone	0.858	1663
Benzophenone	0.857	1664
1,8-Pyrenequinone	0.833	1645
Naphthophenone	0.820	1644
Diphenoquinone	0.819	1626

[a] Berthier *et al.* [*50*].

References

1. B. Pullman and A. Pullman, "Les Theories Electroniques de la Chimie Organique," p. 226. Masson, Paris, 1952.
2. G. W. Wheland, "Resonance in Organic Chemistry," p. 98. Wiley, New York, 1955.
3. M. J. S. Dewar and G. J. Gleicher, *J. Amer. Chem. Soc.* **87**, 3255 (1965).
4. L. Watts, J. D. Fitzpatrick, and R. Pettit, *J. Amer. Chem. Soc.* **87**, 3253 (1965).
5. W. Baker, W. D. Ollis, and V. D. Poole, *J. Chem. Soc., London* p. 307 (1949).
6. M. Cynitti and L. Paoloni, *Theor. Chim. Acta* **7**, 383 (1967).
7. E. Clar, and J. W. Wright, *Nature (London)* **163**, 921 (1949).
8. Y. Syrkin and M. Diatkina, *Acta Physicochim. (USSR)* **21**, 641 (1948).
9. R. Daudel, R. Lefebvre, and C. Moser, "Quantum Chemistry," Ch. XI. Wiley (Interscience), New York, 1959.
10. G. W. Wheland, *J. Amer. Chem. Soc.* **64**, 900 (1942).
11. A. Streitwieser, "Molecular Orbital Theory for Organic Chemists," Wiley, New York, 1961.
12. M. Szwarc, *J. Phys. Chim.* **61**, 40 (1957).
13. H. Baba, *Bull. Chem. Soc. Jap.* **30**, 147 (1957).
14. L. B. Kier, *J. Pharm. Sci.* **55**, 98 (1966).
15. R. Hoffmann, *J. Chem. Phys.* **39**, 1397 (1963).
16. J. C. Slater, "Quantum Theory of Molecules and Solids," Vol. I, p. 108, McGraw-Hill, New York, 1963.
17. L. C. Allen and J. D. Russell, *J. Chem. Phys.* **46**, 1029 (1967).
18. B. P. Van Eijck, *Rec. Trav. Chim.* **85**, 1129 (1966).
19. L. B. Kier, *Tetrahedron Lett.* p. 1233 (1967).
20. F. Jordan and B. Pullman, *Theor. Chim. Acta* **9**, 242 (1968).
21. W. Giordano, J. Hamann, J. Hawkins, and J. Kaufman, *Mol. Pharmacol.* **3**, 307 (1967).
22. W. Herndon, J. Fever, and L. Hall, *Tetrahedron Lett.* p. 2625 (1968).
23. L. B. Kier, *J. Pharmacol. Exp. Ther.* **164**, 75 (1968).
24. H. Kato, K. Morokuma, T. Yonezawa, and K. Fukui, *Bull. Chem. Soc. Jap.* **38**, 1749 1965).
25. W. Adam and A. Grimison, *Tetrahedron* **22**, 835 (1966).
26. R. B. Hermann, *Int. J. Quantum Chem.* **2**, 165 (1968).
27. H. H. Jaffe and M. Orchin, "Theory and Applications of Ultraviolet Spectroscopy," Wiley, New York, 1962.
28. C. Sandorfy, "Electronic Spectra and Quantum Chemistry," Prentice-Hall, Englewood Cliffs, New Jersey, 1964.
29. L. B. Kier and E. B. Roche, *J. Pharm. Sci.* **55**, 807 (1966).
30. K. Fukui, T. Yonezawa, and H. Shingu, *J. Chem. Phys.* **20**, 722 (1952).
31. A. Streitwieser and P. M. Nair, *Tetrahedron* **5**, 149 (1959).
32. A. Streitwieser, *J. Amer. Chem. Soc.* **83**, 4123 (1961).
33. R. S. Mulliken, *J. Amer. Chem. Soc.* **72**, 600 (1950).
34. A. R. Lepley, *J. Amer. Chem. Soc.* **84**, 3577 (1962).
35. P. Millie, J. P. Molrieu, J. Benaim, J. Y. Lallemand, and M. Julia, *J. Med. Chem.* **11**, 207 (1968).
36. G. W. Wheland, "Resonance in Organic Chemistry," p. 207. Wiley, New York, 1955.
37. L. B. Kier, *Tetrahedron Lett.* p. 3272 (1965).
38. G. Del Re, *J. Chem. Soc., London* p. 4031 (1958).
39. J. A. Pople and M. Gordon, *J. Amer. Chem. Soc.* **89**, 4253 (1967).
40. L. Pauling and G. W. Wheland, *J. Amer. Chem. Soc.* **57**, 2086 (1935).

41. C. A. Coulson and H. C. Longuet-Higgins, *Rev. Sci.* **85**, 929 (1947).
42. G. Berthier and B. Pullman, *C. R. Acad. Sci.* **229**, 761 (1949).
43. A. Julg, *C. R. Acad. Sci.* **239**, 1498 (1954).
44. K. Fukui, T. Yonezawa, and C. Nagata, *Bull. Chem. Soc. Jap.* **27**, 423 (1954).
45. M. Holik, V. Skala, and J. Kuthan, *Coll. Czech. Chem. Commun.* **33**, 394 (1968).
46. E. K. Kooyman and E. Forenhorst, *Trans. Faraday Soc.* **49**, 58 (1953).
47. C. A. Coulson and A. Golebiewski, *Proc. Phys. Soc., London* **78**, 1310 (1961).
48. G. V. Boyd and N. Singer, *Tetrahedron* **22**, 3383 (1966).
49. C. A. Coulson and H. C. Longuet-Higgins, *Proc. Roy. Soc., Ser. A* **193**, 456 (1948).
50. G. Berthier, B. Pullman, and J. Pontis, *J. Chim. Phys.* **49**, 367 (1952).
51. E. Clar, "Aromatische Kohlenwasserstoffe." Springer, Berlin, 1952.

Chapter V

PRACTICAL CONSIDERATIONS OF MOLECULAR ORBITAL APPLICATIONS

Before proceeding with a discussion of the application of MO theory to studies on drug molecules, it is important that some limitations be defined. We have spent three chapters on quantum mechanics, MO theory, and calculated indices, and have reached a certain level of understanding as to what we can accomplish in deducing molecular structure and properties. This is only half of the drug structure–activity dualism that we ultimately seek to relate. It is necessary to consider what is meant by activity, what experimental data we can use, and what factors contribute to pharmacological activity.

I. Biological Events

To begin, we must accept the fact that MO calculations, as they are currently employed, hopefully relate strictly to the drug–receptor interaction. It is presumed that the drug is in the biophase and ready for action. How it got there is a considerably involved process, however, and the barriers encountered may well be the limiting events controlling activity. A comparison between MO-calculated indices and an observed biological response may not be reflecting a rate-limiting reaction at the receptor, but may be reflecting another limiting event prior to the drug entering the biophase. The structural features controlling this prebiophase event may be considerably different from features controlling receptor events.

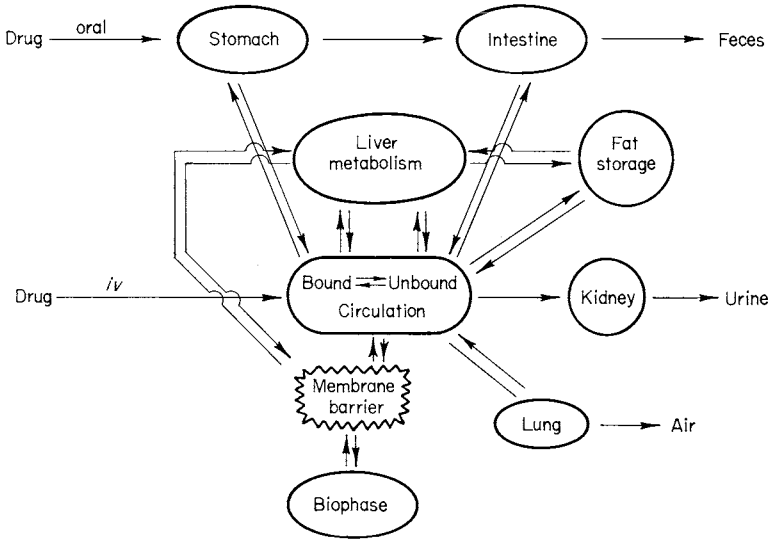

Fig. 1. Schematic diagram of *in vivo* drug events and compartments.

It is useful to consider the events encountered by a drug prior to the time it actually engages the receptor. These can be summarized diagrammatically as in Fig. 1. A brief discussion of each prebiophase event is necessary.

A. Drug Absorption

The route of administration of the drug determines whether the limiting factors of the gastrointestinal tract are invoked. Absorption of most drugs from the stomach is dependent on whether the drug is capable of existing in an un-ionized, hence more lipid-soluble form in the acid stomach. Acidic drugs and weakly basic amines will be largely un-ionized, hence absorption through the stomach wall is possible.

The small intestine is increasingly less acidic at increasing distance from the stomach. As a result, neutral to basic drug molecules will be un-ionized in this environment and the chances of absorption through the wall are increased.

These factors are pK_a-dependent and are therefore amenable to study, using MO theory as an approximation of the relative energy involved in protonation in a closely related series. Chapter IX will deal with this problem.

The presence of a favorable pK_a in a molecule does not insure that it will be absorbed or diffuse across a membrane barrier. The actual diffusion or passage through a barrier, if active transport is not involved, is controlled by thermodynamic factors. A further complication arises from the possi-

bility of forming a nonabsorbable complex with some molecule such as mucopolysaccharide in the lumen or on the walls of the gastrointestinal tract. These last two effects are not directly relatable to MO-calculated indices, but must be factored out of absorption data, if possible, in order to relate absorption due to pK_a with an MO-calculated index.

The contribution of the membrane diffusion process, due to thermodynamic forces, to the overall activity of a drug molecule has been treated by a procedure developed by Hansch [*1*]. He has defined a comparative substituent constant, π, in terms of the partition coefficient P as

$$\pi = \frac{P \text{ (octanol/water) drug with substituent}}{P \text{ (octanol/water) drug with no substituent}}$$

The term π is a free energy-related term like the Hammett σ function and is a measure of the free energy change resulting in the passage of a substance from one phase to another. It is essentially the contribution of the substituent on a molecule to this free energy, relative to the same molecule without the substituent.

It has been found that these π values for different substituents are quite constant among different molecular series, hence standard values of these contributions can be tabulated. Further, it has been found that these π values are additive, hence the contributions to the ability of a molecule to pass into an organic phase can be approximated by summing the π values for its substituents.

This technique makes it possible to determine if the activity-limiting factor in a drug molecule series is the ability to pass a barrier, based upon the prominence of the π term in the equation

$$\log 1/\mathrm{ED}_{50} = -k\pi^2 + k'\pi + \rho\sigma + k''$$

where ED_{50} is the effective dose giving a 50% response, $\rho\sigma$ the Hammett equation terms describing the electronic contribution, and the k's, constants. Regression analyses of these equations reveal the importance of the terms. The Hammett σ term can be replaced by an MO-calculated index reflecting the enthalpy contribution to the relative free energy of activation for a particular reaction.

Rogers and Cammarata have sought to relate the partition coefficients of a series of aromatic molecules with MO-calculated indices [*2*]. They found that the log of the partition coefficients, P, were related to the sum of the electrophilic superdelocalizabilities for the aryl atoms, $\sum S_r$, and the sum of the π-electron charge densities, $\sum |Q_r|$ according to the regression equation

$$\ln P = 0.6670 \sum S_r - 2.5395 \sum |Q_r| + 0.4777$$

The correlation coefficient for the equation, $r = 0.978$, indicates a good level of agreement (see Table I). These authors dissected the equation into a hydrophilicity factor, $\sum |Q_r|$ contributing negatively and a lipophilicity factor, $\sum S_r$, contributing positively. The Q_r term was thought to reflect an aqueous solubilization due to a charge–dipole interacting mechanism. The S_r term, conceded to be more complex, was suggested as representing the ability to form a weak bond in a charge transfer state involving the compound and the organic solvent.

The study is encouraging and suggests that MO theory may have expanded utility in correlating with and predicting some thermodynamic properties of molecules.

It is possible to minimize or eliminate the absorption or partitioning factor in studying structure–activity relationships by designing drug evaluation experiments which, as closely as possible, reflect a direct action of the drug on the receptor. This necessitates the virtual abandonment of

TABLE I

TOTAL ABSOLUTE CHARGE DENSITIES (ΣQ_r), TOTAL ELECTROPHILIC SUPERDELOCALIZABILITIES (ΣS_r) AND LOGARITHMS OF PARTITION COEFFICIENTS ($\ln \bar{P}$) FOR AROMATIC MOLECULES[a]

Compound	$\sum S_r$	$\sum \lvert Q_r \rvert$	Calcd. $\ln \bar{P}$	Exptl. $\ln \bar{P}^*$	$\ln \bar{P}^*/\ln \bar{P}^b$
Carbazole	12.177	0.448	7.576	7.462	0.985
Diphenylamine	12.302	0.496	7.427	7.423	0.999
Biphenyl	10.292	0.000	7.272	7.342	1.010
Thianaphthene	14.698	1.340	7.113	6.878	0.967
Naphthalene	8.874	0.000	6.932	6.397	0.922
5-Bromoindole	11.451	0.552	6.906	6.714	0.972
1,2-Dimethylindole	12.051	0.744	6.498	6.626	1.020
5-Methylindole	10.427	0.614	6.180	5.873	0.950
N,N-Dimethylaniline	10.226	0.315	6.026	6.498	1.078
3-Methylindole	10.691	0.529	5.984	6.265	1.047
Indole	9.114	0.518	5.182	5.241	1.011
Toluene	6.253	0.170	4.852	4.217	0.869
Quinoline	8.333	0.484	4.754	4.807	1.011
Anisole	7.672	0.235	4.700	4.998	1.063
Benzothiazole	12.000	1.426	4.673	4.860	1.040
Indazole	8.991	0.708	4.190	4.677	1.116
Benzoxazole	8.114	0.884	3.664	3.645	0.996
Benzene	4.998	0.000	3.584	3.811	1.063
Oxindole	8.843	1.558	2.639	2.419	0.917

[a] Rogers and Cammarata [2].

[b] Ratio expresses closeness of calculated data to experimental data.

in vivo studies and requires the use of *in vitro* isolated tissue or cell studies. Although the structure–activity relationship problem is simplified, the correspondence of the *in vitro* study to *in vivo* events now comes under question.

B. Drug Distribution

Referring again to Fig. 1, following absorption into the circulating fluids in the body, most drugs bind to proteins such as the albumin fraction in the plasma. In this complex, the drug is capable of being transported in the body. The bound drug is far less susceptible to metabolism, excretion, and distribution into tissues, hence to the exertion of its action at a receptor. The rate of dissociation from plasma protein may be the limiting factor in achieving a sufficient concentration in the biophase to produce a desired response level.

Once again, the use of *in vitro* isolated tissue systems to derive biological activity data relatable to structural modification is an approach. The relationship to *in vivo* response comes under the same criticism as previously mentioned.

C. Drug Metabolism

An event may occur prior to the entrance of the drug into the biophase, severely limiting the effective concentration. The metabolic change of an appreciable amount of the circulating drug by enzymes in the plasma or the liver may well be the limiting factor influencing activity. Isolated enzyme studies are necessary to reveal this. Metabolism may also convert a molecule into an active form, the phenomenon also being rate-limiting as far as the final receptor activity. The structural requirements for metabolic change are likely just as specific as are the requirements for receptor activity, but, at the same time, may be quite different. It is necessary to have biological data which are free from metabolic effects if MO calculations are to be used to reflect drug–receptor events.

II. Biological Data

As we have seen, the use of *in vivo* biological data to correlate with molecular structure is severely limited by the complexity of events, giving rise to the ultimately measured *in vivo* response. In an *in vitro* experiment on isolated tissue or organ, suspended in a fluid, the influence of absorption, transport, metabolism, and excretion is reduced to a minimum. If confidence can be obtained in the relationship between a suitable *in vitro* experiment and *in vivo* events, then the biological data can be used to study structural requirements for activity.

III. MO Calculations

Some general remarks on the choice of MO indices and the interpretation of relationships with biological data are in order.

A. MO Indices

It is one thing to calculate an index from MO theory in a series of molecules, but it is another matter to relate this index to a realistic reaction in which the drug may undergo in a biological environment. The index calculated must therefore represent an event in which the drug may participate. This would exclude certain high energy reactions and would therefore render MO indices reflecting spectral transitions as comparatively meaningless. Other combinations of indices reflecting certain types of high energy bond-forming reactions would also have little bearing on biological events. Where a correlation exists between a biological action and an MO index representing an improbable reaction, it is likely that embodied within the index are other relationships more directly related to the possible chemical event. Thus a correlation between activity and an index reflecting a $\pi \rightarrow \pi^*$ electron transition may in fact be correlating activity with an E_{HOMO}, with a relatively constant E_{LEMO}. This would then be more realistically interpreted as implying a relationship with charge transfer donation rather than an electronic transition.

It is equally important that the index calculated for a particular position on a molecule reflect a chemical event that can actually take place at that position, in a biological environment. In other words, classical chemical intuition and experience must serve as a guide and a check on MO-calculated predictions.

Finally, the quality of the MO indices themselves must be evaluated. We can say with some assurance that indices calculated with Hückel theory involving virtual orbitals are not too reliable. The value of correlations relating such indices to biological activity then comes under some question.

B. Value of Correlations

From statistics we can establish the criteria for meaningful, marginal, or nonexistant correlations between variables. The questions that should be asked in evaluating or designing a study are: (*a*) are the number of cases enough to be meaningful, and (*b*) is the correlation sufficient to account for most of the variation? Neglect of these factors may render a study meaningless.

References

1. C. Hansch and T. Fujita, *J. Amer. Chem. Soc.* **86**, 1616 (1964).
2. K. S. Rogers and A. Cammarata, *J. Med. Chem.* **12**, 692 (1969).

Chapter VI

DRUG MECHANISMS TREATED AS COVALENT BOND PHENOMENA

It is generally felt that most drug agonists engage their biological receptors in a highly reversible manner, thus permitting the possible intrusion of competitive antagonist molecules at the same or nearby sites. This reversibility of drug–receptor complex formation implicates fairly weak forces such as dipole–dipole, hydrogen bonding, or dispersion interactions. It is not very likely that covalent bond formation is involved in these cases.

A number of cases are known or hypothesized in which covalent bond formation between a drug molecule and some receptor feature is involved. Prominent in this group are the alkylating and esterifying agents with biological activities. Other examples are found or proposed for receptor blocking agents or enzyme inhibitors with prolonged, hence irreversible action. The metabolism of all drugs involves covalent bond formation or breaking reactions.

A number of studies have been made using MO calculations in an effort to seek correlations between indices reflecting covalent bond formation and biological activity.

I. Antimicrobial Agents

One of the earliest attempts to study drug action with molecular orbital calculations was in the class of compounds with antifungal and antibacterial activities. These studies employed simple Hückel theory and used super-

delocalizability indices to reflect chemical activity. A number of interesting features arise from these studies, and it will be instructive to review these after a discussion of each study.

A. Antifungal Agents

The finding that the antifungal activity of derivatives of 1,4-napthaquinone roughly paralleled the reduction potential, led Ikeda to presume that the ability of these agents to react with SH groups was the main factor in determining activity [*1*]. This same presumption of the ability to undergo a covalent reaction prompted Fukui and his colleagues to examine a series of quinoline and pyridine-*N*-oxides, using MO theory and to seek a correlation between a reactivity parameter and antifungal activity [*2*]. These workers chose the superdelocalizability index as an MO measure of reactivity. They found a relationship between the Hückel nucleophilic superdelocalizability index $S^{(N)}$ at the nitro group-bearing carbon atom and the degree of antifungal activity. The relationship is illustrated in Table I.

The attack by a nucleophilic reagent would be expected to be most likely, based upon chemical experience, at this carbon atom. Thus if a nucleophilic reaction is indeed involved in the antifungal phenomenon, the ordering of the index and activities are significant. The authors rationalized the inactivity of the 4,6-dinitroquinoline-*N*-oxide, in spite of the very high $S^{(N)}$ value at carbon-4, by assuming that the molecule exceeded the upper threshold of reactivity, i.e., it was suggested to be so reactive that it was consumed at other reactive sites before reaching the vital reaction center in the fungi.

In support of this finding, *in vitro* experiments have shown that 4-nitroquinoline-*N*-oxide can be easily substituted at the 4 position by the SH group of cysteine, and that the substituted compound was biologically inactive [*3*].

B. Nitrofuran Antibacterial Agents

Since the report of Stillman and Dodd that 5-nitrofuran derivatives (*I*) possess notable bacteriacidal activity, considerable attention has been devoted to these substances [*4*].

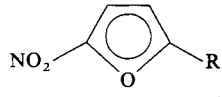

I

From numerous studies it has been shown that the nitro group is essential

TABLE I
ANTIFUNGAL ACTIVITY AND REACTIVITY INDEX RELATIONSHIP[a]

Compound	$S^{(N)}$ at nitro carbon	Activity[b]
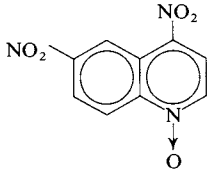	1.014[c]	−
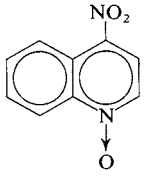	0.630	+ + +
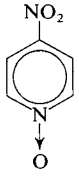	0.297	+ +
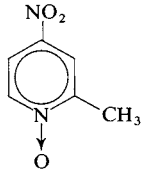	0.279	+
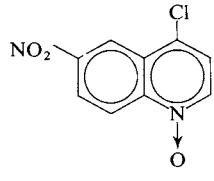	0.205	+
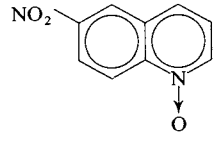	0.168	−

[a] Reference [2].
[b] Activity against *Aspergillus oryzae*, *Tolura utilis*, *Saccharomyces sake*, and *Zygosaccharomyces soja*.
[c] Index at position 4.

and that the nitrofuryl moiety is the active antibacterial moiety with the R substituent serving to enhance or diminish the action.

Yoneda and Nitta have examined a series of 12 nitrofuran derivatives using several molecular orbital indices calculated for the 2 position on the ring of these molecules in an effort to find some indication of the nature of the initial reaction leading to antibacterial action [5]. The structures and MO indices are shown in Table II.

The index of nucleophilic reactivity exhibits a correlation with the antibacterial activity up to a maximum value, followed by a decrease in activity proportional to the increase in $S^{(N)}$ (Fig. 1). The conclusion was reached that an important factor determining antibacterial activity is the chemical reactivity of nitrofuran derivatives at the 2 position with a nucleophilic group, presumably from some component of the bacteria.

The appearance of increasing then decreasing antibacterial activity with a decrease in $S^{(N)}$ (decreasing reactivity) is reminiscent of the previous observation of antifungal activity in the pyridine- and quinoline-*N*-oxide derivatives. In both cases it was proposed that an upper and lower threshold of reactivity exists for biological activity. In the case of the nitrofuran derivatives in this study, strong antibacterial activity appears at $S^{(N)}$ values between 2.4 and 3.0. Greater nucleophilic reactivity was proposed to be a result of a premature loss of the compound at another reactive site before it could achieve a significant concentration at a vital reaction site in the microorganism.

A subsequent study of a similar group of nitrofuran derivatives, employing different parameters revealed no correlation with $S^{(N)}$ at the nitro

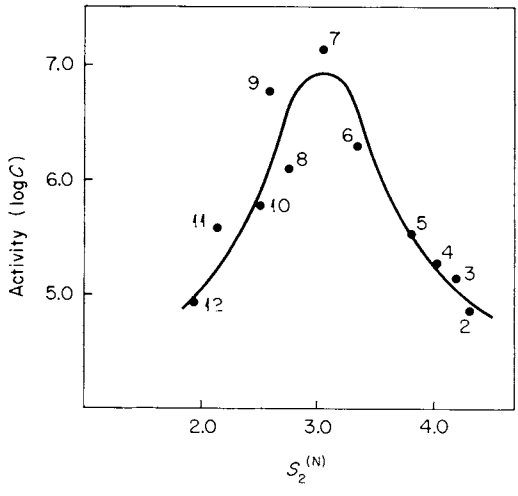

Fig. 1. The relation between $S_2^{(N)}$ at 2 position of nitrofuran derivatives and antibacterial activity [5]. Numbers refer to compounds in Table II. *C* is maximum bacteriostatic dilution.

TABLE II

RELATIONSHIP BETWEEN REACTIVITY INDICES AND ANTIBACTERIAL ACTIVITIES IN NITROFURAN DERIVATIVES[a]

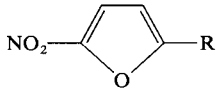

No.	R	$S_2^{(N)}$	Activity
1	—CHO	—[b]	+
2	—$CONH_2$	4.098	+
3	—CONH— 	4.030	++
4	—CH=CH—$CONH_2$	3.960	+++
5	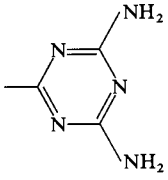	3.463	+++
6	—CH=CH— 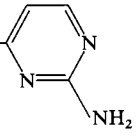	2.973	++++
7	—CH=CH— 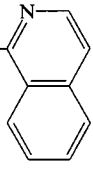	2.866	+++++
8	—CH=N— 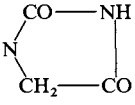	2.532	+++
9	—CH=CH— 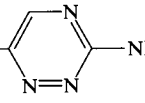	2.458	+++++
10	—CH=CH—CH=N—NH—CO—NH_2	2.355	+++
11	—CH=CH—CH=CH—CH=N—OH	2.127	+++
12	—CH=N—NH—CO—NH_2	2.117	++

[a] Yoneda and Nitta [5].

[b] LEMO is +, hence $S^{(N)}$ cannot be calculated.

group-substituted carbon atom [6]. A correlation was claimed between acidity and the E_{LEMO} but a plot of the data does not reveal any relationship. It was concluded from this study that electron attraction in the form of a complex was the likely mode of reaction in the crucial step. Calculations of the frontier electron density (nucleophilic) for several of the molecules indicated that the nitro group was the most likely recipient of the electron donation. This surprising result is hard to explain from chemical experience. On the other hand, the product of E_{LEMO} and $S^{(N)}$ for the nitro group-bearing carbon atom showed that this atom should have a fairly large $f^{(N)}$ in each molecule, suggesting that it could in fact be a site of a nucleophilic attack, as presumed by earlier work on nitrofurans [5].

C. General Comments

The use of nucleophilic superdelocalizability indices calculated with HMO theory should be approached with caution. This index employs the virtual orbitals which, using Hückel theory, are not reliably calculated due to the failure to reflect any configuration interaction. Although correlations with nucleophilic reactivity have been reported for chemical series, the general applicability of this index is questionable. In studies of the kind reviewed above, corroborative chemical evidence relative to the predicted reactivity would greatly strengthen confidence in this index.

Another aspect of the studies just described worth noting is the limited number of examples used in one study, and the use of nonnumerical biological activity parameters in all cases. Statistical significance is questionable when only four compounds show any activity. The biological activity parameters used do not really permit any kind of statistical evaluation of the correlation with the MO index.

The curvilinear relationship described between the $S^{(N)}$ and the relative activity parameter should be based upon an actual regression analysis, otherwise it could be suggested that the graphic relation is a curve drawn through a scatter of points.

II. Ester Hydrolysis

A number of MO studies have been directed toward correlating hydrolysis rates involving cholinesterases and cholinergic-like drugs. These studies have relied on ground state MO indices in spite of the successful correlations shown between hydrolysis rates and localization energies.

A. Carbamate Cholinesterase Inhibitors

Carbamates are known to be potent inhibitors of the enzyme cholinesterase. These molecules have clinical utility as well as roles as insecticides.

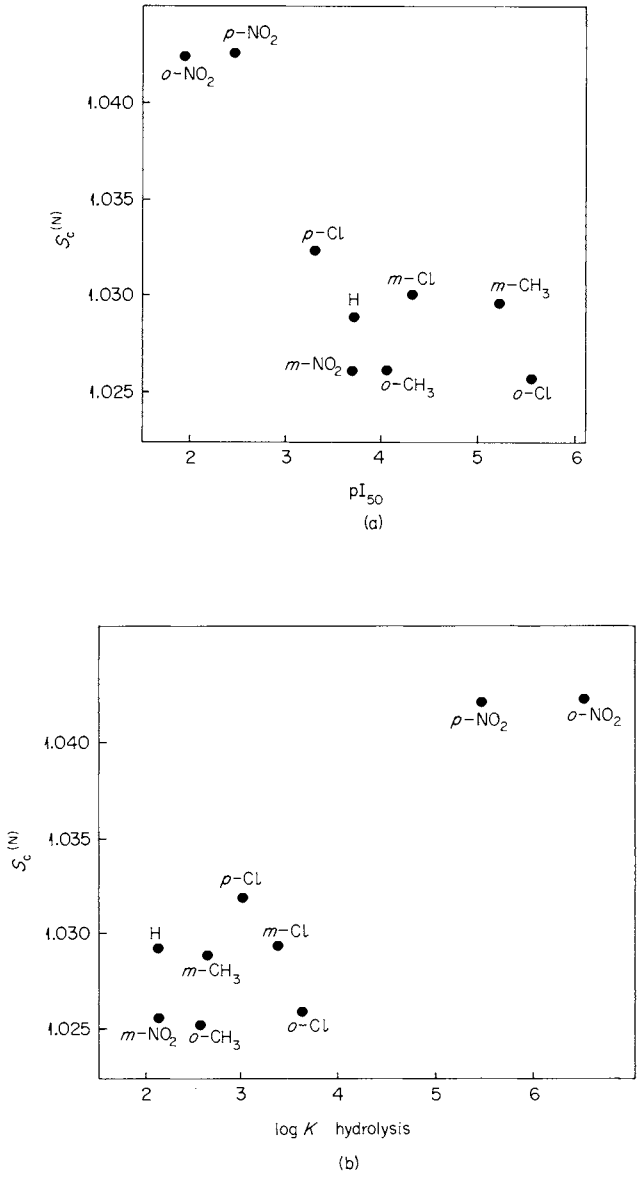

Fig. 2. (a)Relationship between $S_c^{(N)}$ of carbamate derivatives (**II**) and cholinesterase inhibition [7]. (b) Relationship between $S_c^{(N)}$ of carbamate derivatives (**II**) and log K of hydrolysis [7].

A series of substituted phenyl *N*-methylcarbamates (**II**) have been studied by Ban and Nagata using HMO theory [*7*].

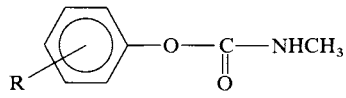

II

A correlation was noted, in a series of eight derivatives, between the π charges on both oxygen atoms of the ester group and the inhibitory potency pI_{50} against cholinesterase (fly brain). It should be stated, however, that the charge variation on the ester oxygen atom among all eight molecules was only $0.015e$ while the variation of charge on the carbonyl oxygen was only $0.002e$ for the series. It is not realistic to attach much significance to this very minor variation.

On the other hand, there was found an inverse relationship between inhibitory potency and nucleophilic reactivity, $S^{(N)}$, at the carbonyl carbon atom (Fig. 2a). The $S^{(N)}$ roughly paralleled the ease of hydrolysis (Fig. 2b). This inverse relationship in Fig. 2a was explained on the basis of an assumed two-step process occurring on the enzyme [*8*, *9*]. The inverse relationship of the $S_C^{(N)}$ value with inhibitory potency was explained on the basis of the second process, k_3 being the rate-determining step in the carbamoylation of the enzyme (Fig. 3). The correlations exhibited in Fig. 2a,b, do not appear good enough to attach too much significance to the proposed mechanism.

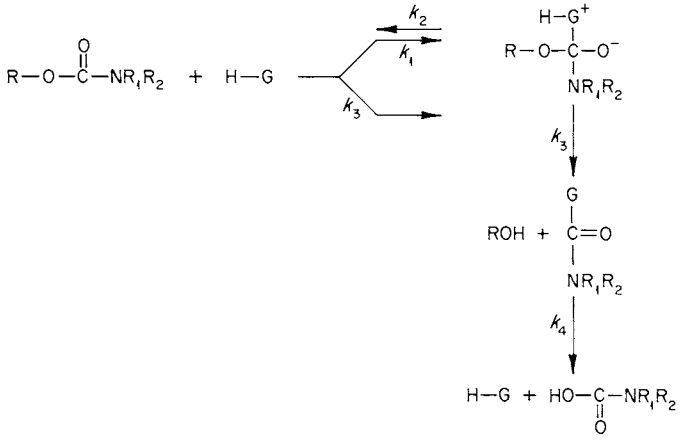

Fig. 3. Postulated scheme for carbamoylation of cholinesterase.

Neely has also studied the carbamates seeking MO-calculated properties related to the cholinesterase inhibiting potencies [*10*]. In this study, charge densities were calculated on the substituted phenol portion of the carbamate (**III**) using π-Hückel theory (see Table III).

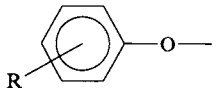

III

TABLE III
CHARGE DENSITIES ON OXYGEN AND ATTACHED CARBON ATOMS OF SUBSTITUTED PHENOL PORTION OF CARBAMATE INHIBITORS[a]

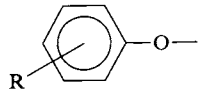

R	q_c	q_o	pK_a
3-Cl	+0.055	+0.076	9.2
2-Cl	+0.076	+0.079	8.4
2,4-Dichloro	+0.087	+0.081	7.7
2,4,5-Trichloro	+0.086	+0.080	7.2
2-CH_3	+0.039	+0.075	10.2
3-CH_3	+0.057	+0.076	10.1
2-NO_2	+0.090	+0.084	7.2
2,4-Dinitro	+0.117	+0.090	4.0
H	+0.056	+0.076	9.9

[a] Neely [*10*].

There was a relationship noted between the dispositive character of the C—O atoms in **III** and the pK_a of the phenol, interpreted as a measure of the stability of the phenoxide anion (Fig. 4).

Although a single conclusion was not reached, it was noted that stability of the phenoxide anion, as correlated with the C—O dispositivity is related to the ease of hydrolysis in the step represented by rate k_3 in Fig. 3. This results in a restoration of the enzyme with no prolonged inhibition. In this discussion, Neely emphasized that, in addition to covalent reactivity, suitable stereochemistry of secondary binding sites to the enzyme were undoubtedly important. This is most assuredly the case in any enzymic reaction.

B. ORGANOPHOSPHATES

Pullman and Valdemoro have also considered the relationship between

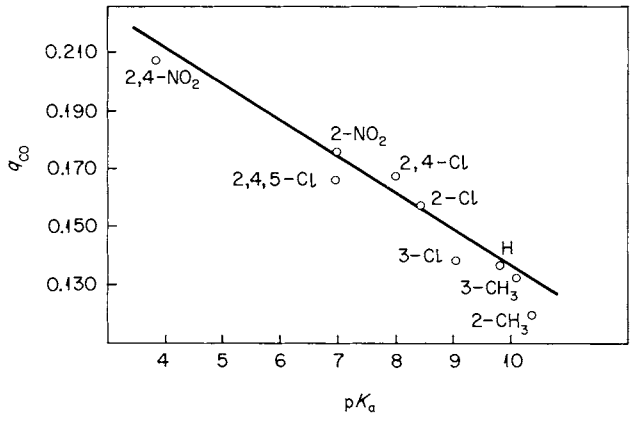

Fig. 4. Relationship between the pK_a and calculated electron deficiency, q_{co} at C—O centers for **III** [*10*].

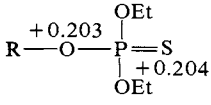

E 605

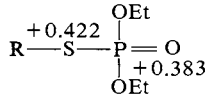

S-Phenyl isomer of E605

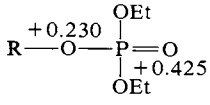

E 600

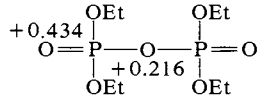

TEPP

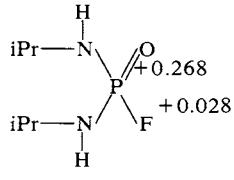

Mepafox

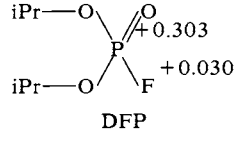

DFP

Fig. 5. Calculated π charges on several organophosphorus esterase inhibitors [*11*].

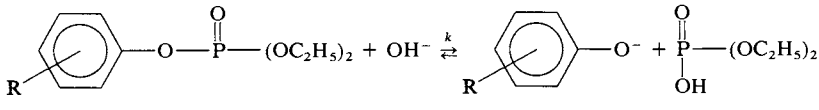

Fig. 6. Alkali hydrolysis scheme for organophosphate ester derivatives.

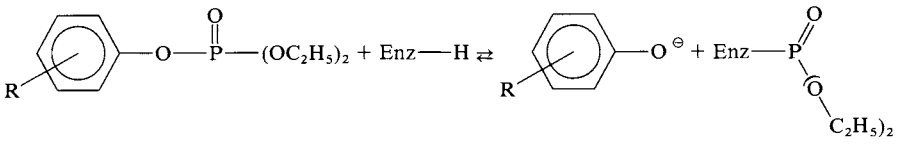

Fig. 7. Postulated scheme of enzyme inhibition with organophosphate derivatives.

a labile dispositively charged π bond and enzymic hydrolysis in a study on a number of organophosphorus esterase inhibitors [*11*]. The Pullmans had earlier made the observation that practically all the fundamental biochemical substrates undergoing enzymic hydrolysis have the common feature of undergoing this reaction on a π-electron-deficient bond [*12*]. Hückel MO calculations on several organophosphorus esterase inhibitors showed dispositive bonds between the phosphorus atom and the bonded atom severed in phosphorylating an enzyme (Fig. 5). It was noted that the inhibitory power seemed to parallel the charge on the P atom. Relative inhibitory potency is observed in two series, E 605 < *S*-phenyl isomer of E 605 < E 600 and in the fluoro series mepafox < DFP [*13*]. This reflects the electron affinity of the P atom for a nucleophile on the esteratic site of the enzyme. The limited number of examples used in the comparison demand caution in the conclusion, although it is intuitively reasonable. This hydrolysis mechanism could be studied with MO energy indices.

In a later study, Fukui *et al.* calculated the superdelocalizability and electron density of the phosphorus atom of each of a series of 15 substituted phenyl diethyl phosphates [*14*]. The $S_P^{(N)}$ was found to correlate with the ease of alkali hydrolysis in the reaction in Fig. 6. A rough relationship was found between $S_P^{(N)}$ and the average molar concentration to inhibit fly brain cholinesterase (see Table IV). In the same table, the insecticidal activity is shown for each compound. Again a rough relationship is seen between insecticidal activity and the $S_P^{(N)}$. These results were used to support the view that both enzyme-inhibitory activity and insecticidal activity involve the attack of an enzyme nucleophile on the phosphorus atom with a resulting phosphorylation of the enzyme (cholinesterase or insect enzyme) shown in Fig. 7. It would be of considerable interest to calculate a localization energy for nucleophilic attack on the phosphorus atom, to see if these correlations could be improved.

A question arises when charge-related indices are used to correlate reactivity such as ester hydrolysis. Where a preliminary orienting effect of a base and the ester are important in determining subsequent rate-limiting events, this index has some validity. An energy such as a localization energy may be generally superior. In all proposed mechanisms based upon MO

TABLE IV

SUPERDELOCALIZABILITY, $S_P^{(N)}$ AT PHOSPHORUS ATOM IN DIETHYL, SUBSTITUTED PHENYL PHOSPHATES, AND ALKALI HYDROLYSIS RATE, CHOLINESTERASE INHIBITORY ACTIVITY, AND INSECTICIDAL ACTIVITY[a]

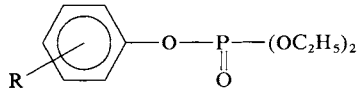

R	$S_P^{(N)}$	k_{OH} hydrol. (min^{-1})	Median inhibitory molar conc. (ChE)	Insecticidal activity
2,4-Dinitro	1.132	5.7×10^{-3}	3.0×10^{-9}	+
o-Nitro	1.120	3×10^{-4}	5.0×10^{-8}	++
p-Nitro	1.119	2.7×10^{-4}	2.6×10^{-8}	+++
p-Formyl	1.106	—	1.5×10^{-7}	−
p-Cyano	1.106	—	1.3×10^{-7}	+++
2,4,5-Trichloro	1.100	7.9×10^{-5}	6.0×10^{-9}	++
2,4-Dichloro	1.100	4.8×10^{-5}	5.0×10^{-7}	+
o-Chloro	1.099	5.1×10^{-5}	2.0×10^{-5}	±
p-Chloro	1.099	3.2×10^{-5}	3.0×10^{-5}	±
H	1.097	9.2×10^{-5}	1.0×10^{-8}	−
m-Nitro	1.097	9.8×10^{-5}	5.0×10^{-8}	++
p-Methyl	1.097	—	1.0×10^{-3}	−
m-Methoxy	1.096	8.9×10^{-6}	1.3×10^{-4}	−
p-Methoxy	1.096	—	1.0×10^{-3}	−
p-Dimethylamino	1.094	1.9×10^{-6}	4.0×10^{-7}	+

[a] Fukui *et al.* [*14*].

calculations, the intervention of an enzyme in the reaction requires a stereochemical parameter not treated in the simple Hückel π-electron schemes. This requirement may override a reactivity limitation calculated by these methods.

C. ACETYLCHOLINE HYDROLYSIS

A recent study has employed all-valence electron EHT to consider the hydrolysis of acetylcholine *in vivo* [*15*]. The charge densities and bond orders were calculated for a series of acetylcholine analogs in which the nitrogen was successively methylated (see Table V).

The major electronic influence calculated for a successive nitrogen methylation was, as expected, the change of charge on the nitrogen atom. Alteration in the electronic structure of the ester group was not apparent, although the probable change in conformation of the molecule, as a result of the methylation, may possibly introduce some nonbonded influence on the

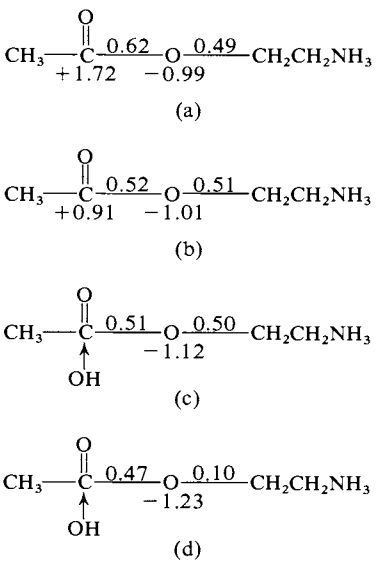

Fig. 8. Calculated electronic structures of the ester group of acetylcholine in (a) nonreacting state, (b) nonreacting excited state, (c) transition state, and (d) transition excited state [*15*].

ester group. Conformational changes were not included in this study, a constant conformational preference being assumed.

The study also included a comparison between the charges and bond orders in the ester group of the molecule in the nonreacting state and in a transition state (**IV**). It was further presumed that the acetylcholine was bound to the enzyme prior to and after hydroxyl attack, by a charge transfer complex in which an electron on the carbonyl oxygen was donated to the enzyme. Accordingly, the excited states for the nonreacting state and the transition state were also calculated (see Fig. 8).

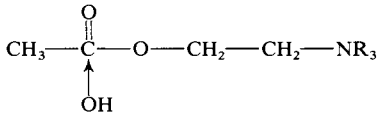

IV

The authors concluded that the dramatic lowering of the O—C bond order from 0.50 to 0.10 upon excitation (complexation) of the transition state indicates that the breakdown of the complex and acetylcholine occurs with scission of the oxygen–choline bond. This mode of ester hydrolysis is not consistent with the commonly viewed mechanism, namely, CO—O cleavage.*

* These authors have observed an *o*-alkyl cleavage in $H_2{}^{18}O$ (personal communication).

TABLE V
CALCULATED EHT INDICES FOR ACETYLCHOLINE DERIVATIVES[a]

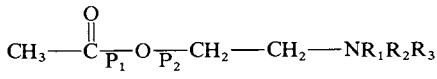

R_1	R_2	R_3	$P_1(0)$[b]	$P_1(1)$[c]	$P_2(0)$	$P_2(1)$	$q_N(0)$	$q_N(1)$
CH_3	CH_3	H	0.622	0.519	0.479	0.508	−0.166	−0.161
CH_3	H	H	0.621	0.519	0.487	0.510	−0.299	−0.287
H	H	H	0.621	0.519	0.487	0.509	−0.427	−0.396

[a] Farkas and Kruglyak [*15*].
[b] (0) refers to ground state values.
[c] (1) refers to first excited state values.

The premise that a calculated electronically excited state of the molecule simulates the molecule in the enzyme–substrate complex is probably an unwarranted one. Even if a charge transfer complex was the mode of binding, a complete transfer of an electron is unlikely from energetic considerations. Furthermore, since the carbonyl oxygen atom is implicated as being the donor atom, these calculations should reflect this dramatic change in the electronic structure of this oxygen by placing an assumed acceptor atom or group close to it and performing the calculations with the acceptor included. This, of course, was the technique employed in considering the hydroxyl ion attack in the transition state. This could materially alter the reported bond order for the O—C bond.

The use of EHT to calculate and utilize charges and bond orders is a tenuous application of the method. The gross exaggeration of charges and bond orders makes derived results questionable.

The question also arises concerning the validity of the use of charge and bond order indices to correlate with and predict bond rupturing reaction phenomena. It has been shown that indices such as localization energies are superior in approximating the relative free energies of activation in such a reaction.

III. Agricultural Agents

Although herbicides and pesticides are not classified as drugs, it is worthwhile including a consideration of some MO studies made in this area. The biochemical processes interfered with by many agricultural control chemicals often have their counterpart in animals; thus upon exposure to man these agents may give rise to adverse manifestations. Some knowledge

of these mechanisms is thus useful in furthering compound design and in understanding human toxicity. A consideration of these studies is also useful in what can be learned from the application of MO calculations to relate biological activity with chemical structure.

A. Auxinic Activity

The auxins are a class of compounds with plant growth-stimulating properties. Since the discovery of the natural plant growth hormone, indole-3-acetic acid (**V**) a large number of compounds have been synthesized and tested.

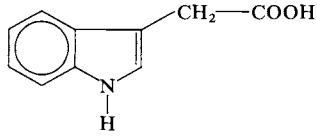

V

One such series of compounds, the substituted benzoic acids, were studied by Fukui, using MO theory in an effort to find a correlation between some reactivity parameter and the auxinic activity [*16*]. Thirty-two substituted benzoic acid molecules were calculated by the π-electron Hückel method using the superdelocalizability index for nucleophilic, electrophilic, and radical attack at all ring positions (see Table VI).

Only eight of the compounds possess any auxinic activity. All of these had $S^{(N)}$ values for the *ortho* carbon atom, above a value of 0.669, although three molecules in the list with a larger value were not active. There was no apparent correlation between the relative activity of the active compounds and the $S^{(N)}$ index.

The conclusion reached was that an *ortho* attack on the ring by a nucleophile from a plant constituent is a necessary event in the plant growth activity, although the calculations only indicate a minimum numerical value of this index as being necessary for activity. This conclusion was considered to be consistent with observations made previously by Muir and Hansch that the carboxyl group and a nucleophilic attack at an *ortho* ring carbon were involved in eliciting an early reaction with a plant substrate, leading to growth stimulation [*17*].

In a more recent study by Cocordano *et al.* on chlorinated benzoic acid derivatives with auxinic activity, MO theory was used to study the reactivity of the ring positions [*18*]. A modified free valence index, a_r, was defined as

$$a_r = \sqrt{3} - \frac{1}{\beta} \sum_{\text{adj}} \beta_{rs} p_{rs}$$

TABLE VI

RELATION BETWEEN AUXINIC ACTIVITY AND SUPERDELOCALIZABILITY, $S^{(N)}_{ortho}$ FOR SUBSTITUTED BENZOIC ACIDS[a]

Compound	$S^{(N)}_{ortho}$	Auxinic activity
2,5-Dichloro	0.7771	+ +
2,4-Dichloro	0.7186	–
2,3,6-Trichloro	0.7108	+ + + +
2-Chloro	0.7093	+
2,3,5-Trichloro	0.7074	+ + + +
2,4,6-Trichloro	0.6918	–
2-Bromo	0.6825	+
2-Iodo	0.6810	±
2-Bromo-6-chloro	0.6777	+
3-Methyl	0.6705	–
2,6-Dichloro	0.6693	+
2,6-Dibromo	0.6501	–
2-Methyl	0.6483	–
3-Chloro	0.6430	–
3-Fluoro	0.6364	–
3-Hydroxy	0.6351	–
3-Bromo	0.6327	–
3-Iodo	0.6312	–
4-Chloro	0.6199	–
4-Iodo	0.6160	–
4-Bromo	0.6142	–
2-Hydroxy	0.6133	–
2-Fluoro	0.6096	–
3,4,5-Triiodo	0.6079	–
Benzoic acid	0.6020	–
2-Amino	0.6010	–
4-Amino	0.5733	–
4-Nitro	0.5567	–
4-Fluoro	0.5564	–
4-Hydroxy	0.5538	–
4-Methyl	0.5427	–
2-Nitro	0.3764	–

[a] Fukui *et al.* [*16*].

The results of the calculation of a_r values for each of the ring positions and the activities are shown in Table VII. A correlation was noted between the activity of the four active molecules listed and the sum of the a_r values for positions 4 and 5 (*meta* and *para* to the carboxylate). A minimum value of $(a_4 + a_5)$ was apparently necessary. It is to be noted that the first six compounds in Table VII, which are inactive as auxins, have at least one of the *meta* or *para* positions blocked by a chlorine atom. Thus their inactivity may be due to an inaccessibility of adjacent *meta–para* positions to attack.

Compound 7 in Table VII has a free *meta–para* position which results in a significantly higher $(a_4 + a_5)$ value. This molecule, however, is not active. Thus a correlation is to be found by considering the *meta–para* substituent free acids from compounds 7 through 12. In this case, there is a definite correlation between $(a_4 + a_5)$ and auxinic activity. The number of cases, however, is too small to attach anything but preliminary interest in the relationship.

The interpretation of this correlation was that the pair of adjacent atoms are involved in a bonding phenomenon with some receptor component of the plant. It has been suggested that an —SH group from a plant protein is involved in this bonding [*19*]. The finding of an MO correlation with activity supports this view, in at least the limited number of examples studied. The nature of the bond cannot be inferred from the study, although the free valence index has been considered to relate to ease of bond formation, usually through a radical attack. This could possibly be involved here.

The results of these two studies on auxinic benzoic acid derivatives appear to conflict as far as the position on the ring involved in bonding with a plant receptor feature. Eight of the twelve chlorobenzoic acid derivatives calculated in the second study were also calculated in the first study, leading to this ambiguity. In spite of the correlation with the free valence index, it is hard to escape the fact that the presence of an *ortho* chloro group is

TABLE VII

RELATION BETWEEN AUXINIC ACTIVITY AND a_r VALUES[a]

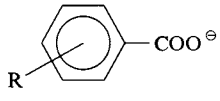

Compound	a_1	a_2	a_3	a_4	a_5	a_6	$a_4 + a_5$	Activities
3,4,5-Trichloro	0.1462	0.4612	0.2322	0.2763	0.2322	0.4612	0.5085	0
4-Chloro	0.1487	0.4317	0.4176	0.2263	0.4176	0.4317	0.6439	0
3,5-Dichloro	0.1388	0.4631	0.2070	0.4546	0.2070	0.4631	0.6616	?
2,4-Dichloro	0.1686	0.4303	0.4248	0.2241	0.4400	0.2440	0.6641	0
3,4-Dichloro	0.1476	0.4542	0.2340	0.2509	0.4156	0.4391	0.6665	0
2,4,6-Trichloro	0.1882	0.2426	0.4468	0.2212	0.4468	0.2426	0.6680	0
3-Chloro	0.1406	0.4563	0.2093	0.4331	0.3936	0.4405	0.8267	0
2-Chloro	0.1615	0.4324	0.4023	0.4091	0.4183	0.2461	0.8274	+
2,6-Dichloro	0.1811	0.2451	0.4250	0.4072	0.4250	0.2451	0.8322	+ +
2,3-Dichloro	0.1599	0.2722	0.2352	0.4309	0.4007	0.4390	0.8316	?
2,5-Dichloro	0.1603	0.4552	0.2190	0.4317	0.4167	0.2561	0.8484	+ + +
2,3,6-Trichloro	0.1794	0.2708	0.2448	0.4292	0.4240	0.2548	0.8532	+ + + +

[a] Cocordano *et al.* [*18*].

TABLE VIII
RELATION BETWEEN AUXINIC ACTIVITY AND a_r VALUES[a]

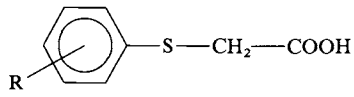

Phenylthioacetic acid derivative	$a_3 + a_6$	Activity rank
3,5-Dichloro	0.684	0
2,6-Dichloro	0.684	0
2,4,6-Trichloro	0.715	0
Unsubstituted	0.844	±
5,6-Dichloro	0.697	+
5-Chloro	0.864	+
2-Chloro	0.865	+
4-Chloro	0.866	+ +
4,5-Dichloro	0.885	+ +
2,5-Dichloro	0.885	+ +
2,4-Dichloro	0.886	+ +
2,4,5-Trichloro	0.905	+ +

[a] Cocordano [*20*].

essential for auxinic activity. It will be interesting to see the results of calculations on a larger series of active molecules using other reactivity indices.

The indices correlating with activities in these studies and the apparent involvement of adjacent atoms in the ring in the second study suggest that it might be profitable to consider a localized charge transfer complex formation with a portion of the ring. The use of localization energies as correlating indices would reveal perhaps more firmly whether a covalent bond was involved in the activity-limiting step. It would also strengthen future work in this class of agents to have a larger number of examples of active molecules.

In a later study by Cocordano [*20*], a series of chloro-substituted phenylthioacetic acids (**VI**) with auxinic activity were studied using the same modified free valence index, a_r. A relationship was noted between activity, expressed in plus values, and the sum $a_3 + a_6$, an index used by Cocordano *et al.* in an earlier study [*18*] (Table VIII). This study implicates the *para*-3,6 positions in some type of bond formation reflected by this index. It is possible, as previously suggested, that a localized charge transfer complex is involved, although in the three studies on auxinic agents reviewed, different positions are implicated. A *para* localization energy would be worth calculating for these molecules.

It is desirable to have numerical biological data rather than ranking designations as in these three studies. This would permit a statistical evaluation of any apparent correlation.

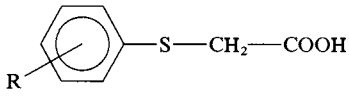

VI

IV. Enzymic Acetyl Group Transfer

The enzyme acetyl transferase, along with coenzyme A as a cofactor, catalyzes the acetylation of many biological substrates including amine groups. Included in this group of amine substrates are the biologically active *p*-aminosalicylic acid, isoniazide, the sulfonamides, and the amino nicotinamides. At the same time the enzyme can acetylate a wide variety of arylamines, and can employ an acetylated arylamine rather than coenzyme A thioacetate as a cofactor [*21*]. The enzyme thus transfers the acetyl group from one aromatic amine to another.

The susceptibility of a series of aromatic amines to enzymic acetylation has been studied by Perault and Pullman using HMO theory [*22*]. In Table

TABLE IX
ARYLAMINE ACETYLATION RATES AND MO INDICES[a]

Amine	Relative acetylation rate[b]			q_N	F_N
p-Bromoaniline	1.12			1.849	1.021
p-Chloroaniline	1.09			1.849	1.020
p-Methylaniline	1.00			1.853	1.028
Aniline	0.70	0.79		1.851	1.023
Benzidine		0.74		1.846	1.020
p-Nitroaniline	0.34			1.827	0.996
Sulfanilamide	0.18	0.17	1.00	1.841	1.010
Sulfathiazole			0.30	1.841	1.011
Sulfadiazine			0.20	1.836	1.012
p-Anisidine		Acetylated		1.861	1.042
o-Phenylenediamine		Acetylated		1.862	1.048
o-Anisidine		Acetylated		1.859	1.041
o-Toluidine		Acetylated		1.852	1.027
m-Nitroaniline		Acetylated		1.851	1.024
o-Nitroaniline		Not acetylated		1.824	0.991

[a] Perault and Pullman [*22*].
[b] From different sources.

IX the comparative data are shown between acetylation rate and MO indices. It was observed that, on the whole, there was a parallelism between the MO indices and acetylation rate. It was noted that the halogen derivatives did not obey the correlation very well, possibly due to poor MO parameterization of these atoms.

In spite of these exceptions, the correlation is not strong, and although the reactivity at the amine nitrogen atom is undoubtedly important, the presence of secondary binding features on the molecule are certainly important in promoting the intimate relationship necessary between enzyme and substrate which leads to the observed reaction rate. In an enzyme-catalyzed reaction, the rate-limiting feature in a series of molecules may well be the preciseness of the fit of secondary binding sites.

The use of a localization energy index in this study would overcome the deficiencies previously cited for the ground state indices, and would permit a more rigorous consideration of the possible correlation of activity with acylation.

A point should be made here concerning the inadvisability of using data from different sources. Although the problem may not be severe in this case, a clear correspondence should be evident whenever this is done. The use of biological data from different sources is definitely not advisable.

V. Skin Photosensitizing Agents

A number of naturally occurring substances are capable of photosensitizing skin after contact. Irradiation with sunlight results in a photodermatitis. One such class of compounds are the furocoumarins or psoralens (**VII**) [*3*]. It has been shown that the psoralen derivatives which show activation peaks around 340–380 mμ and concomitent fluorescence at 420–460 mμ can cause the photosensitization of the skin [*24*].

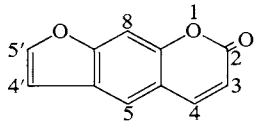

VII

A recent approach to the problem of relating the structural variation with photosensitizing activity has been taken by Yeargens and Augenstein who calculated a number of HMO indices on a group of psoralens [*25*]. Calculations were made on the following molecules:

1. psoralen
2. 4-methylpsoralen
3. 5′,8-dimethylpsoralen
4. 4,5′,8-trimethylpsoralen
5. 8-methoxypsoralen
6. 4,5′-dimethyl-8-propylpsoralen
7. 8-bromo-4,5′-dimethylpsoralen
8. 8-acetyl-4,5′-dimethylpsoralen
9. 4,4′-dimethylpsoralen
10. 3,4,5′8-tetramethylpsoralen
11. 3-*n*-butyl-4,5′,8-trimethylpsoralen
12. 8-acetyl-4,5′-dimethylpsoralin semicarbazide
13. 8-acetamido-4,5′,8-dimethylpsoralen
14. 3,4-benzo-5′,8-dimethylpsoralen
15. 8-amino-4,5′-dimethylpsoralen
16. 5-bromo-8-methoxypsoralen

A correlation was reported between the *in vivo* activity rank (a numerical conversion of plus rankings) and the sum of nucleophilic localization energies for the 3,5, and 8 positions of psoralen (see Fig. 9).

The interpretation of the $\sum L^{\ominus}$ was that it is a measure of combined reactivity of psoralen at the indicated atoms or that it measured simultaneous reactivities from multiple biological sites. This latter interpretation is reminiscent of *ortho–meta* or *para* localization energies used to correlate with multiple site bonding as in Diels-Alder addition reactions. From the correlation in Fig. 9, the suggestion was made that at least a two-point attachment was made with position 8 and either 3, 4, or 5. The nature of this attachment is speculative, but a covalent bond or a charge transfer complex were suggested.

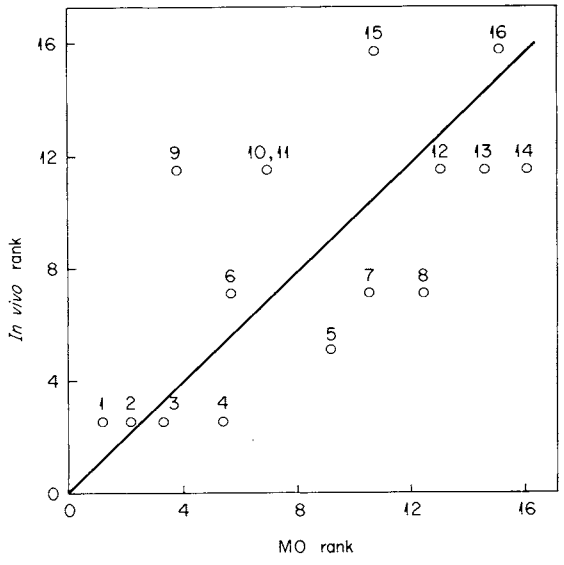

Fig. 9. *In vivo* activity rank vs. MO rank expressed as the sum of localization energies at positions 3, 5, and 8 in **X** [*28*].

The use of localization energies is a reasonable approach; however, the value of the activity ranking leaves much to be desired. In addition, the relationship shown in Fig. 9 can only be said to be suggestive rather than informative. The necessity of irradiation prior to the dermatitis indicates the need for consideration of the potential reactivity of the molecules in the excited state.

VI. Chemical Carcinogenesis of Hydrocarbons

The pioneering application of MO theory to study a major biological problem was the work of the Pullmans on the electronic structures of carcinogenic hydrocarbons [*26*]. Based upon an earlier proposal that the electronic structure was decisive in determining the carcinogenicity of hydrocarbons [*27*], and the observation that MO calculations showed more olefinic character in some regions of hydrocarbon molecules [*28*], the Pullmans devised a generalized theory on the structure–activity relationships of these molecules [*29*].

It was observed that the majority of the polycyclic hydrocarbons contained two regions of importance to their chemical behavior, and subsequently shown, to their carcinogenic activity. These are the olefinic *K* region and the transannular *L* region (Fig. 10).

The *K* region has the lowest bond localization energy or *ortho* localization energy, whereas the *L* region has atoms with the largest atom localization energy or *para* localization energy. These calculations agree with the chemical experience of these polycyclic hydrocarbons.

The Pullmans stated two postulates based upon their calculations.

1. The appearance of carcinogenic activity in aromatic hydrocarbons is determined by the existence of an active *K* region.

2. If the molecule contains an active *L* region, its presence will diminish or cancel the influence of the *K* region.

Two complex indices were defined to reflect reactivity at the *K* and *L* regions. For the *K* region the index used was the sum of the bond localization energy and the lowest of the two-atom localization energies for the

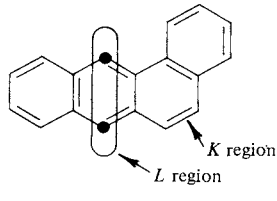

Fig. 10. Benzanthracene showing *K* and *L* regions.

bond. For the *L* region they used the index derived from summing the *para* localization energy and the lowest value of the two-atom localization energies. Calculations on over 40 aromatic polycyclic hydrocarbons using these indices indicated that the appearance of carcinogenic activity is determined by the existence of a *K* region index smaller than 3.31β. The presence of an *L* region with an *L* region index greater than 5.66β, nullifies the *K* region effect on activity. The limiting values, of course, depend upon the parameters chosen for the calculations. Some of the data are summarized in Table X.

TABLE X
HYDROCARBON CARCINOGENICITY AND CALCULATED INDICES[a]

Hydrocarbon	*K* region index (β)	*L* region index (β)	Activity
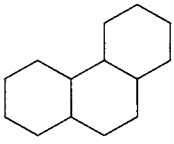	3.36	—	−
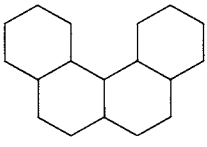	3.41	—	+
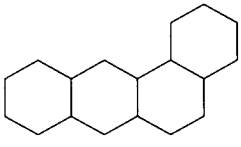	3.29	5.53	?
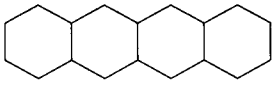	3.33	5.25	0
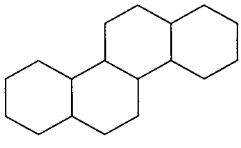	3.38	—	0
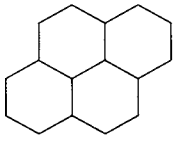	3.33	—	0

[a] Pullman and Pullman [29].

TABLE X *(continued)*

Hydrocarbon	*K* region index (β)	*L* region index (β)	Activity
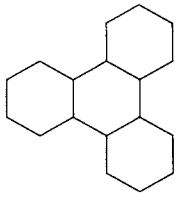	3.81	—	0
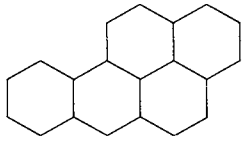	3.23	—	++++
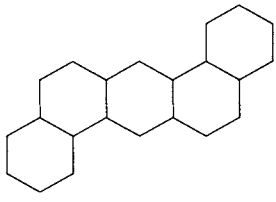	3.30	5.69	++
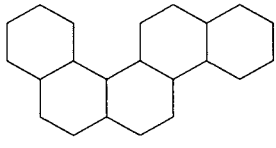	3.41	—	+
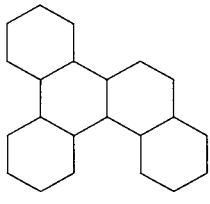	3.42	—	+
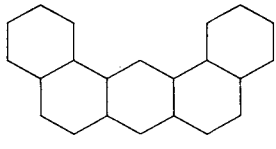	3.31	4.38	+
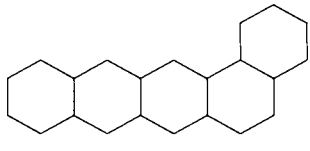	3.20	5.25	−

TABLE X *(continued)*

Hydrocarbon	*K* region index (β)	*L* region index (β)	Activity
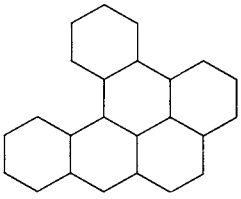	3.24	—	+++
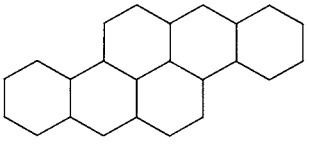	3.17	—	++++
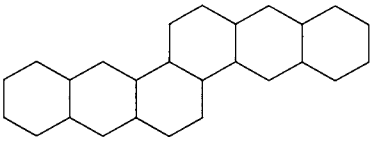	3.24	5.44	–

The mechanism implicated by these correlations is that a key reaction in the carcinogenic process is a covalent bond forming at the *K* region. The reaction at the *L* region, also covalent bond formation, may be an alternate noncarcinogenic reaction.

The use of alternative MO reactivity indices has been used by Mainster and Memory in a more recent study [*30*]. They employed the sum of superdelocalizabilities at the *K* or *L* regions to reflect reactivity. The relationship between the *K* region index, I_K and the *L* region index, I_L and the activity ranking was found to be the same as observed by the Pullmans [*29*]. The aromatic hydrocarbon was found to be carcinogenic if $I_K \geqq 2.05\ (1/\beta)$ and $I_L \leqq 2.30\ (1/\beta)$.

The metabolism of hydrocarbons by liver microsomal mixtures has been studied with the thought of learning more of the reactions undergone *in vivo* by molecules of known carcinogenic potency [*31*]. The predominant derivatives formed in the study were phenolic, either mono- or 1,2- derivatives (Fig. 11).

A proposed common intermediate leading to many of the observed products was thought to be an epoxide, although this has never been isolated.

In at least some of the cases of hydrocarbons incubated with liver microsomes, the relative proportions of products involving one or both members of a bond appear to correlate with an MO-calculated bond order.

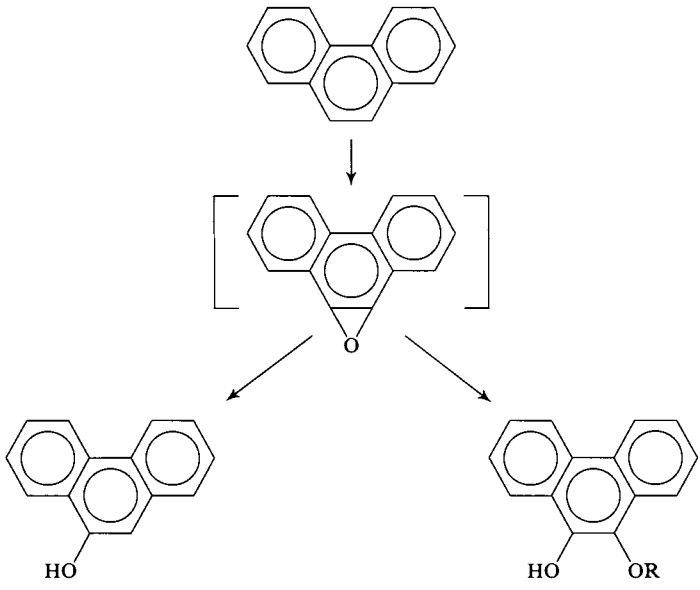

Fig. 11. Phenolic metabolites of phenanthrene [*31*].

Such a correlation is found for phenanthrene (Table XI) and benzanthracene (Table XII). The evident relationship here implies that the bond order index is a measure of the bond reactivity in a reaction such as epoxidation. The epoxide intermediate so formed would open in the aqueous medium to give a dihydrol, followed by rearrangement to a phenol or with acetylcysteine to give the mercapturic acid. It is interesting to note that the two favored bonds in phenanthrene and benzanthracene are the *K* bonds proposed by the Pullmans as being necessary in a polycyclic hydrocarbon to elicit carcinogenicity [*26*]. The mercapturic acid derivative formed (**VIII**) could be the ultimate arylating carcinogen, arylating an essential protein or nucleic acid [*32*].

The susceptibility of the bond may also be related to its ability to *in vivo* oxidize to a hydroperoxide, then to the observed products.

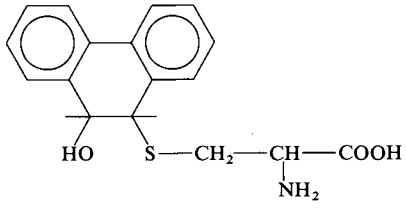

VIII

TABLE XI

RELATIVE AMOUNTS OF METABOLITES OF PHENANTHRENE PRODUCED IN RELATION TO BOND ORDERS[a]

Phenanthrene:

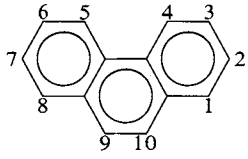

Bond	Bond order	Relative proportion of metabolites involving the bond	
		In urine	By microsomes
2–3 (6–7)	0.623	–	–
3–4(5–6)	0.702	+	+ +
1–2 (7–8)	0.705	+ + +	+ + +
9–10	0.775	+ + + +	+ + + +

[a] Boyland [*31*].

TABLE XII

RELATIVE AMOUNTS OF METABOLITES OF BENZANTHRACENE PRODUCED BY RATS, RABBITS, OR MICE IN RELATION TO BOND ORDERS[a]

Benzanthracene:

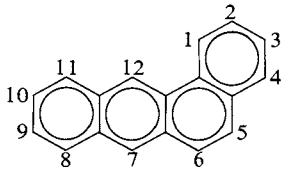

Bond	Bond order	Relative amounts of metabolites
9–10	0.593	–
2–3	0.628	–
1–2	0.695	+
3–4	0.700	+ +
10–11	0.731	+
8–9	0.732	+ + +
5–6	0.783	+ + + + +

[a] Boyland [*31*].

VII. General Summary

These MO studies leading to conclusions of covalent bonding or bond-breaking as limiting reactions in drug or biochemical processes point the way to future applications of the method. Similarly, these studies illustrate some pitfalls which should be guarded against when designing MO studies of biological phenomena.

Perhaps the most pertinent point to be gained from examining these MO applications and covalent phenomena interpretations is the selection of MO indices to reflect the chemical phenomena presumed or assigned. In theory, the indices derived from energy differences between a nonreacting and a transition state should parallel more closely the relative free energies in a series under study. The choice of a reasonable model for the transition state is critical here. Realistic bond distances, geometry, and hybridization assignments must reflect, as closely as is possible, the maximum energy state of the reacting molecule, giving rise to the rate-limiting event.

The biological data used in structure–activity correlations should, as far as is possible, reflect receptor reactions. It should be as free as possible from activity-limiting events such as absorption or distribution. The data should be adequate to permit the application of statistical analyses to determine the validity of a suspected correlation.

References

1. N. Ikeda, *Yakugaku Zasshi* **75**, 1073 (1955).
2. K. Fukui, A. Imamura, and C. Nagata, *Bull. Chem. Soc. Jap.* **33**, 122 (1959).
3. T. Okabayashi, *Hakko Kogaku Zasshi* **31**, 373 (1953).
4. M. C. Dodd and W. B. Stillman, *J. Pharmacol. Exp. Ther.* **82**, 11 (1944).
5. F. Yoneda and Y. Nitta, *Chem. Pharm. Bull. Jap.* **12**, 1264 (1964).
6. K. Hirano, S. Yoshina, K. Okamura, and I. Suzuka, *Bull. Chem. Soc. Jap.* **40**, 2229 (1967).
7. T. Ban and C. Nagata, *Jap. J. Pharmacol.* **15**, 32 (1965).
8. I. B. Wilson, M. A. Hatch, and S. Ginsburg, *J. Biol. Chem.* **235**, 2312 (1960).
9. I. B. Wilson, M. A. Harrison, and S. Ginsburg, *J. Biol. Chem.* **236**, 1498 (1961).
10. W. B. Neely, *Mol. Pharmacol.* **1**, 137 (1965).
11. B. Pullman and C. Valdemoro, *Biochim. Biophys. Acta* **43**, 548 (1960).
12. A. Pullman and B. Pullman, *Proc. Nat. Acad. Sci. U.S.* **45**, 1572 (1969).
13. W. N. Aldridge, *Biochem. J.* **57**, 692 (1954).
14. K. Fukui, K. Morokuma, C. Nagata, and A. Imamura, *Bull. Chem. Soc. Jap.* **34**, 1224 (1961).
15. M. Farkas and J. A. Kruglyak, *Nature (London)* **223**, 523 (1969).
16. K. Fukui, C. Nagata, and T. Yonezawa, *J. Amer. Chem. Soc.* **80**, 2267 (1958).
17. R. M. Muir and C. Hansch, *Plant Physiol.* **28**, 218 (1953).
18. M. Cocordano, J. Ricord, and A. Julg, *J. Theor. Biol.* **12**, 291 (1966).
19. R. Muir and C. Hansch, *Annu. Rev. Plant Physiol.* **6**, 157 (1955).

20. M. Cocordano, *C. R. Acad. Sci.* **226**, 897 (1968).
21. S. P. Bessman and F. Lipmann, *Arch. Biochem. Biophys.* **46**, 252 (1953).
22. A. Perault and B. Pullman, *Biochim. Biophys. Acta* **66**, 86 (1963).
23. L. Masajo and G. Rodighiero, *Experientia* **13**, 153 (1962).
24. M. A. Pathak and J. H. Fellman, *Nature (London)* **185**, 382 (1960).
25. E. Yeargens and L. Augenstein, *Nature (London)* **212**, 251 (1966).
26. A. Pullman, *C. R. Soc. Biol.* **139**, 1956 (1945).
27. O. Schmidt, *Naturwissenschaften* **29**, 146 (1941).
28. N. Svartholm, *Ark. Kemi* **15**, 1 (1942).
29. A. Pullman and B. Pullman, *Advan. Cancer Res.* **3**, 117 (1955).
30. M. A. Mainster and J. D. Memory, *Biochim. Biophys. Acta* **148**, 605 (1967).
31. E. Boyland, *in* "Electronic Aspexts of Biochemistry" (B. Pullman, ed.), p. 155. Academic Press, New York, 1964.
32. A. Pullman and B. Pullman, "Cancerisation Pay les Substances Chimiques et Structure Moleculaire." Masson, Paris, 1955.

Chapter VII

CHARGE TRANSFER MECHANISMS

The quantum mechanical treatment of charge transfer complex formation, first described by Mulliken [*1*], depicts an intimate relationship between two molecules in which there is a mutual propensity for the partial exchange of an electron from the donor to the acceptor. In the cases studied by Mulliken, proximity and exchange propensity existed, but the complete exchange of the electron did not. In the ground state, the structures of the donor and acceptor were essentially unperturbed. The intimacy and the modest contribution of a function denoting a full exchange, to the total complex wavefunction, provided enough energy improvement for at least transient stability, relative to the isolated pair.

To effect a complete transfer of an electron from the donor to the acceptor molecule in the complex, sufficient energy must be put into the system to promote the components to an excited state. The absorption of this energy leads to the new, characteristic band of the charge transfer complex in the uv or visible spectrum.

In the biological milieux, sources of energy are not readily identified or comparable with those obtainable *in vitro*. Nevertheless, Karreman, Isenberg, and Szent-Györgyi have reported that complexes are possible involving some biologically active molecules in which there is practically a complete exchange of an electron while the components are in the ground state [*2*]. These authors cite the involvement of phenothiazine (**I**) and its derivatives, in chemical reactions such as color changes upon freezing, and new colors produced when complexation occurs with iodine, which implicate a charge

transfer mechanism involving an electron exchange in the ground state. Other cases will be discussed later.

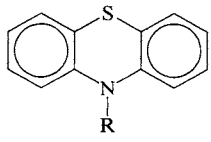

I

It must be concluded that rather specialized conditions must be met to effect some electron exchange between ground states of a complex pair. First, the geometry of the donor and acceptor must be such that a very intimate relationship ensues between the molecules. The overlapping of appropriate orbitals between the two then permit the exchange with a minimum energy requirement. The second condition requires that energy levels of donor and acceptor are so disposed that again a minimum expenditure of energy is necessary for the transfer of an electron. This means that the donor molecule must have a very high-lying HOMO energy, and the acceptor molecule must have a very low-lying LEMO energy. When these conditions are met, the need for significant amounts of external energy are obviated and the electron exchange becomes relatively facile. Attention may then be focused on the HOMO energy as a calculable index of the spontaneous donor ability of a molecule.

The formation of charge transfer complexes among drugs and biologically important molecules may have a consequence in itself or may lead to a subsequent event important in the action of the molecules. A complex may lead to the creation of a new conformation, not present in the donor or acceptor, imparting a biological activity. An allosteric effector may engage the appropriate site in a charge transfer complex. The formation of a complex may influence reactivity resulting in altered chemical stability. The complex may bring together two molecules in sufficient intimacy so that hydrogen or electron transfer may ensue. Further bonding in the form of covalent or hydrogen bonds may be a consequence of the complex.

Molecular orbital theory has been used to study charge transfer phenomena involving drugs and biologically important molecules. The indices usually examined have been the E_{HOMO} and E_{LEMO}.

I. Antimalarial Drugs

One example of an MO study of a drug class, leading to a conclusion of a charge transfer mechanism is the antimalarials. It has been shown that the antimalarial agents chloroquine, quinacrine, and quinine (Fig. 1)

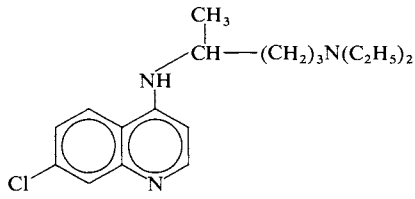

Chloroquine

	Neutral	Protonated
E_{HOMO} =	+0.603	+0.719
E_{LEMO} =	−0.601	−0.486

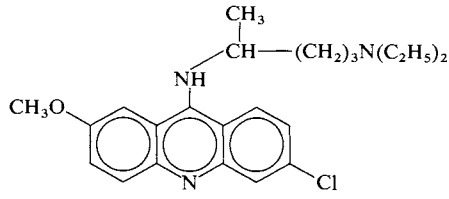

Quinacrine

	Neutral	Protonated
E_{HOMO} =	+0.405	+0.507
E_{LEMO} =	−0.421	−0.291

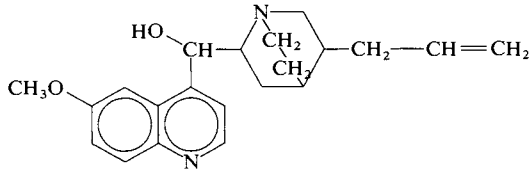

Quinine

E_{HOMO} = +0.647

E_{LEMO} = −0.539

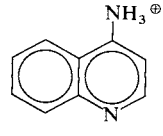

4-Aminoquinoline salt

E_{HOMO} = +0.279

E_{LEMO} = −0.481

Fig. 1. Antimalarial drugs with calculated $E_{(HOMO)}$ and $E_{(LEMO)}$ [5].

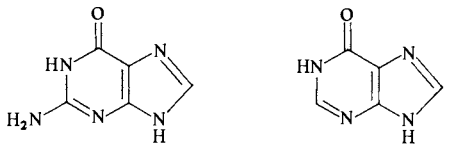

Guanine
$E_{(HOMO)} = 0.481$
$E_{(LEMO)} = 0.754$

Inosine
$E_{(HOMO)} = 0.546$
$E_{(LEMO)} = 0.677$

Fig. 2. Calculated $E_{(HOMO)}$ and $E_{(LEMO)}$ for guanine and inosine [5].

complex with malaria parasite DNA and block the synthesis of DNA and RNA [3].

Chloroquine was shown to be specific for native, double-stranded DNA. The spectra of chloroquine was markedly altered in the presence of DNA, and further evidence suggested that the 2-amino group of guanine was a specific attachment site. It was suggested that electrostatic interaction occurred between the 7-chloro- and onium groups of chloroquine and the 2-amino group of guanine and the anionic phosphates of DNA, respectively.

This mode of binding and the 2-amino group requirement in guanine have been questioned [4]. The spectral influence of guanine on chloroquine was suggested as being due to the superior electron-donor ability of guanine.

Singer and Purcell [5] and Purcell and Sundaram [6] have studied several antimalarial agents using MO theory. They concluded that the 2-amino group of guanine was a major contributor to the electron-donor properties of guanine (see Fig. 2). Removal of the amino group (inosine) showed a marked loss of donor properties. The relative electron donor and acceptor properties of the molecules were predicted, using as indices the energies of the HOMO and LEMO. This is consistent with the comparative abilities of the double-stranded polymers of these two purines to alter the chloroquine spectra [3].

To study the effect of protonation of chloroquine and quinacrine, the energy levels were calculated using an appropriately higher Coulomb integral for the nitrogen attached to the aryl ring.*

The effect can be seen in Fig. 1 as markedly lowering the LEMO energy, indicating that the electron-acceptor properties of these molecules is greatly increased. Finally, calculation on the protonated chloroquine molecule, neglecting the chlorine atom (Fig. 1), showed that the chlorine group has

*Ω-Hückel calculations have shown that protonation is preferable at the ring nitrogen. The resulting relationship of E_{HOMO} and E_{LEMO} indices remains similar. (V. Marquez, personal communication.)

little influence on the electron-donor properties, as measured by the very modest change in the LEMO energy.

The observation that chloroquine interacted only with base-paired DNA polymers [3] led Singer and Purcell to find the intercalation model of binding attractive [5]. The consequences of intercalation, or the insertion of a planar molecule between adjacent base pairs, are far reaching. The reaction can lead to a disruption of the genetic code, hence mutuation, or it can result in a complete functional disruption of the nucleic acid strand. This latter result may well be the mode of action of many antimalarial agents.*

II. Hallucinogenic Activity

The hallucinogenic agents provide another example of MO calculations implicating a charge transfer mechanism of action. Hallucinogens as a class of agents are capable of producing profound, similar effects on the subjective mental functioning of human subjects. Two major classes of compounds with this action are the tryptamine (**II**) and the phenylethylamine-related molecules (**III**).

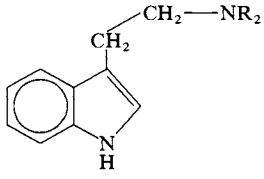

II

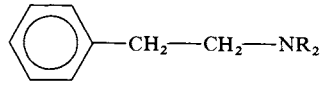

III

Snyder and Merril have studied series of molecules in both of these classes, using π-electron HMO theory to seek correlations between the electronic structures and the relative hallucinogenic potency [7]. Calculations on a series of α-methylphenethylamines revealed a correlation between the E_{HOMO} and hallucinogenic potency in a small number of molecules (Table I). In the same study, calculations on a series of phenethylamines showed that mescaline had the most energetic HOMO and was the most potent hallucinogen. The other molecules in this series were not hallucinogenic (see Table II). These two tables indicate that some minimum level of HOMO energy is necessary for hallucinogenic activity.

The same calculations were made on a series of tryptamine derivatives of varying hallucinogenic potency [7]. As with the phenylethylamines, a definite correlation was noted between hallucinogenic potency and the E_{HOMO} (see Table III).

* An alternate possibility is that antimalarials are not active until they are first oxidized to a quinone which, in turn, may act by covalent bond formation.

TABLE I
E_{HOMO} VERSUS RELATIVE HALLUCINOGENIC POTENCY IN A SERIES OF α-METHYL PHENETHYLAMINES[a]

Compound	Designation	Potency relative to mescaline	$E_{HOMO}(\beta)$
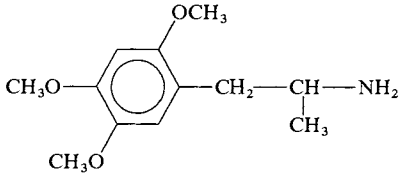	TMA-2	17	0.4810
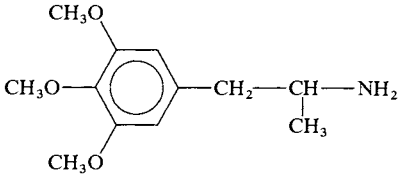	TMA	2	0.5357
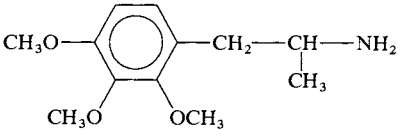	TMA-3	<2	0.5696

[a] Snyder and Merril [7].

TABLE II
E_{HOMO} OF A SERIES OF PHENETHYLAMINES[a]

Compound	Designation	$E_{HOMO}(\beta)$
3,4,5-Trimethoxy	Mescaline	0.5357
2,3,4-Trimethoxy	—	0.5696
3,4-Dimethoxy	—	0.5702
4-Methoxy	Methoxytyramine	0.6583
3-Methoxy	Methoxymetatyramine	0.7240
3,4-Dihydroxy	Dopamine	0.6586
4-Hydroxy	Tyramine	0.7209
—	Phenethylamine	0.8619

[a] Snyder and Merril [7].

The most potent hallucinogen, LSD (**IV**), was calculated by Karreman *et al.* [2] and found to have an E_{HOMO} of 0.218β, far more energetic than any of the molecules calculated by Snyder and Merril.

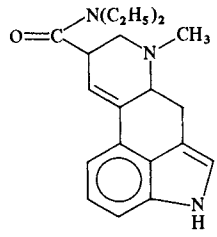

IV

In the case of LSD and the tryptamine derivatives in Table III, the 2 position had the highest free valence, which suggests that this position may be a local site involved in electron donation in a charge transfer complex.

As a more rigorous test of the hypothesis of charge transfer donor ability correlating with hallucinogenic potency, Snyder and Merril compared the E_{HOMO} of five dissimilar molecules with the hallucinogenic potency. The correlation was very good (Table IV) in this limited series.

The study lends credence to the possibility that a potent hallucinogenic agent is an electron donor in some key step involving a charge transfer complex with a biological acceptor molecular entity. It cannot be overlooked, however, that the studies at this point deal only with the conjugated portion of the molecule. Subsequent studies have considered the stereochemistry of the side chains as well [8].

TABLE III

E_{HOMO} VERSUS HALLUCINOGENIC POTENCY IN A SERIES OF TRYPTAMINE DERIVATIVES[a]

Compound	Designation	Potency[b]	$E_{HOMO}(\beta)$
4-Hydroxy-*N*,*N*-dimethyl	Psilocin	31	0.4603
6-Hydroxy-*N*,*N*-dimethyl	—	25	0.4700
5-Hydroxy-*N*,*N*-dimethyl	Bufotenin	Weak	0.5147
N,*N*-Diethyl	—	Weak	0.5164

[a] Snyder and Merril [7].

[b] Potency as a ratio of effective dose of mescaline to a given drug.

TABLE IV

E_{HOMO} VERSUS HALLUCINOGENIC POTENCY IN DIFFERENT DROG CLASSES[a]

Compound	MED (mg/kg)	Activity[b]	$E_{HOMO}(\beta)$
LSD	0.001	3700	0.2180
Psilocin	0.12	31	0.4603
6-Hydroxydiethyltryptamine	0.15	25	0.4700
TMA-2	0.22	17	0.4810
TMA	1.70	2.2	0.5357
Mescaline	3.75	1	0.5357

[a] Snyder and Merril [7].

[b] Ratio of effective dose of mescaline to that of drug.

III. Carcinogenic Hydrocarbons

The possibility that carcinogenic aromatic hydrocarbons might function at the molecular level by the formation of a charge transfer complex as a crucial event, was first considered by Pullman and Pullman [*9*]. They concluded that there was no general relationship between charge transfer capability and carcinogenesis, although some rough correlations were observed in some limited series of molecules.

Mason has postulated that carcinogenic activity depends upon the transfer of an electron from a high-lying protein band to an empty level in the hydrocarbon [*10*]. To possess carcinogenicity, according to Mason's MO calculations, the hydrocarbon should have an unfilled energy level 1.10–1.18β above the highest filled level. He assumed that the unfilled level of the hydrocarbon matched the energy of the highest filled band of the protein (Fig. 3).

Thirty-four hydrocarbons were calculated. Five of these were known to be carcinogens. In each of these five cases, the energy difference between the highest filled and one of the empty levels was in the range 1.10–1.18β (see Table V).

Chalvet and Mason extended this work to a series of methyl-1,2-benzanthracene derivatives [*11*]. These calculations included overlap. Most of the active molecules had ΔE values between the limits of 1.3341 γ and 1.4462 γ (see Table VI).

The consequences of this complexation with a protein donor molecule in terms of the induction of carcinogenesis have been discussed by Mason [*10*].

Pullman and Pullman have commented critically on the theory of charge transfer as a mechanism in carcinogenesis, questioning the validity of the correlation and the concept of a protein donor in the complex [*12–14*]. An alternate suggestion has been offered in which the nucleic acids are

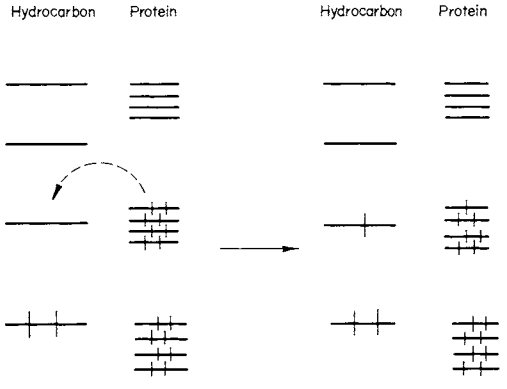

Fig. 3. Electron transfer from protein to carcinogenic hydrocarbon.

implicated in the charge transfer, complexing with a carcinogenic hydrocarbon [*15*]. It has also been suggested that electrons are transferred from the protein to an empty level in the hydrocarbon [*16*]. Allison and Nash postulated that carcinogenicity arises as a consequence of a molecule possessing both electron-donating and electron-accepting properties [*17*].

A statistical approach has been taken by Sung to determine the validity of the correlations between charge transfer capability of hydrocarbons and their carcinogenicity [*18*]. He concluded that the data of Mason does reveal

TABLE V

ENERGY DIFFERENCE BETWEEN A HYDROCARBON FILLED LEVEL AND ONE OF ITS EMPTY LEVELS, AND CARCINOGENIC ACTIVITY[a]

Molecule	$\Delta E_1(\beta)$	$\Delta E_2(\beta)$	$\Delta E_3(\beta)$	$\Delta E_4(\beta)$	Activity
Benzene	2.000	2.000	3.000	—	–
Naphthalene	1.2361	1.6180	1.9208	2.2361	–
Anthracene	0.8284	1.4142	1.4142	1.8284	–
Naphthacene	0.5899	1.0724	1.2950	1.4855	–
Pentacene	0.4394	0.8377	1.2197	1.2197	–
Phenanthrene	1.2105	1.3743	1.7476	1.9110	–
3,4-Benzophenanthrene	1.1352	1.2297	1.5676	1.6910	+
Chrysene	1.0402	1.3124	1.3954	1.7365	–
1,2-Benzanthracene	0.9046	1.1673	1.4523	1.6179	+?
Pyrene	0.8901	1.3244	1.4450	1.6920	–
Triphenylene	1.3681	1.5634	1.9696	2.0313	–
Pentaphene	0.8743	0.9580	1.4372	1.4372	–
Picene	1.0038	1.1822	1.3614	1.5019	–
Perylene	0.6946	1.3473	1.3473	1.3473	–
1,2:3,4-Dibenzanthracene	0.9982	1.2131	1.2899	1.5940	–
1,2:5,6-Dibenzanthracene	0.9470	1.1578	1.2601	1.5431	++
1,2:7,8-Dibenzanthracene	0.9834	1.097	1.3652	1.4917	+
3,4:5,6-Dibenzophenanthrene	0.0709	1.1922	1.3227	1.6027	–
3,4-Benzpyrene	0.7425	1.1730	1.3712	1.3712	
3,4:8,9-Dibenzopyrene	0.6054	0.0960	1.1314	1.3027	
1,12-Benzoperylene	0.8784	1.1235	1.4329	1.4392	?
Coronene	1.0784	1.0784	1.5392	1.5392	–
Anthanthrene	0.5818	1.0409	1.1657	1.3944	–
Diphenyl	1.4092	1.7046	1.7046	2.0221	–
p-Diphenylbenzene	1.1853	1.5926	1.5926	1.5926	–
m-Diphenylbenzene	1.3243	1.4275	1.6622	1.6622	–
o-Diphenylbenzene	1.2206	1.4346	1.6103	1.6103	–
1,3,4-Triphenylbenzene	1.3243	1.5681	1.6622	1.6622	–
Styrene	1.3242	1.6622	2.0764	2.7979	–
Stilbene	1.0086	1.5043	1.5043	1.6577	–
Biphenylene	1.8901	1.3244	1.6920	1.7923	?
2,3:6,7-Dibenzofluorene	0.9687	1.0107	1.1518	1.6211	?
3,4:5,6-Dibenzofluorene	0.7466	1.2002	1.2151	1.4433	–
1,2:7,8-Dibenzofluorene	0.8326	1.1848	1.3793	1.5207	?

[a] Mason [*10*].

a correlation between carcinogenicity and some property related to the calculated energy levels.

In Chapter VI, we have discussed the reactivity theory of the Pullmans centering on the *K* and *L* regions of these hydrocarbons. The presence of correlations between carcinogenicity and reactivity criteria is apparent from their work. It is not unreasonable to suggest that the charge transfer

TABLE VI

DIFFERENCES IN ENERGY BETWEEN THE HIGHEST FILLED AND SUCCESSIVE UNFILLED LEVELS IN UNITS OF γ, THE RESONANCE INTEGRAL[a]

Molecule	$\Delta E_{1-\bar{1}}(\gamma)$	$\Delta E_{1-\bar{2}}(\gamma)$	$\Delta E_{1-\bar{3}}(\gamma)$	$\Delta E_{1-\bar{4}}(\gamma)$	Activity
5,9,10-Trimethyl-	0.8711	1.1025	1.3868	1.5509	+
6,9,10-Trimethyl-	0.8733	1.1129	1.3919	1.5593	+
9,10-Dimethyl-	0.8769	1.1154	1.3978	1.5637	+
8,10-Dimethyl-	0.8842	1.1266	1.4122	1.5752	+
5,10-Dimethyl-	0.8848	1.1244	1.4114	1.5747	+
5,9-Dimethyl-	0.8851	1.1312	1.4156	1.5292	+
1',10-Dimethyl	0.8909	1.1484	1.4229	1.5895	+
10-Methyl-	0.8909	1.1379	1.4229	1.5885	+
5,8-Dimethyl-	0.8867	1.1376	1.4252	1.5860	−
9-Methyl-	0.9931	1.1463	1.4287	1.5966	+
5,6-Dimethyl-	0.8910	1.1469	1.4309	1.5956	+
5-Methyl-	0.8965	1.1517	1.4387	1.6021	+
3-Methyl-	0.8977	1.1592	1.4390	1.6048	+
8-Methyl-	0.8974	1.1552	1.4409	1.6038	+
4-Methyl-	1.8975	1.1562	1.4411	1.6039	+
6,7-Dimethyl-	0.8984	1.1569	1.4413	1.6062	+
2',6-Dimethyl-	0.8985	1.1602	1.4428	1.6071	+
7-Methyl-	0.9002	1.1587	1.4462	1.6097	+
6-Methyl-	0.9014	1.1644	1.4462	1.6133	+
3',6-Dimethyl-	0.9004	1.1671	1.4473	1.6119	−
3',7-Dimethyl-	0.8996	1.1618	1.4477	1.6087	−
4-Methyl-	0.9022	1.1724	1.4480	1.6144	−
2-Methyl-	0.9012	1.1631	1.4485	1.6114	−
1-Methyl-	0.9046	1.1177	1.4523	1.6186	−
3-Methyl-	0.9036	1.1703	1.4536	1.6167	−
1'-Fluoro-10-methyl	0.8806	1.2190	1.4126	1.6184	?
2'-Fluoro-	0.8274	1.0728	1.3794	1.5061	?
3'-Fluoro-	0.8622	1.1412	1.4304	1.5736	+
4'-Fluoro-	0.8173	1.1397	1.3779	1.5542	Toxic
3-Fluoro	0.7911	1.0519	1.2824	1.4560	−
4-Fluoro	0.8116	1.0381	1.3462	1.4609	+
5-Fluoro	0.8161	1.0097	1.3286	1.4836	?
6-Fluoro	0.8205	1.0771	1.3341	1.5773	+
7-Fluoro	0.8321	1.0482	1.3667	1.5271	+
8-Fluoro	0.8035	1.0233	1.3327	1.6199	?
9-Fluoro	0.7806	1.0802	1.2712	1.4141	?

[a] Chalvet and Mason [*11*].

theory and the chemical reactivity theory may really be providing insights into the same general event leading to carcinogenesis, but that each theory seeks correlation with a different, although closely related, phase of that event. It is possible that some form of intimate complex precedes a covalent bond formation reaction with an active hydrocarbon. In some cases, this complexing ability may be the limiting step in the process. There is then an apparent correlation noted between subsequent biological activity and an electronic parameter relating to the propensity to form such a complex. In other cases, the molecule may not be so limited but instead, some structural requirement at the point of covalent bond formation may be a limiting feature. Hence, correlation with reactivity at a particular site may prevail. It is conceivable also that the hydrocarbons may function in different ways insofar as their metabolism to ultimate carcinogens. Entering into structural requirements then may be overall size and shape as well as reactivity and complexing ability. Clearly the last word is not in on this matter, but studies to date have narrowed the range of mechanisms of these molecules.

IV. Solution Stabilization of Menadione

The formation of complexes may greatly alter the rate of a chemical reaction involving one of the complexing molecules. Advantage can be taken of this alteration by employing a complexing agent to retard some destructive reaction of a medicinal agent in solution. It has been noted that the rate of hydrolysis of local anesthetic esters can be reduced by introducing a substance which will form a molecular complex [*19*]. This phenomenon can be of advantage in designing systems to stabilize aqueous solutions of labile drugs.

A study on the stabilization of menadione (**V**) and the MO relationship of electron donor molecules to this phenomenon was reported by Hata *et al.* [*20*]. The objective was to seek a correlation between some MO energy level index and an experimental manifestation of complexation. This would offer an opportunity to approach stability problems from a predictive point of view rather than trial and error [*21*]. The energies of the HOMO and LEMO were calculated, using π-electron HMO theory, on a number of molecules of known complexing ability as well as menadione (see Table VII).

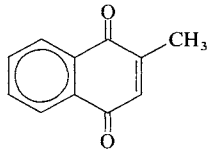

V

TABLE VII
ENERGY LEVELS OF HOMO AND LEMO[a]

Compound	$E_{HOMO}(\beta)$	$E_{LEMO}(\beta)$
Menadione	0.972	0.228
Salicylic acid	0.438	0.555
Caffeine	0.633	0.687
Theophylline	0.656	0.690
Theobromine	0.633	0.688
Nicotinamide	0.563	0.465
Ethyl aminobenzoate	0.363	0.386
Dehydroacetic acid	0.822	0.546
6-Hydroxynaphthoic acid	0.384	0.450

[a] Hata *et al.* [*20*].

A series of molecules were added to solutions of menadione and spectral changes observed. Formation constants were obtained from these studies and the free energies of complexation, ΔG, calculated. Some relationship was noted between this ΔG of complexation with menadione and the E_{HOMO} of the electron donor molecule (see Fig. 4). It was concluded from this curvilinear relationship that the complex formation was at least partly due to charge transfer interaction.

The stabilization of menadione in electron donor solutions was found to protect the molecule from photodecomposition [*22*]. Absorption spectra of menadione and complexed menadione were observed before and after irradiation and a rate of stabilization calculated. The rate increased with the complexing of superior electron-donating molecules as shown in Fig. 5.

In an effort to assess whether the complex formed by menadione and the

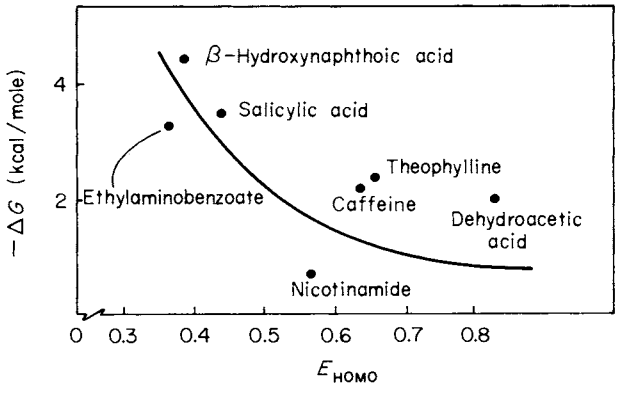

Fig. 4. Relation between apparent free energy change, ΔG, and $E_{(HOMO)}$ [*21*].

other molecules considered was of the charge transfer type, further MO calculations were made on the molecules in the study [*23*]. Specifically, it was presumed that the orientation of the molecules in the complex would be governed to a considerable degree by the matching of complimentary electronic charges so as to maximize electrostatic or dipole attraction. Schematically, the complex was depicted as in Fig. 6. Using this model, Nagata *et al.* [*24*] has defined a stabilization energy, δE, and a quantity of charge transfer, δQ, as

$$\delta E = -2\left[\sum_{j}^{\text{occ}}\sum_{k}^{\text{vac}} - \sum_{j}^{\text{vac}}\sum_{k}^{\text{occ}}\right]\frac{(C_r^j C_s^k I_1 + C_t^j C_u^k I_2 + \cdots)^2}{E_{1j} - E_{2k}}(\beta')^2$$

$$\delta Q = 2\left[\sum_{j}^{\text{occ}}\sum_{k}^{\text{vac}} - \sum_{j}^{\text{vac}}\sum_{k}^{\text{occ}}\right]\frac{(C_r^j C_s^k I_1 + C_t^j C_u^k I_2 + \cdots)^2}{(E_{1j} - E_{2k})^2}(\beta')^2$$

where C_r^j is a coefficient of the rth atomic orbital in the jth molecular orbital, E_{1j} is the energy of the jth molecular orbital of molecule 1, and both $\sum^{\text{occ}}$ and $\sum^{\text{vac}}$ are the summation of the occupied and vacant orbitals, respectively. The

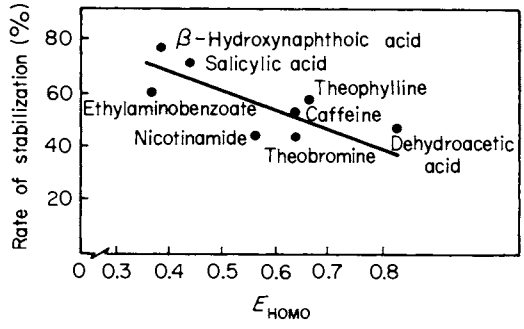

Fig. 5. Relation between rate of stabilization and $E_{(\text{HOMO})}$ [*22*].

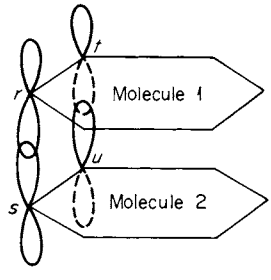

Fig. 6. Schematic representation of δ–δ overlap of π orbitals [*23*].

TABLE VIII
REACTIVITY INDICES BASED ON ASSUMED OVERLAPPING ATOMS IN THE DONOR–MENADIONE COMPLEX[a]

Compound	$\delta E\frac{(-\beta')^2}{\beta}$	$\delta Q\left(\frac{\beta'}{\beta}\right)^2$
p-Hydroxybenzoic acid	2.3372	2.4149
Salicylic acid	1.6109	0.6092
Ethylaminobenzoate	1.1946	0.4670
Theophylline	1.0198	0.2196
Caffeine	0.9966	0.1866
Dehydroacetic acid	0.9575	0.1223
Nicotinamide	0.7712	0.1740
Theobromine	0.6236	0.0943

[a] Hata *et al.* [23].

term β' is the resonance integral between the atomic orbitals of carbon atoms of the charge transfer complex, as depicted in Fig. 6.

An arbitrary assumption was made concerning which atoms were involved in the charge transfer overlap between each electron donor and menadione. The δE and δQ indices were calculated from these overlapping patterns (see Table VIII).

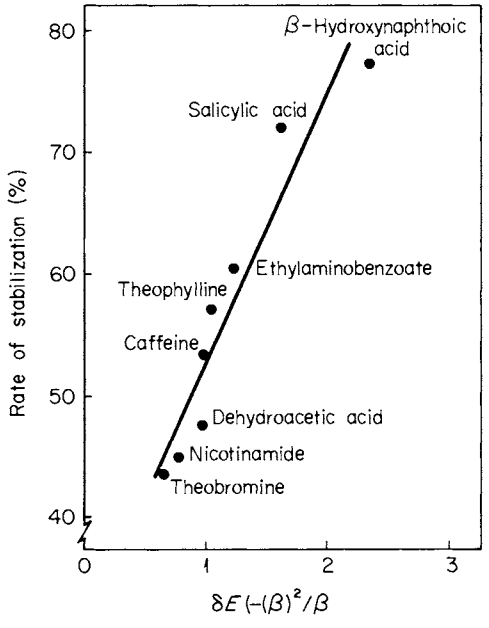

Fig. 7. Relation between rate of stabilization and stabilizing energy, δE [23].

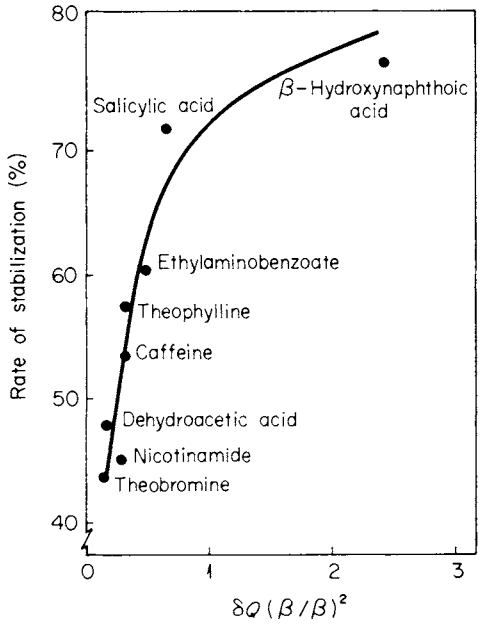

Fig. 8. Relation between rate of stabilization and the quantity of charge transfer [*23*].

A relationship is shown between the rate of stabilization of menadione and the stabilization energy, δE (Fig. 7). The stability of menadione was also found to correlate with the quantity of charge transfer, δQ (Fig. 8).

The conclusion reached was that the suppression of photodecomposition of menadione with various electron donors was due to charge transfer complex formation among them. The possibility exists that the complexes do form, as concluded from the studies; however, the MO-calculated indices, δE and δQ, certainly are heavily dependent on the assumed overlapping patterns of atoms between donor and menadione.

The case for a charge transfer complex stabilizing menadione was strengthened by Hata when a new charge transfer band was noted when menadione was dissolved in aqueous solution with the electron donors previously studied [*25*]. The energies of the charge transfer absorption maxima formed between menadione and several electron donors correlated with the stabilization energies, δE, and the E_{HOMO} of the donors, as shown in Figs. 9 and 10, respectively.

This type of study offers considerable promise in the potential ability of MO calculations to predict charge transfer capabilities of molecules in solution with an acceptor. The benefit to studies on drug stabilization could be significant.

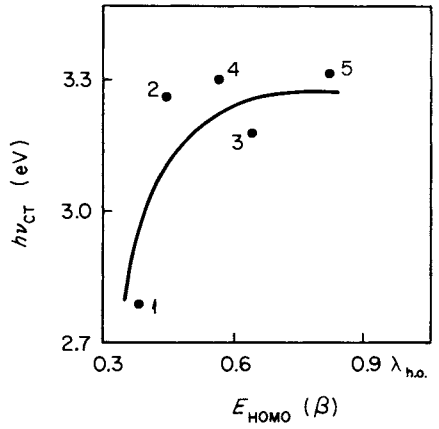

Fig. 9. Relation between charge transfer band, $h\nu_{CT}$ and $E_{(HOMO)}$: (1) β-hydroxynaphthoic acid, (2) salicylic acid, (3) caffeine, (4) nicotinamide, (5) dehydroacetic acid [*25*].

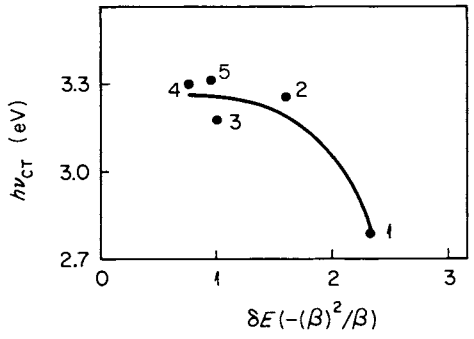

Fig. 10. Relation charge transfer band, $h\nu_{CT}$, and stabilization energy, δE. Numbers refer to Fig. 9 [*25*].

V. Local Anesthetics

The δE and δQ indices reflecting the stabilization energy and quantity of charge transfer have also been calculated in studies on local anesthetics. It has been recognized that thiamine participates in some manner in nerve conduction, although its role cannot be precisely defined [*26*]. Eckert has investigated the interaction of local anesthetics and thiamine with absorption spectroscopy and has concluded that charge transfer complexation takes place [*27*]. He postulated that local anesthetics may inhibit nerve conduction by such a process.

In a recent study by Yoneda and Nitta, the electronic structures of several local anesthetics were calculated in an effort to find a reactivity index correlating with activity [*28*]. The calculations were made using π-electron Hückel theory. The molecules were postulated to form charge transfer complexes by pairing complementary charged atoms so as to maximize

electrostatic attraction. In these models, the stabilization energy of the complex, δE, and the quantity of charge transfer, δQ, indices were calculated. These are the same indices just described in the work on menadione [*23*]. The results of the calculations are shown in Table IX.

TABLE IX
CHARGE TRANSFER INDICES CALCULATED FOR SEVERAL LOCAL ANESTHETICS AND ACTIVITY[a]

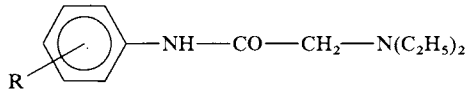

No.	R	$\delta E \frac{(-\beta')^2}{\beta}$	Conc. with 1 hr anesth. duration (%)
1	2-Chloro, 6-methyl	0.4350	0.8
2	2,6-Dimethyl	0.5397	1.05
3	2-Methyl	0.4000	1.4
4	H	0.3706	1.8
5	2-Chloro	0.3689	2.0
6	3,4-Dimethyl	0.4117	2.1
7	2-Chloro, 4-methyl	0.4254	2.3
8	2-Methyl, 3-chloro	0.3531	2.7
9	2-Methyl, 5-chloro	0.3341	3.25

[a] Yoneda and Nitta [*28*].

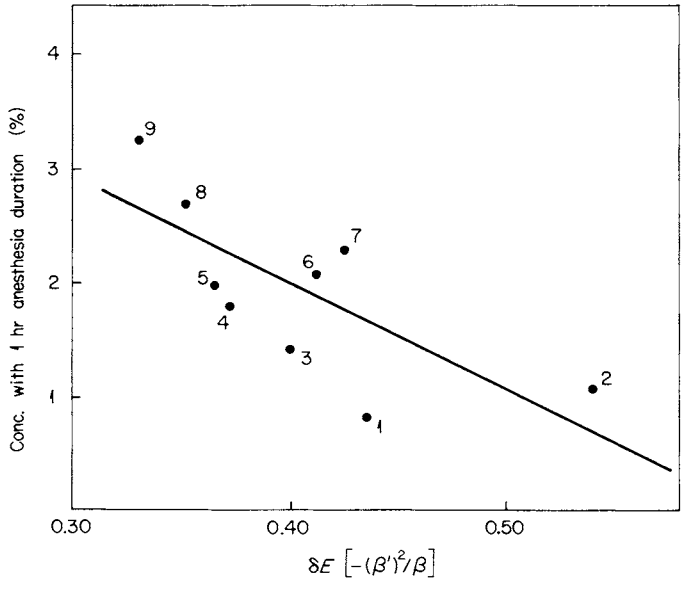

Fig. 11. Relation between charge transfer stabilization energy, δE, and local anesthetic activity. Numbers refer to Table IX.

There appears to be some relationship between the stabilization energy index and the activity as seen in Fig. 11. This calculated relationship suggests that a charge transfer complexation may play a role in the activity of these molecules. It should be noted here that the values of δE in the series are dependent on the assumed pattern of atoms interacting between the local anesthetic and thiamine. The choice of a different, but equally reasonable pattern of interacting atoms may result in an entirely different picture.

VI. Phenothiazine Tranquilizers

In their classic paper, Karreman, Isenberg, and Szent-Györgyi proposed that a charge transfer reaction may play a prominent role in the biological activity of drug molecules [*2*]. They noted the powerful tranquilizing action of chlorpromazine (**VI**) as well as the striking electron-donating properties of this molecule and raised the possibility of a causal relationship.

They discussed the possibility of an electron donor transferring an electron at the electric double layer at the cell surface resulting in depolarization of the cell and thus excitation (Fig. 12).

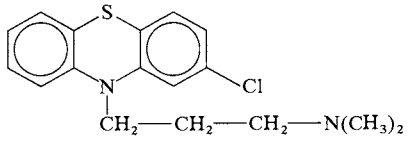

VI

An alternative event could be the donation of an electron in the interior of the cell leading to hyperpolarization and inhibition (Fig. 13).

The E_{HOMO} and E_{LEMO} were calculated by these authors for chloropromazine. They found:

$$E_{\text{HOMO}} = -0.217\beta \qquad E_{\text{LEMO}} = -1.000\beta$$

The finding of an antibonding MO for the highest filled level is startling. This suggests an almost spontaneous tendency to donate a high-lying electron. This situation has been somewhat clarified by other MO calculations in which the sulfur atom has been treated by considering the *d* orbitals [*29*]. These calculations showed chlorpromazine to have:

$$E_{\text{HOMO}} = 0.191\beta$$

with the lowest empty orbital being a nonbonding orbital on sulfur. Nevertheless, this high-lying filled MO suggests that chloropromazine may be an excellent electron donor in a charge transfer complex.

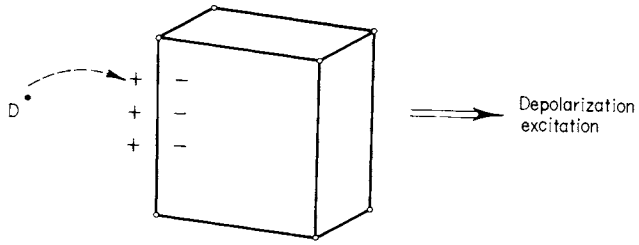

Fig. 12. Schematic representation of an electron donor transferring an electron at the cell surface.

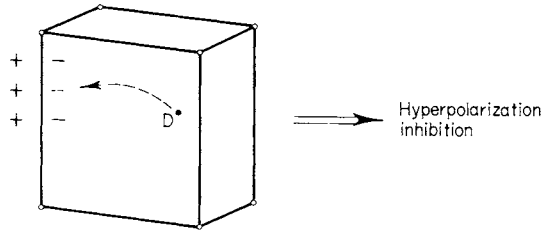

Fig. 13. Schematic representation of an electron donor transferring an electron within the cell.

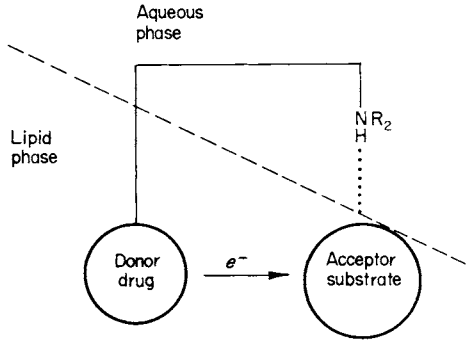

Fig. 14. Model proposed for chlorpromazine activity involving a charge transfer complex [*30*].

Nash and Allison have hypothesized that chlorpromazine may form a charge transfer complex with a suitable acceptor molecule, permitting the close approach of the chlorpromazine side chain to a hydrogen bond acceptor feature on the acceptor molecule (Fig. 14) [*30*].

VII. Nicotinic Agents

An MO study of phenylcholine ethers (**VII**) has led to the conclusion that

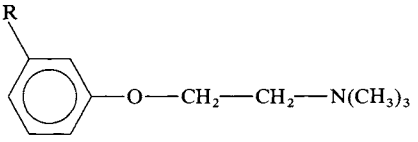

VII

charge transfer may be an important mechanism in the nicotinic action of these agents. The phenylcholine ethers are known to possess nicotinic action which varies in potency with the substitution on the phenyl ring. Attempts have been made to relate this structure with the natural ganglionic

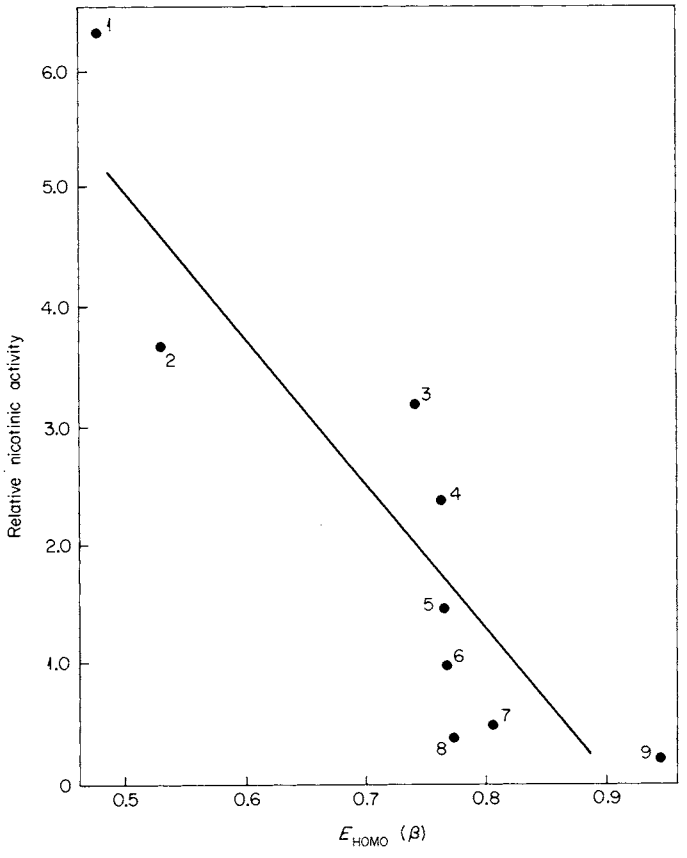

Fig. 15. Relationship between nicotinic activity of a series of phenylcholine ethers and $E_{(HOMO)}$. Numbers refer to Table X [*32*].

TABLE X
RELATIVE NICOTINIC ACTIVITY AND MO INDICES[a]
R—CH_2—CH_2—$N(CH_3)_3^+$

	R	Rel. nicotinic activity[b]	$S_2^{(E)}$	$S_6^{(E)}$	$E_{HOMO}(\beta)$
1.	*m*-I—C_6H_4—O—	6.3	0.9947	0.9928	0.4812
2.	*m*-NH_2—C_6H_4—O—	3.7	1.2800	1.2781	0.5322
3.	*m*-Br—C_6H_4—O—	3.2	0.9869	0.9837	0.7671
4.	*m*-Cl—C_6H_4—O—	2.4	0.9779	0.9742	0.7671
5.	*m*-F—C_6H_4—O—	1.5	0.9746	0.9706	0.7685
6.	C_6H_5—O—	1.0	0.9751	0.9751	0.7692
7.	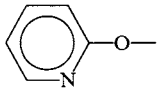	0.5	—	—	0.8040
8.	*m*-NO_2—C_6H_4—O—	0.4	0.9483	0.9228	0.7738
9.	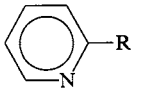	0.2	—	—	0.9467

[a] Crow *et al.* [*32*].
[b] Coleman *et al.* [*33*].

stimulant (nicotinic agent) acetylcholine. Fukui has studied these ethers using MO theory and found no correlation between activity in a series and the ether oxygen charge density [*31*]. A correlation was found between the frontier electron density at the ether oxygen and also the superdelocalizability at the ring *ortho* position and activity.

Crow, Wasserman, and Holland have extended these studies on a series of *meta*-substituted phenylcholine ethers, using simple Hückel theory [*32*]. The results, shown in Table X and Fig. 15, reveal a correlation between nicotinic activity and E_{HOMO}, $S_2^{(E)}$, and $S_6^{(E)}$. They concluded that a charge transfer mechanism was indicated involving the aromatic ring as a donor.

A further inference that can be drawn from the calculations is that the complexation which may ensue between the aromatic ring and the receptor is possibly localized at the 2 or 6 positions of the ring. Thus the $S^{(E)}$ indices show a correlation with activity. It is noteworthy that the 2 position of the phenyl ring in the phenylcholine ethers bears the same relationship to the ether oxygen atom as does the carbonyl oxygen atom to the ether oxygen atom of acetylcholine. Assuming that the ethylammonium side chains in both the phenylcholine ether series and acetylcholine are comparable as far as conformation is concerned,* it is possible to identify the secondary

* Recent MO calculations of the conformation of phenylcholine ether justify this assumption (L. B. Kier and J. M. George, *J. Med. Chem.*, in press).

binding site in these nicotinic agents and to approximate its distance from the quaternary group. Kier, in studies of the conformations of nicotine and acetylcholine, predicted that this secondary site was negatively charged and about 4.85 Å from the onium group [*34*]. The study of Crow, Wasserman, and Holland supports this hypothesis and provides further insight into the possible role of the secondary binding site in nicotinic agents [*32*].

VIII. Imidazoline Analgesics

The complications arising when attempts are made to correlate a chemical reactivity parameter with an observed biological response were touched on in Chapter V. In particular, the ability of a drug molecule to partition between the fat and aqueous phases *in vivo* in an optimum manner may limit the availability of the drug to the receptor. It may, in some cases, be the sole limiting factor for activity in a series of molecules. Hansch has provided an empirical approach to the evaluation of the relative contribution of substituent groups and atoms to the lipophilic character of a molecule [*35*]. This was described briefly in Chapter V.

It is thus possible to add to a calculated electronic index, a term reflecting the lipophilic or partitioning properties of molecules in a series and to relate these, via regression analyses, to the observed biological activity.

Such an effort was made by Neely *et al.* who considered a series of analgesic imidazoline derivatives (**VIII**) [*36*].

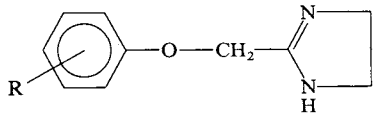

VIII

The calculations were made using π-electron Hückel theory to obtain E_{HOMO} values for the substituted phenoxy portion of the molecule. The results are shown in Table XI, along with the Hansch partition substituent constants, π.

An examination of the relationship of activity to the π and E_{HOMO} indices was made using separate then combined regression analyses. From Eqs. (1) and (2)

$$\text{Log ED}_{50} = -0.445\pi + 1.015 \qquad r = 0.640 \tag{1}$$

$$\text{Log ED}_{50} = 0.655\pi^2 - 1.00\pi + 0.455 \qquad r = 0.728 \tag{2}$$

it is evident that the correlation between activity and the substituent parameters was nonexistent. When the E_{HOMO} was compared with activity, there

TABLE XI
ANALGESIC POTENCIES, MO INDICES, AND SUBSTITUENT CONSTANTS FOR A SERIES OF IMIDAZOLINES[a]

Substituent	ED_{50}[b]	π[c]	$E_{HOMO}(\beta)$
2,6-Dimethyl	0.6	1.36	0.716
2-Br, 6-Cl	2.0	1.34	0.802
2,6-diBr	3.2	1.50	0.797
2,6-diCl	3.3	1.18	0.808
2,6-diCl, 3-methyl	5.4	1.69	0.789
2,6-Dimethoxy	25	−0.66	0.618

[a] Neely *et al.* [*36*].
[b] Oral dose in mg/kg in writhing test.
[c] Fujita *et al.* [*37*].

was not found any correlation. However, when both π and E_{HOMO} terms were included in the regression equation,

$$\text{Log } ED_{50} = 0.945\pi^2 - 1.850\pi + 7.90\,E_{HOMO} - 5.117 \qquad r = 0.975 \quad (3)$$

the correlation becomes apparent. The significance of the E_{HOMO} term in the equation is at the 5% level.

The activity of the molecules was concluded to relate to a combination of favorable partitioning and the ability of the ring to engage a receptor feature in a charge transfer complex, as reflected in the E_{HOMO} index. The calculations provide a working model for the design of additional related molecules which may have greater potency.

IX. Benzothiadiazine Antihypertensive Agents

Wohl has recently studied antihypertensive potency in a series of benzothiadiazines (**IX**) using EHT [*38*].

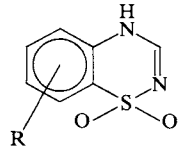

IX

A number of indices were calculated, including polarizability, frontier density and superdelocalizability. The latter index employs the vacant orbitals from EHT calculations. The value of these virtual orbitals is questionable in view of the fact that the LEMO is of the same sign as the HOMO and that the two are unrealistically close together [*39*].

The antihypertensive potency was found by regression analysis to relate to eight MO-calculated indices in the regression equation, considering 25 derivatives of **IX**. The calculations showed that a reactivity index reflecting charge transfer capacity at position 5 in the benzene ring was of determinantal importance.

X. General Comments

It would appear from a limited number of studies to date that some correlations have been observed between biological activity and calculated MO indices. Insofar as these indices reflect charge transfer phenomenon, the assignment of a charge transfer mechanism to the event under study is reasonable. The problem is present in using π-only Hückel theory, that the realism of the calculated energy levels is always suspect. The nonbonded interactions are not part of the calculation, so the influence of these on the higher lying π MO's is not apparent. Still, in a closely related series, the relative energies of the HOMO levels should bear some relationship to physical properties and may be a fair index of charge transfer. SCF π-only calculations would certainly be superior.

The value of individual energy levels as calculated by EHT is questionable. Thus the E_{LEMO} and E_{HOMO} levels are too close and are of the same sign. The $S^{(N)}$ index would thus be derived from a virtual orbital with a negative sign relative to the zero of energy.

References

1. R. S. Mulliken, *J. Amer. Chem. Soc.* **74**, 811 (1952).
2. G. Karreman, I. Isenberg, and A. Szent-Györgyi, *Science* **130**, 1191 (1959).
3. F. E. Hahn, R. L. O'Brien, J. Ciak, J. L. Allison, and J. G. Olerick, *Mil. Med. Suppl.* **131**, 1071 (1966).
4. I. H. Goldberg, *Military Med.* **131**, *Suppl.*, 1092 (1966).
5. J. A. Singer and W. P. Purcell, *J. Med. Chem.* **10**, 754 (1967).
6. W. P. Purcell and K. Sundarem, *J. Med. Chem.* **12**, 18 (1969).
7. S. H. Snyder and C. R. Merril, *Proc. Nat. Acad. Sci. U.S.* **54**, 258 (1965).
8. S. H. Snyder and E. Richelson, *Proc. Nat. Acad. Sci. U.S.* **60**, 206 (1968).
9. A. Pullman and B. Pullman, "Cancerisation par les Substances Chimiques et Structure Moleculaire." Masson, Paris, 1955.
10. R. Mason, *Nature (London)* **181**, 820 (1958).
11. O. Chalvet and R. Mason, *Nature (London)* **192**, 1070 (1961).
12. A. Pullman and B. Pullman, *Nature (London)* **196**, 228 (19[illegible]).
13. B. Pullman and A. Pullman, *Nature (London)* **199**, 4892 (196[illegible]).
14. A. Pullman "Quantum Aspects of Polypeptides and Polynucleotides" (M. Weissbluth, ed.), p. 47. Wiley (Interscience), New York, 1963.
15. J. Ladik, *Acta Phys.* **11**, 239 (1960).

16. J. B. Birks, *Nature (London)* **190**, 232 (1961).
17. A. C. Allison and T. Nash, *Nature (London)* **197**, 758 (1963).
18. S. Sung, *Sci. Sinica* **14**, 583 (1965).
19. T. Higuchi and L. Lachman, *J. Pharm. Sci.* **44**, 521 (1955).
20. S. Hata, M. Hamakawa, S. Tomoiko, and H. Sano, *Chem. Pharm. Bull. Jap.* **13**, 96 (1965).
21. S. Hata, K. Mizuno, and S. Tomoiko, *Chem. Pharm. Bull. Jap.* **15**, 1791 (1967).
22. S. Hata, K. Mizuno, and S. Tomoiko, *Chem. Pharm. Bull. Jap.* **15**, 1796 (1967).
23. S. Hata, K. Mizuno, and S. Tomoiko, *Chem. Pharm. Bull. Jap.* **16**, 1 (1968).
24. C. Nagata, A. Imamura, K. Fukui, and H. Saito, *Gann* **54**, 401 (1963).
25. S. Hata and S. Tomoiko, *Chem, Pharm. Bull. Jap.* **16**, 1397 (1968).
26. A. von Muralt, "Neue Ergebuisse der Nervenphysiologie." Springer, Berlin, 1958.
27. T. Eckert, *Arzneim.-Forsch.* **12**, 8 (1962).
28. F. Yoneda and Y. Nitta, *Chem. Pharm. Bull. Jap.* **13**, 574 (1965).
29. M. K. Orloff and D. D. Fitts, *Biochim. Biophys. Acta* **47**, 596 (1961).
30. T. Nash and A. C. Allison, *Biochem. Pharmacol.* **12**, 601 (1963).
31. K. Fukui, C. Nagata, and A. Imamura, *Science* **132**, 87 (1960).
32. J. Crow, O. Wasserman, and W. C. Holland, *J. Med. Chem.* **12**, 764 (1969).
33. M. E. Coleman, A. S. Hume, and W. C. Holland, *J. Pharmacol. Exp. Ther.* **148**, 66 (1965).
34. L. B. Kier, *Mol. Pharmacol.* **4**, 70 (1968).
35. C. Hansch and T. Jujita, *J. Amer. Soc.* **86**, 1616 (1964).
36. W. B. Neely, H. C. White, and A. Rudzik, *J. Pharm. Sci.* **57**, 1176 (1968).
37. T. Fujita, J. Iwasa, and C. Hansch, *J. Amer. Chem. Soc.* **86**, 5175 (1964).
38. A. J. Wohl, *Mol. Pharmacol.* **6**, 189, 195 (1970).
39. R. Hoffmann, *J. Chem. Phys.* **39**, 1397 (1963).

Chapter VIII

MOLECULAR CONFORMATION

If we accept the premise that the pattern of essential atoms and groups in a drug molecule must bear some distinct relationship to complementary features on the receptor molecule, then it follows that we must understand the spatial relationship of these essential moieties in order to relate structural modification to biological activity. It also follows that with an understanding of the electron distribution on the essential atoms and groups of a drug, and an understanding of the drug molecule stereochemistry, we are in a position to deduce something of the nature of the topology of the receptor.

The importance of the stereochemistry of active molecules in many pharmacological classes is well known. The high degree of receptor specificity for active substrates is also appreciated. The problem has persisted, however, as to the deduction of a probable conformation of a "flexible" drug molecule. Direct experimental evidence and indirect evidence from studies on series of molecules has been the approach used to date. This has certainly led to some progress in the understanding of structure–action relationships, drug mechanisms, and new drug design.

There are now available MO methods capable of treating all-valence electrons, leading to a total energy which is a function of geometry. These methods are the EHT [*1*] and the Pople-Segal CNDO 2, SCF method [*2*]. They have been previously described (Chapters III and IV).

The relationship between an MO-calculated conformation and the experimentally determined conformations of a crystal and of a substance in solution should be briefly considered. The MO calculations are on a single conservative molecule; the crystal studies are on a molecule frozen into

an array of its kind; and solution-derived conformations are on a molecule surrounded by solvent. Thus, the MO calculations do not consider the perturbations introduced by the neighboring molecules or solvent. Consequently, there is uncertainty in the calculated expectation values. Where correlation between MO-calculated and experimental values has been achieved, the additional forces must not be of a sufficient magnitude to alter the conformation. Whether this is generally true is not known and will be answered only in time. Most results to date are encouraging. It is well at this time, however, to seek correlation between calculated and experimental conformations.

Another area of concern regarding MO-calculated conformations is whether drug molecules so treated can be used to map complementary features of a receptor. The working hypothesis that has been used in several studies using MO methods is that these molecules engage the receptor in their preferred conformations. An alternative hypothesis is that the receptor is capable of a significant perturbing influence on a drug molecule in its vicinity, and that a nonpreferred conformation engages the receptor. This still would not violate the concept of optimum stereochemistry maximizing efficacy, since the perturbed conformation would arise from an initial presentation of the drug molecule in its preferred conformation. This would, however, require that different, active molecules would have to be perturbed into nonpreferred conformations in which the pattern of essential atoms was closely related.

Another observation on this matter that has emerged from recent work is that, in several cases so far studied, at least two different, active molecules in a pharmacological class, in their calculated preferred conformation, presented nearly identical patterns of like-charged atoms. This supports the view that, at least in the cases cited, the drug molecules involved function in a preferred conformation. The alternative view would require a series of fortuitous perturbations of each molecule. From Occam's Razor, the former hypothesis appears more acceptable.

Applying the principles and assumptions described, several pharmacologically important molecules have been studied using all-valence electron MO-calculated conformations. The molecules considered in these studies have been among the most potent in a particular class, the reasoning being that these molecules present optimum electronic patterns to their receptors. The bonds under study in these molecules were rotated and calculations of total energy made at regular angular increments. An energy vs. angle profile results, from which preferred conformation can be deduced (Fig. 1). Also available from such a graph is information on the relative height of rotation barriers and the possible presence of secondary energy minima.

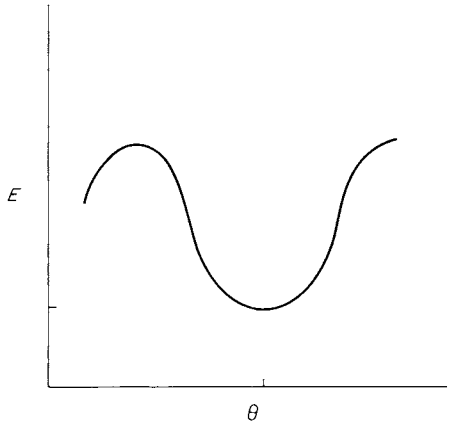

Fig. 1. Plot of calculated total energy, E, vs angle of rotation, θ.

I. Muscarinic Pharmacophore

The first attempt to apply MO-calculated conformations to drug molecules was with the muscarinic agonists. Most attempts to deduce the pattern of essential atoms in muscarinic agonists have centered around chemical modification, in an effort to simulate the important features of acetylcholine (**I**), and then to depart from this structure in a regular manner to assess the importance of the structural feature being varied.

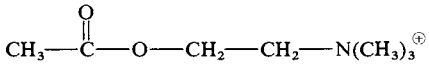

I

The problem is compounded, of course, by the fact that the conformation of acetylcholine is not predictable from classical considerations. As a result, one approach has been to design molecules constraining the functional groups of acetylcholine into a rigid structure in order to predict unequivocally their interatomic distances and relationships. Comparative cholinergic activities of these molecules have been used to predict the pharmacologically active conformation of acetylcholine and, hence, the pattern of essential atoms necessary for activity.

Clearly, the rigid-conformation model possesses inherent weaknesses. In the process of spatially fixing the key functional groups to simulate various conformations of acetylcholine, several additional atoms must be

added to the molecule. The neglect of the possible interaction of these atoms with the receptor and their subsequent effect on the measured activity is questionable.

In spite of the limitations inherent in these approaches, there have evolved over the years a number of useful empirical rules concerning the structures of active muscarinics.

Physical approaches to the acetylcholine conformation have been made by several investigators. Infrared studies have been carried out by Fellman and Fujita [*3–5*], Canepa and Mooney [*6*], and Martin-Smith, Smail, and Stenlake [*7*]. Culvenor and Ham have used NMR in various solvents to study acetylcholine conformation [*8*]. Finally, Canepa, Pauling, and Sorum [*9*] and Chothia and Pauling [*10*] have studied the acetylcholine crystal conformation using X-ray crystallography.

In addition to acetylcholine, two other molecules, muscarine (**II**) and muscarone (**III**) are potent muscarinic agonists.

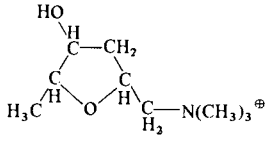

II

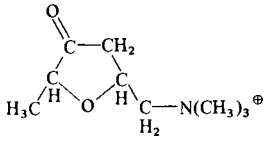

III

Studies on muscarine have established its crystal conformation using X-ray crystallography [*11*]. It is interesting to note that the crystal structures of acetylcholine and muscarine locate the three heteroatoms of each molecule in approximately the same positions with respect to each other.

In a recent study, the conformation of these three agonists using EHT was considered [*12*]. It was hoped that a common pattern of similarly charged atoms would be found in each of the three agonists. This would then furnish the basis for deducing a common pharmacophoric pattern for muscarinic agents, assuming retention of each preferred conformation, and would possibly permit a prediction concerning the complementary receptor features.

In the case of muscarine and muscarone in this study, total energy versus the ring-to-methylene bond rotation was calculated and the preferred conformation assigned to the angle of minimum energy. In both cases, the barriers to rotation away from the preferred conformations (Figs. 2 and 3) were very high. The barriers were maximal (maximum energy) when the side chain was twisted over the ring in each case. Although the EHT-calculated barriers are known to be exaggerated, their magnitude in these cases

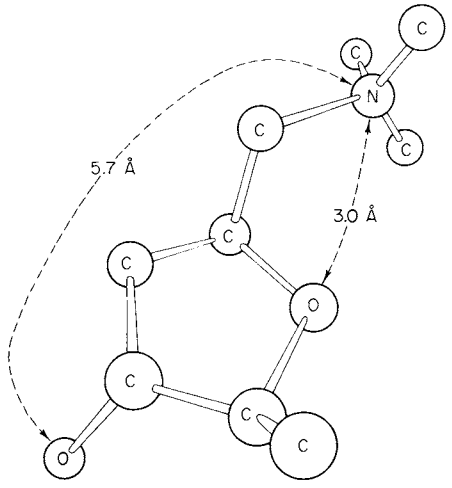

Fig. 2. Calculated preferred conformation of muscarine [*80*].

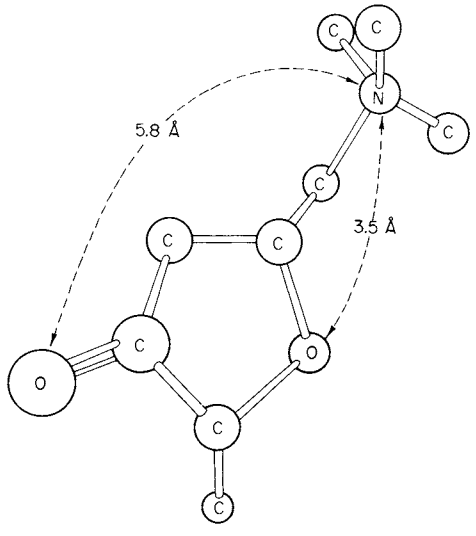

Fig. 3. Calculated preferred conformation of muscarone [*80*].

is likely to be considerable, so that the two molecules are predicted to be comparatively rigid. Waser has proposed that the onium group of muscarone is located over the ring [*13*] a view which is inconsistent with the high energy that was calculated for the conformation.

The third molecule studied in this series [*12*], acetylcholine, was found to prefer a conformation in which the carbonyl group was free to rotate 60°

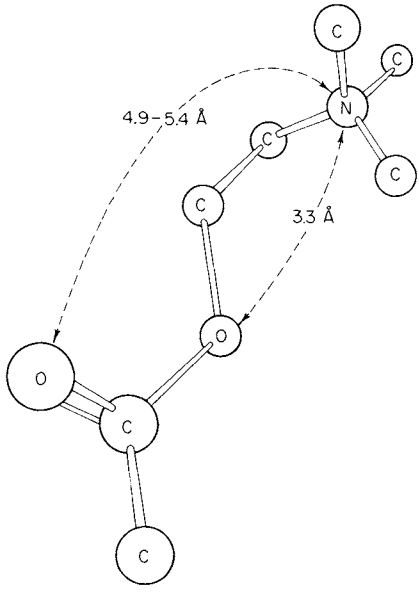

Fig. 4. Calculated preferred conformation of acetylcholine [*80*].

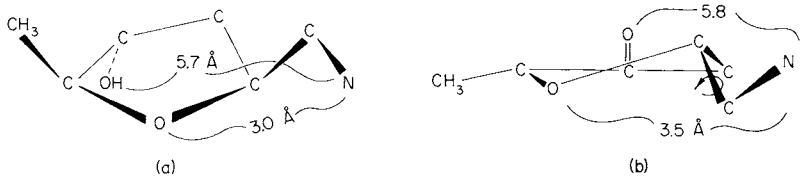

Fig. 5. Calculated conformations of (a) muscarine and (b) muscarone [*80*].

to either side of a *cis* relationship with the O—CH_2 bond, and the CH_2—CH_2 bond was at an angle of 80° from the eclipsing* of the O and N (Fig. 4). The calculated conformation of muscarine agreed with Jellinek's X-ray data [*11*]. The calculated conformation of acetylcholine agreed with Culvenor and Ham's NMR interpretation [*8*], but not with the X-ray study of Chothia and Pauling [*10*].

The calculated interatomic distances between comparable heteroatoms in each molecule are close. The two oxygen atoms in all three molecules were negatively charged ($\sigma + \pi$ charge) though the ether oxygen atoms in each case were more nearly neutral. The onium group in each molecule $CH_2N(CH_3)_3$ bore a total charge near +1.

* This angle was incorrectly stated in the original paper to be 80° from the staggered arrangement.

Several hypotheses can be drawn from a consideration of these studies. The calculations indicate that a similar pattern of atoms is presented to a receptor by each of the three agonists in its preferred conformation. It is, however, necessary to assume that muscarone approaches the receptor with the opposite face (relative to the side-chain configuration) than does muscarine (Fig. 5). This is in opposition to the assumption of Waser [*13*], but in agreement with the proposal of Belleau and Puranen [*14*]. The calculations leave little doubt that the three ether oxygens play comparable roles in the drug–receptor engagement. Similarly, the carbonyl oxygens and the hydroxyl group must also play comparable roles.

Another conclusion from the calculations was that acetylcholine is energetically permitted some latitude in its conformational preference. This latitude was found in the rotation of the carbonyl group relative to the ether oxygen bond. A rotational freedom of 120° around a planar conformation with the methylene groups permits the acetylcholine molecule to exist in more than one pattern of heteroatoms. The significance of this finding became apparent in subsequent studies on the nicotinic receptor.

From the charge–density calculations, the ether oxygen was found to possess a modest negative total ($\sigma + \pi$) charge. This is contrary to a positive-charge assignment for the ether oxygen atom that is occasionally stated in the literature, which may arise from a consideration of just the π electrons.

From a consideration of the calculations of the preferred conformations of these three potent muscarinics and a comparison of interatomic distances, it is possible to conjecture on the pattern of key atoms imparting activity to these molecules (Fig. 6). This is very similar to a pattern proposed by Beckett *et al.*, based on extensive classical structure–activity relationship studies [*14*].

A test of this pharmacophoric pattern, derived solely from MO theory, arose in a consideration of the oxotremorine molecule (**IV**) currently proposed to be a central muscarinic agent [*16–17*].

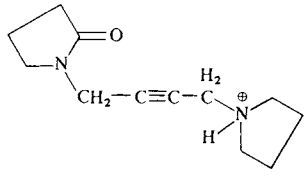

IV

An assumed structural dissimilarity between oxotremorine and known muscarinic agents has been commented upon [*18*]. However, if the acetylenic

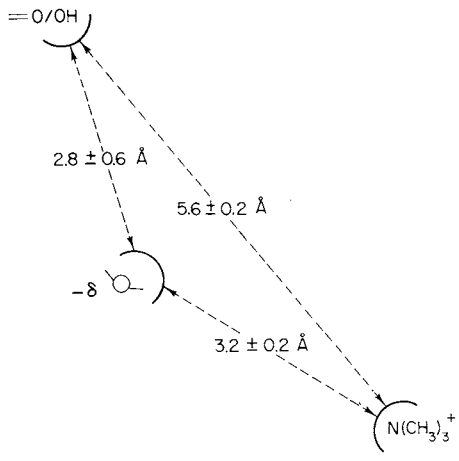

Fig. 6. Pattern of atoms calculated for muscarinic pharmacophore [*80*].

group is postulated to interact with the site on the muscarinic receptor responsive to the ether oxygen atom of acetylcholine or muscarine, then the molecule might mimic the essential atom placement at a muscarinic receptor [*19*].

If oxotremarine does act directly on central muscarinic receptors, some explanation of its activity like this one must be invoked. Such an effective presentation of essential atoms in the oxotremorine molecule to the receptor requires a conformational preference in which the muscarinic pharmacophore is reproduced.

An approach to the conformation of this molecule has been taken using EHT-MO theory [*20*]. The results of these calculations showed that the molecule can exist in a variable preferred conformation. The two rings exhibit considerable independence as far as their influence on the conformation of the other. When the distance separating any two first row atoms on opposite rings is greater than 4 Å, the two rings were calculated to have conformational freedom. Energies within 1 kcal or less of each other were considered to be equivalent as far as influencing conformational preference. The pyrrolidine ring was calculated to be symmetrically disposed relative to the triple bond (Fig. 7). The two rings were predicted to be able to assume any relationship to each other except that in which the methylene groups are eclipsed (Fig. 8). The lactam ring was predicted to be able to assume two zones of conformational preference to within 60° of coplanarity with the acetylenic bond (Fig. 9).

The distance separating the protonated nitrogen from the center of the triple bond is fixed at 3.0 Å. In the energy-permitted conformations, the

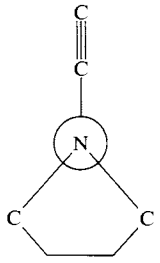

Fig. 7. Calculated conformation of oxotremorine viewed down pyrrolidine–methylene bond [*20*].

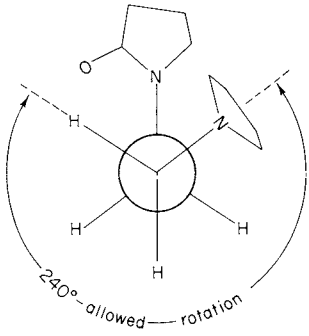

Fig. 8. Calculated conformation of oxotremorine viewed down triple bond [*20*].

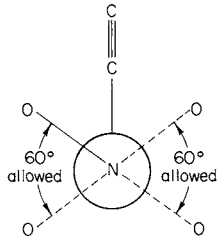

Fig. 9. Calculated conformation of oxotremorine viewed down lactam–methylene bond [*20*].

distance separating the carbonyl oxygen and the protonated nitrogen ranges from 4.3 to 7.2 Å and the energy-allowable distance from the carbonyl oxygen to the center of the triple bond is 3.1 to 4.2 Å. This results in a calculated energy-permitted pattern of atoms and groups as shown in Fig. 10.

It was found from the calculations of preferred conformation of oxotremorine that the molecule is permitted to assume a pattern identical to that previously calculated for the muscarinic pharmacophore (12) (Fig. 6).

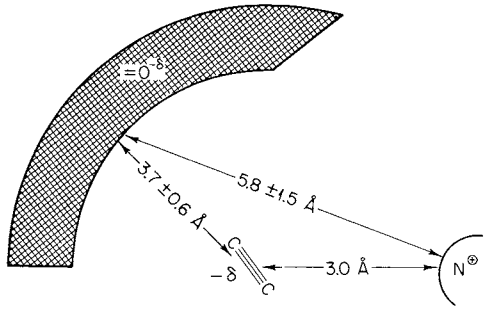

Fig. 10. Calculated pattern for oxotremorine [*20*].

These calculations support the explanation offered that oxotremorine is a central muscarinic agent by virtue of being able to mimic the muscarinic pattern [*19*].

II. Nicotinic Pharmacophore

Another application of EHT conformation prediction was made in a study of the potent nicotinic agent, nicotine [*21*]. Two points of view prevail concerning the key electronic features that are necessary in a molecule eliciting nicotinic cholinergic activity. The first point of view, advanced by Hey, is that activity is dependent upon the presence of a partial positive charge some distance from a quaternary nitrogen [*22*]. Hey concluded that maximum nicotinic activity would be found in a series of choline ethers (**V**) in which a polarized structure with a positively charged ether oxygen atom contributed appreciably.

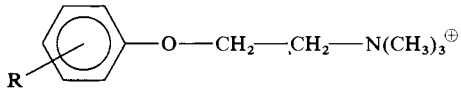

V

This was predicted upon the assumption that the nicotinic agent acetylcholine was similarly polarized when absorbed at the receptor.

Barlow and Hamilton also reached the conclusion that a slightly positively charged secondary site was necessary for activity [*23*]. The range of distances proposed for this site was 3.4–4.5 Å from the onium group.

The second point of view, based on a study of esters of choline by Sekul and Holland, is that a partial negative charge at some distance from the onium group is essential for nicotinic activity [*24*]. This negative charge is

assumed to be in a position analogous to the partial negative charge assigned to the carbonyl oxygen atom of acetylcholine.

Ormerod studied a series of substituted benzoylcholine esters and observed that electron-releasing substituents enhance activity, presumably by increasing the partial negative charge on the carbonyl oxygen atom [*25*]. Triggle feels that the combined evidence suggests the need for two secondary sites, one partially negative and the other partially positive in character, such as found at the two oxygen atoms of acetylcholine [*26*]. Barlow and Hamilton compared the activities of (+) and (−) nicotine in an effort to ascertain any significant difference [*27*]. Such a finding would implicate the presence of a third site in the molecule, imparting stereospecificity. They observed a varying degree of specificity from one group of receptors to another, suggesting some difference in receptor structure. Barlow concluded that any possible stereospecificity of nicotine may be a result of a portion of the molecule in a less active isomer functioning as a deterrent to affinity rather than the actual presence of a third pharmacodynamic group optimally placed in the more active isomer.

The problem of the secondary charge and its relationship to the onium group in nicotinic agonists is one ideally suited to consideration using molecular orbital theory. Such a study was recently reported using EHT [*21*]. The calculations on the nicotinium ion indicated two equally preferred conformations (Fig. 11) in which the pyridyl ring is predicted to be perpendicular to the pyrrolidine ring. The pyridyl nitrogen atom is negatively charged. Two sets of internitrogen distances then prevail in two conformers present in about equal concentrations, based on the energy calculations. The calculated preferred conformations are in agreement with a recently reported study of the NMR spectra of several nicotine derivatives [*28*]. Barlow and Hamilton had suggested the possibility of two conformations after a consideration of models [*27*].

A comparison was made between nicotine and acetylcholine in its preferred conformations, previously calculated [*12*]. Only one calculated conformation of nicotine (Fig. 11a) agreed with any energy-permitted acetylcholine conformation which is shown in Fig. 12. The conclusions were reached that (*a*) Fig. 11a is the nicotinic conformation of nicotine, (*b*) the secondary binding site is partially negatively charged, (*c*) the two sites are separated by about 4.85 ± 0.10 Å, and (*d*) the preferred conformation of acetylcholine in Fig. 12 is the "nicotinic" conformation of that molecule. From this latter observation and the previous conclusion of the "muscarinic" conformation of acetylcholine, it was proposed that the dual activity of acetylcholine could be explained by its ability to exist in two equally preferred conformations. This idea has been advanced by Archer [*29*] and Martin-Smith *et al.* [*30*] in an effort to explain the dual action of acetylcholine.

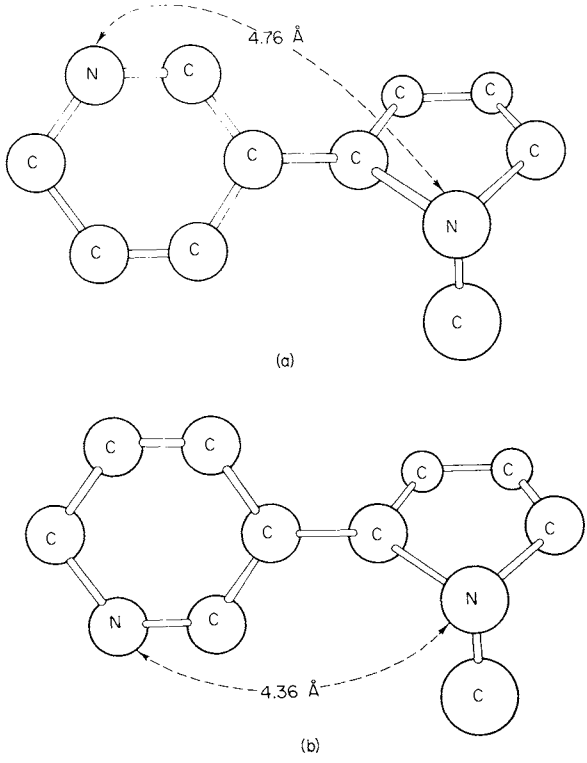

Fig. 11. Calculated conformations of nicotine [*80*].

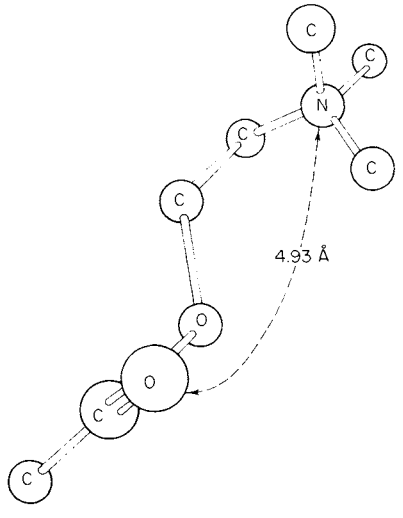

Fig. 12. Calculated "nicotinic" conformation of acetylcholine [*80*].

III. Histamine Pharmacophores

Histamine is known to produce a series of well-characterized biological responses when it is released from storage cells by the influence of trauma or chemical agents. A number of other molecules are known to produce these responses, but histamine is the most active compound known and remains the prototype of histaminic activity. It is reasonable to assume that the histamine molecule must present near-optimal electronic features to its receptor. To date, several studies have been directed toward elucidating the features of the molecule that are necessary to elicit biological activity. Lee and Jones have suggested that an important structural feature is a small heteroaromatic ring [*31*]. Neimann and Hays have suggested that the univalent cation (the predominant form at physiological pH) will exist in an intramolecular hydrogen-bonded form, and that the ability to form this hydrogen bond is a necessary condition for histaminic activity [*32*]. Lee and Jones, however, observed that although all of the active compounds they studied were capable of forming such a bond, many were inactive [*31*]. Alterations in the imidazole ring of histamine have led to abrupt lowering of activity [*31*, *33*]. It is generally believed that the fragment necessary for activity is **VI**.

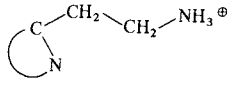

VI

π-Electron density calculations on the histamine imidazole ring by Brown [*34*] and of a thiazole ring modification by Pullman and Metzger [*35*] failed to explain the different levels in the activities. Stereochemical differences seem to emerge from all of these studies as a structural feature just as important as atom placement in the small aromatic ring [*36*].

A recent study employing EHT has considered the preferred conformation of histamine [*37*]. The calculations revealed two conformations of nearly equal preference for this molecule as the univalent cation (Fig. 13). The conformation shown in Fig. 13a is in agreement with a recently reported X-ray analysis of the histamine phosphate crystal [*38*].

The calculations predicted no preference for intramolecular hydrogen bonding. This prediction has recently been supported by experimental evidence [*38a*].

The finding of two significantly different but nearly equally preferred conformations for the histamine cation by these calculations raised the interesting question as to whether the histamine molecule can function

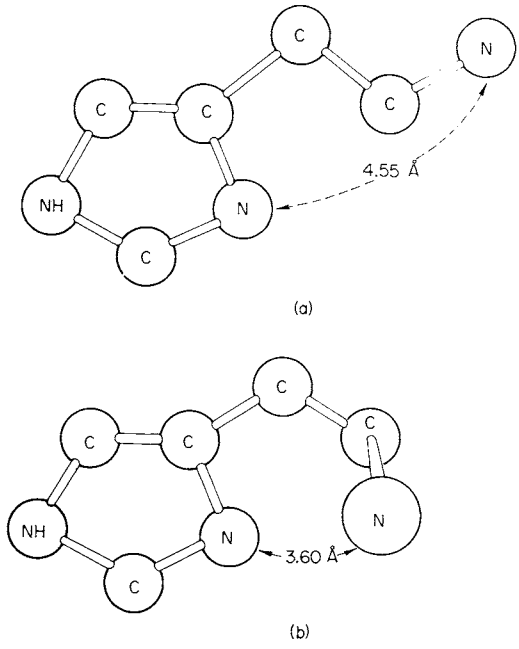

Fig. 13. Calculated conformations of histamine [*80*].

in vivo to elicit two types of biological responses from two different receptors, one for each conformation. Experimental evidence suggests that this is quite possibly the case. This dualistic behavior manifests itself as guinea pig ileum stimulation on one hand and gastric secretory stimulation on the other. Ash and Schild have obtained evidence supporting the view that histamine receptors may be differentiated into at least these two classes [*39*]. In their study of histamine analogs, they observed structural requirements for the histamine receptor in the guinea pig ileum designated H_1, different than those for the rat uterus and stomach designated H_2. Further evidence of the existence of two types of histamine receptors is found in the fact that antihistaminics fail to suppress the action of histamine in stimulating secretion on guinea pig ileum.

As an approach to the question of which calculated histamine conformer may be associated with which receptor, the more potent antihistaminics were considered in an effort to find one in which the spatial relationship of key atoms could be reasonably well established [*37*]. These key interatomic distances in the antihistaminic molecule were then compared with those calculated structures in Fig. 13 in order to ascertain which histamine con-

former was reasonably close enough to be designated as the conformation associated with the H_1 receptor.

Such a molecule is found in the potent antihistaminic triprolidine (**VII**).

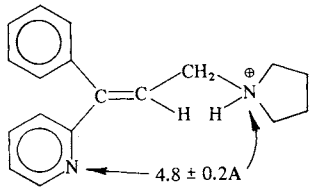

VII

This molecule has been shown by ultraviolet absorption to exist with the pyridyl ring coplanar with the olefinic bond [*40*]. If triprolidine is placed in a conformation permitting the closest approach of the two nitrogen atoms, an internitrogen distance of about 4.8 Å is found. This conformation is not an unreasonable one, although quantum chemical calculations on this molecule as well as physical evidence to support it are lacking. Nevertheless, the internitrogen distance in triprolidine is quite close to the comparable internitrogen distance of 4.55 Å calculated for histamine in conformation (a) in Fig. 13.

From these calculations and the assumptions made, it was proposed that the conformation shown in Fig. 13a is the histamine structure specific for the histamine H_1 receptor. It is not possible at this time to conclude that the histamine conformation shown in Fig. 13b is the prototype of histamine receptor H_2 activity, since no H_2 blockers are well established. However, it was offered as a possible conformation pending further work.

As an interesting sidelight to this study, the calculated charge densities for the histaminium ion revealed that the quaternary nitrogen atom was negatively charged, whereas the adjacent atoms were positively charged. The net charge of the onium group was approximately +1. An SCF calculation and an *ab initio* Gaussian-based treatment confirmed these findings on the ammonium ion. This is undoubtedly a matter which will have to be reckoned with in considering the onium group of other drug molecules and their interactions with receptor features. Thus the positive charge of the onium group cannot always be considered to be geometrically centered on the nitrogen, especially if the nitrogen is asymmetrically alkylated.

IV. Serotonin Pharmacophore

Over the past decade, an enormous amount of information has accumulated on serotonin (5-hydroxytryptamine) [*41*]. After a series of investigations, Gaddum and his group concluded that the effect of serotonin on

smooth muscle is specific and is not related to the effect of acetylcholine or histamine [*42*].

A further elaboration of the serotonin-receptor concept was proposed by Gaddum and Hameed, who offered evidence for two types of serotonin receptors, M and D [*43*]. The M receptors were those blocked by morphine and the D receptors those blocked by dibenzyline. They found that the D receptors, located in the plain muscle fibers, were also blocked by LSD, Gramine, or dihydroergotamine, while the M receptors (not accurately localized) were not easily blocked by these drugs [*44*]. Other investigators have explained the dual-receptor type of effects by suggesting that serotonin stimulates organs containing smooth muscle by a direct action on the smooth muscle fiber and by an indirect action on the nervous tissue [*45*, *46*].

The question of whether serotonin interacts with two different types of receptors or functions both as a direct and indirect acting agent persists up to the present time. The two-receptor concept is reminiscent of that proposed for the action of acetylcholine and histamine, whereas the direct–indirect action is typified by ephedrine.

Molecular orbital calculations of the preferred conformation of serotonin have recently been performed in an effort to shed light on the nature of the serotonin receptor [*47*]. The calculated preferred conformation was found to be as depicted in Fig. 14. The pharmacophoric pattern presented in the preferred conformation is shown in Fig. 15. The choice of the three heteroatoms as being the essential ones for activity is speculative but reasonable. A comparison of this heteroatom pattern with the comparable interheteroatom distances in two potent serotonin antagonists, LSD (**VIII**) and 2-methyl-3-ethyl-5-dimethylaminoindole (medmain) (**IX**) shows close agreement between atoms of comparable charge.

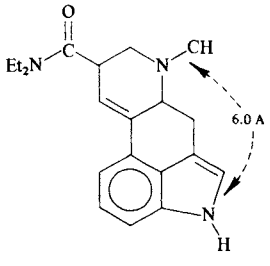

VIII

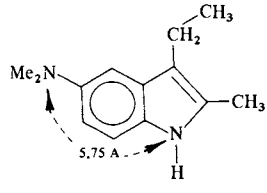

IX

It is readily conceivable that LSD could block serotonin action at a receptor by occupying only two of the receptor features. Similarly, the medmain molecule has an internitrogen distance of 5.75 Å. This approximates the indole nitrogen-to-oxygen distance of 5.71 Å in serotonin. Thus

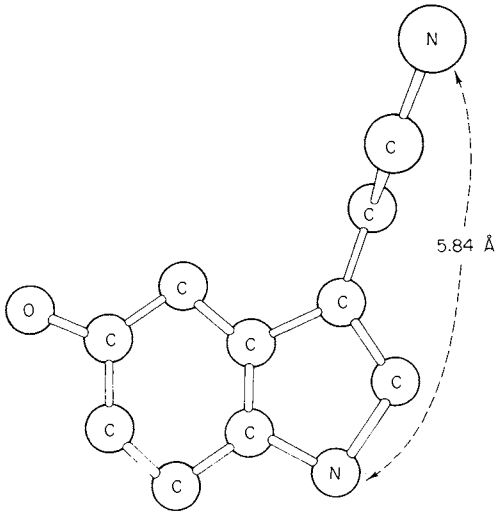

Fig. 14. Calculated conformation of serotonin [*80*].

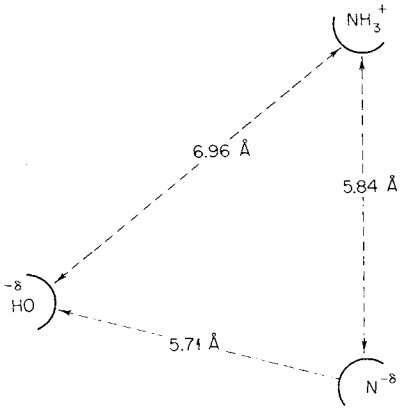

Fig. 15. Calculated serotonin pharmacophore [*80*].

its blocking activity might also be explained on the basis of competitive occupation of the serotonin receptor.

It was suggested from these calculations that there is only one preferred conformation of serotonin and this is potentially capable of being blocked by LSD and medmain. It was suggested that serotonin responses not antagonized by LSD and medmain may be due to an indirect action of serotonin.

V. Cortisol and Antiinflammation

A. Steroid Conformation

From a structural standpoint, nearly all of the positions and substituents of the pregnane hormones, such as progesterone, corticosterone, and cortisol (**X**), are easily defined because of the fused nature of the four rings.

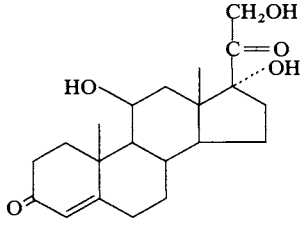

X

The only exception is the two-carbon keto side chain at C-17 which, in a conventional sense, is "free" to rotate to some extent. The biological activity of these steroids is markedly influenced not only by the C-21 hydroxyl group, but also by a hydroxyl group in the C-17 α position. Any realistic approach to the consideration of a possible receptor for these steroid hormones must ultimately come to grips with the problem of assigning a preferred conformation to the side chain, whether it be an acetyl, α-ketol, or dihydroxyacetone grouping at C-17.

Numerous investigators have approached the problem of the side-chain conformation by considering the chemical reactivities of various derivatives of these steroids [*48–50*]. These efforts have centered mainly around the reduction products of the 20-oxo group. It is certainly debatable whether the rates of reaction and relative yields of reduction products can be used to deduce the preferred conformation of the ground state of a molecule, since a perturbation in this conformation is necessarily introduced in passing through the transition states of the reaction.

Physical measurements have been used to deduce the 20-oxo group conformation in steroids. Allinger and DaRooge have proposed a conformation of the side chain of pregnane 20-one (**XI**) based on dipole moment measurements [*51*]. Optical rotatory dispersion and circular dichroism studies have

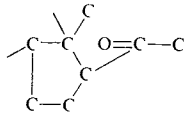

XI

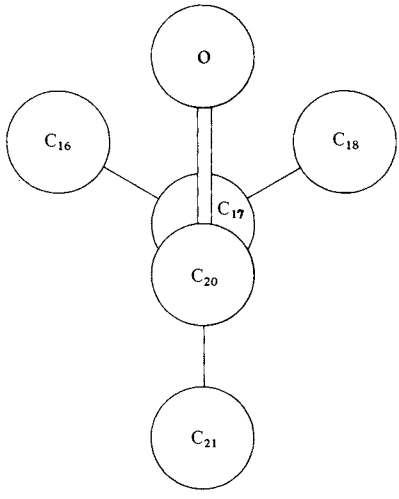

Fig. 16. Calculated side chain conformation for progesterone, corticosterone, and cortisol.

led to the prediction of the same side chain conformation [*52*]. This conformation is in agreement with a recent X-ray analysis of the crystal [*53*].

Molecular orbital calculations of the preferred conformation of the C-17 side chains of progesterone, corticosterone, and cortisol have recently been reported, in which the molecules were dissected into portions involving just the D ring and the appended groups [*54*]. A theoretical justification of the neglect of distant atoms in calculating the side-chain conformation was presented.

The calculated side-chain conformations for progesterone, corticosterone, and cortisol are depicted in Fig. 16. These conformations are within 30° of the assignments from studies using dipole moment [*51*], ORD [*52*] and X-ray analysis [*53*]. Other experimental evidence in solution supports these predictions [*54a, 54b*].

The results of these calculations led to a consideration of the three steroid molecules and the key interatomic distances in their predicted preferred conformations. These reflected patterns of heteroatoms are illustrated in Fig. 17 for progesterone and in Fig. 18 for corticosterone and cortisol. The pattern presented by cortisol is of interest due to the known antiinflammatory action of this compound [*55*].

There are two key interatomic distances in the cortisol molecule in its calculated preferred conformation (Fig. 18). One distance is the approximately 4.8 Å separating the C-20 oxygen atom from the C-11 hydroxyl group hydrogen. The second distance is the approximately 6.0 Å spacing between the C-3 oxygen atom and the C-11 hydroxyl group hydrogen.

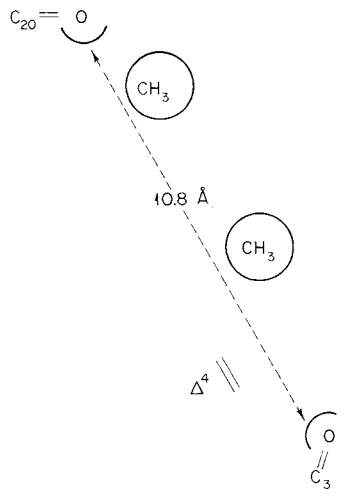

Fig. 17. Reflection onto a planer surface of key atoms of progesterone in calculated preferred conformation [*54*].

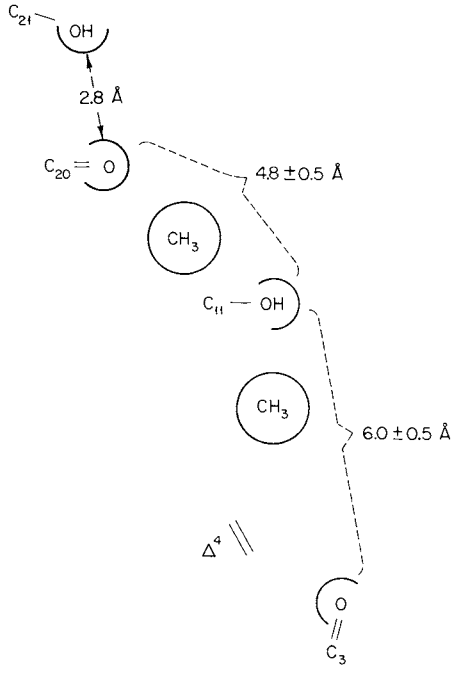

Fig. 18. Reflection onto a planer surface of key atoms of corticosterone and cortisol in calculated preferred conformations [*54*].

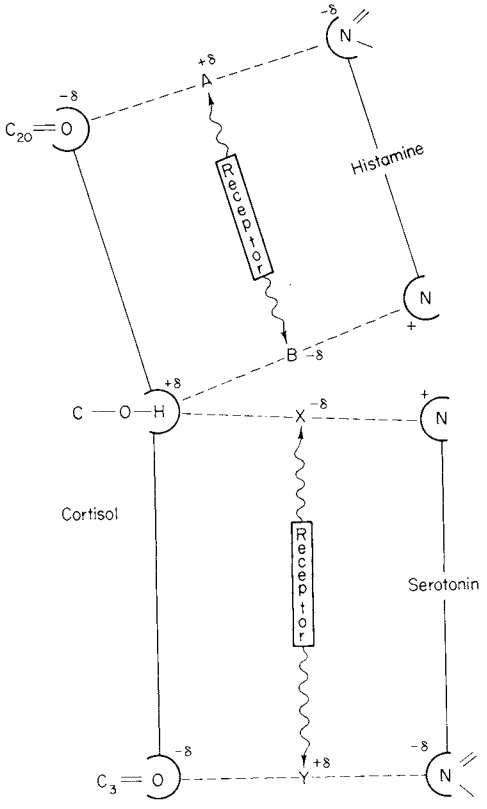

Fig. 19. Relationship of key atoms in cortisol in calculated preferred conformation to histamine and serotonin in their calculated preferred conformations [*54*].

The significance of these proposed charges and distances in terms of a possible cortisol receptor remains to be firmly established. It is of interest, however, to note the similarity of these charges and distances to previous calculations of the preferred conformations of histamine [*37*] and serotonin [*47*] (Fig. 19). It is possible to show how cortisol might interfere with both serotonin and histamine (Fig. 19), which have been implicated, among other substances, as inflammatory mediators [*56*, *57*]. Cortisol is known to protect against, and to antagonize the results of the intrusion of foreign substances into tissues [*50*, *58*, *59*].

These calculated relationships between the interatomic distances in cortisol, a potent antiinflammatory drug, and histamine and serotonin do not necessarily prove that receptors for the latter two compounds are involved in the inflammatory process. It does offer an explanation as to how cortisol might function as an antagonist if these amine receptors were

involved in directing the inflammatory response. In any event, a pattern of atoms has been calculated for the cortisol molecule which may reflect some features of the long-sought steroid receptor(s).

B. Nonsteroidal Antiinflammatory Agents

To test this hypothesis of cortisol antiinflammatory activity [*54*] it was necessary to ascertain if the numerous nonsteroidal antiinflammatory agents could assume the conformation and pattern of charges necessary to match the proposed pattern in cortisol. Such a study was recently made on several of these active molecules of diverse chemical structure [*60*]. This study included EHT-MO calculation on 5-methoxy-2-methyl indole-acetic acid (MeO-MIAA) (**XII**),

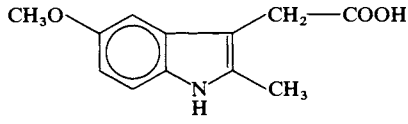

XII

a presumed metabolic hydrolysis product of the potent antiinflammatory agent indomethacin (**XIII**).

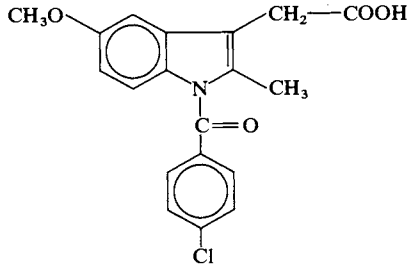

XIII

The MeO-MIAA molecule was found to prefer equally two conformations from these calculations (Fig. 20). If it is assumed that the nitrogen atom and the carboxyl group proton meet the demands of the inflammatory receptor for a negatively and positively charged feature, it is noteworthy that in conformation (b), Fig. 20, these charges are 6.17 Å apart. This is close to the 5.84 Å calculated for the serotonin charge separation [*47*]. Thus, this indomethacin metabolite may satisfy the charge and conformation requirements hypothesized from the cortisol studies [*54*].

It is well known that phenylbutazone (**XIV**) the *N*-arylanthranilates (**XV**) and the salicylates (**XVI**) also mimic cortisol in suppressing acute inflamma-

(a) (b)

Fig. 20. Calculated conformations of 5-methoxyl-2-methylindole acetic acid viewed down methylene–carboxyl bond.

tion [*61*]. A consideration of these molecules in likely conformations showed that they could present a pharmacophore consistent with the previously stated hypothesis, when in a likely conformation as shown in Table I [*60*]. This supports the hypothesis proposed for the inflammagenic antiinflammatory interrelation.

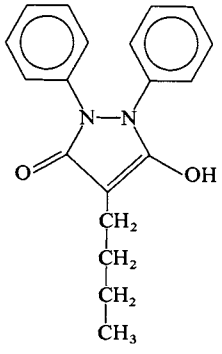

XIV

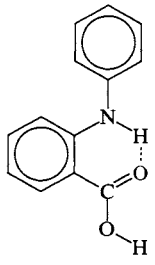

XV

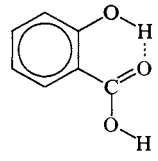

XVI

TABLE I

INTERATOMIC DISTANCES IN CORTISOL, SOME NONSTEROID ANTIINFLAMMATORY ACIDS (OR THEIR METABOLIC DERIVATIVES), AND INFLAMMAGENIC AMINES[a]

Molecule	Inflammation activity[b]	Distance (Å)
Cortisol	A	20-oxo to 11-oxy-H = 4.8
Histamine	P	Ring N to NH_3^+ = 4.55
Cortisol	A	3-oxo to 11-oxy-H = 6.0
5-HT	P	Ring N to NH_3^+ = 5.84
5-MeO-MIAA[c]	A	Ring N to carboxyl-H = 6.17 or 5.05
3′-Oxophenylbutazone[c]	A	3′-oxo to ring-ene-3(5)-ol-H = 6.0 or 4.4
N-Arylanthranilic acids	A	N to carboxyl-H = 4.65
Salicylic acids	A	Phenolic-O to carboxyl-H = 4.60

[a] Kier and Whitehouse [*60*].
[b] A = Antiinflammatory. P = Proinflammatory.
[c] Metabolites.

VI. α-Adrenergic Agents

A. Ephedrine Isomer Conformations

The isomers of ephedrine, D(−)- and L(+)-ephedrine, and D(−)- and L(+)-ψ-ephedrine (**XVII**) are known to produce effects comparable to many sympathomimetics [*62*]. The current view is that these four isomers elicit their pharmacological responses by combinations of two mechanisms, a direct action on α-adrenergic receptors and an indirect action on norepinephrine storage sites, the combination depending on the isomer and the organ [*63*]. The extent of the direct α-adrenergic effect of each isomer can be factored from the total response by pretreatment with reserpine, which depletes stored norepinephrine. The decreasing order of α-adrenergic potency of the ephedrine isomers has been found to be D(−)-ephedrine > L(+)-ephedrine > L(+)-ψ-ephedrine > D(−)-ψ-ephedrine. It is apparent that the differences in potency of these isomers must be due to stereochemical differences involving the essential features of the molecules. These features have been assumed to be the nitrogen and oxygen atoms and the phenyl ring.

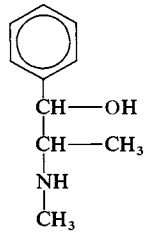

XVII

X-ray studies by Phillips on a crystalline salt of L(+)-ephedrine indicated that the amino and hydroxyl groups are comparatively close, i.e., 3.0 Å [*64*]. Hyne has studied the conformations of the free bases of ephedrine and ψ-ephedrine in chloroform solution by NMR [*65*]. He concludes that ephedrine and ψ-ephedrine possess "off-staggered" conformations related to those in Fig. 21. More recently, Portoghese examined these isomers as free bases and as their salts using NMR [*66*]. He interpreted his data to indicate Fig. 21a as the most prominent conformer of ephedrine and Fig. 21b as the most prominent conformer of ψ-ephedrine.

A theoretical approach to the conformation of these two diastereoisomers has recently been reported using EHT [*67*]. The preferred conformation of D(−)-ephedrine was predicted from these calculations to be as shown in Fig. 22a. This calculated value is in agreement with X-ray analysis

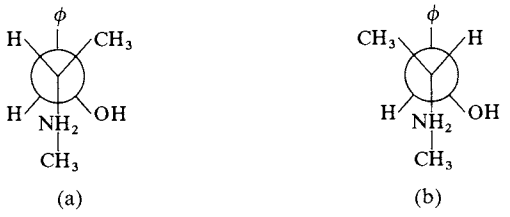

Fig. 21. Conformations of (a) ephedrine and (b) ψ-ephedrine predicted from NMR studies.

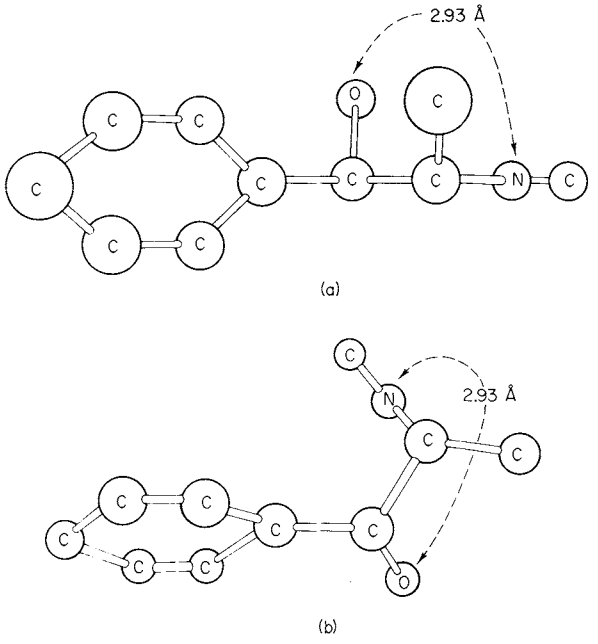

Fig. 22. Calculated conformation of (a) D(−)-ephedrine and (b) L(+)-ψ-ephedrine [67].

of the crystal [64], and NMR analysis [65, 66]. The conformation depicted in Fig. 22b was predicted for L(+)-ψ-ephedrine. This calculated value agreed with a minor contributing conformation in an equilibrium composition based on NMR studies [66]. From a consideration of the ranking of the four isomers as far as α-adrenergic potency and the assumption that the onium group, the hydroxyl group, and the phenyl ring are key participants in a receptor interaction, a pharmacophoric pattern was proposed (Fig. 23). The lower activities of L(+)-ephedrine and the ψ-ephedrine isomers were explained on the basis of a correct placement of the hydroxyl and onium groups, but a less favorable presentation of the phenyl ring and the intrusion

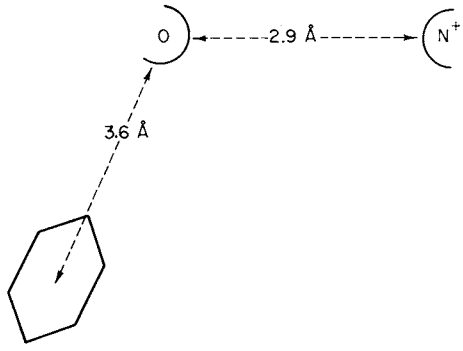

Fig. 23. Postulated α-adrenergic pharmacophore from calculations [*67*].

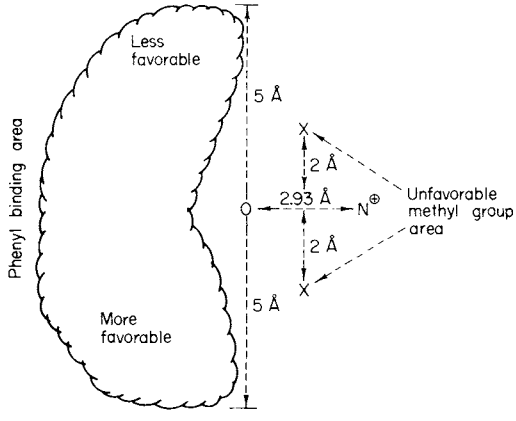

Fig. 24. Postulated features of α-adrenergic receptor topology [*67*].

of the α-methyl groups into the hypothetical receptor plane in the ψ-ephedrine isomers (Fig. 24).

B. Norepinephrine Conformation

A logical extension of the studies on the ephedrine isomers was a consideration of the preferred conformation of the α-adrenergic transmitter, norepinephrine (noradrenaline) (**XVIII**). If a comparable pattern of atoms could be found for both receptor agonists, in their calculated preferred conformations, it would lend considerable validity to the speculation on the nature of the α-adrenergic pharmacophore [*67*] and lend support to the

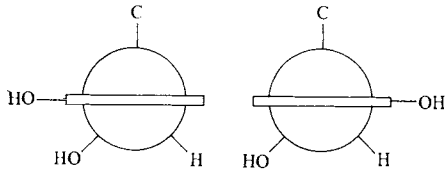

Fig. 25. Relationships of phenyl ring *m*-hydroxyl group to β-hydroxyl group in the calculated preferred conformations of norepinephrine [*68*].

hypothesis that the efficaciously significant interaction between drug and receptor occurs while the agonist is in its preferred conformation.

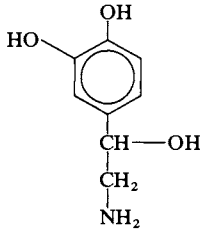

XVIII

EHT-MO calculations on the norepinephrine molecule [*68*] have resulted in a predicted conformation identical to that found by X-ray analysis of (−)-norepinephrine hydrochloride [*69*]. The calculations also showed that the onium, hydroxyl, and phenyl groups were in the same relationship sterically as previously calculated for (−)-ephedrine (Fig. 22a) [*67*]. The ring *m*-hydroxyl group could assume either of two relationships to the side chain (Fig. 25).

The results for norepinephrine are consistent with the model postulated for the features of the α-adrenergic receptor [*67*]. This finding of more than one agonist molecule in a pharmacological class having comparable calculated steric placement of key features lends support to the hypothesis that many drug molecules engage their receptors in an efficacious manner while in their preferred conformations.

C. Dopamine Conformation

A study on the catecholamine, dopamine (3,4-dihydroxyphenylethylamine) (**XIX**),

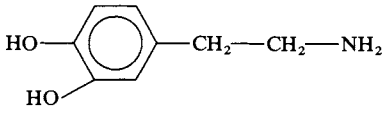

XIX

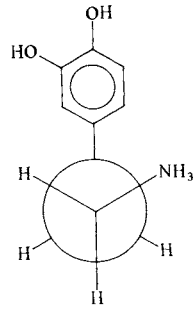

Fig. 26. Calculated conformation of dopamine salt [*70*].

using EHT, has been conducted to determine its calculated conformational preference [*70*]. Although dopamine is known to be a precursor to norepinephrine its presence in a particular tissue has been shown to reflect a receptor response differing from that of norepinephrine. This is particularly true in the central nervous system [*71*].

The superficial chemical similarity of the dopamine and norepinephrine molecules suggests that if the two molecules engage different receptors, they likely are specific for their own receptors due to differing conformational preferences. The MO calculations support this supposition [*70*]. Dopamine was calculated to prefer a conformation shown in Fig. 26. This was confirmed by NMR analysis [*70*]. This *gauche* relationship of the nitrogen and phenyl ring is in marked contrast to the calculated trans placement of the same groups in norepinephrine [*68*].

VII. Nucleoside Conformation

Jordan and Pullman have calculated the conformation of the bond joining the sugar moiety with the purine or pyrimide bases in the nucleosides cytidine (**XX**), uridine (**XXI**), adenosine (**XXII**), and guanosine (**XXIII**) [*72*]. The method used was EHT.

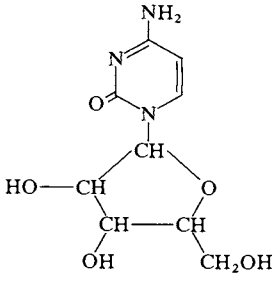

XX

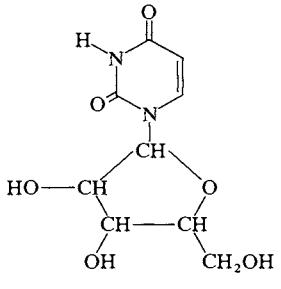

XXI

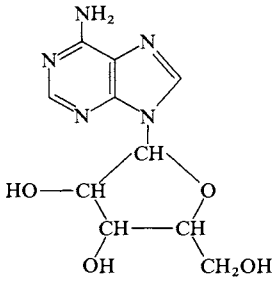

XXII

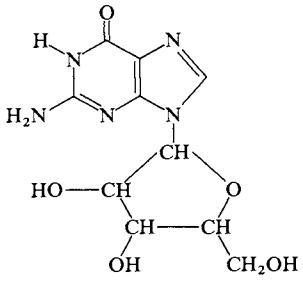

XXIII

The calculated conformation in each case agreed well, within 30°, with the experimental values (see Table II).

TABLE II
TOTAL ORBITAL ENERGY OF VARIOUS DEGREES OF ROTATION IN NUCLEOSIDES[a]

Rotation of sugar clockwise (degrees)	E_{total} (kcal/mole)			
	Cytidine $\phi_{CN} = -24°$ [b] at 0° rotation	Adenosine $\phi_{CN} = -18°$ at 0° rotation	Uridine $\phi_{CN} = -43°$ at 0° rotation	Guanosine $\phi_{CN} = +138°$ at 0° rotation
0	−43532.681	−46122.656	−44345.897	−49498.588
60	−43522.151	−46117.172	−44342.011	−49492.034
120	−43523.590	−46121.105	−44342.532	−49497.284
180	−43508.875	−46105.370	−44335.881	−49497.662
240	−43436.417	−46080.072	−44329.306	−49338.243
300	−43464.723	−46108.884	−44339.892	−49494.787

[a] Jordan and Pullman [72].
[b] Experimental ϕ_{CN}.

VIII. Sugar Conformation

Neely has studied several conformational possibilities of glucopyranose using EHT (Fig. 27) [73].

The calculations showed that the Cl conformation is preferred and that further the β form is more stable, Table III. This is in agreement with experiment [74].

The results on the nucleosides and the sugars are most encouraging, considering the complexity of these molecules in terms of the large number of heteroatoms present. It is distinctly possible that other stereochemical problems in the carbohydrate area can now be successfully assaulted with MO theory.

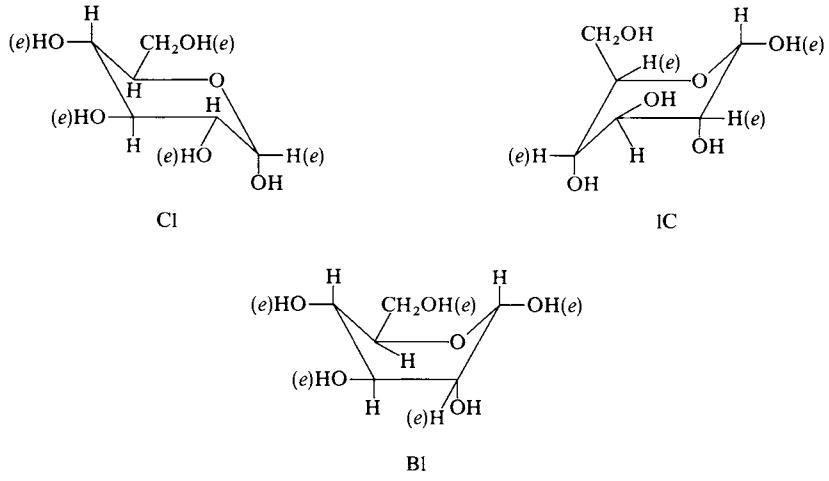

Fig. 27. Conformation of β-D-glucopyranose calculated [73].

TABLE III
TOTAL ENERGY OF VARIOUS CONFORMATIONS OF GLUCOSE AND RELATED SUGARS[a]

Sugar	Conformation	Energy (kcal)
Glucooyranose	α-D-Cl	−34,969
	β-D-Cl	−34,978
	α-D-lC	−34,920
	α-C-Bl	−34,963

[a] Neely [73].

IX. Amino Acid Conformation

A number of investigators have recently turned their attention to calculating the preferred conformation of amino acids. The objective is ultimately to be able to predict the conformation of more complex polypeptides from theoretical considerations. The conformation of a protein in solution is a complex resultant of such factors as the preference of the individual amino acid residues, the interaction of side chains, interresidue hydrogen bonds, and solvent–protein interaction. As a first approximation, the conformation preference of each amino acid residue may give a crude picture of the conformation of a polypeptide (realistically only a short-chain molecule) when assembled into the proper sequence.

Hoffmann and Imamura have calculated the conformation of glycine and alanine residues using the *N*-acetyl, *N*-methyl amides as model compounds

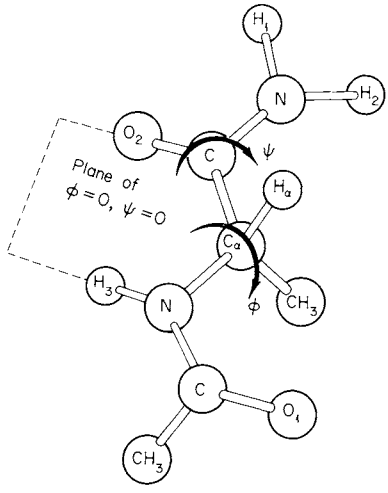

Fig. 28. Illustration of convention for designating peptide conformation. ψ is the clockwise angle of rotation of the CO group, and ϕ is the clockwise angle of rotation of the $CH(CH_3)$ group.

[*75*]. For glycine, they calculated an energy minimum at $\phi = 0°–120°$, $\psi = 300°–60°$, using the convention of Edsall to describe the angles of the C—C and C—N bonds in amino acid residues [*79*] (Fig. 28). For alanine, they calculated an energy minimum at $\phi = 30°–120°$, and $\psi = 300°–0°$. A ϕ, ψ contour map of these two residues, plotting the relative energies above the minimum value, gives a contour map of energies as a function of coordinates. This map is useful in predicting regions of high energy and secondary conformation preferences.

In another study, Kier and George have made calculations on several amino acid residue model compounds [*76*, *78*]. These predicted conformations compare favorably with experimental conformations which can be achieved by these residues in polypeptides (see Table IV).

A recent study on chains of 4 and 5 peptide unit polyglycine model compounds, indicates an increasing stabilization energy per peptide unit with increasing chain length [*77*], possibly reflecting the formation of the hydrogen bonds. The preferred conformation of these peptides was calculated to be $\phi = 137°$, $\psi = 128°$, very close to the α-helix structure.

These pioneering efforts into the very complex subject of polypeptide conformation are of great interest and hopefully portend more extensive application of MO techniques to this area.

TABLE IV
SUMMARY OF CALCULATED AND EXPERIMENTAL ϕ, ψ ANGLES OF RESIDUES[a]

	Calculated (deg)		Experimental conformations (deg)		
Residue	ϕ	ψ	Structural type	ϕ	ψ
Glycine	0–120	0	I β-antiparallel pleated sheet	38	325
			II Collagen-like	100	330
Alanine	240	240	Right-handed α-helix	132	123
			β-antiparallel pleated sheet	41	315
Phenylalanine	30	330	Right-handed α-helix	132	123
			β-parallel pleated sheet	61	293
Proline	120	330	I	300	300
			II	120	330
Serine	60–120	330	β-parallel pleated sheet	61	293
Leucine	60	0	In Gramicidin	30	0
			Right-handed α-helix	132	123
Isoleucine	60– 90	300	β-form	38– 61	293–325
Valine	60– 90	300	β-form	38– 61	293–325
			Right-handed α-helix	132	123

[a] Kier and George [*78*].

X. Summary

The success of all-valence electron theories in predicting the preferred conformation of drug molecules has been impressive to date. The biological significance of these predictions lies in the ability now to offer explanations for the similar actions of apparently dissimilar drug molecules and to speculate on the key features of these molecules and their mechanisms of action. Insofar as the shape of a drug molecule is important, the calculation of the conformations of potent agonists, and the calculation of the conformations of potential agonist and antagonist molecules makes the approach hopefully predictive in new drug design.

References

1. R. Hoffmann, *J. Chem. Phys.* **39**, 1397 (1963).
2. J. A. Pople and G. A. Segal, *J. Chem. Phys.* **44**, 3289 (1966).
3. J. H. Fellman and T. S. Fujita, *Biochim. Biophys. Acta* **56**, 227 (1962).
4. J. H. Fellman and T. S. Fujita, *Biochim. Biophys. Acta* **71**, 701 (1963).
5. J. H. Fellman and T. S. Fujita, *Nature (London)* **211** 848 (1966).

6. F. G. Canepa and E. F. Mooney, *Nature (London)* **207**, 78 (1965).
7. M. Martin-Smith, G. Smail, and J. Stenlake, *J. Pharm. Pharmacol.* **19**, 649 (1967).
8. C. Culvenor and N. Ham, *Chem. Commun.* p. 537 (1966).
9. F. G. Canepa, P. Pauling, and H. Sorum, *Nature (London)* **210**, 907 (1966).
10. C. Chothia and P. Pauling, *Nature (London)* **219**, 1156 (1968).
11. F. Jellinek, *Acta Crystallogr.* **10**, 277 (1957).
12. L. B. Kier, *Mol. Pharmacol.* **3**, 487 (1967).
13. P. G. Waser, *Pharmacol. Rev.* **13**, 465 (1962).
14. B. Belleau and J. Puranen, *J. Med. Chem.* **6**, 325 (1963).
15. A. H. Beckett, N. J. Harper, and J. W. Clitherow, *J. Pharm. Pharmacol.* **15**, 362 (1963).
16. R. George, W. L. Haslett, and D. J. Jenden, *Life Sci.* **2**, 361 (1962).
17. A. Bebbington and R. W. Brimblecomb, *Advan. Drug Res.* **2**, 143 (1965).
18. A. K. Cho, W. L. Haslett, and D. J. Jenden, *J. Pharmacol. Exp. Ther.* **138**, 249 (1962).
19. A. Bebbington, R. W. Brimblecomb, and D. Shakeshaft, *Advan. Drug. Res.* **2**, 161 (1965).
20. L. B. Kier, *J. Pharm. Sci.* **59**, 112 (1970).
21. L. B. Kier, *Mol. Pharmacol.* **4**, 70 (1968).
22. J. Hey, *Brit. J. Pharmacol.* **7**, 117 (1952).
23. R. B. Barlow and J. T. Hamilton, *Brit. J. Pharmacol.* **18**, 510 (1962).
24. A. A. Sekul, W. C. Holland, and R. House, *Arch. Int. Pharmacodyn.* **141**, 404 (1963).
25. W. E. Ormerod, *Brit. J. Pharmacol.* **11**, 267 (1956).
26. D. J. Triggle, "Chemical Aspects of the Autonomic Nervous System," p. 89. Academic Press, New York, 1965.
27. R. B. Barlow and J. T. Hamilton, *Brit. J. Pharmacol.* **25**, 206 (1965).
28. T. R. Simpson, J. C. Craig, and W. D. Kumler, *J. Pharm. Sci.* **56**, 708 (1967).
29. S. Archer, A. M. Lands, and T. R. Lewis, *J. Med. Pharm. Chem.* **5**, 423 (1962).
30. M. Martin-Smith, G. Smail, and J. Stenlake, *J. Pharm. Pharmacol.* **19**, 561 (1967).
31. H. M. Lee and R. G. Jones, *J. Pharmacol. Exp. Ther.* **95**, 71 (1949).
32. C. C. Neimann and J. T. Hays, *J. Amer. Chem. Soc.* **64**, 2288 (1942).
33. M. I. Grossman, C. Robertson, and C. E. Rosiere, *J. Pharmacol. Exp. Ther.* **104**, 277 (1952).
34. R. D. Brown, *Aust. J. Chem.* **8**, 100 (1955).
35. A. Pullman and M. Metzger, *Bull. Soc. Chim. Fr.* **15**, 102 (1948).
36. R. B. Barlow, "Introduction to Chemical Pharmacology," p. 344. Wiley, New York, 1964.
37. L. B. Kier, *J. Med. Chem.* **11**, 441 (1968).
38. M. V. Veidis and G. J. Palenik, *Chem. Commun.* p. 196 (1969).
38a. T. B. Paiva, M. Tominaga and A. C. M. Paiva, *J. Med. Chem.*, **13**, 689 (1970).
39. A. S. F. Ash and H. O. Schild, *Brit. J. Pharmacol.* **27**, 427 (1966).
40. D. W. Adamson, P. A. Barrett, J. W. Billinghurst, and T. S. G. Jones, *J. Chem. Soc. London* p. 2315 (1957).
41. S. Garattini and L. Valzelli, "Serotonin." Elsevier, New York, 1965.
42. J. H. Gaddum, K. A. Hameed, D. E. Hathway, and F. F. Stephens, *Quart. J. Exp. Physiol.* **40**, 49 (1955).
43. J. H. Gaddum and K. A. Hameed, *Brit. J. Pharmacol.* **9**, 240 (1954).
44. J. H. Gaddum and Z. P. Picarelli, *Brit. J. Pharmacol.* **12**, 323 (1957).
45. I. R. Innes, H. W. Kosterlitz, and J. A. Robinson, *J. Physiol. (London)* **137**, 396 (1957).
46. N. Ambache, "5-Hydroxytryptamine" (G. P. Lewis, ed.), p. 203. Macmillan (Pergamon), New York, 1958.
47. L. B. Kier, *J. Pharm. Sci.* **57**, 1188 (1968).
48. G. P. Mueller, R. E. Stobaugh, and R. S. Winneford, *J. Amer. Chem. Soc.* **75**, 4888 (1953).
49. G. Just and R. Nagarajan, *Can. J. Chem.* **39**, 548 (1961).

50. C. R. Engel, S. Rakhit, and W. W. Haculak, *Can. J. Chem.* **40**, 921 (1962).
51. N. L. Allinger and M. A. DaRooge, *J. Amer. Chem. Soc.* **83**, 4256 (1961).
52. K. M. Wellman and C. Djerassi, *J. Amer. Chem. Soc.* **87**, 60 (1965).
53. A. Cooper and W. L. Duax, *J. Pharm. Sci.* **58**, 1159 (1969).
54. L. B. Kier, *J. Med. Chem.* **11**, 915 (1968).
54a. W. G. Cole and D. H. Williams, *J. Chem. Soc. London* p. 1849 (1968).
54b. W. G. Cole and D. H. Williams, *J. Chem. Soc. London* p. 748 (1970).
55. L. H. Sarett, A. A. Patchett, and S. Steelman, *Fortschr. Arzneimittelforsch,* **5**, 13 (1963).
56. R. W. Schayer, *Amer. J. Physiol.* **202**, 66 (1962).
57. W. G. Spector and D. A. Willoughby, *Ann. N.Y. Acad. Sci.* **116**, 839 (1964).
58. R. Cass and P. B. Marshall, *Arch. Int. Pharmacodyn.* **136**, 311 (1962).
59. R. W. Schayer, *Perspect. Biol. Med.* **10**, 409 (1967).
60. L. B. Kier and M. W. Whitehouse, *J. Pharm. Pharmacol.* **20**, 793 (1968).
61. T. Y. Shen, "Topics in Medicinal Chemistry" (J. L. Rabinowitz and R. M. Myerson, eds.), pp. 27–78. Wiley (Interscience), New York, 1967.
62. R. B. Barlow, "Introduction to Chemical Pharmacology," p. 310. Wiley New York, 1964.
63. U. Trendelburg, *Pharmacol. Rev.* **15**, 225 (1963).
64. D. C. Phillips, *Acta Crystallogr.* **7**, 159 (1954).
65. J. B. Hyne, *Can. J. Chem.* **39**, 2536 (1961).
66. P. S. Portoghese, *J. Med. Chem.* **10**, 1057 (1967).
67. L. B. Kier, *J. Pharmacol. Exp. Ther.* **164**, 75 (1968).
68. L. B. Kier, *J. Pharm. Pharmacol.* **21**, 93 (1969).
69. D. Carlstrom and R. Bergin, *Acta. Crystallogr.* **23**, 313 (1967).
70. L. B. Kier and E. B. Truitt, *Pharmacol. Exp. Therap.* **174**, 94 (1970).
71. O. Hornykiewicz, *Pharmacol. Rev.* **18**, 925 (1966).
72. F. Jordan and B. Pullman, *Theor. Chim. Acta.* **9**, 242 (1968).
73. W. B. Neely, *J. Med. Chem.* **12**, 16 (1969).
74. R. E. Reeves, *J. Amer. Chem. Soc.* **71**, 215 (1949).
75. R. Hoffmann and A. Imamura, *Biopolymers* **7**, 207 (1969).
76. L. B. Kier and J. M. George, *Theor. Chim. Acta* **14**, 258 (1969).
77. A. Rossi, C. W. David, and R. Schor, *Theor. Chim. Acta* **14**, 429 (1969).
78. L. B. Kier and J. M. George, "Molecular Orbital Studies in Chemical Pharmacology" (L. B. Kier, ed.), Ch. 3. Springer-Verlag, New York, 1970.
79. J. Edsall, *Biopolymers* **4**, 121 (1966).
80. L. B. Kier, "Fundamental Concepts in Drug-Receptor Interactions" (J. Danielli, J. Moran, and D. Triggle, eds.), p. 15. Academic Press, New York, 1970.

Chapter IX

ACID–BASE PHENOMENA

I. General Considerations

A. Drug Action and pK_a

The role of acid–base phenomena, or more specifically protonation–deprotonation equilibria, in biological processes is very large. There is hardly a known biochemical scheme or pharmacological mechanism which is not dependent in some way on the ability of an acid to release a hydrogen ion or the ability of a base to accept a proton.

The ability of an acid or base to ionize has been shown to influence the absorption properties of a drug molecule from different regions of the gastrointestinal tract. Absorption through a membrane is generally facilitated by conversion of a molecule to an undissociated form, this being, in the main, more soluble in the lipodal material comprising the barrier. It follows then that a molecule prone to dissociate in the environment of the barrier will be retarded in its efforts to cross that barrier. A moderately weak acid, therefore, will be essentially undissociated in the acid stomach, hence absorption through the stomach wall is a possibility. This same acid molecule, on the other hand, in the more alkaline environment of the intestine, will be appreciably ionized. Absorption through the intestinal wall may not be considered too likely.

Basic amines present the opposite set of circumstances. In the acid stomach it is certainly ionized, hence not in a form suitable for absorption. The prominence of the dissociated form diminishes in the intestine and absorption is more likely.

The same reasoning can be applied to the passage of drug molecules into a cell to exert their action. The undissociated form, if it prevails in the equilibrium dictated by the pK_a of the molecule, will possibly penetrate the cell wall. Thus the antibacterial actions of many acids and phenols are enhanced by insuring a predominance of the undissociated form. Many antibacterial agents have increased activity if a significant contribution from an ionized form is present. Thus protonated amines may function by competing with hydrogen ions for essential anionic sites.

B. MO Relationships

The ability to correlate relative acidity or basicity with activity in a series of molecules can put the design of new, more active molecules on a sound basis. Carrying this one step further, the ability to predict the relative dissociation constant of an acid or base could afford a tremendous short cut to drug design, by eliminating the necessity of synthesizing large numbers of molecules and assessing experimentally their acid and base strengths.

Molecular orbital theory has been employed in the study of equilibrium constants. The equilibrium constant, K expresses the ratio

$$K = \frac{[A][H^+]}{[AH^+]}$$

for the reaction

$$AH^+ \overset{K}{\leftrightarrows} A + H^+$$

The equilibrium constant between the protonated and unprotonated form is related to the change in free energy, ΔF, the gas constant, R, and temperature, T.

$$K = e^{-\Delta F/RT}$$

The free energy is related to the enthalpy change, ΔH, and entropy change, ΔS, by the well-known expression

$$\Delta F = \Delta H - T\Delta S$$

hence the expression relating the equilibrium constant and the energies involved in the protonation is

$$\text{Log } K = -\frac{\Delta H}{RT} + \frac{\Delta S}{R}$$

In MO considerations of equilibria, it has been common to assume a linear relationship between ΔS and ΔH, particularly in a related series of molecules, and then to neglect the entropy contribution.

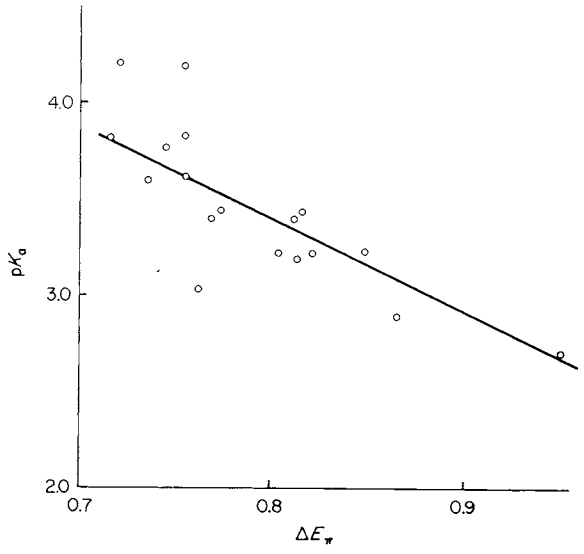

Fig. 1. Relation between ΔE_π and pK_a. Elliott and Mason [*1*].

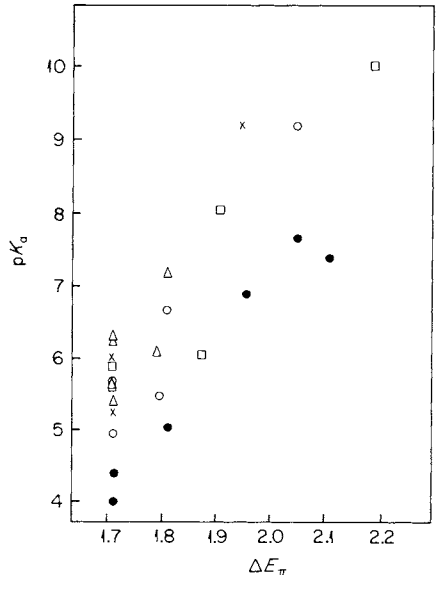

Fig. 2. Relation between Hückel-calculated ΔE_π and pK_a. Chalvet *et al.* [*2*]. (×) Pyridine derivatives. (△) Isoquinoline. (○) Quinoline. (□) Acridine. (●) *Ortho* and *peri* effect.

The enthalpy, ΔH, hence the log K or pK, is a function of several factors. These include (*a*) the energy change in the σ bonds, ΔE_σ, (*b*) the energy change in the delocalized or π bonds, ΔE_π, (*c*) the energy change due to nonbonded interactions or a steric energy, ΔE_{st}, and (*d*) the solvation energy change, ΔE_s, so that

$$\Delta H = \Delta E_\alpha + \Delta E_\pi + \Delta E_{st} + \Delta E_s$$

In studies of the pK of conjugated molecules, the contribution of ΔE_π has been considered to be the most important.

1. *π-Electron Calculations*

Elliott and Mason have plotted ΔE_π values obtained from HMO calculations and the associated pK values [*1*] (Fig. 1). The calculations, in this case, permit the prediction of the pK to within 1 unit. A test of this modest precision has been made to determine if the method of arriving at the calculated ΔE_π may be at fault [*2*]. Calculations using HMO theory [*3*] (Fig. 2), were repeated using an SCF–MO treatment [*4*] (Fig. 3). The more sophisticated calculation obviously produces a better prediction. Within a structural family of bases, the precision is much closer than in a diverse group.

TABLE I
CORRELATIONS OF CALCULATED HMO QUANTITIES WITH PROTON SHIFTS, HAMMETT σ VALUES, AND pK_a'S OF SUBSTITUTED ANILINES[a]

	Substituent(s)	q[b]	k_{C-N}[c]	ΔE[d]	Amino proton shift ν[d]	Hammett σ	pK
1	2,6-Me_2	1.782	1.00	0.8176	263		3.95
2	4-OMe	1.764	1.00	0.9078	270	−0.268	5.44
3	2-OMe	1.748	1.00	0.9064	276		4.56
4	2-Me	1.751	1.00	0.9330	278		4.52
5	4-Me	1.743	1.00	0.9710	282	−0.170	5.16
6	3-Me	1.730	1.00	1.0140	287	−0.069	4.69
7	H	1.729	1.00	1.0020	288	0.000	4.69
8	3-OMe	1.712	1.05	1.0540	295	0.115	4.30
9	4-Ph	1.707	1.00	1.0150	309	0.160	4.35
10	4-Cl	1.694	1.10	1.0946	309	0.227	4.07
11	3-Cl	1.669	1.15	1.1654	319	0.373	3.60
12	3-NO_2	1.651	1.20	1.2200	345	0.710	2.47
13	4-NO_2	1.531	1.20	1.3600	398	1.270	1.04
14	2-NO_2	1.502	1.25	1.4400	440		−0.24

[a] Lynch [*5*].
[b] π-Electron density at amino nitrogen.
[c] $\beta_{C-N} = k_{C-N}\beta_{C-C}$.
[d] Difference in π-electron energy (in β units) between corresponding anilines and anilium ions.

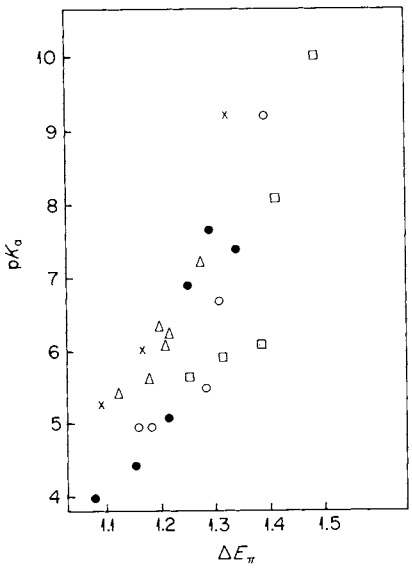

Fig. 3. Relation between SCF-calculated ΔE_π and pK_a for same compounds shown in Fig. 2. Chalvet *et al.* [2]. (×) Pyridine derivatives. (△) Isoquinoline. (○) Quinoline. (□) Acridine. (●) *Ortho* and *peri* effect.

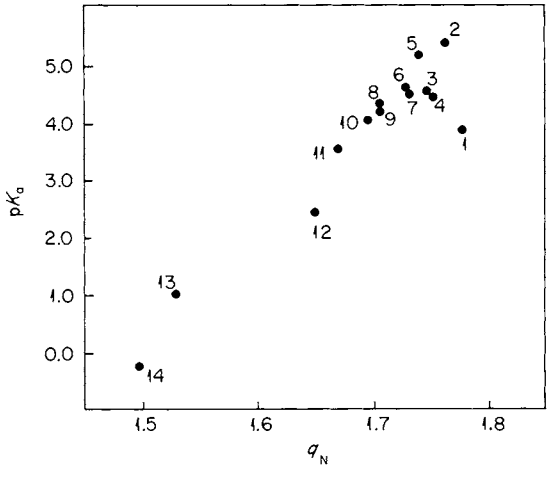

Fig. 4. Relation between electron density on nitrogen, q_N, in a series of anilines and pK_a. Numbers refer to Table I. Lynch [5].

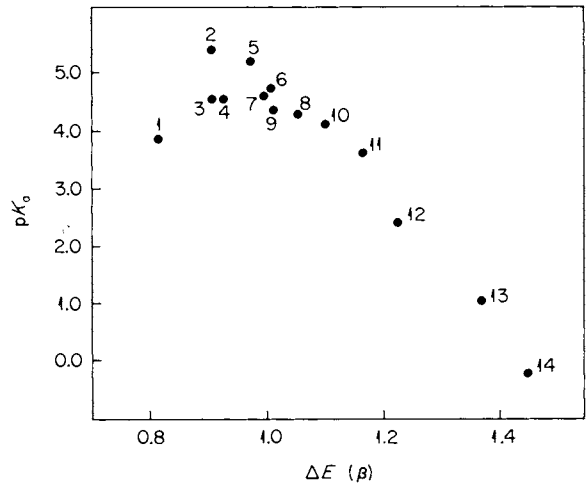

Fig. 5. Relation between energy index, ΔE, and pK_a in a series of anilines listed in Table I. Lynch [5].

The data dispersion noted then in a heterogeneous group of molecular classes must be due to factors associated with each molecular group.

Another approach to the prediction of basicity has been to regard the π-electron charge density at an atom, say an amino nitrogen, as being influential in the ultimate course of a protonation reaction. This approach follows the same line of reasoning used by some investigators in predicting chemical activity from MO-calculated ground state properties. The charge density index is on a less sound footing than an energy difference index reflecting the free energy of activation to the protonation transition state. The superior correlation of pK with an energy index rather than with a charge index has been the usual observed result. An example of this is the recent work of Lynch on a series of substituted anilines [5]. The data (Table I), when plotted for the charge (Fig. 4), and the energy (Fig. 5), clearly show the superiority of the energy index in correlating with the pK.

2. *All-Valence Electron Calculations*

With the advent of all-valence electron MO methods, it is now possible to include an approximation to the energy contribution from π electrons to the enthalpy change occurring in a protonation reaction. Hermann has recently used the CNDO/2 MO method in a study of bicyclooctanecarboxylic acids (Fig. 6) [6]. Calculations were made of total electronic energies on both species in a series. In some cases water was assumed to be hydrogen bonded to the substituent X in an optimum arrangement. The values of the total energy and the difference in energy from the loss of a proton,

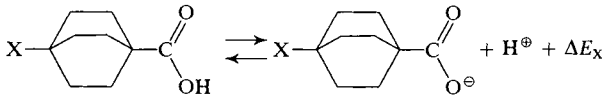

Fig. 6. Bicyclooctanecarboxylic acid equilibrium. Herrmann [6].

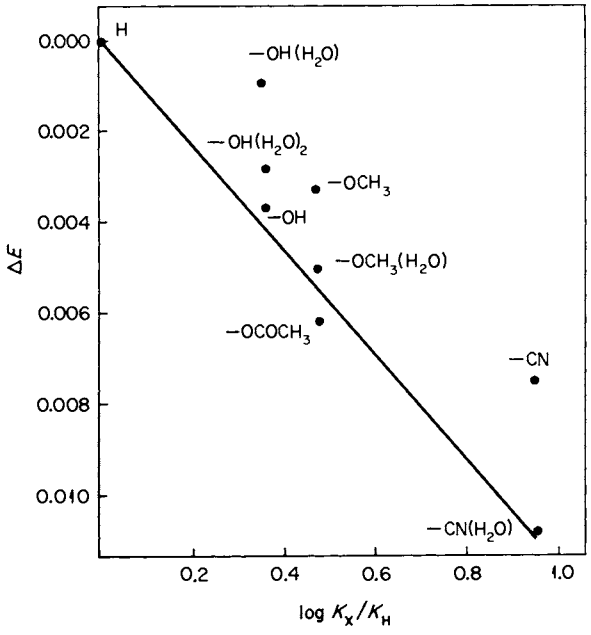

Fig. 7. Plot of ΔE vs. log K_X/K_H for the substituted bicyclooctanecarboxylic acids shown in Table II. Hermann [6].

$E_X - E_H$, were compared with experimental values of K_X/K_H in 1:1 ethanol–water (see Table II and Fig. 7). The calculations are correctly ordered except for X = OH. When this substituent is treated in a hydrated form, then all molecules considered are correctly ordered. These results are heartening, for they indicate that MO methods of this type may become reasonably predictive since σ bond energies and solvent effect approximations may be incorporated into the calculations.

Recent literature provides examples of the use of MO calculations to correlate with and predict pK_a, with the frequent objective of seeking explanations for the biological activities of drug molecules. A discussion of some of these is instructive to show the possible applicability of MO calculations to this physical phenomenon.

TABLE II
CALCULATED ENERGIES AND EXPERIMENTAL LOG K/K_H FOR THE REMOVAL OF THE PROTON FROM BICYCLOOCTANECARBOXYLIC ACID WITH SUBSTITUENT X[a]

X	E_X	$E_X - E_H$	log K/K_H
H—	−0.84446		
HO—	−0.84085	0.00361	0.370±0.044
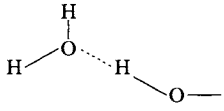	−0.84363	0.00083	
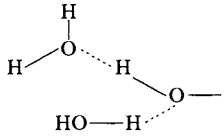	−0.84135	0.00311	
CH_3O	−0.84109	0.00337	0.472±0.032
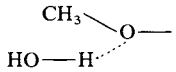	−0.83883	0.00563	
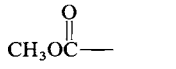	−0.83843	0.00603	0.48[b]
F—	−0.83687	0.00759	
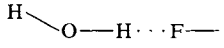	−0.83407	0.01039	
N≡C—	−0.83724	0.00722	0.93
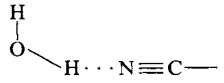	−0.83346	0.01100	
NH_3^+—	−0.72574	0.11872	1.50[c]

[a] Hermann [6].
[b] Value is for the ethyl ester.
[c] Value is for the substituent $(CH_3)_3N^+$.

II. Dissociation of Amino Acids

Using an MO method developed by Del Re [7] for the calculation of properties of σ-bonded systems, Yonezawa, Del Re, and Pullman have sought a relationship between the calculations on amino acids and their

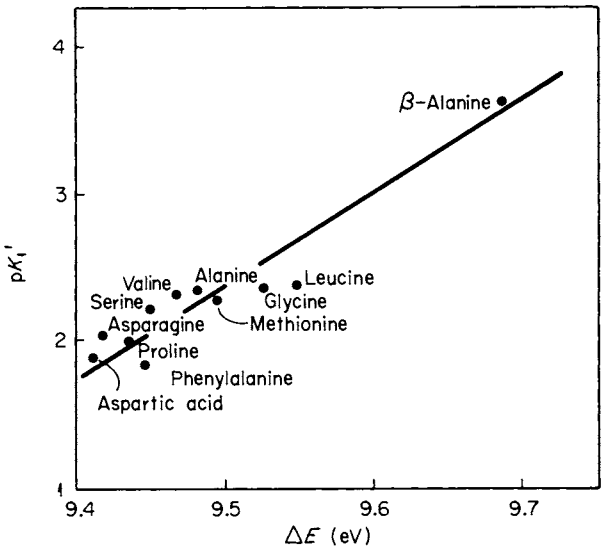

Fig. 8. The dissociation constant pK_1' vs. calculated energy index from column 3, Table III. Yonezawa *et al.* [8].

dissociation constants [8]. In this study, it was assumed that the major contribution to the dissociation constants in a series of related molecules is the change in the sum of the bond energies, $E_{\mu\nu}$, between a dissociated and undissociated form

$$E_{\text{bond}} = \sum E_{\mu\nu}$$

and the change in the electrostatic energy of the proton

$$E_{\text{elec}} = \sum_{\mu} \frac{Q_{\text{H}} Q_{\mu} e^2}{R_{\text{H}\mu}}$$

where the charges are Q and the separation distance is R. In a closely related series it was assumed to a first approximation that the change in solvation energy is constant.

The expression relating to the dissociation constant is thus

$$\Delta E = E_{\sigma(\text{dissoc})} - E_{\sigma(\text{undissoc})} - \sum_{\mu} \frac{Q_{\text{H}} Q_{\mu} e^2}{R_{\text{H}\mu}}$$

In the study, where π electrons are involved, the Q_{μ} term is the sum

$$Q\mu = Q_{\mu}^{\sigma} + Q_{\mu}^{\pi}$$

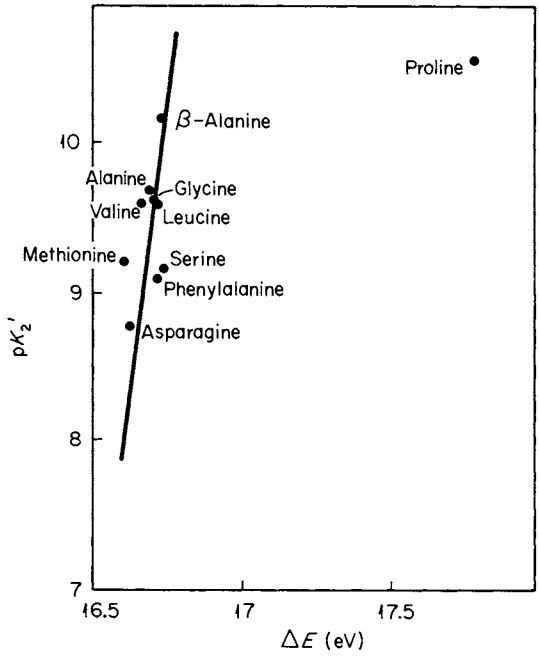

Fig. 9. The dissociation constant pK_2' vs. calculated energy index from column 3, Table IV. Yonezawa *et al.* [8].

the Q_μ^π term being obtained from π-electron Hückel calculations. Also in the bond energy summation, an energy term reflecting the total π energy, E_π was included. A value of -5.2 eV was arbitrarily assigned to the β parameter.

Table III shows the results of the calculations and includes the contribution of bond energy difference and the electrostatic energy. Table IV shows the calculations for the amine protonation equilibria. A plot of these ΔE values and their respective pK values shows a fair correlation (Figs. 8 and 9).

Considering that the method takes no account of preferred conformation and that the $R_{H\mu}$ term was calculated using an average distance based upon free bond rotation, the correlation is encouraging and suggests that further refinements might afford significant improvement in the predictive value of this MO method.

Because of the superior treatment of the interaction between σ and π electrons afforded by the all-valence electron methods, it would be of great interest to determine the predictive capability of these methods to amino acid pK_a.

TABLE III
THE DISSOCIATION CONSTANT pK_1' AND CALCULATED RESULTS[a]

Compound	ΔE_σ $(-\beta)$	$\sum_\mu \frac{Q_H Q_\mu}{R_{H\mu}} e^2$ (eV)	$\Delta E_\sigma - \sum_\mu \frac{Q_H Q_\mu}{R_{H\mu}} e^2$ (eV)	Apparent dissociation constants (pK_1')
Glycine	1.852	−0.037	9.527	2.34
Alanine	1.821	−0.014	9.483	2.34
Valine	1.815	−0.031	9.469	2.32
Serine	1.815	−0.010	9.448	2.21
Proline	1.803	−0.062	9.437	1.99
β-Alanine	1.818	−0.235	9.689	3.60
Leucine	1.815	−0.094	9.548	2.36
Methionine	1.821	−0.024	9.493	2.28
Aspartic acid	1.821	+0.057	9.412	1.88
Asparagine	1.815	+0.017	9.421	2.02
Phenylalanine	1.811	−0.032	9.449	1.83

[a] Yonezawa *et al.* [8].

TABLE IV
THE DISSOCIATION CONSTANT pK_2' AND CALCULATED RESULTS[a]

Compound	ΔE_σ $(-\beta)$	$\sum_\mu \frac{Q_H Q_\mu}{R_{H\mu}} e^2$ (eV)	$\Delta E_\sigma - \sum_\mu \frac{Q_H Q_\mu}{R_{H\mu}} e^2$ (eV)	Apparent dissociation constants (pK_2')
Glycine	3.367	0.799	16.709	9.60
Alanine	3.363	0.794	16.694	9.69
Valine	3.357	0.782	16.674	9.62
Serine	3.367	0.791	16.717	9.15
Methionine	3.363	0.891	16.597	9.21
Proline	3.603	0.871	17.784	10.60
β-Alanine	3.387	0.877	16.735	10.19
Asparagine	3.363	0.850	16.638	8.80
Leucine	3.371	0.811	16.718	9.60
Phenylalanine	3.366	0.789	16.714	9.13

[a] Yonezawa *et al.* [8].

III. Basicity and Folic Acid Inhibition

An example of pK_a directly influencing biological activity, as reflected by an MO-calculated relationship, is illustrated by a study of folic acid inhibition. Neely has made a study of structural features imparting activity to 7,8-dihydrofolic acid (DHFA) reductase inhibitors [9]. Folic acid (FA) (**I**)

is the substrate for this enzyme, whereas analogs such as aminopterin (**II**) are prominent inhibitors.

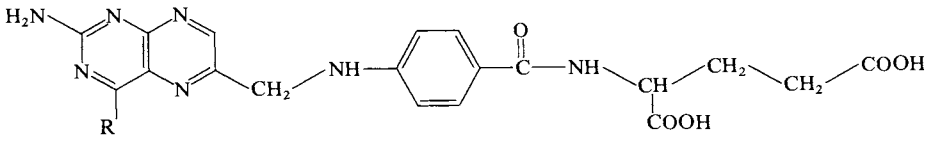

I: R = OH
II: R = NH_2

TABLE V
ELECTRONIC PARAMETERS FOR VARIOUS FOLIC ACID ANALOGS CALCULATED BY MEANS OF LCAO[a]

1–12 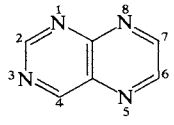

13–15 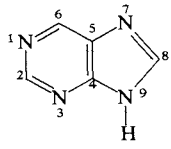

Compound	Basicity $-\sum Qp$ (pp/dd) N-1	Electron density 2-NH_2	4-NH_2	4-OH	C-6	C-7	DHFA reductase inhibition (K_i)
1. 2-Amino,4-hydroxy enol	2.15	0.188	—	0.102	0.042	0.099	—
2. 2-Amino,4-hydroxy keto	1.23	0.209	—	0.426	0.010	0.085	—
3. 2-Amino,4-hydroxy, 7,8-dihydro	1.91	0.185	—	0.092	0.049	—	—
4. 2-Amino,4-hydroxy, 5,6,7,8-tetrahydro	2.21	0.163	—	0.079	—	—	—
5. 2,4-Diamino	2.48	0.187	0.219	—	0.033	0.095	4.7×10^{-7}
6. 2,4-Diamino,7,8-dihydro	1.94	0.183	0.185	—	0.156	—	—
7. 2,4-Diamino,5,6,7,8-tetrahydro	2.51	0.163	0.160	—	—	—	—
8. 2,4-Diamino,6-formyl	2.16	0.191	0.223	—	0.002	0.120	8.1×10^{-6}
9. 2,4-Diamino,6-formyl, 7,8-dihydro	1.67	0.192	0.201	—	−0.043	—	—
10. 2-Amino,4-hydroxy, 6-formyl	2.06	0.193	—	0.104	0.010	0.123	2.9×10^{-4}
11. 2-Amino,4-hydroxy, 6-formyl,7,8-dihydro	1.23	0.192	—	0.096	−0.027	—	—
12. 2,4-Diamino,6-hydroxy	2.01	0.168	0.198	—	0.200	0.074	9.0×10^{-6}
13. 2,6-Diamino	2.22						1.5×10^{-6}
14. 2-Amino	1.39						Inert
15. 2-Amino,6-hydroxy	1.70						Inert

[a] Neely [9].

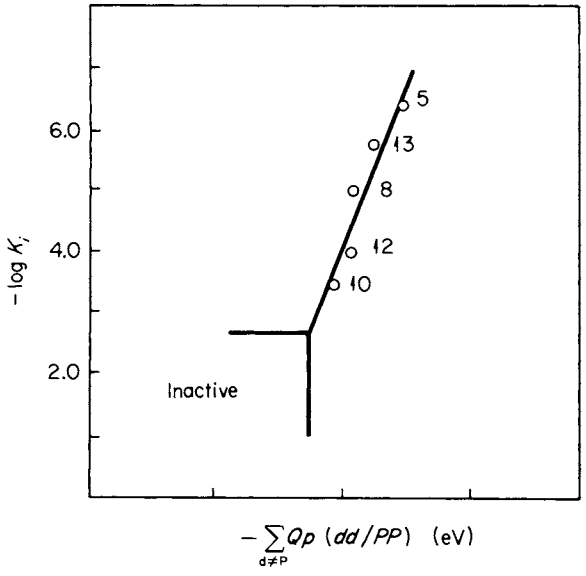

Fig. 10. Relation between calculated basicity and inhibition constant $-\log K_i$ in Table V. Neely [9].

The importance of specific sites on FA and its analog inhibitors has been the subject of several previous studies [*10–12*]. The general conclusion reached is that the conjugated portion of the molecule represented by the pteridine rings is alone responsible for binding to the enzyme. Further, the enol form of FA is considered to be the tautomer actually engaging the receptor.

Neely has proposed that the moiety **III**

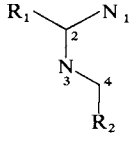

III

is the critical binding portion of FA and its analog inhibitors [*9*]. MO calculations were accordingly made on a series of FA analogs (Table V). The basicity of the N positions were calculated using Nakajima and Pullman's expression [*13*]

$$-\sum Qp(dd/pp)$$

where Q is the π charge density on atom p and (dd/pp) is the two-center integral between an electron of the lone-pair orbital, d, on the nitrogen

atom, and the π electron on atom p. The summation is over all π atoms. The integrals (dd/pp) were calculated according to a prescription of Pariser and Parr [*14*].

The data indicate that a certain level of basicity of the N-1 position is essential for activity, correlating with the inhibition constant (Fig. 10). A minimum basicity of the N-1 position is necessary to maintain the molecule at the enzyme surface. This supports the basicity hypothesis advanced by Colin and Pullman [*11*].

IV. Sulfonamide Activity

A prominent view is held that the mechanism of sulfonamide action is a competitive antagonism of *p*-aminobenzoic acid at an enzyme [*15*, *16*]. The sulfonamides (**IV**) are weak acids, the dissociable proton coming from the amide nitrogen.

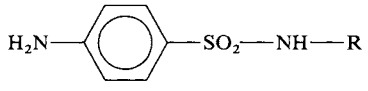

IV

The influence of the R group must account for the experimental differences observed in the pK_a. Foernzler and Martin have studied a large number of sulfa derivatives seeking a correlation between charge densities, experimental pK_a's, and bacteriostatic activity indices [*17*]. The simple Hückel theory was employed. Only the π electrons of sulfur were considered. The electron densities for the *p*-amino group, the sulfur and oxygen atoms were essentially constant. A variation occurred, however, in the density on the amide nitrogen, q_N (see Table VI).

The relationship between pK_a and the amide q_N was not evident when all 30 sulfonamides in the study were considered. The authors, in reflecting on this lack of correlation, noted that solvation effects of the R group were not considered. It is not surprising that in such a diverse group of substituents, R, the assumption of a reasonably constant solvation would be in serious violation of reality.

Foernzler and Martin reduced the list of 30 derivatives to six classes of molecules based upon the nature of the R group. Three such classes, **V–VII**

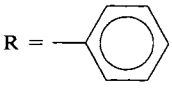

V Class A

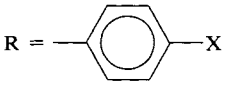

VI Class B

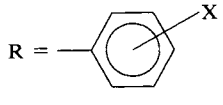

VII Class C

TABLE VI
SULFONAMIDE DERIVATIVES USED FOR LCAO-MO CALCULATIONS[a]

No.	Compound[b]	pK_a	q_{N-1}	$C \times 10^4$ [c]
1	*p*-Aminobenzoic acid	4.68	—	
2	Sulfanilamide	10.43	1.919	20.0
3	N^1-Methylsulfanilamide	10.77	1.853	30.0
4	N^1,N^1-Dimethylsulfanilamide	—	1.795	30.0
5	N^1-Hydroxyethylsulfanilamide	10.92	1.851	50.0
6	Sulfanilylglycine	3.52	1.855	90.0
7	N^1-Phenylsulfanilamide	9.60	1.794	3.0
8	N^1-*o*-Tolylsulfanilamide	9.96	1.791	10.0
9	N^1-*m*-Tolylsulfanilamide	9.74	1.792	5.0
10	N^1-*p*-Tolylsulfanilamide	9.82	1.793	5.0
11	N^3-Sulfanilylmetanilamide	8.23	1.792	2.0
12	N^4-Sulfanilylmetanilamide	7.85	1.790	0.5
13	N^1-*p*-Aminophenylsulfanilamide	10.22	1.805	5.0
14	N^1-Furfurylsulfanilamide	10.88	1.856	20.0
15	Sulfapyridine	8.43	1.781	0.6
16	3-Sulfanilamidopyridine	7.89	1.793	0.2
17	2-*S*-5-Bromopyridine	7.15	1.781	0.5
18	5-*S*-2-Bromopyridine	7.12	1.794	0.2
19	2-*S*-5-Aminopyridine	8.47	1.793	0.6
20	5-*S*-2-Aminopyridine	8.82	1.805	2.0
21	2-Sulfanilamidoimidazole	9.72	1.790	40.0
22	3-Sulfanilamidopyridazine	7.06	1.780	0.08
23	Sulfadiazine	6.48	1.770	0.08
24	2-*S*-4-Methylpyrimidine	7.06	1.770	0.2
25	2-*S*-4,6-Dimethylpyrimidine	7.37	1.769	0.3
26	2-*S*-4-Aminopyrimidine	9.44	1.769	20.0
27	4-*S*-Pyrimidine	6.17	1.768	0.1
28	5-*S*-Pyrimidine	6.62	1.793	0.2
29	5-*S*-2-Chloropyrimidine	5.80	1.797	0.1
30	2-Sulfanilamidopyrazine	6.04	1.779	0.08

[a] Foernzler and Martin [*17*].
[b] *S* = Sulfanilamido.
[c] Minimum molar concentration of drug to cause stasis of *E. coli*.

were considered in detail. The plots of pK_a vs. q_N in each of these classes showed a relationship in each case (see Fig. 11). The authors regarded these relationships as being evidence supporting the view that the pK_a of the molecule influences the activity of the sulfonamides.

Cammarata has extended the studies on the sulfonamides by parameterizing the sulfur atom to include the *d*-orbitals within the Hückel framework [*18*]. He noted an influence of the R group on the charge density of the *para* amino group, depending upon the nature of R group, i.e., electron-donating or -withdrawing. This effect was not observed by Martin and Foernzler who considered the sulfur from a π-only standpoint.

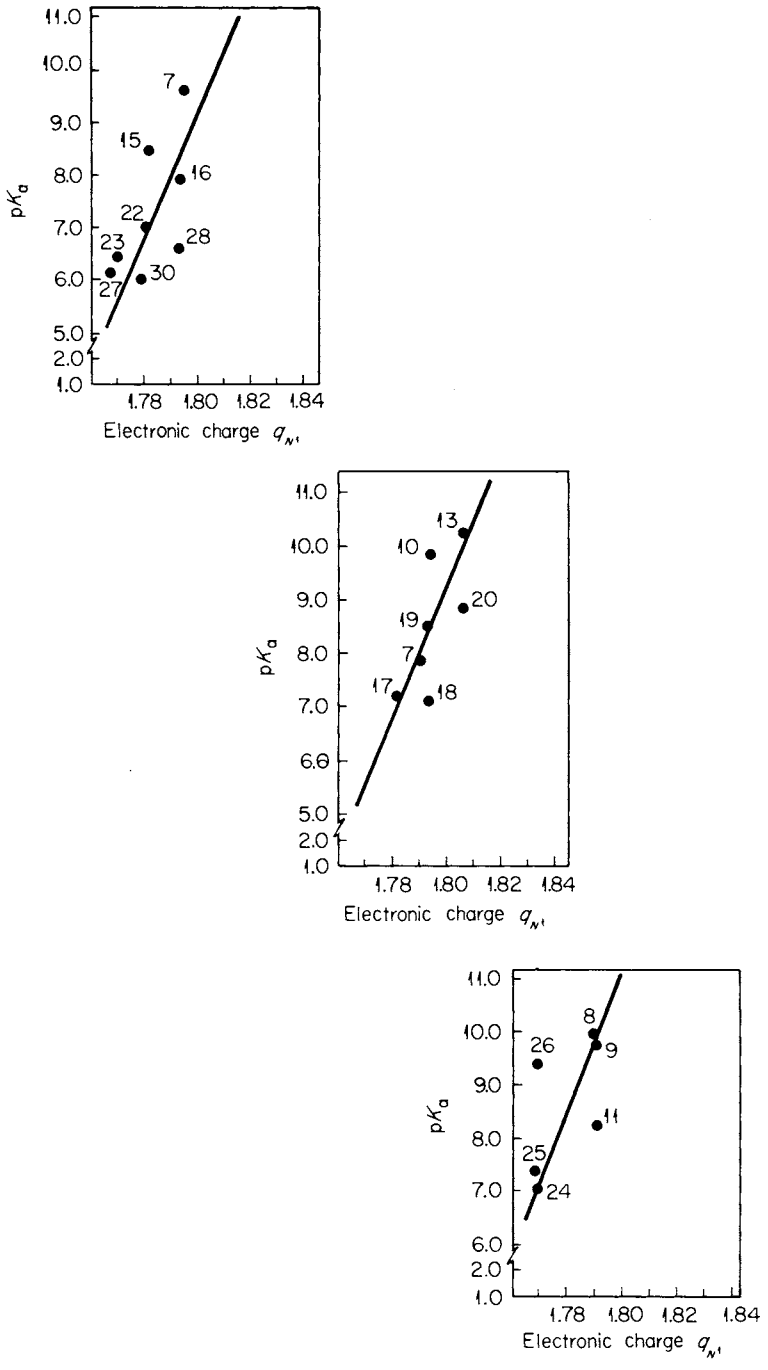

Fig. 11. Relation between sulfonamide N_1 electronic charge and pK_a of derivatives (top) class A, (middle) class B, and (bottom) class C. Foernzler and Martin [*17*].

The net effect of these studies is to show a relationship between electronic charge and pK_a, a point which is theoretically justified, assuming the approximations previously described and selecting the cases carefully to balance out the effect of the neglect of solvation.

It would be of interest to repeat these studies, using an energy index rather than a ground state index.

IV. Summary

It would appear that the applicability of π only MO methods to the prediction of pK_a is severely limited to closely related series where solvation and entropy effects are fairly constant or slowly varying. Predictions in a mixed series of structural types breaks down rather badly.

There have yet to be performed many calculations using all-valence electron methods and correlating these with experimental pK_a's. These methods would at least consider such contributions to the enthalpy of protonation as the energy change in the σ bonds, ΔE_σ, and the energy change due to nonbonded interactions (steric energy), ΔE_{st}.

Thus either EHT or the SCF–CNDO methods might provide a more powerful method to approximate these factors. An immediately obvious application of all-valence electron methods would be in the reassessment of the sulfonamides.

References

1. J. J. Elliott and S. F. Mason, *J. Chem. Soc. London* p. 2352 (1959).
2. O. Chalvet, R. Daudel, and F. Peradejordi, "Molecular Orbitals in Chemistry, Physics and Biology" (P. Lowdin and B. Pullman, eds.), p. 475. Academic Press, New York, 1964.
3. H. C. Longuet-Higgins, *J. Chem. Phys.* **18**, 275 (1950).
4. F. Peradejordi, *Cah. Phys.* **1**, No. 158, 159 (1963).
5. B. M. Lynch, *Tetrahedron Lett.* p. 1357 (1969).
6. R. B. Hermann, *J. Amer. Chem. Soc.* **91**, 3152 (1969).
7. G. Del Re, *J. Chem. Soc., London* p. 4031 (1958).
8. T. Yonezawa, G. Del Re, and B. Pullman, *Bull. Chem. Soc. Jap.* **37**, 985 (1964).
9. W. B. Neely, *Mol. Pharmacol.* **3**, 108 (1967).
10. B. R. Baker, D. V. Santi, P. I. Almaula, and W. C. Werkheiser, *J. Med. Chem.* **7**, 24 (1964).
11. R. Colin and B. Pullman, *Biochim. Biophys. Acta* **89**, 232 (1964).
12. S. F. Zakrzewski, *J. Biol. Chem.* **238**, 148 (1963).
13. T. Nakajima and A. Pullman, *J. Chim. Phys.* **55**, 793 (1958).
14. R. Pariser and R. G. Parr, *J. Chem. Phys.* **21**, 767 (1953).
15. D. D. Woods, *Brit. J. Exp. Pathol.* **21**, 74 (1940).
16. P. Fildes, *Lancet* No. 238, 955 (1940).
17. E. C. Foernzler and A. N. Martin, *J. Pharm. Sci.* **56**, 608 (1967).
18. A. Cammarata, *J. Pharm. Sci.* **55**, 1469 (1966).

Chapter X

HYDROGEN BONDING

I. Theory

The hydrogen bond plays a very significant role in biological systems in uniting molecules into functional complexes without resorting to the mechanism of a stronger, less reversible covalent bond. It is not surprising to find this bond so ubiquitously distributed in living systems since groups and atoms capable of engaging in this phenomenon are widespread among biological compounds. The bond is formed when a hydrogen atom bridges, in some equilibrium position, two electronegative atoms. Oxygen and nitrogen are two prominent atoms found in the bond, although Cl, F, S, and perhaps C are also known.

The energy of the hydrogen bond as a function of the distance between the two bridged atoms X—H----Y results in a double-welled minimum. The shape of this curve is symmetrical when X = Y (Fig. 1), and unsymmetrical when $X \neq Y$ (Fig. 2). In the latter case, the dissimilar bridged atoms X and Y are not equivalent in the electronegativity (X > Y), hence a deeper minimum occurs on the X side of the midpoint.

The energy of these bonds, in the usual cases encountered in biological systems, is 4–8 kcal/mole. The distance between bridgehead atoms ranges from 2.5 to 3.2 Å. The angle of the three atoms ranges from 180° to about 125° [*1*].

A considerable amount of thought has gone into the theoretical interpretation of the hydrogen bond. Coulson has described the forces involved as (*a*) the classical interaction of fixed charge distributions, or the more

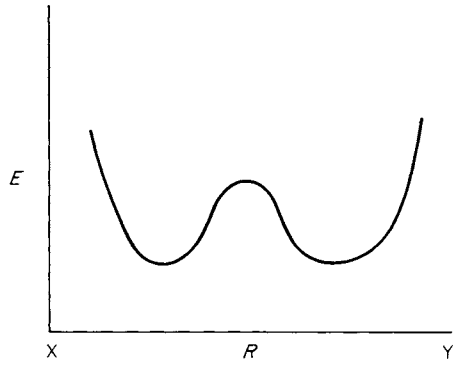

Fig. 1. Relationship between position, *R*, of hydrogen atom between two atoms, X and Y of equal electronegativity and the energy of the system.

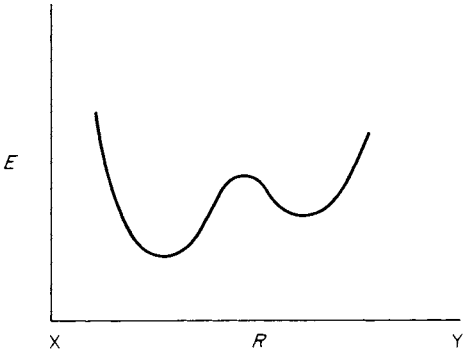

Fig. 2. Relationship between position, *R*, of hydrogen atom between two atoms X and Y, of unequal electronegativity and the energy of the system.

familiar electrostatic interaction of point charges, (*b*) delocalization effects, (*c*) orbital overlap repulsions, and (*d*) dispersion or charge fluctuation interactions [*2*]. The acceptance of the role of the last three forces contributing to the stability of the bond has replaced the earlier view that the bond was entirely an electrostatic phenomenon.

A. Electrostatic Approach

It has been possible, however, to achieve reasonable estimates of the bond energy by considering the interaction from the view of an electrostatic phenomenon between two charge distributions, the magnitude of which has been fairly accurately evaluated. Thus Nash and Bradley have used this approach to predict the pairing schemes between the nucleotide base pairs

adenine, uracil, cytosine, and quanine [3]. The π-electron charges were evaluated using Hückel and SCF calculations, whereas the σ-electron charges were calculated using Del Re's method [4]. These separately calculated charges were summed to give a total charge at each atom of the base. Various geometrical patterns of pairing were then evaluated using Coulomb's law to sum the interactions. The minimum energy was sought by varying the pairing scheme. The predicted pairing schemes were in every case but one consistent with existing experimental evidence.

B. Charge Transfer Approach

A theory put forth by Puranik and Kumar has considered the delocalization contributing to the bond as arising out of a mutual polarization of the charge clouds as the atoms of the bond approach each other [5]. This leads to a model which can be thought of as a charge migration or charge transfer. As an approach then, charge transfer formalism as proposed by Mulliken [6] was used to develop a relationship for the hydrogen bond to explain such phenomena as X—H infrared frequency shifts and increased infrared intensity.

The wavefunction of the ground state of the hydrogen bond ψ_m is represented in Eq. (1).

$$\psi_m = a\psi_0 + b\psi_1 \tag{1}$$

where ψ_0 is the no-bond function for X—H----Y and ψ_1 is the dative bond function for $X^{\ominus}$----H—$Y^{\oplus}$ as in Mulliken's charge transfer theory. The first term in Eq. (1), $a\psi_0$ corresponds to recognized forces between molecules like dispersion, electrostatic interaction, and repulsive forces. The second term in Eq. (1), $b\psi_1$, is conceived to represent the migration of an electron from a nonbonding orbital on Y (the donor) to an antibonding orbital on X (the acceptor). A covalent bond of modest strength due to the distance is thus presumed to form.

An approximation for the energy of the complex, E_m, can be derived from perturbation theory as in Eq. (2)

$$E_m = E_0 - (H - SE)^2/(E_1 - E_0) \tag{2}$$

where E_0 is the energy of the separate donor and acceptors represented by ψ_0, and E is the energy of the complex represented by ψ_1. H is the Hamiltonian of the system and S is the overlap integral between the donor orbital and the anion of the acceptor orbital.

The normalization condition gives

$$a^2 + 2abS + b^2 = 1$$

whereas from perturbation theory we have

$$\frac{b}{a} = -\frac{(H_{01} - SE_0)}{E_1 - E_0}$$

so that

$$b = \frac{cS}{E_1 - E_0}$$

where c is a constant.

$E_1 - E_0$ in Eq. (2) can be replaced by $I_d - A$, where I_d is the ionization potential of the donor molecule and A is the sum of the electron affinity of the acceptor molecule and the net energy of attraction between X^- and Y^+. As a result we can write for b,

$$b = \frac{cS}{I_d - A}$$

The frequency shifts in the infrared for the stretching vibration of X—H on complex formation provides a means of evaluating the coefficients a and b, thus

$$\frac{\Delta\nu}{\nu} = \frac{(5/2)\lambda c^2 S^2}{(I_d - A)^2}$$

where ν is the frequency of the stretching vibration and λ the polarity of the orbitals. An extensive testing of this theory is still awaited.

C. Delocalization Approach

The view that the delocalization contribution to the structure of the hydrogen bond is considerable, has led to a number of studies in which higher energy orbitals of hydrogen have been invoked. A strong argument against the use of $2p$ atomic orbitals of hydrogen in hydrogen-bonding is that the promotion of a hydrogen $1s$ electron to a $2p$ orbital probably requires more energy than would be gained by the resulting strengthening of the hydrogen bond. However, the hydrogen in a hydrogen-bonded condition may actually require less energy, due to favorable geometry. This may be particularly true in cases where there is extensive π character in the molecules.

Pullman and Pullman have considered the π character of hydrogen in hydrogen bonds to be important enough to incorporate this into the framework of π-electron Hückel theory [7]. In the system

—X—H----Y

The usual heteroatom parameters are employed for X, Y, and the X—Y

bond, h_X, h_Y, and k_{X-Y} in the Coulomb and resonance integral expressions

$$\alpha = \alpha + h\beta$$

$$\beta = k\beta$$

The parameter h_X was decreased by 0.2, reflecting the loss of electronegativity upon acquiring some partial charge due to the extension of the X—H bond toward Y. The h_Y term is correspondingly increased by 0.2 due to the drift of charge from Y toward the hydrogen. The resonance integral between X and Y, in which H intervenes but is ignored in the mechanics of the method, is assumed to be 0.2.

TABLE I

THE CARBONYL STRETCHING FREQUENCIES ν_{C-O} (MEASURED IN DILUTE CARBON TETRACHLORIDE SOLUTION) AND THE CORRESPONDING BOND ORDERS, P_{C-O} [a]

No.	Compound	P_{C-O}	ν_{C-O} cm^{-1}
1	Benzaldehyde	0.851	1708
2	1-Naphthaldehyde	0.841	1700
3	2-Naphthaldehyde	0.849	1702
4	9-Phenanthrenealdehyde	0.840	1698
5	Salicylaldehyde	0.809	1670
6	1-Hydroxy-2-naphthaldehyde	0.800	1651
7	2-Hydroxy-1-naphthaldehyde	0.792	1649
8	3-Hydroxy-2-naphthaldehyde	0.813	1670
9	10-Hydroxy-9-phenanthrenealdehyde	0.786	1637
10	*o*-Benzoquinone	0.823	1669
11	1,2-Naphthoquinone	0.819	1678
12	9,10-Phenanthraquinone	0.826	1684
13	1-Hydroxy-9,10-phenanthraquinone	0.780	1639
14	1,4-Naphthoquinone	0.793	1675
15	9,10-Anthraquinone	0.794	1676
16	5,8-Dihydroxy-1,2-naphthoquinone	0.736	1623
17	1-Hydroxy-9,10-anthraquinone	0.750	1636
		0.792	1673
18	1,4-Dihydroxy-9,10-anthraquinone	0.743	1627
19	1,5-Dihydroxy-9,10-anthraquinone	0.748	1639
20	1,2-Dihydroxy-9,10-anthraquinone	0.749	1636
		0.781	1660
21	1,3-Dihydroxy-9,10-anthraquinone	0.743	1635
		0.792	1675
22	1,2,4-Trihydroxy-9,10-anthraquinone	0.733	1623
		0.742	
23	2-Hydroxy-1,4-naphthoquinone	0.774	1663
		0.778	
24	2,3-Dihydroxy-1,4-naphthoquinone	0.757	1649
25	Benzophenone	0.786	1659
26	1-Hydroxybenzophenone	0.746	1626

[a] Grinter [8].

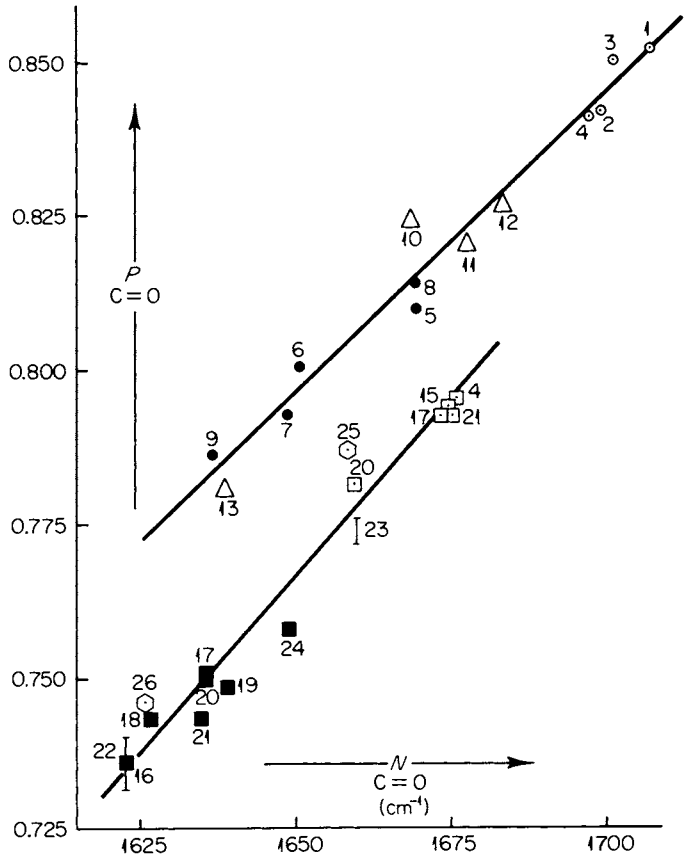

Fig. 3. Relationship between carbonyl stretching frequency, N_{CO} and calculated bond orders P_{CO} for groups of compounds listed in Table I. Grinter [8].

Grinter has tested this approach by considering the known relationship between the MO bond order of a conjugated carbonyl group and its infrared stretching frequency [8]. Two groups of molecules were studied, quinones, and aldehydes. Within each group were a number of molecules capable of intramolecular hydrogen-bonding, as for example salicylaldehyde (**I**). (See Table I.)

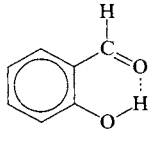

I

The calculated bond orders within each group showed a good correlation with the carbonyl stretching frequencies (Fig. 3).

These findings do not prove the involvement of hydrogen $2p\ \pi$ orbitals, but they indicate that methods using this approximation may give results in reasonable agreement with experiment.

D. United Molecule Approach

1. *Extended Hückel Calculations*

A more extensive consideration of the delocalization stabilization of the hydrogen bond has been considered, using an all-valence electron MO treatment [*9*]. This approach considered the entire molecule in the isolated state and the entire complex as a molecule in the hydrogen-bonded state. The EHT was used for the calculations.

A delocalization energy was calculated as the difference between the total electronic energy of the isolated molecules and the total electronic energy of the molecules hydrogen-bonded. The distance between the bridge atoms in the bond was varied to a limited extent to seek the minimum energy separation.

The calculations on the formic acid dimer (**II**)

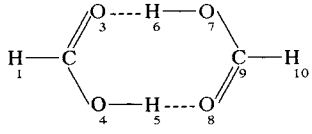

II

are shown in Table II for various distances separating the monomers. The most stable distance separating the oxygen atoms is 2.7 Å, in good agreement with the separation distance of 2.72–2.73 Å found in the gas phase [*10*]. The calculated delocalization energy, 0.164 eV, 3.77 kcal/mole is about one-quarter of the observed ΔH of 14.2 kcal/mole of two hydrogen bonds in the gaseous dimer [*1*]. This calculated value may be too low based on Coulson's estimate of the delocalization contribution to the hydrogen bond of water of 8 $\pm$ kcal/mole [*11*]. This low value may be due to overemphasis of the bond polarity in this approximation, which would hinder electron delocalization. Another cause of the apparent low value may be due to the fact that, in this approximation, the delocalization energy is exclusively attributed to the σ electrons including the lone pairs, and not at all to the π electrons. Since a hydrogen has no π orbital in this approximation, the delocalization must occur between oxygens by direct overlap. This value is, of course, very small (0.0014) considering the interoxygen distance.

TABLE II
DELOCALIZATION ENERGY OF HYDROGEN BOND IN FORMIC ACID DIMER (II)[a,b]

Model	O_3----O_7 distance (Å)	O_7----H_6 distance (Å)	O_3----H_6 distance (Å)	Total energy (eV)	Delocalization energy (eV)
2 Monomers	—	0.96	—	−805.8540	—
1	2.8	0.96	1.89	−806.0106	+0.1566
2	2.7	0.96	1.79	−806.0181	+0.1641
3	2.6	0.96	1.69	−806.0031	+0.1491
4	2.7	1.06	1.69	−805.6966	−0.1574
5	2.6	1.06	1.60	−805.7198	−0.1342

[a] ∠COH was assumed to be tetrahedral.
[b] Morokuma *et al.* [9].

In the same study, a calculation was performed on the π levels of formic acid and its dimer with and without consideration of the $2p\pi$ orbital of hydrogen. A Coulomb integral of −3.4 eV was assigned to the hydrogen $2p$ π orbital and an effective nuclear charge of 1.0 was assumed. The π delocalization energy without this orbital was found to be 0.0002 eV and 0.002 eV with inclusion of the orbital. The amount is still negligible however, and the conclusion reached was that this orbital does not play a role in the delocalization.

These investigators considered an intramolecular hydrogen bond by calculating the energies of several conformations of salicylaldehyde (**III**–**V**) [9].

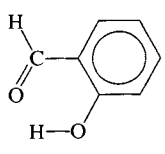

III

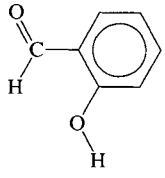

IV

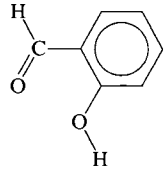

V

Configuration **III** was preferred over **IV** and **V** by about 0.07 eV (1.61 kcal). Assuming that this preference is due entirely to the gain in energy from the hydrogen-bonding, this value can be considered to be the delocalization energy of the bond.

This same approach to the hydrogen bond has more recently been applied by Hoffmann to a consideration of the pyridine lone pair and the bond formed with water and methanol [12]. Extended Hückel MO calculations were performed on a number of modes of approach of water and the pyridine nitrogen lone pair (Fig. 4).

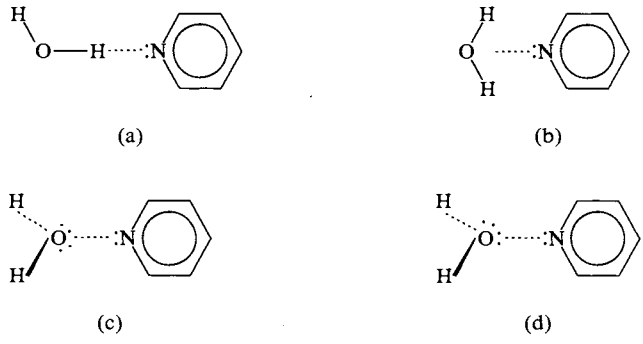

Fig. 4. Various modes of water–pyridine hydrogen-bonding assumed in energy calculations. Adam *et al.* [*12*].

In mode (a) the O—H bond approaches so that the O—H----N system is linear. Mode (b) has the hydrogens bisecting the lone pair, whereas (c) has the nitrogen lone pair bisecting the oxygen lone pairs. Mode (d) has one oxygen lone pair in a direct line of approach to the nitrogen lone pair. In each case the H----N distance was varied from 3.0 Å to 1.0 Å by 0.5 Å incremenets. Only total energy vs distance plot for mode (a) in Fig. 4 gave an energy minimum. At this minimum the bridged atoms are 2.76 Å apart, in excellent agreement with experiment. The position of the other hydrogen atom of water is apparently irrelevent to the energy vs distance relationship.

Results of calculations of methanol approaching the pyridine lone pair again showed that a linear O—H----N system gave a minimum in a total energy vs. distance plot. Little difference was calculated in the total energy for several arrangements of the methyl group of methanol (about 0.5 kcal).

Another series of calculations were made in which the O and the N distances were held at the equilibrium distance ± 0.25 Å, whereas the position of the hydrogen atom was allowed to vary between the bridging atoms. A double minimum plot was obtained for each of the three bridge atom distances (Fig. 5). The energy barrier to transfer of the hydrogen from O to N for the equilibrium distance of 2.76 Å is about 15 kcal/mole. The energy minimum for the N—H bond is 50 kcal/mole lower than the O—H minimum. Thus nitrogen has a greater affinity for the hydrogen than does oxygen in this system. At the O—H minimum the structure of the system is O—H----N with little charge separation, while at the N—H minimum the structure is $O^{\ominus}$----H—$N^{\oplus}$ with considerable charge separation. The former would be expected to be more stable from simple electrostatic considerations. This points up the fault in the Hückel method in which electron repulsion is not considered, leading to exaggerated charge separation. This

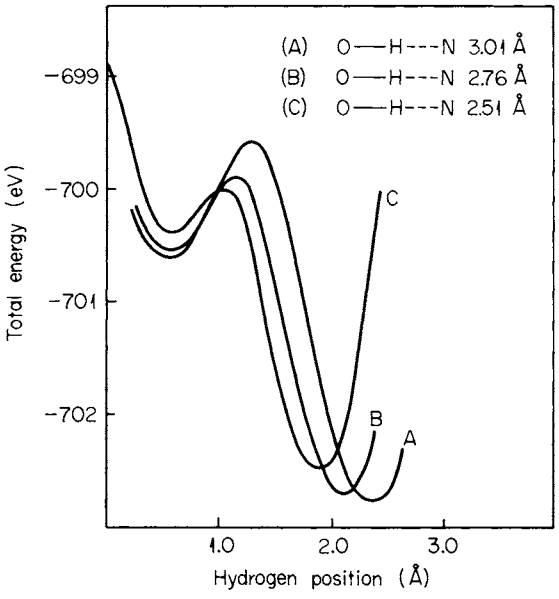

Fig. 5. Total energy of the configuration shown in Fig. 4a of the water–pyridine system as a function of the position of the hydrogen atom. Adam *et al.* [*12*].

makes details of the barriers of this double minimum questionable, although the finding of a double minimum is certainly encouraging.

As would be expected, when the hydrogen migrates away from the oxygen, a large negative charge is left, while a commensurate decrease in the negative charge on the nitrogen develops. The charge on the hydrogen remains relatively constant, being somewhat more positive near the oxygen atom.

From this study, it is evident that EHT, in spite of the limitations of a Hückel scheme, can adequately account for features of a hydrogen bond such as geometry and equilibrium separations as well as a fair estimate of the energy of the bond.

2. *CNDO/2 Calculations*

The limitations of Hückel theory, carrying over into the EHT method, has led to research on the hydrogen bond using all-valence SCF methods in the hope that a closer account of the bond can be realized. Pullman and Berthod have used the CNDO/2 method to study the dimers of formamide, a hydrogen-bonded system [*13*]. In this study, an energy distance profile was not developed, but an arrangement was assumed, based on experimental data. The stabilization energies and the charge densities were the main focus of attention.

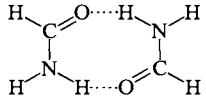

Fig. 6. Formamide cyclic dimer found in the crystal and preferred from CNDO/2 calculations.

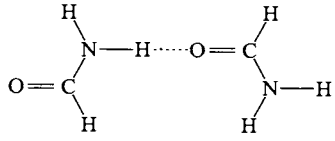

(a)

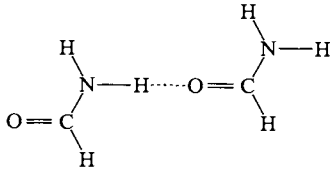

(b)

Fig. 7. Formamide dimer arrangements used in CNDO/2 calculations.

The stabilization energy for the cyclic dimer (Fig. 6) found in the crystal was calculated as the difference between the total energy of the dimer and the two isolated monomers. This was found to be 11.7 kcal/mole or 5.8 kcal/mole per hydrogen bond. The dimer arrangements found in parallel polypeptide chains (Fig. 7a) and in antiparallel polypeptide chains (Fig. 7b), have stabilization energies calculated to be 4.9 and 4.6 kcal/mole, respectively, for the hydrogen bond. All of these values are in good agreement with experimental hydrogen bond energies in similar systems.

The electron distribution, as a result of the formation of the hydrogen bond, can be studied with CNDO/2 in a more reliable way than with EHT. In the formamide dimers, the proton-donating nitrogen atom showed a net gain in electrons as does the proton-accepting oxygen atom, compared to the formamide monomer. The hydrogen atom increased in positive charge when it participated in the hydrogen bond. The electron gain of the nitrogen is the net result of a σ charge gain and a π charge loss. The electron gain of the oxygen, in contrast, is the net result of a σ charge loss and a π charge gain. It appears from these calculations that the net electron transfer, via the hydrogen bond, is essentially a σ-electron transfer.

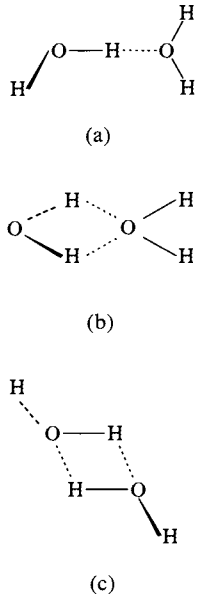

Fig. 8. Hydrogen-bonded water dimers considered in MO studies [*14*].

Hoyland and Kier have also employed the CNDO/2 method to study the hydrogen bond in several representative systems [*14*]. Several conformations of hydrogen-bonded water molecules were considered (Fig. 8), including a linear (a), bifurcated (b), and cyclic (c) dimer. The geometry of the bonded water was assumed to be invariant: O—H = 0.96 Å, H—O—H = 104.5 Å. The equilibrium distances of bridging atoms and stabilization energies calculated are shown in Table III. The linear dimer has a stabilization energy in good agreement with the experimental value of hydrogen bond strength of 5–6 kcal/mole [*1*]. The equilibrium distance of oxygen atoms is about 10% lower than the experimental value for ice of 2.74–2.77 Å [*1*]. The bifurcated and cyclic dimers are clearly less preferred than the linear form.

Two trimers of water were also considered in this study. Trimer I considers both hydrogens of the central molecule bonded to adjacent molecules, whereas trimer II considers the oxygen atom and one hydrogen atom of a central water molecule to be bonded to two adjacent molecules (Fig. 9).

These results are also shown in Table III. Trimer II is preferred over trimer I by about 2 kcal/mole. Trimer II has a stabilization energy of 6.80 kcal/mole for each hydrogen bond, hence it is somewhat larger than the linear dimer.

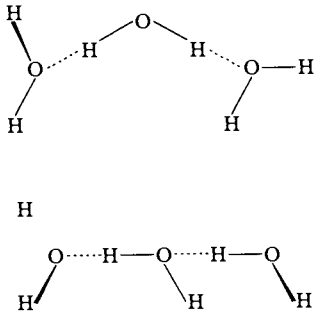

Fig. 9. Hydrogen-bonded water trimers considered in MO studies [*14*].

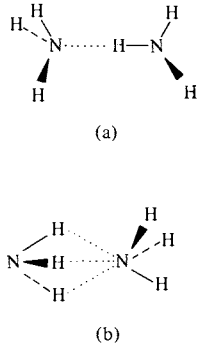

Fig. 10. Hydrogen-bonded ammonia dimers considered in MO studies [*14*].

The final calculation on water was on a pentamer in which four waters are tetrahedrally arranged about a central water molecule. Such an arrangement occurs in ice. The equilibrium bridging distance was calculated to be 2.54 Å and the stabilization energy per hydrogen bond, 5.81 kcal/mole (see Table III).

Hoyland and Kier considered several other hydrogen-bonded systems in the same study [*14*]. A linear dimer of ammonia (a) was found to be preferred over a trifurcated arrangement (b) (Fig. 10).

The stabilization energy for (a) (Fig. 10) was calculated to be 4.06 kcal/mole, in good agreement with experimental bond strength of 3.7–4.4 kcal/mole [*1*]. The calculated energy minimum occurred at 2.77 Å.

Calculations were also made on several hydrogen fluoride arrangements including a dimer, trimer, tetramer, hexamer, and cyclic hexamer [*14*]. The results, shown in Table IV indicate that the chain polymers prefer a zig-zag arrangement with an HFH angle of 145° and an F—F distance of 2.43 Å.

TABLE III
CALCULATED STABILIZATION ENERGIES AND EQUILIBRIUM DISTANCES FOR VARIOUS CONFORMATIONS OF HYDROGEN FOR BONDED WATER[a]

Polymer	R_o(Å)	$E(R_o + 0.05)$[b]	$E(R_o)$	$E(R_o - 0.05)$	R_{eq}[c]	$E(R_{eq})$
Linear dimer	2.55	− 6.14	− 6.30	− 6.23	2.54	− 6.30
Bifurcated dimer	2.40	− 2.82	− 2.84	− 2.77	2.41	− 2.84
Cyclic dimer	2.67	− 1.87	− 1.91	− 1.87	2.67	− 1.91
Trimer I[d]	2,55	−11.34	−11.46	−11.04	2.56	−11.48
Trimer II[d]	2.55	−13.02	−13.52	−13.58	2.52	−13.60
Pentamer	2.55	−22.84	−23.16	−22.44	2.56	−23.24

[a] Hoyland and Kier [*14*].
[b] ΔH in kcal/mole for the reaction $n H_2O \rightarrow (H_2O)_n$.
[c] Predicted O—O equilibrium separation.
[d] See text for a discussion of the geometry of the two trimers.

TABLE IV
COMPUTED RESULTS FOR HYDROGEN FLUORIDE[a]

Polymer	R_o(Å)	$E(R_o + 0.05)$[b]	$E(R_o)$	$E(R_o - 0.05)$	R_{eq}[c]	$E(R_{eq})$
Dimer	2.45	− 6.68	− 6.90	− 6.87	2.43	− 6.92
Trimer	2.40	−15.26	−15.56	−15.18	2.40	−15.56
Tetramer	2.40	−24.05	−24.78	−24.58	2.39	−24.82
Chain hexamer	2.37	−43.16	−44.10	−43.21	2.37	−44.10
Ring hexamer	2.35	−55.16	−56.59	−55.78	2.34	−56.61

[a] Hoyland and Kier [*14*].
[b] ΔH in kcal/mole for the reaction $n HF \rightarrow (HF)_n$.
[c] Predicted F—F equilibrium separation.

This is in good agreement with electron diffraction studies which show the angle to be 140 ± 5 and the separation of F—F to be 2.55 Å. The calculations show an increasing ΔE with increasing chain length. The ring hexamer is substantially more preferred from the calculated ΔE. With increasing chain length, however, entropy considerations will become increasingly prominent so that the presence of hexamer, either linear or cyclic, may not be likely. On the basis of the electron diffraction results, it would appear that chain length would not likely exceed the tetramer or pentamer [*15*].

Hoyland and Kier also studied the ammonium ion and methylammonium ion–water systems [*14*]. In view of the tremendous importance of quaternary ammonium ions in many drug classes, it is of particular interest to consider this system with theoretical methods. A comparison between computed and experimental results is difficult. The heat of hydration of the ammonium ion is known to be −79 kcal/mole [*16*]. Pearson and Vogelsong have estimated that the heat of hydration of the tetramethylammonium ion

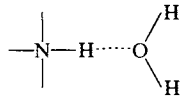

Fig. 11. Hydrogen-bonded ammonium ion–water model considered in MO studies [*14*].

is −48 kcal/mole, and have concluded that substitution of a methyl group for a proton raises the heat of hydration of the quaternary amines by 8 kcal/mole per methyl group [*17*]. Thus they estimate the heat of hydration of $CH_3NH_3^+$ to be −71 kcal/mole.

An alternate approach is to assume that the interaction energy between each methyl group and the surrounding medium is −12 kcal/mole. This is one fourth of the value of −48 kcal/mole estimated by Pearson and Vogelsong for tetramethylammonium ion [*17*]. These values then can serve as a basis for comparison with calculated values.

Calculations on the ammonium ion were made on a model in which the bonded water molecules were assumed to be planar with each N — H bond (Fig. 11). A minimum energy was found at an N — O distance of 2.49 Å with a stabilization energy of −22.26 kcal/mole for each bonded water molecule, or a total of 89 kcal/mole for the system. An approximate comparison with experiment can be made by assuming that four water–water hydrogen bonds must be broken to form the $(NH_4)^+ \cdot 4H_2O$ complex. Assuming a value of 5.5 kcal/mole for the water–water hydrogen bonds, 22 kcal/mole must be deducted from the 89 kcal calculated. The interaction of the complex with the aqueous medium through various dipole–dipole, dipole-induced dipole, and dispersion forces must be considered. This was estimated to be the difference between the computed and experimental heat of hydration or about −12 kcal/mole.

Calculations on the CH_3—$NH_3 \cdot 3H_2O$ system indicated a value of −62 kcal/mole for the energy of formation with an N—O separation of 2.48 Å. Additional calculations were made to determine if the C—H bonds were capable of participating in hydrogen-bonding. It was found that this is unlikely. It was, however, assumed that the methyl group interacted with surrounding water to produce an orienting effect. This was concluded to be the −12 kcal/mole from the work of Pearson and Vogelsong. [*17*]. The estimate of the heat of hydration of methylammonium is a sum of contributions including the energy to rupture three water–water bonds and an estimated 9 kcal/mole of dipole–dipole and dispersion energy between the complex and surrounding water. The total of these contributions is −66.5 kcal/mole.

Estimates of the heats of hydration of the di- and trimethylammonium ions were made by extrapolation from the above results. The values are shown in Table V. It is likely that these results are closer to reality than those

TABLE V
PREDICTED CONTRIBUTIONS TO THE HEAT OF HYDRATION OF METHYL-SUBSTITUTED AMMONIUM IONS[a,b]

Quaternary amine	NH—O hydrogen bonding	Water–water cleavage	NH—OH_2 medium interaction	Methyl group contribution	Total
NH_4^+	−89.0	+22.0	−12.0	—	−79.0
$CH_3NH_3^+$	−62.0	+16.5	− 9.0	−12.0	−66.5
$(CH_3)_2NH_2^+$	−39.2	+11.0	− 6.0	−24.0	−58.2
$(CH_3)_3NH^+$	−19.2	+ 5.5	− 3.0	−36.0	−52.6
$(CH_3)_4N^+$	—	—	—	−48.0	−48.0

[a] Hoyland and Kier [*14*].
[b] All values are in units of kcal/mole.

TABLE VI
COMPUTED RESULTS FOR METHANOL[a]

Polymer	R_o[b]	$E(R_o + 0.05)$[c]	$E(R_o)$	$E(R - 0.05)$	R_{eq}[d]	$E(R_{eq})$
Linear dimer	2.55	− 6.29	− 6.50	− 6.49	2.53	− 6.52
Cyclic dimer[e] $\alpha = 60°, \beta = 0°$	2.05	− 1.93	− 1.98	− 1.97	2.03	− 1.98
Cyclic dimer $\alpha = 75°, \beta = 0°$	1.95	− 2.50	− 2.55	− 2.54	1.93	− 2.55
Cyclic dimer $\alpha = 90°, \beta = 0°$	2.00	− 1.96	− 2.04	− 2.04	1.97	− 2.05
Cyclic dimer $\alpha = 75°, \beta = 30°$	1.95	− 2.31	− 2.33	− 2.27	1.96	− 2.33
Tetramer	2.55	−23.30	−23.90	−23.65	2.54	−23.92

[a] Hoyland and Kier [*14*].
[b] The O—O distance (Å) for the linear dimer and tetramer, and the O—H distance (Å) for the cyclic dimer.
[c] ΔH is kcal/mole for the reaction $n CH_3 \rightarrow (CH_3OH)_n$.
[d] Predicted equilibrium separation.
[e] α = angle of H—O----H; β = angle between C—O bond and plane containing hydrogen bonded atoms.

obtained by adding 8 kcal/mole for each methyl group to the ammonium ion result.

Hoyland and Kier's studies on various methanol dimers included several cyclic forms [*14*]. The results indicated that the linear dimer was significantly lower in energy than any of the cyclic forms considered, in contrast to indications from experiment [*18–20*]. The linear dimer bond strength was found to be −6.52 kcal/mole, in good agreement with experimental measurements of −4.0 to −6.7 kcal/mole [*1*]. This is slightly lower than the value of −6.3 kcal/mole found for the linear water dimer.

The heat of formation of a cyclic tetramer was computed to be −23.92

kcal/mole in good agreement with experimental studies on methanol vapor, indicating a cyclic tetramer with a heat of formation of −24.2 kcal/mole [*21*]. Table VI summarizes these results.

Less satisfactory results were calculated for formic and acetic acid dimers [*14*]. Calculations showed enthalpies of formation of −22.96 kcal/mole and −23.62 kcal/mole for formic and acetic acid dimers, respectively. The O—O equilibrium separation in each case was predicted to be 2.42 Å. Experimental studies in the gas phase show enthalpies of formation of −14.2 and −15.0 kcal/mole for formic and acetic acid dimers with an O—O separation of 2.70 Å. Pullman and Bethod's studies on formamide dimers with CNDO/2 led to good agreement with experimental energies; however, they adopted the experimental geometry in which the O----H bond distance is considerably longer than would be predicted by a variation of this distance [*13*]. These poor results from CNDO/2 methods seem to imply that the carbonyl oxygen atom cannot be adequately treated using present parameterization. Choosing the same valence-state electronegativities for both alcohol and carbonyl oxygen atoms is apparently not valid.

The studies using the CNDO/2 method suggest that calculations on some hydrogen-bonded systems using a united molecule model may be on the threshold of significant achievement in explaining and predicting hydrogen bond phenomenon.

II. Anticonvulsants

Andrews had utilized the CNDO/2 MO method to study the possible role of hydrogen-bonding in the activities of several anticonvulsant drugs [*22*]. Two theories on the activities of these molecules involve different portions of the ring system common to all anticonvulsants. The first theory implicates the imide atoms (**VI**)

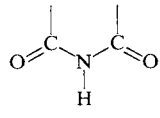

VI

as being involved in hydrogen-bonding at a receptor. The second theory implicates the charge at the ring atom bearing the substitution **VII**.

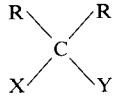

VII

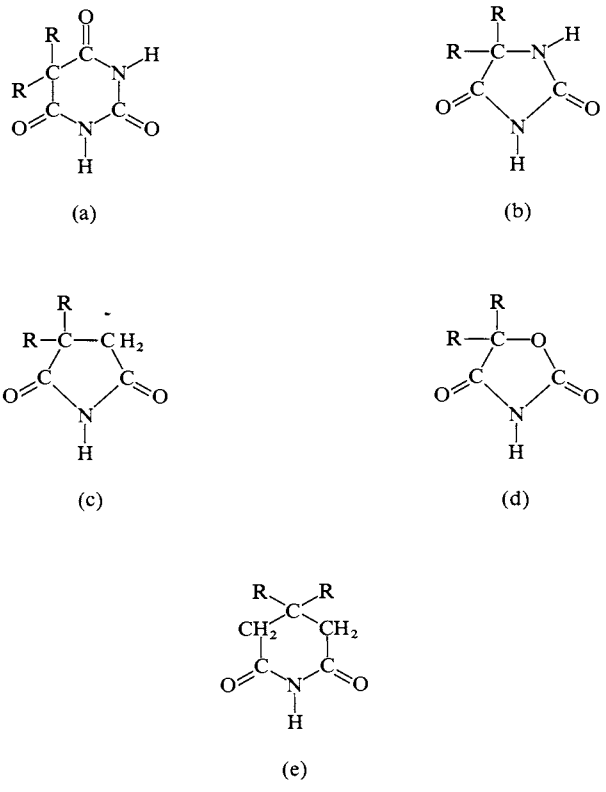

Fig. 12. Anticonvulsant compound classes considered in MO study [*23*]. (a) barbiturates, (b) hydantoins, (c) succinimides, (d) oxazolidine-2,4-diones, (e) glutarimides.

Andrews calculated the charges at these atoms, with both CNDO/2 and EHT, using this index as a measure of hydrogen-bonding ability.

The choice of the charge density to predict hydrogen bond strength is open to some question. Andrews felt that because of the similar structures involved, this was not an unreasonable choice; however, as can be seen in Fig. 12, the structures are not all that similar.

Andrews found no correlation between the substituted ring carbon charge and activity, nor did he find a correlation between the charge at the imide atoms and activity. The latter finding led Andrews to conclude that hydrogen-bonding ability is unrelated to the extent of biological activity. The charges on the imide atoms remained fairly constant throughout the series. It is possible that the imide portion of these rings may be involved in a strong and specific hydrogen bond with the receptor and that the extent of action depends upon the substituents [*22*]. It has been suggested recently that

the activity of the barbiturates may be due to their disruption of the coenzyme flavin-adenine dinucleotide [*23*].

A further look at this problem is indicated before abandoning the prospect that the hydrogen-bonding ability of the imide atoms quantitatively influences activity. The ground state charge density does not reflect the extent of change in the charge density at these atoms when they are involved in a hydrogen-bonded complex. This change in charge density would parallel the strength of the bond, as found by Hoyland and Kier [*14*]. Calculations could be performed on a supermolecule modeling the anticonvulsant drug with a standard hydrogen bond acceptor or donor. Enthalpies of formation or charge density exchanges could then be obtained for correlation with activities.

III. Purine and Pyrimidine Base Pairing

One of the most intriguing examples of hydrogen-bonding in nature is that of the purine–pyrimidine base pairs in RNA and DNA macromolecules. These bonds and their rupturing appear to control or regulate the replication of the genetic code, hence are at the core of species reproduction.

In a series of articles, Rein and Harris have used MO calculations to study the base-pairing scheme and associated phenomena [*24–27*]. A π-electron SCF method was used for the delocalized system, while the σ electrons were separately calculated using an SCF scheme. The guanine–cytosine complex was used as a model in the first study [*24*] (Fig. 13).

Reasonable descriptions of these hydrogen bonds are reported relative to charge distribution, the double well potential of the N—H---N bond, proton tunneling, and tautomeric equilibria.

Lunell and Sperber have extended these studies to include the adenine–thymine base pair, and the rare adenine–cytosine and guanine–thymine pairs [*28*]. Again reasonable potential energy surfaces and tautomeric distributions are reported.

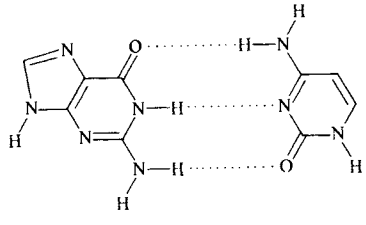

Fig. 13. Hydrogen-bonding in the guanine–cytosine base pair.

IV. Cholinesterase Inhibitor Binding

Cammarata and Stein have studied the relative potency of several substituted 3-hydroxyphenyltrimethylammonium salts (**VIII**), using MO theory [*29*]. They considered both the π and σ electrons by employing, separately, the simple Hückel scheme, and the Del Re σ treatment. The indices calculated by the π Hückel scheme were the charge, $S^{(N)}$ and $S^{(E)}$. From the Del Re calculations were obtained just charges. The inhibition potencies were used in the correlation attempts. The results are shown in Table VII. There is no apparent correlation between inhibitory potency and π-electron indices. When the σ and π charges are summed at an atom, however, a good correlation is obtained between potency and the total charge on the oxygen plus the $S^{(E)}$ at the oxygen. Thus the phenolic oxygen atom is implicated as interacting with an electrophilic species on the enzyme. This is consistent with the observation of Wilson and Quan that the *m*-hydroxy

TABLE VII
INHIBITION CONSTANTS (pK_I), ACIDITY CONSTANTS (pK_a), AND CALCULATED MO QUANTITIES FOR SOME 3-HPTA DERIVATIVES[a]

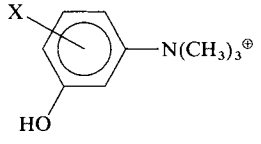

			σ and π Charges on Positions[b]			Superdelocalizabilities[c]		
X	pK_a	pK_I	C_1	C_3	O of 3-OH	C_1	C_3	O of 3-OH
4-CH_3	8.2	8.995	−0.039	0.034	0.075	0.835	0.805	1.063
			(0.055)	(0.116)	(−0.446)	(0.825)	(0.795)	(0.061)
6-CH_3	8.3	7.954	−0.041	0.035	0.075	0.835	0.805	1.062
			(0.053)	(0.119)	(−0.446)	(0.825)	(0.795)	(0.061)
5-CH_3	8.2	7.792	−0.037	0.037	0.075	0.830	0.799	1.061
			(0.55)	(0.119)	(−0.446)	(0.830)	(0.799)	(0.061)
6-OCH_3	8.6	7.716	−0.178	0.035	0.074	1.946	0.839	1.069
			(0.064)	(0.119)	(−0.446)	(1.254)	(0.839)	(0.070)
H	8.1	7.491	−0.037	0.037	0.075	0.830	0.799	1.061
			(0.056)	(0.119)	(−0.446)	(0.830)	(0.799)	(1.094)
4-OCH_3	8.0	6.068	−0.069	−0.001	0.071	0.950	0.939	1.094
			(0.056)	(0.127)	(−0.445)	(0.766)	(0.756)	(0.057)

[a] Cammarata and Stein [*29*].
[b] σ Charges in parentheses.
[c] $S^{(N)}$ values in parentheses.

group enhanced acetylcholinesterase binding by a factor of 120, suggesting a hydrogen bond.

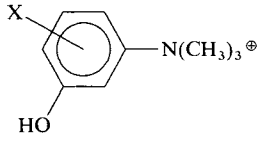

VIII

The separate treatment of σ and π electrons has limitations. In particular, the neglect of interaction of these orbitals is likely to lead to a distortion of the charge density picture on the atom. This would be particularly true for the highly electronegative oxygen atom. Reliance on the total charge of oxygen under these circumstances is not prudent. Nevertheless, these studies are illuminating, and could possibly reflect the receptor mechanism.

References

1. G. Pimental and A. McClellan, "The Hydrogen Bond," Freeman, San Francisco, California, 1960.
2. C. A. Coulson, "Hydrogen Bonding" (D. Hadzi, ed.), p. 339 Macmillan (Pergamon) New York, 1959.
3. H. A. Nash and D. F. Bradley, *J. Chem. Phys.* **45**, 1380 (1966).
4. G. Del Re, *J. Chem. Soc., London* p. 4031 (1958).
5. P. G. Puranik and V. Kumar, *Proc. Indian Acad. Sci., Sect. A* **58**, 29 (1963).
6. R. S. Mulliken, *J. Amer. Chem. Soc.* **72**, 600 (1950).
7. B. Pullman and A. Pullman, "Quantum Biochemistry," Ch. III. Wiley (Interscience), New York, 1963.
8. R. Grinter, *J. Mol. Spectrosc.* **17**, 240 (1965).
9. K. Morokuma, H. Kato, T. Yonezawa, and K. Fukui, *Bull. Chem. Soc. Jap.* **38**, 1263 (1965).
10. J. Karle and L. O. Brockway, *J. Amer. Chem. Soc.* **66**, 574 (1944).
11. C. A. Coulson, *Research* **10**, 149 (1957).
12. W. Adam, A. Grimison, R. Hoffmann, and C. Ortiz, *J. Amer. Chem. Soc.* **90**, 1509 (1968).
13. A. Pullman and H. Berthod, *Theor. Chim. Acta* **10**, 461 (1968).
14. J. R. Hoyland and L. B. Kier, *Theor. Chim. Acta* **15**, 1 (1969).
15. S. H. Bauer, J. Y. Beach, and J. H. Simons, *J. Amer. Chem. Soc.* **61**, 19 (1939).
16. A. P. Altshuller, *J. Amer. Chem. Soc.* **77**, 3480 (1955).
17. R. G. Pearson and D. C. Vogelsong, *J. Amer. Chem. Soc.* **80**, 1038 (1958).
18. M. Van Thiel, E. D. Becker, and G. C. Pimental, *J. Chem. Phys.* **27**, 95 (1957).
19. U. Liddel and E. D. Becker, *Spectrochim. Acta* **10**, 70 (1957).
20. E. D. Becker, U. Liddle, and J. N. Shoolery, *J. Mol. Spectrosc.* **2**, 1 (1958).
21. L. Pauling and L. O. Brockway, *Proc. Nat. Acad. Sci. U.S.* **20**, 336 (1934).
22. P. R. Andrews, *J. Med. Chem.* **12**, 761 (1969).
23. Y. Kyoguku and B. S. Yu, *Bull. Chem. Soc. Jap.* **41**, 1742 (1968).
24. R. Rein and F. E. Harris, *J. Chem. Phys.* **41**, 3393 (1964).

25. R. Rein and F. E. Harris, *J. Chem. Phys.* **42**, 2177 (1965).
26. R. Rein and F. E. Harris, *J. Chem. Phys.* **43**, 4415 (1965).
27. R. Rein and F. E. Harris, *J. Chem. Phys.* **45**, 1797 (1966).
28. S. Lunell and G. Sperber, *J. Chem. Phys.* **46**, 2119 (1967).
29. A. Cammarata and R. L. Stein, *J. Med. Chem.* **11**, 829 (1968).

Chapter XI

DISPERSION FORCES

Intermolecular forces are either electrostatic or magnetorelativistic [*1*]. Electrostatic forces can be conveniently classified as:

1. Direct electrostatic (long range)
2. Polarization or induction (long range)
3. Dispersion or London-van der Waal's (long range)
4. Resonance (long range)
5. Charge transfer (intermediate range)
6. Valence or chemical (short range)

The first four are termed "long range" forces since the energies involved decrease slowly with distance, such as R^{-n} where $n = 3,4,5,6$, etc. A short-range force decreases exponentially with distance, since it is dependent on the orbital overlap. The valence or chemical bond is such an example.

I. Dispersion Force Theory

We have discussed the roles of several of these forces in drug–receptor phenomena and have described how quantum mechanical calculations can approximate the relative energies of these forces in series of molecules. It is generally presumed that molecular mechanisms at a receptor involve some combination of strong and weak forces, the latter being termed a secondary or a reinforcing binding of the molecule to the receptor. These secondary forces are generally presumed to be dispersion or London-van der Waal's binding phenomena. An element of this binding is undoubtedly

present in every bond involving polar groups, but its prominence emerges when nonpolar groups are involved. These forces are so ubiquitously distributed among biologically important molecules that some mention should be made of them and the role that quantum mechanics can play in assessing their contributions to binding.

Charge fluctuation interactions are due to two different effects, the thermal motion of charges and the quantum mechanical random motion of electrons inherent in the Heisenberg uncertainty principle. The quantum mechanical effect in the case of molecules is called a London or dispersion interaction. In essence, this force, always attractive, arises between two neutral molecules as a result of the instantaneous fluctuation of charge distribution in one molecule inducing a dipole in a nearby molecule. The potential energy of system is approximately described by an equation, due to London [2]

$$V = -\frac{3\alpha_1\alpha_2}{2d^6}\frac{I_1 I_2}{I_1 + I_2}$$

where α is the polarizability of the molecule, I, the ionization potential of the molecule, and d, the distance between molecules. It can be seen that the force of attraction due to dispersion dies off very rapidly with distance, and is therefore only important between nearest-neighbor molecules or groups. London's equation gives values for the interaction energy somewhat lower than indicated by experiment.

The interaction energy between methylene groups 5 Å apart, is approximately 0.1 kcal/mole; however, the interaction between adjacent saturated chains is the sum of pair interactions along the chain. Thus the forces of attraction between molecules like long-chain fatty acids can become considerable. These forces undoubtedly play a prominent role in micelle formation. This attractive force is probably the key feature in what has been termed "hydrophobic bonding" of nonpolar side chains of macromolecules [3].

II. Molecular Orbital Treatment of Dispersion

An example of the use of MO theory to calculate molecular properties influencing dispersion interaction and the relationship of these to biological activity is the study by Agin, Hersh, and Holtzman on a number of local anesthetics [4]. It is known that a wide variety of chemical structures ranging from the inert gases to complex molecules are capable of reversibly blocking electrical activity. These authors considered a model in which the drug molecule confronted a membrane assumed to be a conducting wall. Since the drug molecules considered were neutral or possessed only small permanent moments, the major contribution to the energy of interaction was assumed

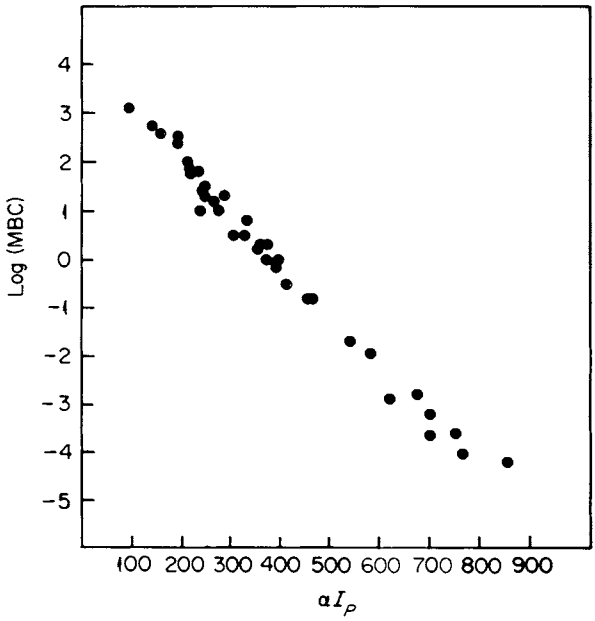

Fig. 1. Relationship between calculated dispersion binding ability at constant distance expressed as αI and local anesthetic activity expressed as log (MBC) (minimum blocking concentration) [*4*].

to be a London or dispersion energy. Casimer and Polder have derived an expression for the interaction energy between a neutral molecule and a conducting wall as

$$E = \alpha I/8r^3$$

where α and I refer to the neutral molecule [*5*].

A biological parameter was employed, the minimum blocking concentration (MBC), which defines the minimum concentration in an external solution necessary to completely block excitability. Assuming that the distance separating the drug from the membrane is constant, the MBC or the log (MBC) should be linearly related to αI for the series, if dispersion forces are the limiting feature controlling activity.

The polarizability term, α, was derived from atomic refraction constants. Experimental ionization energies were used when available. In the absence of such data, the ionization potentials were calculated using HMO theory. The ionization potential was equated to the E_{HOMO}. Numerical values of I were obtained by calculating the E_{HOMO} of those molecules with known experimental values and deriving an expression relating the two.

The results of the α, the I, either from experiment or calculations, and

TABLE I
POLARIZABILITY, IONIZATION POTENTIAL, AND MINIMUM BLOCKING CONCENTRATION OF LOCAL ANESTHETICS[a]

Anesthetic	α	I (eV)	log (MBC) (mM)
Methyl alcohol	8.2	10.85	3.09
Ethyl alcohol	12.9	10.48	2.75
Acetone	16.2	9.69	2.6
Isopropanol	17.6	10.16	2.55
Propanol	17.5	10.20	2.4
Urethane	23.2	9.0	2.0
Ethyl ether	22.5	9.53	1.93
Butanol	22.1	10.04	1.78
Antipyrine	29.8	7.7	1.78
Pyridine	24.1	9.32	1.77
Chloroform	21.4	11.42	1.5
Hydroquinone	29.4	8.1	1.4
Aniline	31.6	7.70	1.3
Benzyl alcohol	32.5	8.8	1.3
Acetanilide	30.5	8.4	1.17
Pentanol	26.8	9.85	1.2
Phenol	27.8	8.50	1.0
Toluene	31.1	8.82	1.0
Benzimidazole	40.2	8.24	0.8
Hexanol	31.4	9.75	0.56
Nitrobenzene	32.5	9.92	0.47
Quinoline	42.1	8.5	0.3
8-Hydroxyquinoline	44.7	8.1	0.3
Heptanol	36.0	9.7	0.2
2-Naphthol	45.4	8.1	0.0
Methyl anthranilate	48.9	8.1	0.0
Octanol	40.6	9.65	−0.16
Thymol	47.3	8.7	−0.52
o-Phenalthroline	57.8	8.0	−0.8
Ephedrine	50.2	9.1	−0.8
Procaine	67.0	8.1	−1.67
Xylocaine	72.5	8.0	−1.96
Diphenhydramine	79.5	8.5	−2.8
Tetracaine	79.7	7.76	−2.9
Phenyltoloxamine	79.9	8.8	−3.2
Quinine	93.8	8.0	−3.6
Eserine	82.4	8.5	−3.66
Caramiphen	87.0	8.8	−4.0
Dibucaine	103.6	8.25	−4.2

[a] Agin *et al.* [4].

the log (MBC) are shown in Table I. The relationship between log (MBC) and αI is shown in Fig. 1. The results show a close relationship between αI and log (MBC) for a widely diverse group of molecules over an 8-fold concentration range of activity. All other calculated MO indices failed to reveal any correlation with biological activity. The conclusion is inescapable that dispersion interaction, as calculated using these approximations, is related to the anesthetic activity of these molecules.

The failure of many other molecules to exhibit anesthetic activity is attributed to the possibility that other molecules like sugars and amino acids can engage in stronger interactions with water, thus precluding adsorption to a van der Waal's surface.

This study presents the exciting possibility that dispersion forces may be approached using MO theory. It is conceivable that with all-valence electron methods like CNDO/2, a better approximation of the molecular ionization potential may be achieved and a wider range of molecules studied.

References

1. J. O. Hirschfelder, *J. Chem. Phys.* **43**, S199 (1965).
2. F. London, *Discuss. Faraday Soc.* p. 8 (1936).
3. L. Salem, *in* "Electronic Aspects of Biochemistry" (B. Pullman, ed.), p. 297. Academic Press, New York, 1964.
4. D. Agin, L. Hersh, and D. Holtzman, *Proc. Nat. Acad. Sci. U.S.* **53**, 952 (1965).
5. H. B. G. Casimer and D. Polder, *Phys. Rev.* **73**, 360 (1948).

Chapter XII

FUTURE DIRECTIONS OF MOLECULAR ORBITAL STUDIES

I. Methods

A. MO Techniques

Many applications of MO theory to research in pharmacology and medicinal chemistry have been relatively primitive to date. This is primarily due to the fact that comparatively primitive MO methods have been all that has been available, until recently, to study large molecules. With the introduction of all-valence electron methods, the potential ability to make more meaningful calculations of molecular properties is available. Certainly the last word is not at hand with these techniques, for each has its limitations [*1*].

The EHT can be expected to undergo some revision which may take the form of iterating the integrals in an effort to improve the calculated charges. The parameters employed can be expected to be reviewed with the objection of equal Coulomb integrals for nonequivalent heteroatom hybrids in mind. It is not likely that the EHT method will be greatly improved. Because of the fundamental deficiencies in the primary assumptions, EHT will probably have to stand as a method which gives good conformations, but which has severe limitations for other molecular properties.

It is reasonable to assume that the SCF all-valence electron methods such as CNDO/2 and INDO/2 will profit more by studies directed toward reparameterization. This is likely because of the fundamentally more

sound basis for their construction. This is the direction to look in the immediate future for progress in the ability to calculate drug molecule properties.

B. Combination Techniques

At the present time there is an emerging interest in the union of MO-calculated indices with thermodynamic properties such as parameters reflecting partitioning between lipid and water phases in the body. The latter technique has been pioneered by Hansch [*2*], while the union of the two methods has been reported by several investigators [*3*]. This approach can be fruitful if the deficiencies in the MO methods can be minimized, and if the MO methods are wisely employed. The great danger here is the oversimplification of relationships between the two methods.

Heavy reliance should be placed on the indicators of statistical validity when MO indices and hydrophobic substituent constants are regressed with an index of biological activity. The inclusion of a large number of terms in a regression equation may lead to a good correlation coefficient, but the utility of the equation to predict may be negligible.

II. Future Areas of Study

A number of areas of interest to the medicinal chemist and pharmacologist appear to lend themselves to the application of MO studies to afford answers to some questions related to the structures and reactivities of drug molecules. The citation of a number of potential problems are useful to stimulate further thoughts on applying MO theory.

A. Irreversible Dihydrofolic Acid Reductase Inhibitors

Over the past few years, Baker has synthesized an enormous number of compounds with potential dihydrofolic acid reductase inhibitory action [*4*]. The objective of the studies has been to selectively inhibit the enzyme in leukemia L1210 cells. Many compounds studied were derived from 2,4-diaminopyrimidines (**I**) or 2,4-diamino-*S*-triazines (**II**).

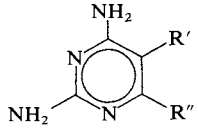

I

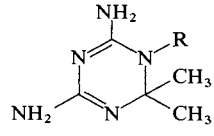

II

Although a number of compounds were made which were capable of inhibiting the enzyme *in vitro*, these same compounds were found to be

ineffective *in vivo*. The excellent biological data available for this large number of compounds, most of which contain extensive aromatic character, suggests that this collective data is ripe for MO considerations. Either SCF π-electron calculations or all-valence electron calculations could shed light on essential molecular features. These studies should be coupled with treatments of the hydrophobic contributions of substituent groups.

Probing deeper in the area of potential antitumor agents, it is apparent that a very large number of compounds have been synthesized and tested. These are of diverse chemical types and are presumed to act on a variety of cellular mechanisms such as enzyme inhibition, RNA synthesis inhibitors, and alkylating agents. These studies are readily available from publications of the National Cancer Institute and in the scientific journals. In many cases, large numbers of compounds in a chemical class have been studied and good biological data are available. MO studies could be applied in many cases to further the effort of compound design.

B. Skin Photosensitizing Effect of Furocoumarins

Over a period of several years studies have been conducted by Musajo and collaborators on the reaction of some furocoumarins with the skin, resulting in a photosensitizing upon irradiation [5]. A series of psoralen derivatives (**III**) have been tested for this activity. Irradiation of skin,

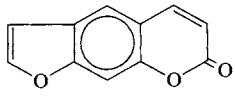

III

exposed to certain of these compounds, at 3655 Å, results in an erythma, followed by pigmentation. Studies to date have shown that the active compounds bind weakly to DNA and to nucleic acids in the dark, the complex breaking up completely upon precipitation of the DNA with ethanol. On the other hand, irradiation of the complex results in a more stable complex, resistant to disruption. A parallelism has been shown between the photoreactivity of the compound with DNA and the skin photosensitizing activity of the compound.

These compounds lend themselves to SCF π-electron MO calculations, since they are extensively conjugated. The biological reactivity of interest probably occurs in the photoexcited state, hence the calculations would have to be on the molecule under these conditions.

C. The Conformation of the Analgesic Methadol Isomers

In recent studies, Portoghese has investigated the stereochemistry of

methadol, (**IV**) isomers and the relationship to analgesic activity [6]. Using

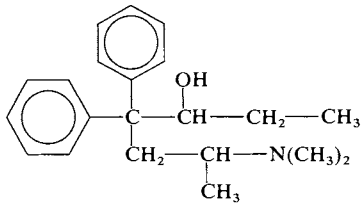

IV

pK_a, infrared, and NMR techniques, the possible conformations of the isomers have been proposed. The relationship of the conformation of the more active isomers of methadol to the conformation of methadone and to the hypothesized analgesic receptor was speculated upon.

All-valence electron MO studies would be of value in this case to test the agreement with experiment, to possibly calculate the relative prominence of hydrogen-bonding in each isomer, and to predict secondary conformational preferences which could play a role at the receptor. MO studies could be extended to consider the preferred conformations of other analgesics such as the prodine isomers (**V**).

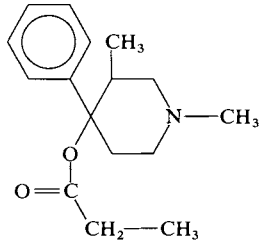

V

D. α- AND β- ADRENERGIC AGENTS

An intriguing problem on which MO calculations may shed some light is the one posed by the series of catecholamines substituted on the onium nitrogen. Norepinephrine (**VI**) R = H unsubstituted on the nitrogen atom

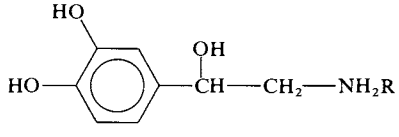

VI

is a potent α-adrenergic agent with no β-adrenergic activity. Epinephrine, with $R = CH_3$ has activity in both categories. With increasing bulk of the R group, i.e., ethyl, isopropyl, and *t*-butyl, the α-adrenergic activity becomes negligible while the β-adrenergic activity is enhanced. A reasonable explanation for this pattern of activity must account for the role of the alkyl group which not only diminishes α activity, but at the same time enhances β activity.

Larsen has suggested that the increasing bulk of the R group results in the change of reaction mechanisms from an aziridine ion to a quinoidal intermediate as illustrated in Fig. 1 [7]. The key to his hypothesis is his assumption that the added bulk of the R group causes an increasing energy barrier to the rotation of the methylene–methylene from a preferred conformation (**VII**) to a reacting conformation (**VIII**) necessary for α activity.

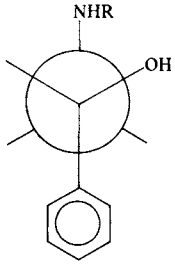

VII

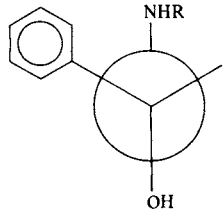

VIII

MO calculations of the relative energy barriers introduced by the increasing bulk of the R group would show whether this hypothesis was reasonable from at least the stereochemical aspect.

At the same time, MO calculations could reveal whether there is a significant change in the electron densities on the atoms of the onium group, and whether an hypothesis on the activity pattern could be built around this structural effect.

E. *N*-Methyl Group Effects

The influence of *N*-methyl groups on onium ions of potent agonists is well known but largely unexplained [8]. Acetylcholine (**IX**) with three methyl groups on the nitrogen atom has maximum muscarinic activity in a series of molecules formed by successively removing methyl groups and replacing them with hydrogen atoms.

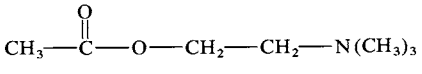

IX

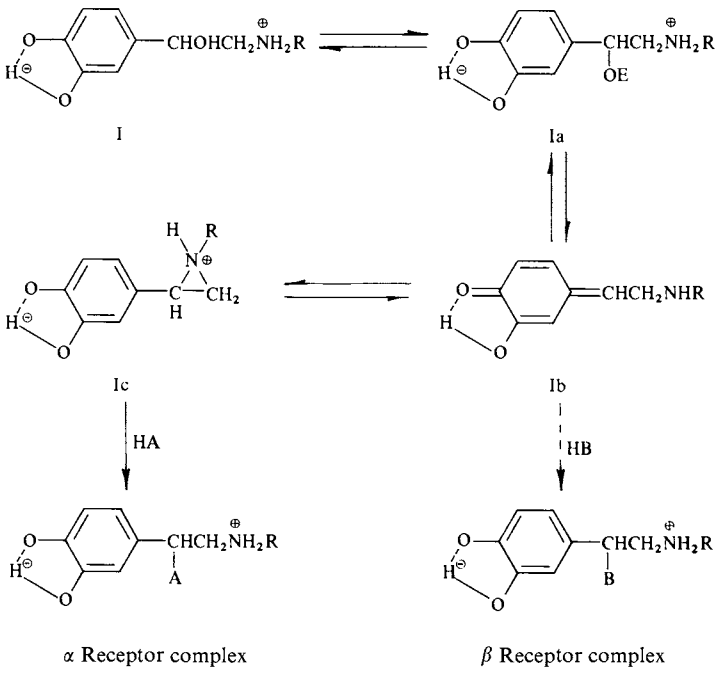

Fig. 1. Proposed mechanism of α and β adrenergic activity as influenced by the *N*-alkyl group in catecholamines. [7].

A contrary situation is noted with histamine (**X**). Successive methylation of the nitrogen atom progressively lowers the activity in this series. Additional examples are known for both trends.

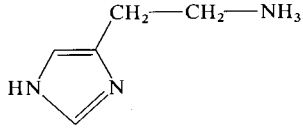

X

The question that MO studies could address themselves to is what is the change in the electronic structure around the onium group in these molecules? What is the bonding phenomenon to a receptor which is enhanced by methyl groups on the one hand and that is retarded in another case? It is conceivable that MO calculations would have to come to grips with dispersion forces to be useful here.

F. Hydrogen-Bonding and Solvation

A vast area remaining fertile for MO theory is the study of hydrogen-

bonding and solvation of groups commonly found on drug molecules. This includes groups variously alkylated, carbonyl groups, and hydroxyl groups. The extent to which these structural features participate in hydrogen bonds and solvation may be a subject in which MO calculations could be illuminating. Some beginnings have been made, as described in Chapter X and in studies by Rein and Harris [*9*], but predictive capability is still not clearly at hand.

Solvation patterns around the carbonyl group seems to be the easiest phenomenon to begin with. It is obvious that a fairly sophisticated MO method is necessary, since eigenvalue properties of the group and the complex would be the logical index of stability to consider. Solvation around the onium group has been considered using CNDO/2 with some success, but much remains to be done [*10*].

G. Structure–Activity Relationships among Aneleptics

A recent study by Andrews has focused attention on the use of MO theory to study the structural features imparting activity to the aneleptics, including the barbiturates (**XI**) and hydantoins (**XII**) [*11*]. A large amount of bio-

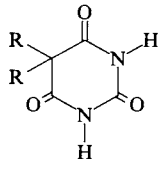

XI

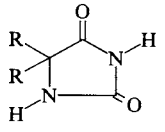

XII

logical data is available on the activities of many compounds in this class but as yet, no unified mechanism has been proposed which relates the electronic structures and reactivities of these molecules to antiepileptic activity.

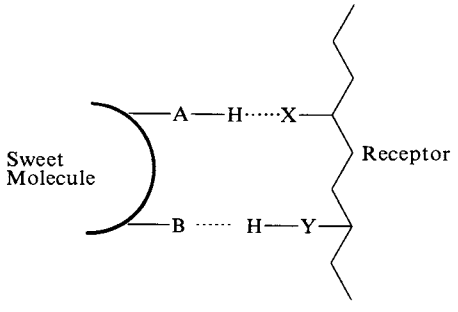

Fig. 2. Proposed sweet molecule–receptor interaction mode. [*12*].

H. Structural Characteristics of Sweetening Agents

A theory of the structural features necessary to impart a sweet taste to a molecule has been proposed by Shallenberger and Acree [*12*]. It was proposed that the key feature in sweet-tasting molecules is the presence of two electronegative atoms, *A* and *B*, with a proton associated with *A* (Fig. 2). From a consideration of a number of sweet-tasting molecules such as β-D-glucose (**XIII**), saccharine (**XIV**), and cyclamate (**XV**), the *A*/*B* distance was concluded to be optimum at 2.5 to 3.5 Å.

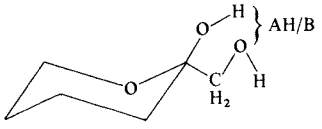

XIII

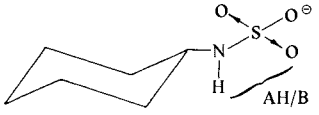

XIV

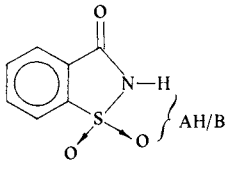

XV

The importance of the stereochemistry and the charges in the theory suggests that MO calculations could be useful to confirm the hypothesis and to possibly predict new structures with the desired properties.

A more recent study by Solms on amino acids has ranked a number of these compounds as bitter or sweet [*13*]. Interestingly, the D-isomers appear to be sweet in many cases, whereas the L-isomers are bitter. This implicates a stereoselective receptor and, of course, the need for an optimally positioned third binding site on the molecule.

III. Final Summary

Molecular orbital theory can advance our understanding of chemical events associated with molecules of biological significance. It is of importance, however, to use this research technique with prudence, bearing in mind that a biological process does not occur in a conservative state, nor does it occur in a reaction vessel. It occurs in a complex milieu which can certainly influence and alter events perhaps at times to a degree beyond the reach of presently available predictive methods.

One of the greatest dangers in the use of MO theory to study drug phenomena is the temptation to carry a correlation too far into the realm of mechanism prediction or receptor characterization. Limits must be placed on conclusions from MO studies so that the relationship between the method and the predicted result is always apparent. Nevertheless, the future opportunities for MO theory as a research technique in the life sciences are such that many scientists should be encouraged to acquaint themselves with this method.

References

1. J. R. Hoyland, *in* "Molecular Orbital Studies in Chemical Pharmacology" (L. B. Kier, ed.), p. 31. Springer-Verlag, New York, 1970.
2. C. Hansch and T. Fujita, *J. Amer. Chem. Soc.* **86**, 1516 (1964).
3. A. Cammarata, B. Neeley, W. Purcell, and A. Wohl, *in* "Molecular Orbital Studies in Chemical Pharmacology" (L. B. Kier, ed.). Springer-Verlag, New York, 1970.
4. B. R. Baker, "Design of Active-Site-Directed Irreversible Enzyme Inhibitors." Wiley, New York, 1967.
5. G. Rodighiero, L. Musajo, F. Dall'Acqua, S. Marciani, G. Caporale, and M. Ciavatta, *Experientia* **25**, 479 (1969).
6. P. Portoghese and D. Williams, *J. Med. Chem.* **12**, 839 (1969).
7. A. A. Larsen, *Nature (London)* **224**, 25 (1969).
8. R. B. Barlow, "Introduction to Chemical Pharmacology." Wiley, New York, 1964.
9. R. Rein and F. E. Harris, *J. Chem. Phys.* **45**, 1797 (1966).
10. J. R. Hoyland and L. B. Kier, *Theor. Chim. Acta* **15**, 1 (1969).
11. P. R. Andrews, *J. Med. Chem.* **12**, 761 (1969).
12. R. S. Shallenberger and T. E. Acree, *Nature (London)* **216**, 480 (1967).
13. J. Solms, *J. Agr. Food Chem.* **17**, 686 (1969).

AUTHOR INDEX

Numbers in parentheses are reference numbers and indicate that an author's work is referred to although his name is not cited in the text. Numbers in italics show the page on which the complete reference is listed.

SUBJECT INDEX